Developing Synthetic Polymer Substrates for Stem Cell Culture

Thesis submitted in accordance with the requirements of the University of Liverpool for the degree of Doctor in Philosophy

by

Laurence Jerome Glennon-Alty

January 2012

Acknowledgements

I would like to thank my supervisors Dr Patricia Murray, Dr Rachel Williams and Dr Haifei Zhang for their help and support throughout this project. I would also like to thank Simon Dixon, Ian Harrison and Fred Laws for their expertise and encouragement.

I am grateful to everyone who has helped and supported me throughout the good and the bad. Thanks to all of my lab group, and especially Iryna, Egon and Marina, who always had time to show me the right way when I was unsure, I wouldn't be the scientist I am today without you.

Finally, thanks to my family and friends for their unwavering support and encouragement. I would not have made it this far without you all. Most of all Becky, you make me smile, smile, smile... and you have always given me something to look forward to.

This work was funded by the Biotechnology and Biological Sciences Research Council and Biomer Technology Ltd.

Abstract

Stem cells hold great promise for use in regenerative therapies. However, current obstacles to their use include the ability to culture them under defined conditions, and the ability to differentiate them cost effectively. Over recent years there has been a great deal of interest in designing artificial substrates that are able to regulate stem cell behaviour, and there is now much evidence to suggest that the chemical composition of the substrate plays an important role in this regulation. The use of chemically defined substrates represents simple and cheap solutions to the effective culturing of stem cells.

In this study, the surface properties of poly-acrylate substrates were altered to enact control over the self-renewal and differentiation of stem cells. Specifically, chemically defined substrates were designed and tested for their ability to support mouse embryonic stem cell (mESC) self-renewal and direct the differentiation of mouse and human mesenchymal stem cells (MSCs) to chondrocytes.

Poly-acrylate substrates were designed with Biomer Technology Limited (BTL), which has developed novel synthetic **ac**celer**a**te™ polymeric coatings for use as biomaterials. The surface of these poly-acrylate substrates presented a combination of amine, carboxylic acid and hydroxyl functional groups at controllable density and proportion. These functionalities are known to influence stem cell behaviour and differentiation; however their combined influence is less studied. Substrates were further developed by modelling the functional group composition and distribution found at common integrin binding sites of key extracellular matrix proteins.

The poly-acrylate substrates were able to modulate stem cell behaviour through alterations in surface chemistry. Results of the mESC studies indicated that while some of the poly-acrylate substrates could support the expansion of undifferentiated mESC colonies in defined serum-free culture medium over the short-term, population expansion was significantly reduced compared with control substrates. Further investigation demonstrated that this was likely due to deficient attachment of cells to the poly-acrylate substrates.

The MSC studies indicated that poly-acrylate substrates modelled on the functional composition and distribution of the RGD integrin-binding motif of fibronectin were able to promote chondrogenesis in mouse and human MSCs, without need of additional stimuli. MSCs began to aggregate following seeding onto substrates, with QPCR and immunostaining confirming the presence of chondrocyte markers within aggregates, reminiscent of limb-bud formation. The mechanism of chondrogenesis induction was thought to occur directly via an RGD-integrin-like interaction.

This work is the first to show that biomaterials designed to mimic specific sites of ECM molecules have the potential to direct MSC chondrogenesis without need of additional stimuli. More broadly, this thesis demonstrates that the surface properties of biomaterials can be tailored to regulate the self-renewal or differentiation of stem cells cultured in contact with them.

Contents

List of figures

List of tables

Abbreviations

AP	Alkaline phosphatase	**m**	Minute
BMP	Bone morphogenetic protein	**MAP**	Mitogen-activated protein
BTL	Biomer Technology Limited	**MSC**	Mesenchymal stem cell
CAM	cell adhesion molecule	**N-cadherin**	Neural cadherin
CBP	CREB-binding protein	**N-CAM**	Neural CAM
cDNA	Complementary DNA	**Oct4**	Octamer-4
DAPI	4',6-diamidino-2-phenylindole	**OD**	Optical density
DCA	Dynamic contact angle	**PBS**	Phosphate buffered saline
DMEM	Dulbeccos modified eagles medium	**PFA**	Paraformaldehyde
		PLGA	Poly(lactic-co-glycolic acid)
E-cadherin	Epithelial cadherin	**PLLA**	poly(l-lactic acid)
ECM	Extracellular matrix	**QPCR**	Quantitative real-time PCR
ERK	extracellular signal-regulated kinase	**RGD**	Arginine-glycine-aspartic acid
		RNA	Ribonucleic acid
ESC	Embryonic stem cell	**ROCK**	Rho-associated protein kinase
ESP	Embryonic stem cell polymer		
FAK	Focal adhesion kinase	**SAM**	Self-assembled monolayer
FCS	Foetal calf serum	**SCID**	Severe compromised immuno-deficient
FGF	Fibroblast growth factor		
gp130	Glycoprotein 130	**S.E.M**	Standard error of the mean
GSK	Glycogen synthase kinase	**SICM**	Scanning ion conductance microsopy
h	Hour		
JAK	Janus kinase	**Sox**	SRY (sex determining region Y)-box
KLF	Krüppel-like family of transcription factor	**STAT**	Signal transducers and activators of transcription
KSC	Kidney-derived stem cell		
LBC	Limb bud cell	**TGF**	Transforming growth factor
LIF	Leukaemia inhibitory factor	**XPS**	X-ray photo-electron spectroscopy
LIFR	LIF receptor		

Chapter 1

1. Introduction

The term "stem cell" was first coined in the mid 19th century and comes from the German "stammzelle", or "family cell". This nomenclature referred to a single cell's ability to produce a variety of specialised progeny. However, its current meaning originates from around the turn of the 20th century, when theories of cell origin and differentiation were being proposed. Among others, the Russian histologist Alexander Maksimov put forward, in 1906, his theory of haematopoietic precursors. This theory proposed common precursors for the diverse and specialised cell types of the blood system, preceding by more than 50 years definitive evidence of haematopoietic stem cells in 1963. That work, conducted by Till and McCulloch, led the way for the present definition.

Stem cells are characterised by their ability to both renew themselves and differentiate into specialised cell types. These specialised cell types can be tremendously diverse, representing every cell type in the body. Due to their unique properties, stem cells hold great promise for regenerative therapies, where tissues and organs could be grown for transplantation.

Stem cells are typically referred to by their means of derivation. The two main mammalian groups are embryonic stem cells (ESCs) and adult stem cells. ESCs are derived from the inner cell mass of early stage embryos,

also called blastocysts. They are pluripotent, and are able to form all the cells of the adult organism. Adult stem cells can be found in most organs, where they are mainly responsible for tissue maintenance and repair. Whilst many adult stem cells are unipotent, tending to generate cell types of their tissue of origin, some types of adult stem cell, such as mesenchymal stem cells (MSCs) and haematopoietic stem cells, can generate a wider range of different cell types. For instance, MSCs can give rise to adipose, bone and cartilage cells. The ability of MSCs to generate chondrocytes means they could have the potential to treat diseases such as osteoarthritis, which are caused by degeneration of articular cartilage.

However, control over the fate of stem cells is not well understood and obstacles to the viable use of stem cell therapies remain. Two significant obstacles to the advancement of stem cell based therapies are the ability to culture them in sufficient numbers under defined conditions, and the ability to direct their differentiation to the required cell type cost effectively. Current culture protocols typically involve undefined mixtures of animal components, expensive and complex growth factors, and complicated culture techniques. In this study, the ability of chemically and physically defined substrates to regulate stem cell self-renewal and differentiation was assessed. Specifically, chemically defined substrates were designed and tested for their ability to support mESC self-renewal and direct the differentiation of mouse and human MSCs to chondrocytes.

1.1. Embryonic stem cell self-renewal

The potential for embryonic stem cells (ESCs) to differentiate into functional adult cell types is now well recognised (Xu 2005; Carr 2009; Fathi 2010). However, many barriers remain to be overcome before they can be used for drug discovery or future therapy applications. One of the foremost is the development of defined conditions to enable consistent and cost effective ESC population expansion. To allow the development of these conditions, the mechanisms behind ESC self-renewal need to be understood. Over recent years considerable progress has been made towards defining the molecular mechanisms that regulate mESC self-renewal. Smith and co-workers have shown that fibroblast growth factor 4 (FGF4) signalling plays a crucial role in inducing mESC differentiation, and that mESC self-renewal can be maintained under relatively defined conditions in the absence of serum as long as inhibitors of FGF4 and its downstream effector, extracellular signal-regulated kinase (ERK1/2), are present (Kunath 2007; Nichols 2009).

Undifferentiated mESCs have a characteristic morphology; namely, prominent nucleoli, a high nuclear:cytoplasmic ratio, and a tendency to grow in compact multi layered colonies (Robertson 1987). These colonies are tightly packed and typically display smooth edges. On differentiation, the cells have a greatly reduced nuclear:cytoplasmic ratio and tend to spread on the surface, forming a monolayer.

1.1.1. The mechanisms of self-renewal

A number of transcription factors are implicated in ESC self-renewal. Among the foremost are OCT4 (Niwa 2000), *NANOG* (Chambers 2003), SOX2 (Masui 2007) and KLF4 (Okita 2007), which serve as key markers for undifferentiated ESCs. These transcription factors share a substantial number of target genes and work synergistically to maintain self-renewal, and to regulate their own expression (Ying 2008; Hall 2009). The importance of these factors in maintaining the ESC phenotype has also been exemplified by the fact that their forced expression in somatic cells can generate induced pluripotent stem (Phillips) cells (Okita 2007). A further key marker for mESC pluripotency is alkaline phosphatase (AP). AP is localised at the cell membrane, where it is expressed at high levels in ESCs, but is rapidly down-regulated during differentiation (Kim 1995; Palmqvist 2005). It is a useful marker, as the phosphatase activity can be easily detected with histochemical assays. Another property of undifferentiated mESCs is that they proliferate rapidly due to the absence of a G1-S checkpoint (Savatier 1994). Therefore, upon differentiation, the proliferation rate of mESCs is reduced.

mESC self-renewal can be maintained through a number of different pathways. Typically, leukaemia inhibitory factor (LIF) is used to maintain mESC self-renewal in culture (Smith 1988; Williams 1988). LIF binds to a LIFR-GP130 complex which acts on multiple downstream pathways, including JAK-STAT and ERK pathways. The JAK-STAT (Janus kinase, signal transducer and activator of transcription) pathway acts via STAT3

(Niwa 1998; Burdon 2002; Cartwright 2005), which is thought to promote self-renewal by inducing transcription of KLF4 (Figure 1-1) (Hall 2009). Several LIF independent pathways have also been identified. A WNT/β-CATENIN signalling pathway has been demonstrated to maintain mESC self-renewal under certain conditions (Haegele 2003; Sato 2004). This is thought to occur by preventing β-CATENIN from switching coactivator usage from CBP to p300, thereby increasing β-CATENIN/CBP-driven transcription at the expense of βCATENIN/p300-driven transcription (Figure 1-1) (Miyabayashi 2007). A role for WNT signalling in promoting ESC self-renewal is supported by findings that inhibition of glycogen synthase kinase 3 (GSK-3) suppresses mESC differentiation (Ying 2008). It is now thought that when cultured under defined conditions in the absence of serum, undifferentiated mESCs are at a normal "ground state", and require external stimuli for differentiation, but not self renewal (Ying 2008; Nichols 2009).

Recent studies have also demonstrated the importance of cell-cell interactions in regulating mESC self-renewal. Several groups have demonstrated the roles of cadherin cell adhesion molecules in differentiation. Inhibition of E-cadherin mediated cell-cell contact has been shown to maintain LIF-independent self-renewal, in addition to blocking colony formation (Soncin 2009). An earlier study had shown that E-cadherin null mESCs remained undifferentiated, but lost pluripotency (Larue 1996). Another study found an E-cadherin substrate could inhibit

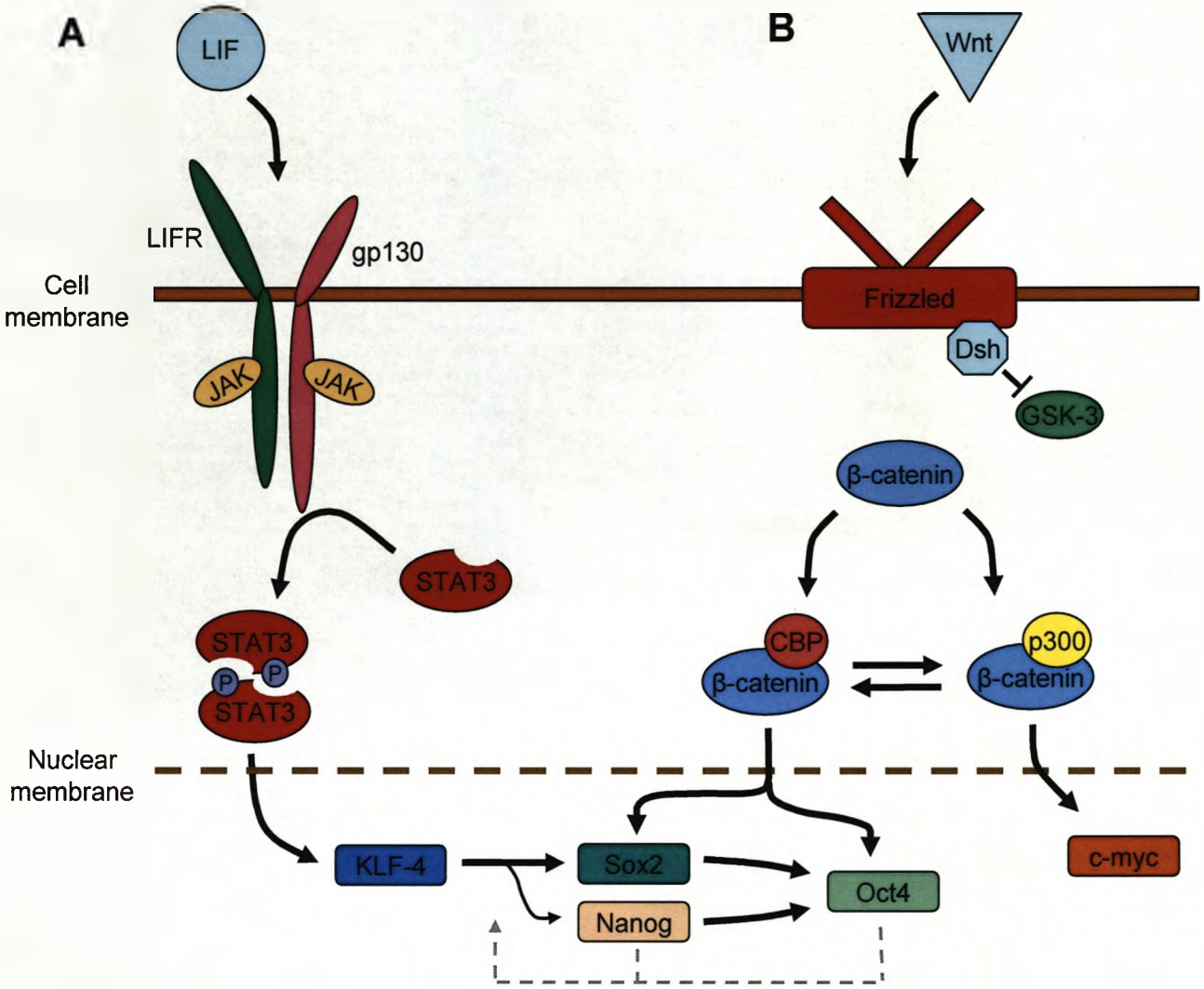

Figure 1-1 LIF and WNT signalling pathways promote mESC self-renewal.

(A) LIF binds to the LIFR-gp130 complex, causing a conformational change in the receptors and activating JAKs by autophosphorylation. STAT3 monomers bind to phosphorylated sites on the LIFR-gp130 receptors and are phosphorylated by JAKs. Activated STAT3 monomers dimerize and translocate to the nucleus, where they induce the expression of KLF-4. KLF-4 mainly activates SOX2 but also *NANOG*, which in turn maintain expression of OCT4. SOX2, *NANOG* and OCT4 autonomously regulate their own expression, leading to maintenance of self-renewal.

(B) WNT binds to its frizzled receptor, activating dichevelled (Dsh) and inhibiting GSK-3 kinase activity and the β-CATENIN degradation complex, stabilising β-CATENIN levels. β-CATENIN can then interact with its co-activators, CBP or p300, to mediate transcription. The β-CATENIN/CBP complex promotes self-renewal, via SOX2 and OCT4 activation. The β-CATENIN/p300 complex initiates differentiation, via c-myc.

colony formation and encourage scattered distributions of undifferentiated mouse embryonal carcinoma cells under serum conditions without LIF (Nagaoka 2008). Furthermore, over-expression of N-cadherin was found to promote the formation of more tightly packed colonies of mESCs and reduced their attachment to the substrate (Karabekian 2009). Taken together, these studies suggest that cell-cell contact might be required for differentiation of ESCs.

The role of cell shape has also been suggested to impact on mESC self renewal, with a recent study by Wells *et al.* (2009) demonstrating that restriction of spreading on carboxyl presenting surfaces could promote self-renewal in mESCs. Another recent study found that reduction of cell spreading on agarose substrata reduced focal adhesion formation and promoted adipogenic differentiation in mESCs in the presence of serum (Szabo 2009). A link between cell shape and behaviour has also been demonstrated with other cell types (Huang 2000; Luo 2008), and other studies have shown that cell shape can be regulated by modifying the culture substrate (Kalaskar 2008). Recently in hMSCs Killian *et al.* (2010) showed that cell shape could encourage differentiation to osteoblasts, by promoting a contractile cytoskeleton, or adipocytes, by disrupting contractility, in the presence of differentiation cues.

1.1.2. Mechanisms of cell attachment

Cell attachment can be described as the binding of cells to a surface, an extracellular matrix (ECM) or another cell, and is involved in numerous

cellular processes, including proliferation, migration and apoptosis (Mousa 2008). Furthermore, it is essential for the assembly of multi-cellular three-dimensional tissues (Gumbiner 1996). Attachment is typically mediated by cell adhesion molecules (CAMs), which are commonly transmembrane receptor proteins, with an intracellular domain that interacts with the cytoskeleton and signalling pathways, a transmembrane domain, and an extracellular domain that interacts with other CAMs on neighbouring cells or proteins of the ECM. Most CAMs belong to one of four protein families: integrins, immunoglobulin superfamily (IgSF), cadherins and selectins (Elangbam 1997; Mousa 2008). *In vivo*, integrins are most commonly associated with cell-ECM interactions, but can also bind IgSF CAMs, whereas IgSF CAMs, cadherins and selectins are involved in cell-cell adhesion. Cadherins exhibit homophilic adhesion, and are important for tissue organisation and maintaining intracellular junctions, binding cells within tissues together (Gumbiner 1996; van der Linden 1996).

In vivo, most cells are in contact with ECM molecules, which have roles in regulating cell attachment, proliferation, differentiation, migration and survival (Hynes 2002). ECMs can regulate these functions by direct interaction with integrins, but also by binding secreted growth factors, such as fibroblast growth factors (FGFs) and bone morphogenetic proteins (BMPs), and subsequently bringing them into intimate contact with cells or regulating their distribution (Hynes 2009). Growth factors can bind directly to ECM proteins, such as the binding of TGF-β1 and BMP-2

to collagen II (Zhu 1999), but also through associated heparan sulphates (Vlodavsky 1996).

Integrins are heterodimeric transmembrane receptors, consisting of a non-covalent association between an α and β subunit. In mammals, 18 α and 8 β subunits have been characterised, with 24 recognised combinations (Figure 1-2) (Hynes 2002). They mediate cell-ECM adhesion by simultaneously binding ECM proteins, such as fibronectin, vitronectin, collagen and laminin, and establishing a linkage to the actin cytoskeleton of the cell. In this way they are able to operate both outside-in and inside-out signalling, being able to transduce information from the ECM to the cell, but also reveal the status of the cell to the outside (Ellis 2009).

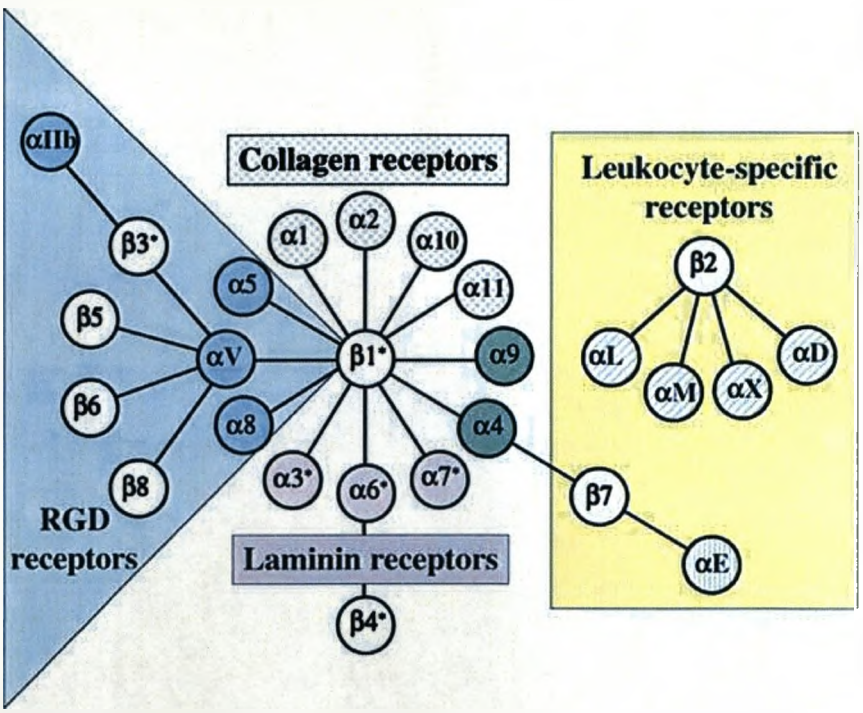

Figure 1-2 Integrin heterodimer combinations and typical ligands. Integrins are obligate heterodimers, containing distinct α and β subunits. In mammals, 18 α and 8 β subunits have been characterised, with 24 recognised combinations. Adapted from (Hynes 2002).

The intracellular action of integrins is regulated by a large multi-protein complex assembled around the integrin. This complex includes integrin-binding proteins, scaffolding proteins, actin-binding proteins, and cell-signalling proteins. Some well described components that bind to the cytoplasmic domain of integrins include talin, vinculin, paxillin and α-actinin, which in turn allow other intracellular signalling proteins, such as focal adhesion kinase and Src kinase, to associate with the complex (Hynes 2002). Through this complex, integrins are able to modulate an extensive number of processes within the cell, including differentiation, proliferation and survival (Legate 2009). However, the intracellular pathways involved are very complex, as highlighted in Figure 1-3 (Delon 2007; Zaidel-Bar 2007).

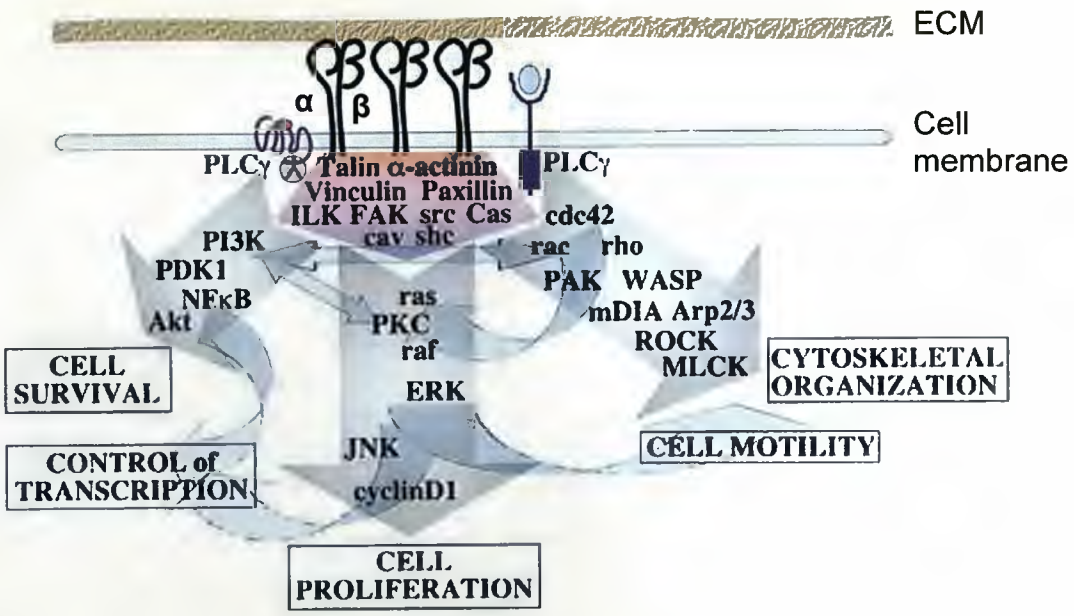

Figure 1-3 Intracellular integrin signalling. The multi-protein integrin-associated complex is large and intricate, with well over 100 associated proteins and factors involved in the multitude of intracellular signalling pathways. The major integrin-associated proteins are highlighted in pink, below the clustered integrins. The major signal transduction pathways, key players in them and the effects on cell behaviour mediated by integrins are summarised. Adapted from (Hynes 2002).

Interaction of integrins with the ECM is modulated in two main ways, either through integrin activation or integrin clustering (Figure 1-4) (Ellis 2009). Integrin activation, or affinity modulation, involves conformational changes, which can be achieved via cytoplasmic factors interacting with the cytoplasmic domain (inside-out signalling), or through interactions with extracellular ligands (outside-in signalling). Integrin clustering is associated with tight adhesion, spreading and focal adhesion formation (Gumbiner 1996).

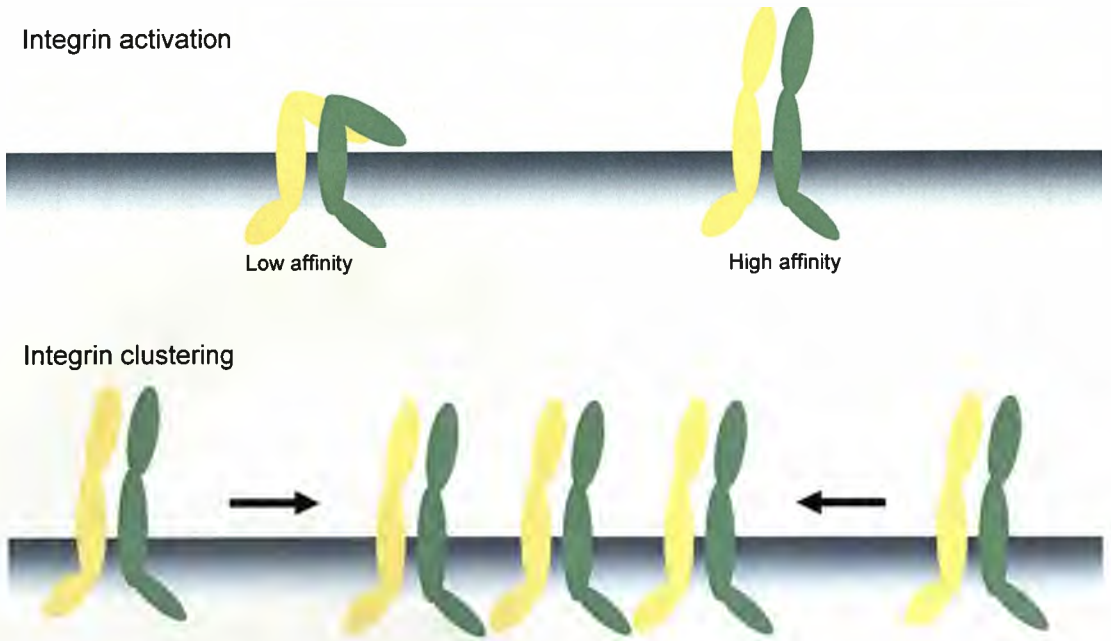

Figure 1-4 Integrin activation and clustering. The upper panel shows different conformations of an integrin that are associated with low and high affinities. The lower panel demonstrates clustering of integrins on the surface of a cell.

Cell adhesion to a substrate is typically mediated by a layer of adsorbed proteins. The initial response of a surface in a biological milieu is for a layer of water to cover it in the order of nanoseconds (Roach 2007). A layer of proteins then adsorbs to the surface in seconds to hours, before cells interact with this protein coating (Roach 2007), and often cells which cannot attach rapidly will apoptose (Pelham 1997). Therefore, cell

attachment to a substrate, like the ECM, is predominantly enacted by integrins. Over time it is likely that cells will deposit their own ECM molecules to provide an optimal substrate (Michelini 2006; Chen 2007).

1.1.3. Regulation of ESC self-renewal by cell-substrate interactions

Cell attachment to the ECM is typically mediated via cell surface receptors, such as integrins (Figure 1-4). When cultured in the presence of serum, ECM proteins present in the serum, such as fibronectin and vitronectin, adsorb to tissue culture plastic and aid in cell attachment and growth (Steele 1992; Steele 1995). Synthetic ECM-based substrates, such as Matrigel™ – a basement membrane-like matrix secreted by Engelbreth-Holm-Swarm mouse sarcoma cells (Kleinman 2005), have been shown to support mESC self-renewal in combination with LIF (Greenlee 2005). Most cell types are known to attach and grow well on ECM protein substrates, such as fibronectin, laminin and vitronectin (Garcia 1999; Webb 2000; Chen 2007). There is also evidence to suggest that production of endogenous ECM is critical in ESC culture (Chen 2007). Virtually all mammalian cell types, including mESCs, express the β1 integrin subunit, which binds to several ECM proteins. In hESCs, both fibronectin (Baxter 2009), via α5β1 integrin, and vitronectin (Braam 2008), via αvβ5 integrin, have been shown to support attachment and self-renewal.

However, some studies have demonstrated that mESCs differentiate when cultured on substrates coated with a single type of ECM protein (Hayashi 2007; Lee 2010). A study by Hayashi *et al.* (2007) found fibronectin and laminin substrates promoted differentiation of mESCs under serum-free conditions with LIF through integrin signalling and activation of ERK1/2. Conversely, collagen type I and type IV, which bind to α1β1, α2β1, α10β1, and α11β1 that are not expressed in mESCs and are suppressed by LIF, were able to support mESC self-renewal. In addition, blocking interactions between ECM and integrins, with anti-integrin β1 antibody, inhibited any differentiation, suggesting that inactivation of integrin signalling is crucial for mESC self-renewal under these conditions (Hayashi 2007).

In contrast to these findings, Lee *et al.* (2010) demonstrated that, under serum conditions with LIF, simultaneous activation of multiple integrin subunits in 3-D culture, via peptide ligands, promoted self-renewal in mESCs, whereas individually they encouraged differentiation (Lee 2010). These key integrins were $\alpha_5\beta_1$, $\alpha_v\beta_5$, $\alpha_6\beta_1$ and $\alpha_9\beta_1$; their normal ECM ligands and the peptide ligands used are listed in table 1-1 below. This result suggests a balance of integrin signalling is required to maintain self-renewal, and suggests parallels with the study of Ying *et al.* (2008), that showed if the balance of signalling becomes skewed, self-renewal is lost.

Table 1-1 List of integrins and their ligands used by Lee *et al.* (2010)

Integrin	ECM Ligand	Peptide Ligand
$\alpha_5\beta_1$	Fibronectin (RGD)	RGDSP
$\alpha_v\beta_5$	Vitronectin (RGD)	RGDSP
$\alpha_6\beta_1$	Laminin	TTSWSQ
$\alpha_9\beta_1$	Tenascin-C	AEIDGIEL

Integrin signalling has been identified as a key regulator of multiple cell processes and has been well reviewed by Berrier *et al.* (2002) and Legate *et al.* (Legate 2009). In mESCs, blocking integrin binding has been found to reduce attachment to ECM proteins, alter morphology and migration, and inhibit differentiation (Fassler 1995; Andressen 1998; Liu 2009). Several groups have shown enhancement of cell-substrate adhesion of ESCs and other cell types by artificial peptide ligands derived from ECM proteins (Derda 2007; Fischer 2007; Kalaskar 2008). Commonly used ligands contain integrin binding motifs, such as the common RGD motif found in fibronectin and several other ECM proteins. The RGD motif has been implicated in almost half of integrin bindings (Hersel 2003), and is, therefore, a key target for aiding in cell attachment. Studies have demonstrated adhesion of many cell types to surfaces presenting RGD peptides (Alvarez-Barreto 2007; Sato 2007).

1.1.4. Regulation of cell-substrate attachment via interaction with an adsorbed protein layer

Protein adsorption is known to depend on the surface properties of the substrate. Surfaces can influence this adsorption through electrostatic, hydrophobic, hydrogen bonding and van der Waals interactions (Garcia 1999; Michael 2003). A typical model for this interaction suggests that, in most cell types, properties that enhance ECM protein adsorption, enhance cell attachment because of the increased concentration of adsorbed proteins (Kalaskar 2008). The wettability of a surface is thought to confer a preference for the adsorption of cell adhesion proteins, such as fibronectin, which are in competition with adhesion inhibiting proteins, such as albumin (Carre 2010). Hydrophilic surfaces are better able to adsorb cell adhesion proteins, resulting in improved cell attachment (Wei 2009) (Carre 2010).

However, substrate-dependent changes in conformation and orientation of ECM proteins have been demonstrated to alter their affinity for cell adhesion (Horbett 1988; Steele 1995; Michael 2003; Lan 2005; Roach 2005; Lord 2006). Keselowsky *et al.* (2003) demonstrated that the adsorption kinetics and conformation of fibronectin was dependent on the surface chemistry of a substrate. They examined alkanethiol self-assembled monolayers (SAMs) presenting methyl, hydroxyl, amine and carboxyl functional groups (Figure 1-5), and found murine MC3T3-E1 osteoblast-like cell adhesion was modulated consistent with the structural

changes in fibronectin. Utilising monoclonal antibodies, they found that fibronectin adsorbed to methyl surfaces demonstrated the most pronounced structural changes, whereas, hydroxyl surfaces induced the least structural change in the fibronectin, and were associated with the highest degree of cell adhesion (Michael 2003). X-ray photoelectron spectroscopy (XPS) was used to demonstrate increased atomic percentage of oxygen or nitrogen in the hydroxyl, carboxyl and amine SAMs, however, the availability of functional groups at the surface was not quantified making it difficult to be certain what fibronectin interacts with. Furthermore defects can occur in the SAMs, which could result in masking of the expected functional group and unexpected interactions with the tail or gold substrate (Love 2005). Other monoclonal antibody studies have also demonstrated conformation changes at specific cell binding sites of ECM proteins (Underwood 1993; Roach 2005), and subsequent effects on proliferation and differentiation (Garcia 1999). In addition, the strength of fibronectin adsorption to defined surfaces has been shown to alter the ability of cultured cells to remodel it (Lan 2005; Pompe 2007).

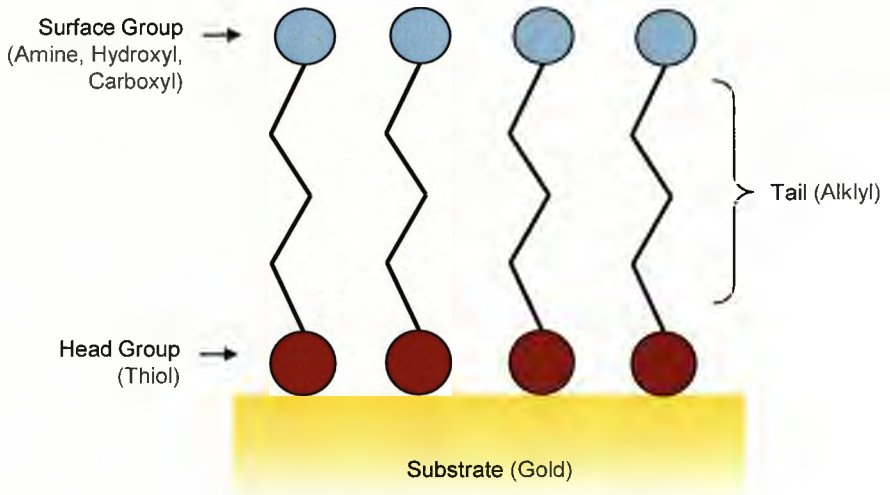

Figure 1-5 Schematic of self assembled monolayers (SAMs). A SAM is an organized layer of amphiphilic molecules with a hydrophilic head group, which has a high affinity for the substrate, and hydrophobic tail region, which will organize alongside closely-packed adjacent molecules. Example components of the most common alkanethiol SAMs are shown in parenthesis.

1.1.5. Regulation of ESC self-renewal using biomaterial substrates

The influence of the local environment on cell behaviour is now well recognised. In particular, surface properties, which will regulate the initial cell response have been widely investigated (Zhu 2004; Curran 2006; Yim 2006). Studies have demonstrated control over many cell properties, including proliferation, attachment, migration and differentiation in multiple cell types (Lan 2005; Curran 2006; Alvarez-Barreto 2007), though common responses have been elusive.

Surface chemistry affects the degree of hydrophilicity and hydrophobicity, or wettability, of the substrate, which can affect cell behaviour in culture. Wettability has long been thought to positively correlate with the degree of cell attachment to a substrate (Vanwachem 1987). Typically,

substrates with a high degree of hydrophilicity are thought to have a higher affinity for protein adsorption than hydrophobic substrates, and therefore, present a more adhesive surface for cell attachment (Horbett 1985). More recently, however, studies with mESCs and other cell types have found that cell behaviour can be influenced by particular functional groups (Webb 2000; Ma 2003; Neuss 2008), irrespective of their wettability characteristics. For example, in one study it was found that substrates presenting amine and hydroxyl functional groups improved cell adhesion, whereas carboxyl groups reduced cell adhesion despite similar increases in wettability (Ma 2003).

Harrison *et al.* (2004) demonstrated that increasing hydrophilicity of poly(alpha-hydroxy ester) substrates by NaOH and oxygen plasma gas treatments significantly increased mESC colonization rate (Harrison 2004). This was attributable to increased surface wettability via hydrolysis of surfaces by these treatments. Additionally, poly(lactic-co-glycolic acid) (PLGA) (Figure 1-6) was found to be the most successful substrate for supporting mESC growth, though this did not correlate with wettability characteristics. The support of short-term mESC growth by PLGA substrates was confirmed by Newman and McBurney (2004). Furthermore, PLGA has been found to be a suitable substrate for the culture of other cell types (Jinming 1998). In hESCs, oxygen plasma etching has also been shown to enhance the ability of tissue culture plastic to support undifferentiated hESC culture in MEF conditioned medium (Mahlstedt 2009).

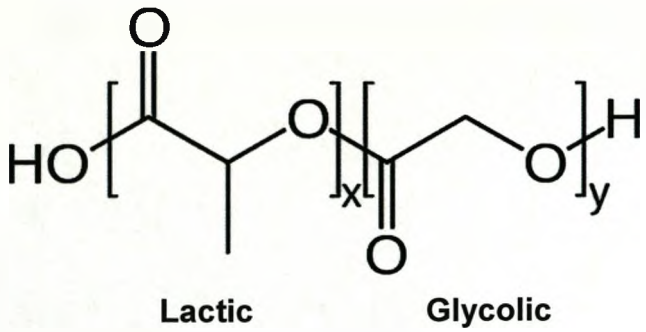

Figure 1-6 Chemical structure of poly(lactic-co-glycolic acid) (PLGA). During polymerization successive units of lactic acid (x) and glycolic acid (y) are joined by ester linkages, yielding a linear aliphatic polyester. Hydrolysis will split the ester linkage, creating two additional hydroxyl groups and increasing the wettability of the polymer.

Other studies have investigated the response of mESCs to known bio-compatible artificial substrates; however, little success in the maintenance of mESC self-renewal has been found with this non-systematic approach. For example, a study by Melville *et al.* (2006) investigated the potential of apatites to support mESC growth. Hydroxyapatite (Figure 1-7) is a commonly found material in the body, the major component in tooth enamel and bone mineral, and has been used extensively in biomedical implants. Melville *et al.* (2006) found that the proliferation of mESCs increased when the carbonate content of the apatite-based substrate increased; however, self-renewal was not maintained.

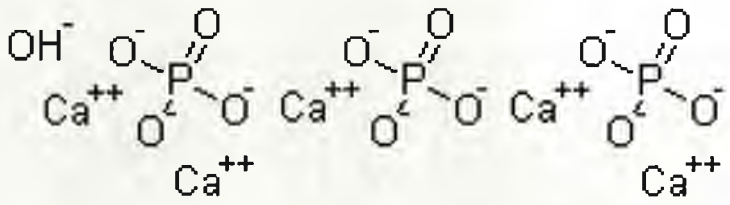

Figure 1-7 Chemical structure of hydroxyapatite. Hydroxyapatite can be found in teeth and bones and is often used in biomedical implants.

Other studies of artificial substrates have found that many promote the differentiation of mESCs despite the presence of LIF (Horak 2004; Melville 2006; Pompe 2007). However, due to the complex nature of the substrates used, the majority of these studies only provide relevant information for a specific material or culture technique. In most cases it is difficult to compare the materials used, which can vary vastly in structure and composition, and to ascertain which components are interacting with the cells. The quantification of components presented at the surface of these substrates, alongside other physiochemical properties, might be more practical for a comparative analysis between different substrates.

Several studies have now demonstrated the potential of specific functional groups to control the behaviour of mESCs and other cell types (Anderson 2004; Keselowsky 2004; Pompe 2007; Wells 2009). Wells *et al.* (2009) demonstrated that the degree of attachment of mESCs to substrates coated with carboxyl groups increased with increasing carboxyl concentration, however, self renewal was maintained only at low concentrations. Keselowsky *et al.* (2004) demonstrated surface chemistry modulated integrin binding, differentiation and focal adhesion signalling of MC3T3-E1 osteoblast-like cells on fibronectin-coated SAMs presenting methyl, hydroxyl, amine and carboxyl functional groups. The highest affinity for $\alpha_5\beta_1$ integrin binding was demonstrated on hydroxyl substrates, whereas $\alpha_v\beta_3$ integrin binding was highest on carboxyl and amine

substrates. As discussed earlier (1.1.3), integrin signalling can regulate self-renewal in mESCs.

In hESCs, recent studies have demonstrated the support of self renewal on diverse biomaterials. Melkoumian *et al.* (2010) found that RGD-containing peptides conjugated to acrylate surfaces were able to maintain hESCs in serum-free medium. Peptides derived from vitronectin and bone sialoprotein were able to support hESC self renewal, however, those derived from fibronectin and laminin were not, suggesting that the RGD sequence alone was insufficient for hESC self renewal. Villa-Diaz *et al.* (2010) demonstrated that a chemically defined substrate, poly[2-(methacryloyloxy)ethyl dimethyl-(3-sulfopropyl)ammonium hydroxide] (PMEDSAH), was able to support hESC self renewal in serum-free medium. Five other polymer coatings were unable to support hESC attachment or self-renewal, however, no explanations for the observed differences in hESC culture between polymer coatings were presented. These differences could be due to altered physicochemical properties or surface chemistry of the coatings. Contact angle was lowest on the hESC supporting substrate, but might not be informative as the chemical composition was different between polymers. Together, these studies suggest that both peptide-presenting and chemically defined substrates may be suitable for long-term growth of undifferentiated hESCs.

1.2. Mesenchymal stem cell chondrogenesis

Mesenchymal stem cells (MSCs) are multipotent adult progenitor cells, which retain the ability to differentiate into a variety of adult cell types, including osteoblasts, chondrocytes and adipocytes. They can be derived from numerous autologous sites, including bone marrow and fat tissue, and have great potential for regenerative therapy due to their proliferative and differentiation ability (Csaki 2008; Meirelles Lda 2009).

Undifferentiated MSCs can be identified by their ability to generate multiple mesenchymal lineages. They have a characteristic spindle-shaped morphology, which is lost on differentiation, and are commonly isolated from bone marrow by their adherence to plastic substrates (Friedenstein 1976). Few specific markers of MSCs have been identified to date; however, a panel of surface antigen markers have been shown to be commonly expressed by MSCs, including Stro-1, CD271 (nerve growth factor receptor), CD29 (β1 integrin subunit), and CD44 (Gronthos 1994; Buhring 2007; Kolf 2007).

1.2.1. Cartilage and osteoarthritis

Cartilage is a connective tissue comprised mainly of matrix with a small population of chondrocytes performing maintenance functions. Three classes of cartilage exist in the body: elastic cartilage, fibrocartilage and

hyaline cartilage. Hyaline cartilage is the most common and most susceptible to disease and damage (Newman 1998). Specifically, the hyaline cartilage of the limb and trunk skeleton is under the most stress. These areas of cartilage originate from the condensation and differentiation of mesenchymal cells during embryogenesis.

Cartilage damage can be a debilitating condition. Cartilage has a limited capacity for autonomous repair; the tissue is aneural and avascular, and chondrocytes are bound in lucanae, restricting migration. Osteoarthritis affects millions of people worldwide and occurs where articular cartilage, a subset of hyaline cartilage, is worn away resulting in painful joints and often erosion of the bones. Current technologies typically focus on treating the end-stage symptoms, with replacement of joints with synthetic substitutes. However, treatments involving stimulation of endogenous ECM production and the generation of replacement tissues are being developed that demonstrate great promise for treatment of cartilage damage (Newman 1998; Csaki 2008).

Cartilage was initially thought to be a relatively simple tissue, consisting mainly of ECM with few cells; however, it is now clear that cartilage consists of several zones with differing properties (Buckwalter 1998). Therefore, generating this tissue will require complex culture techniques and multiple signalling events. Mesenchymal stem cells represent a potential model for cartilage repair. *In vivo*, MSCs are known to migrate to damaged tissues and initiate repair, predominantly via paracrine

signalling (Chapel 2003; Ortiz 2003); for example, in acute myocardial infarction (Kollar 2009). However the mechanisms of this migration are not well known (Brooke 2008). Additionally, it is well reported that MSCs have the potential to differentiate to chondrocytes *in vitro* (Zanetti 1984; Sekiya 2002; Chang 2009). Therefore, this raises the possibility that MSCs could be used in future regenerative therapies, such as the replacement of damaged articular cartilage in osteo-arthritis patients.

1.2.2. *In vitro* differentiation of MSCs

Typically, *in vitro* control over differentiation of MSCs is enacted via soluble cytokine stimulation; in monolayer culture for osteogenesis and adipogenesis, and in micro-mass culture for chondrogenesis. For adipogenesis, differentiation can be induced in confluent monolayer culture. The main factors required for adipogenesis are insulin, which promotes peroxisome-proliferator-activated receptor gamma (PPARγ) expression through cross-activation of the insulin growth factor (IGF) receptor with IGF, and indomethacin, isobutylmethylxanthine and dexamethasone, which promote expression of CCAAT-enhancer-binding protein alpha (C/EBPα) and PPARγ, the key transcription factors for adipogenesis (Pittenger 1999). Typical markers of adipogenesis include PPARγ2, fatty acid binding protein (FABP) and lipoprotein lipase. The cells become rounded and characteristic lipid vacuoles can be observed developing within (Pittenger 1999).

For osteogenesis, differentiation can again be induced in confluent monolayer culture. The main factor required for *in vitro* osteogenesis is dexamethasone, which promotes RUNX2 expression, the main transcription factor required for osteoblast differentiation, as well as alkaline phosphatase (AP) and osteocalcin expression (Marie 2006). In addition, ascorbic acid and glycerophosphate enhance collagen metabolism and mineralised matrix production, respectively (Pittenger 1999). Typical early markers of osteoblastic differentiation include AP, type I collagen and RUNX2. Later markers of osteogenesis characterizing matrix mineralization include osteocalcin, osteopontin and bone sialoprotein (Liu 2003; Marom 2005). AP is an early marker of osteoblast differentiation involved in regulating mineralization. It is a cell-surface glycoprotein and can usually be detected within a week under osteogenic conditions (Marom 2005). It is also known to be down-regulated as the osteoid becomes heavily mineralized (Liu 2003). Osteocalcin is a matrix protein that regulates osteoclast activity and is expressed late in osteogenesis, characterizing the post-proliferative stage, and can take several weeks to appear (Malaval 1999; Liu 2003). Furthermore, following differentiation, osteoblast cell morphology becomes more spread and cuboidal shaped, increasing the surface area in contact with the substrate (Hoemann 2009). Following a couple of weeks in culture, osteogenesis can be observed by nodule formations of mineralized ECM, normally a calcium-phosphate substituted hydroxyapatite similar to that seen in bone and teeth (Landis 1996).

For chondrogenesis, MSCs require micro-mass culture, which typically involves pelleting the cells and culturing them in suspension (Mackay 1998; Yoo 1998). Chondrogenesis is then induced in high-glucose serum-free medium supplemented with TGF-β3 (Mackay 1998; Pittenger 1999). Whilst TGF-β1 and TGF-β2 can also be used to induce chondrogenesis, TGF-β3 supports it best (Mackay 1998; Barry 2001). TGF-β1/2/3 signalling is critical for chondrogenesis and directly promotes up-regulation of chondrogenesis factors, particularly SOX9, a key transcription factor that directs chondrogenesis *in vivo*, via TGF-β type 1 receptor activation of Smad2/3 (Furumatsu 2005). In addition, the high glucose conditions promote survival in pellet culture (Mackay 1998). Apart from SOX9, typical early markers of chondrocyte differentiation also include N-cadherin and neural cell adhesion molecule (N-CAM), which are up-regulated very early in culture and are involved in condensation in the micro-mass and initiating chondrogenesis. Later markers of mature matrix-generating chondrocytes include Collagen II, Aggrecan and Collagen XI, which are commonly detected after two or three weeks in culture (Pittenger 1999). Collagen II is the main collagenous element, making up about 90% of the collagenous fraction (Plainfosse 2007), and is the major fibril component contributing to cartilage properties (Mendler 1989). Aggrecan is the most abundant proteoglycan in cartilage, accounting for about 90% of the proteoglycan content, and forms macromolecular complexes with hyaluronic acid and link protein in the ECM (Quintana 2009). Furthermore, chondrocytes display characteristic spherical cell morphology (Shum 2002).

1.2.3. *In vivo* chondrogenesis in the limb bud

In vivo, chondrogenesis is most prominent in generating the cartilage intermediate that leads to endochondral ossification during skeletal development. A well studied model of *in vivo* chondrogenesis is limb bud formation, and this process is largely mimicked by current techniques for *in vitro* chondrogenesis. During *in vivo* limb bud formation, mesenchymal cells (MCs) migrate into the limb-bud then condense to form a tightly packed aggregate which differentiates to chondrocytes and then begins to develop osteoblasts around the periphery (Figure 1-9).

1.2.3.1. MC condensation the limb bud

In limb bud chondrogenesis, undifferentiated MCs migrate into the limb bud at the earliest stage of formation, before condensing into a tightly packed mass and undergoing chondrogenesis (Figure 1-8). The precartilagenous condensation process itself is thought to be regulated by cell-cell and cell-matrix interactions, mediated through the ECM. Fibronectin has been shown to be critical in migration and aggregation of the limb-bud MCs, and its absence severely inhibits condensation (Downie 1995; Gehris 1997; White 2003). In addition, several proteoglycans, which bind many ECM proteins and factors, have been shown to be necessary for chondrogenesis, such as versican and perlecan, although the mechanism by which they regulate condensation and chondrogenesis are unknown (Arikawa-Hirasawa 1999; Kamiya

2006). Versican in particular can bind fibronectin, enhances MC condensation and is necessary for chondrogenic gene expression (Kamiya 2006).

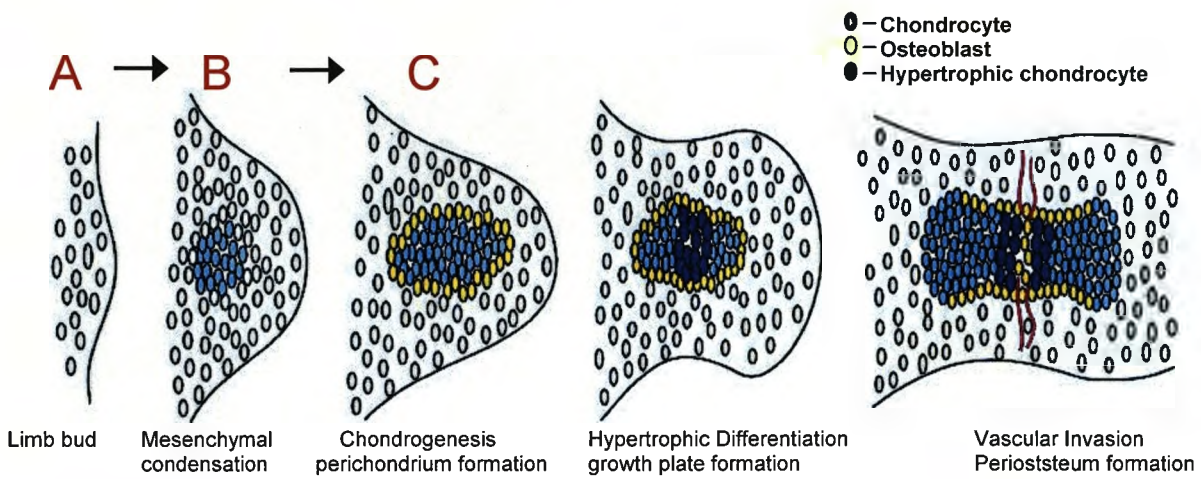

Figure 1-8 *In vivo* limb-bud formation. MCs initially migrate into the limb bud (A), up-regulating early chondrogenesis markers (SOX9) and cell adhesion molecules (N-cadherin). The MCs then condense to form a tightly packed aggregate (B) and begin to differentiate to chondrocytes, expressing collagen II & aggrecan. Osteoblasts then develop around the periphery of the chondrocyte aggregate (C), expressing osteocalcin & alkaline phosphatase. Adapted from Ornitz & Marie (2002).

Cell-cell interactions have also been shown to play distinct roles in limb bud condensation. The cell adhesion molecules N-cadherin and N-CAM are both important in aggregating and compacting MCs during condensation. Up-regulation of these cell-cell adhesion molecules compact the MCs into tightly packed aggregates by enhancing the cells' affinity for each other (Widelitz 1993; Oberlender 1994; DeLise 2002). However, expression of these adhesion molecules is decreased as cells become chondrogenic (Tavella 1994), and other cadherins have been demonstrated to permit chondrogenesis in the absence of N-cadherin (Luo 2005). The molecular mechanisms of this process are yet to be

elucidated; however, TGF-β is one of the earliest genes to be expressed during chondrogenesis and is known to up-regulate the expression of N-cadherin, N-CAM, fibronectin and SOX9 (Chimal-Monroy 1999).

Aggregation and condensation of cells is critical for both limb bud and *in vitro* chondrogenesis. Chondrocytes have been found to de-differentiate when cultured as a monolayer (Benya 1982). Studies have shown the importance of cell-cell interactions in this process, but also cell shape (Estes 2004; Luo 2008; Gao 2010). In both micromass culture and limb bud condensation, cells are tightly packed within the aggregates, and thereby restricted from spreading, conforming to a rounded cell morphology (Shum 2002). Restricting the spreading of human mesenchymal stem cells (hMSCs), and enforcing a rounded morphology, has been shown to promote chondrogenesis in hMSCs, possibly by blocking RHOA/ROCK signalling and inducing RAC1 signalling via rearrangement of the cytoskeleton (Woods 2005; Woods 2007; Kumar 2009; Gao 2010). Furthermore, promoting contractility in hMSCs, via control of cell shape, has been shown to promote osteogenesis when increased or adipogenesis when decreased; however, differentiation promoting media supplements were required for differentiation (Kilian 2010).

1.2.3.2. MC chondrogenesis in the limb bud

Following condensation in the limb bud, the MCs proceed to undergo chondrogenesis. The molecular mechanisms of chondrogenesis following condensation are not fully understood. However, the transcription factor SOX9 is a master regulator of chondrogenesis, playing a critical role in both chondrogenesis and condensation (Akiyama 2002), and all osteo-chondroprogenitors have been shown to derive from SOX9 expressing cells (Akiyama 2005). Inactivation of SOX9 results in a complete lack of cartilage and bone development, and knockout mice die at 11.5 days post-coitum from heart failure (Akiyama 2002; Akiyama 2004). SOX9 is expressed sequentially throughout chondrogenesis; it is first expressed early in limb bud formation, at around 10.5 days post-coitus, and has roles in condensation, proliferation and chondrogenesis. It is known to directly induce the expression of Collagen type II (Bell 1997), in addition to promoting other chondrogenesis related genes, such as aggrecan and N-cadherin.

LSOX5 and SOX6 are not present in early mesenchymal condensations, but are co-expressed with SOX9 during chondrocyte differentiation (Lefebvre 1997). These additional SOX transcription factors are up-regulated by SOX9 following mesenchymal condensation and then cooperate with SOX9 to promote expression of major chondrogenic genes, including Collagen II, aggrecan and link protein (Smits 2001). Following the genesis of cartilage ECM, some chondrocytes enter

hypertrophy, regulated by Indian Hedgehog (IHH)/parathyroid hormone-related protein signalling (PTHrP) (Shimizu 2007), which is antagonized by SOX9 (Huang 2000).

The expression of SOX9 is regulated by multiple pathways, including TGF- β signalling (Goldring 2006; Kawakami 2006), bone morphogenetic proteins (BMPs) (DeLise 2000) and canonical WNT signalling, through β-CATENIN antagonism of SOX9 (Akiyama 2004). TGF-β has a strong chondrogenic effect; up-regulation of SOX9 can be detected after only 30 min following MSC exposure to TGF-β (Chimal-Monroy 2003; Kawakami 2006). Furthermore, TGF-β signalling ultimately initiates expression of multiple other chondrogenic factors, including aggrecan, N-cadherin, N-CAM, Collagen II, Collagen XI and fibronectin (Derfoul 2006).

In addition to TGF-βs, several members of the TGFβ superfamily have been identified that direct and modulate chondrogenic events. Four BMPs are expressed in the developing limb bud; BMP2, BMP4, BMP5 and BMP7, all of which show chondrogenic ability (Zuzarte-Luis 2004). Furthermore, considerable cross-talk has been demonstrated between the TGF-β and BMP signalling pathways (Mehlhorn 2007). The knockout of the BMP receptors BMPR1A and BMPR1B, normally expressed in cartilage condensations, results in severe chondrodysplasia with loss of SOX9 expression, suggesting the BMP signalling is required for chondrocyte proliferation, survival and differentiation (Yoon 2005). BMP signalling can promote chondrogenesis through at least two pathways,

via SMADs and p38 MAP kinase (Yoon 2004; Li 2009). Canonical Smad pathways promote chondrogenesis through mechanisms mediated by SMAD1 or SMAD5 in combination with SMAD4 (Hatakeyama 2003), whereas, the p38 MAP kinase pathway is activated by TGF-β activated kinase 1 (TAK1), and has been shown to be required for expression of Collagen II (Nakamura 1999).

1.2.3.3. Chondrocyte hypertrophy and endochondral ossification

Once the limb bud has formed chondrocytes begin to undergo hypertrophy, expanding to several times their starting size, and commence depositing matrix in preparation for endochondral ossification, mainly collagen X (Shimizu 2007). Hypertrophic chondrocytes undergo terminal differentiation and stop proliferating with the inactivation of SOX9 and expression of RUNX2 transcription factors (Quintana 2009). RUNX2, assisted by RUNX3, promotes the expression of hypertrophic chondrocyte markers, such as collagen X, and instigates Ihh expression (Mackie 2008). Ihh creates a negative feedback gradient with PTHrP, secreted by the perichondrium, delaying hypertophy, but also stimulates osteogenesis in the mesenchymal cells surrounding cartilage, prior to vascular invasion and ossification (Mackie 2008). Vascular invasion of cartilage is stimulated by vascular endothelial growth factor expression in hypertrophic chondrocytes, under the control of RUNX2 (Mackie 2008). The cartilage ECM is partially degraded by matrix metalloproteinase-13 and the hypertrophic chondrocytes undergo apoptosis, creating space for

the invading blood vessels (Mackie 2008). Osteoblast progenitors enter the tissue via blood vessels and the tissue is then converted to bone (Quintana 2009).

1.2.3.4. Limb bud development and patterning

Following early chondrogenesis events in the limb bud further development and patterning of the limb occurs relative to three axes; the proximo-distal, anterior-posterior and dorso-ventral axis (DeLise 2000). Three interdependent signalling centres are present in the embryonic limb: the apical ectodermal ridge (AER), the zone of polarizing activity (ZPA), and the non-AER ectoderm. The AER directs the proximo-distal outgrowth and is formed at the distal tip of the limb bud by a thickening of the overlying ectoderm, initiated and maintained by FGF10 signalling from the mesenchyme (Fernandez-Teran 2008). A progressive zone (PZ) is formed under the AER in which cells remain proliferative and undifferentiated, mediated by FGF4, FGF8, FGF9 and FGFf17 produced by the AER (Fernandez-Teran 2008). As cells leave the PZ they condense and differentiate to chondrocytes (DeLise 2000). The ZPA is located at the posterior of the limb bud and directs the anterior-posterior axis (DeLise 2000). Sonic hedgehog is produced by the ZPA and is the key determinant of the anterior-posterior axis as well as being involved in an essential positive feedback loop with FGFs expressed in the AER (Duboc 2009). The non-AER ectoderm directs the dorso-ventral axis through WNT7a production (Fernandez-Teran 2008). WNT7a is also

involved in sonic hedgehog expression, in the ZPA, and the positive feedback loop between FGF8 from the AER and FGF10 from the mesenchyme (Duboc 2009).

1.2.4. Ability of ECM substrates to regulate chondrogenesis

MSCs have demonstrated great potential as a source for cartilage regeneration, due to their inherent ability to differentiate into chondrocytes (Mackay 1998; Bosnakovski 2004). However, current techniques for chondrogenesis induction are complex and require expensive growth factors, such as TGF-βs, as described above. The extra-cellular environment is well known to regulate chondrogenesis and, therefore, current studies are employing defined substrates to encourage MSC chondrogenesis under simpler and more controllable conditions.

Fibronectin has long been known to be an essential component of the ECM during chondrogenesis (Gehris 1997; Tavella 1997; White 2003). It has been implicated in promoting condensation and the early stages of chondrogenesis (Tavella 1997), following which, *in vivo*, matrix metalloproteinases (MMPs) are involved in breaking it down to be replaced by a more mature ECM (Tavella 1997). Studies have shown positive regulation of *in vitro* chondrogenesis by fibronectin substrates, where it is thought to promote chondrogenesis, in part by enabling migration and aggregation of MSCs (White 2003). Several studies have demonstrated MSC differentiation in response to substrate chemistry, and

this is often attributed to differential fibronectin binding (Lan 2005; Phillips 2009).

1.2.5. Ability of chemically defined substrates to regulate MSC chondrogenesis

Studies of chemically defined substrates have typically analysed the effect of single functional groups on the induction of chondrogenesis in MSCs. Phillips *et al.* (Phillips 2009) used fibronectin-coated SAMs presenting methyl, hydroxyl, carboxyl and amine groups to assess their roles in lineage commitment of hMSCs. However, under chondrogenic media conditions with TGF-β3, they demonstrated no consistent up-regulation of chondrogenic factors in monolayer culture on any of the SAMs. Interestingly, they found hMSC aggregate formation and chondrogenesis on methyl-presenting substrates in the absence of fibronectin, and attributed this to reduced cell adhesion to the substrate. Furthermore, under osteogenic conditions, mineralized nodules were formed on amine substrates, with up-regulation of osteocalcin and other osteoblast markers.

Guo *et al.* (2008) examined the effect of polyallylamine (amine), poly(acrylic acid) (carboxyl) and neutral poly(ethylene glycol) (Figure 1-9), covalently bound to a substrate by photochemical modification, on chondrogenesis in hMSCs under chondrogenic conditions, namely in the presence of TGF-β3 (Guo 2008). They found that hMSCs proliferated to

confluence on most substrates initially, but then gradually aggregated and detached from the substrate to form aggregated clumps after a few days of culture. The rate of aggregation and detachment was found to be substrate-dependent, with the highest rate on the amine substrate. Chondrogenic markers were also up-regulated on the amine substrate.

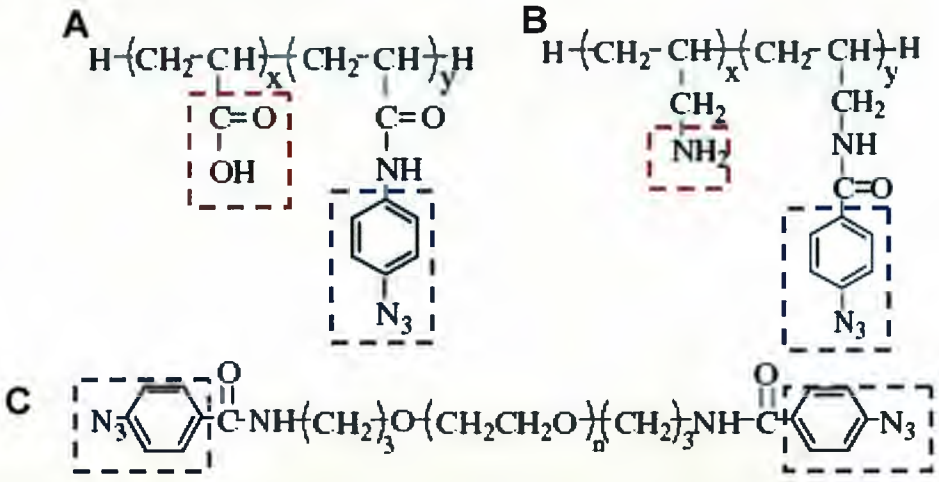

Figure 1-9 Schematics of photo-reactive azidophenyl-derivatives of different polymers. Adizophenyl-derivatised acrylic acid (A), polyallylamine (B) and poly(ethylene glycol) (C). The adizophenyl group (blue) will covalently bind to an organic substrate under UV irradiation. Specific functionality is highlighted (red); poly-ethylene has no discrete functional groups. Adapted from Guo *et al.* (2008).

Curran *et al.* (2006) investigated the effect of silane-modified surfaces, presenting methyl, amine, silane, hydroxyl and carboxyl groups, on MSC differentiation under basal, chondrogenic and osteogenic conditions (Curran 2006). They concluded that chondrogenesis was promoted on amine, hydroxyl and carboxyl substrates under chondrogenic conditions, i.e., in the presence of TGF-β1, and osteogenesis on amine and silane substrates under osteogenic conditions, i.e., in the presence of dexamethasone and ascorbic acid. However, the amine surface was deemed unsuitable for chondrogenesis due to reduced levels of cell

adhesion, which caused the hMSCs to aggregate and detach from the substrate, making further analysis problematic.

In other cell types, substrate chemistry has been widely implicated in modulating differentiation. Lan *et al.* (2005) demonstrated differential differentiation of murine myoblasts on fibronectin-coated SAMs presenting methyl, hydroxyl, amine and carboxyl functional groups. Significant increases in myogenic differentiation were demonstrated on the methyl and hydroxyl surfaces, and this was attributed to surface chemistry-dependent differences in integrin binding to the adsorbed fibronectin. Binding of $\alpha_5\beta_1$ integrin was supported on all substrates; however the carboxyl and amine substrates also supported binding of $\alpha_V\beta_3$ integrin (Keselowsky 2004; Lan 2005).

1.2.6. The use of peptide ligands to promote MSC chondrogenesis

Owing to the 3-D nature of chondrogenesis, both *in vivo* and *in vitro*, chondrocyte differentiation has been extensively studied in 3-D culture. Scaffolds and hydrogels have demonstrated an appropriate environment for chondrogenesis (Williams 2003; Alhadlaq 2004; Park 2009). However, they are typically constructed from inert polymers and require treatment to promote cell adhesion and chondrogenesis. These treatments can involve chemical modification with functional groups (Nuttelman 2005), incorporation of proteins into the matrix (Mi 2006; Chang 2009) and tethering of peptide ligands to the polymers (Mochizuki 2007). Peptide

ligands are typically modelled on specific active sites of proteins that are known to promote cell attachment and growth and considerable progress has been made in identifying appropriate peptide sequences (Santiago 2006; Alvarez-Barreto 2007; Derda 2007; Liu 2010). However, to-date, studies using 2-D peptide-presenting substrates have primarily investigated their ability to promote attachment cell attachment (Santiago 2006; Derda 2007; Fischer 2007; Sato 2007).

The RGD integrin binding motif is unique in that it universally acts as a ligand to multiple integrin dimers (Figure 1-2). For this reason it has been exploited as an attachment "facilitator" to improve cell attachment to inert substrates, particularly hydrogels and scaffolds (Kim 2002; Fischer 2007). The early application of RGD-modified polymers for cell culture has been well reviewed by Hersel *et al.* (2003). More recently, with MSCs, RGD peptide sequences have been shown to promote chondrogenesis, in addition to attachment (Alvarez-Barreto 2007; Salinas 2008; Tigli 2008; Chang 2009; Shao Qiong 2009; Liu 2010; Re'em 2010). This is thought to be regulated by $\alpha_5\beta_1$ signalling (Pulai 2002; Shakibaei 2008) but also $\alpha_v\beta_5$ signalling (Goessler 2008), normally associated with fibronectin and vitronectin RGD interactions, respectively (Martino 2009).

Recent studies by Re'em *et al.* (2010) and Shao *et al.* (2009) have demonstrated that scaffolds and hydrogels incorporating RGD-containing peptides were able to enhance TGF-β induced chondrogenesis of hMSCs (Shao Qiong 2009; Re'em 2010). Re'em *et al.* (2010) employed macro-

porous alginate scaffolds containing immobilised RGD peptides (Figure 1-10) and demonstrated significantly enhanced expression of chondrogenesis markers, including Collagen II and SOX9, in medium supplemented with serum and TGF-β1. They also confirmed enhanced levels of SMAD2 and ERK1/2 phosphorylation in response to TGF-β1 and, surprisingly, found inhibition of aggregation within the RGD-containing scaffolds, demonstrating that aggregation may not be a prerequisite for the initial stages of chondrogenesis. They concluded that chondrogenesis was enhanced via promoting cell adherence to the matrix and increased accessibility to the chondrogenic-inducing molecule TGF-β1.

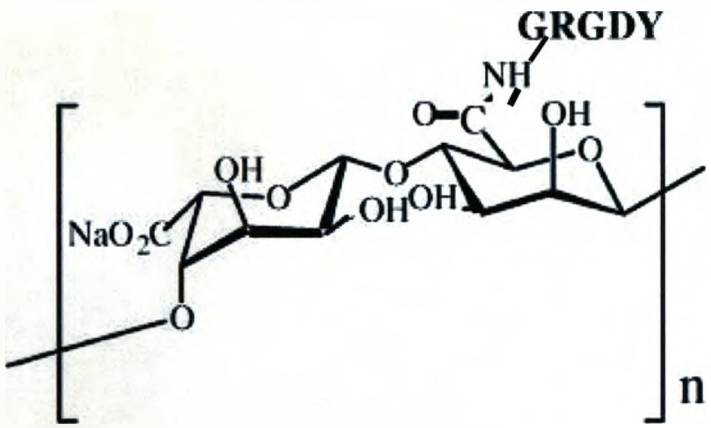

Figure 1-10 Chemical structure of RGD-alginate scaffold. The RGD-containing pentapeptide is immobilised via interaction of the carboxyl group of the alginate and the N-terminal amine of the GRGDY peptide. Adapted from Re'em *et al.* (2010).

Shao Qiong *et al.* (2009) employed RGD-incorporated poly(ethylene glycol) (PEG) hydrogels (Figure 1-11) to examine chondrogenesis under TGF-β3 conditions. Here, significant induction of chondrogenesis was observed using hMSCs encapsulated in the PEG hydrogel, in an RGD

concentration dependent manner. Interestingly, hMSCs were found to spread when seeded onto the surface of hydrogels, but were forced to adopt a rounded morphology when encapsulated. Another study by Salinas *et al.* (Salinas 2008), using RGD modified hydrogels, also found promotion of chondrogenesis with TGF-β1, in addition to enhanced hMSC viability, thereby supporting the conclusions of these studies. Taken together, these studies demonstrate induction of hMSC chondrogenesis by RGD and TGF-β interactions.

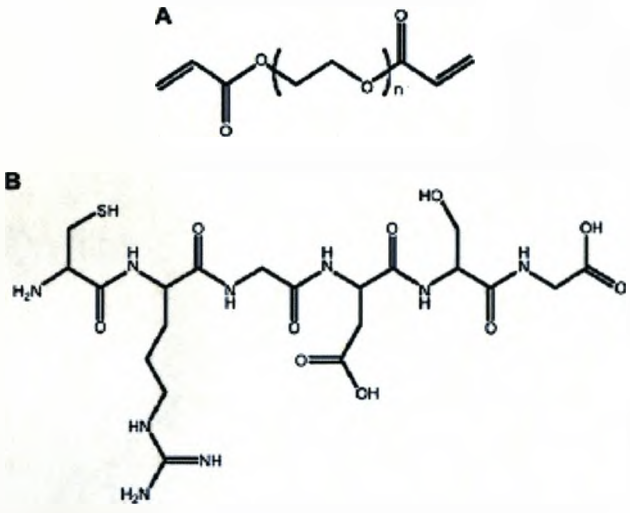

Figure 1-11 Chemical structure of PEG (A) and peptide sequence CRGDSG (B). CRGDSG peptide sequences were incorporated into PEG hydrogels. Adapted from Shao Qiong *et al.* (2008).

Furthermore, a recent study by Chang *et al.* (2009), using rat adipose-derived adult stem cells (ADAS), demonstrated induction of chondrogenesis in 3-D culture with an RGD-chimeric protein embedded in alginate beads (Chang 2009). They determined that RGD acted via $\alpha_5\beta_1$ signalling, which was found to up-regulate SOX9 expression. They also suggested chondrogenesis might be promoted via inhibition of RhoA

activity. This was in light of findings by Woods *et al.* (2005), where the RhoA/ROCK pathway was found to suppress SOX9 expression via repression of its promoter and control of actin organization (Woods 2005).

Current chondrogenic techniques require the presence of expensive growth factors, such as TGF-βs, and a complex 3-D environment to induce chondrogenesis in MSCs. Whilst surface chemistry and peptide ligands can promote chondrogenesis, they still require the presence of growth factors. A more effective technique may be to encourage aggregation and compaction of MSCs, then to allow MSCs to generate their own chondrogenic environment, similar to *in vivo* events. Altering substrate chemistry to mimic integrin binding motifs may activate cell-substrate signalling pathways, such as via RGD/$\beta_1\alpha_5$ integrin interactions, known to be critical in initiation of condensation and chondrogenesis in the limb bud (White 2003; Chang 2009).

1.3. Aims

The effect of substrate chemistry on stem cell behaviour is only just beginning to be understood. In this study poly-acrylate substrates presenting alternate proportions of amine, carboxyl and hydroxyl functional groups were evaluated for their ability to support the maintenance and expansion of stem cell populations, but also their capacity to direct stem cell differentiation.

The main aims of this thesis were:

1. To develop a defined substrate for the culture of mESCs.

2. To develop defined substrates for inducing chondrogenesis in mMSCs and hMSCs.

2. Materials and Methods

2.1. Materials

2.1.1. Polymer substrates

Accelerate™ polymeric coatings were developed with Biomer Technology Ltd. (Runcorn, UK) and manufactured using their proprietary techniques on site in Runcorn. These were all polyacrylates and presented a combination of amine, carboxylic acid and hydroxyl groups at controllable density and proportion. These were statistical polymers, however the BTL proprietary technique promotes equal binding affinity among the base components, therefore the polymers should display an even distribution of base components throughout their polymer chains. For their quality control BTL carried out gel permeation chromatography to confirm consistent polymerisation and chain lengths. Polymer designations: BTL01008, BTL01009, BTL01015, BTL01016, ESP01001, ESP01002, ESP01003, ESP01004, ESP01006, ESP01007.

Plasma polymerised amine substrates were provided by Dr Vasilev (Mawson Institute, University of South Australia). These were split into high and low amine content and had been previously characterised by XPS analysis (Losic 2008).

2.1.2. Organic Solvents

Dimethylformamide (DMF) was purchased from Sigma (Missouri, USA) and used as the primary solvent for BTL polymers.

2.1.3. Water

Purified water was obtained by reverse osmosis using Direct-Q System (Millipore Corp., Massachusetts, USA). This water was further purified by passing through a 0.22 µm filter, and checked for a resistivity higher than 18.2 MΩ cm. Nuclease-free water (Sigma) was used for all molecular biology procedures.

2.1.4. Solutions

Phosphate buffered saline (PBS): 8 g sodium chloride, 1.44 g di-sodium hydrogen orthophosphate, 0.24 g potassium di-hydrogen orthophosphate, 0.2 g potassium chloride in 1 L sterile distilled water, pH adjusted 7.4 with hydrochloric acid. Buffer was autoclaved for 20 min on liquid cycle and stored at room temperature. Sterile PBS (Invitrogen, California, USA) was used for cell culture.

4% (w/v) Paraformaldehyde (PFA): 4 g PFA (Sigma) in 100 ml PBS. Solution was warmed to 60°C on a hotplate until all PFA dissolved. PFA was stored in the dark at 4°C for a maximum of 10 days.

0.1M TrisHCl (pH9.2): 6 g Trizma base (Sigma) in 480 ml dH_2O, pH adjusted with 1N HCl (Sigma). Made up to 500 ml with dH_2O.

Tris-acetate-EDTA (TAE) Buffer: 242 g Trizma base (Sigma), 57.1 ml glacial acetic acid (Sigma), 100 ml 0.5 M EDTA pH8 (Sigma). Made up to 1 L with dH_2O.

2.1.5. General Reagents

Unless otherwise stated all other reagents were laboratory grade and supplied by Sigma. Molecular biology reagents were molecular biology grade and supplied by Sigma.

2.1.6. Cell Lines

2.1.6.1. E14 mESC

The E14 mESC line was derived from blastocysts of the inbred mouse strain 129/Ola in 1985 by Dr Martin Hooper of Edinburgh University (Hooper 1987). The cells were isolated and expanded on STO feeder cell layers. The University of Liverpool Stem Cell Consortium obtained the E14.1a subclone of this line from the laboratory of Mark Boyd at the University of Liverpool. Passages 20-30 were used in experiments.

2.1.6.2. D1 mMSC

The D1 mouse mesenchymal stem cell line was obtained from the American type culture collection (ATCC®) (Virginia, USA) and cultured under supplier's guidelines. Cells from passages 8-15 were used in experiments.

2.1.6.3. H6 kidney-derived stem cells

The H6 cell line was originally derived by Cristina Fuente Mora from a population of kidney-derived stem cells (KSCs) isolated from 2-6 day old CD1 mice (Fuente-Mora 2009) . Cells from passages 10-15 were used in experiments.

2.1.6.4. Limb bud cells

Female CD1 mice (6-8 weeks old) were purchased from Charles River UK (Charles River, Margate, UK) and were housed at constant temperature, with a 12 hours light – 12 hours dark cycle, and free access to food and water. The animal sacrifice was carried out by asphyxiation with CO_2, which was followed by cervical dislocation. Murine limb bud (LB) cells were removed from E11.5 mouse embryos, previously dissected from pregnant mice by E. Ranghini (University of Liverpool Stem Cell Group), under aseptic conditions on a Leica MZFLIII dissecting microscope. Between 10 and 15 buds were placed into 3 ml 1x Trypsin-EDTA solution (Sigma) and incubated at room temperature for 15 min. The solution was then triturated to dissociate into a single cell suspension, washed with 9 ml Dulbecco's Modified Eagle Medium (DMEM) and passed through a 50 µm microsieve to remove large clumps of cells or ECM. Cells were pelleted at 900x g for 3 min, and then resuspended in 1 ml 10% (v/v) FCS and their concentration determined using a haemocytometer (Hausser Scientific Company, PA, USA). LB cells (p0) were then used immediately in experiments.

2.1.6.5. hMSC

Primary hMSCs were purchased from Lonza Walkersville Inc. (Walkersville, USA) and cultured in accordance with the supplier's guidelines. Cells from passages 5-8 were used in experiments.

2.1.7. Media

2.1.7.1. mESC medium

ESC medium was serum-free and contained Advanced DMEM® (Invitrogen) supplemented with 2 mM L-glutamine (Sigma), 1 mM 2-mercaptoethanol (Sigma), 250 U/ml leukaemia inhibitory factor (LIF) (Millipore).

2.1.7.2. mMSC medium

Contained 25 ml foetal calf serum (FCS) (PAA) in 225 ml high glucose DMEM (Invitrogen) supplemented with 2 mM L-glutamine (Invitrogen). medium was filter sterilised before use.

2.1.7.3. mMSC differentiation medium

Chondrogenic medium: high-glucose DMEM (Invitrogen) supplemented with 10 ng/ml TGF-beta3 (R&D), 500 ng/ml BMP-6 (Sigma), 0.1 µM dexamethasone (Sigma), 50 µg/ml ascorbate-2-phosphate (Sigma), 40 µg/ml proline (Invitrogen), 100 µg/ml pyruvate (Invitrogen), 50 mg/ml ITS + 3 liquid supplements (Invitrogen).

Osteogenic media: 10% FCS supplemented with 12 mM L-glutamine (Invitrogen), 20 mM beta-glycerol phosphate (Invitrogen), 50 ng/ml thyroxine (Invitrogen), 1 nM dexamethasone (Sigma), 0.5 µM ascorbic acid (Sigma).

2.1.7.4. hMSC media

MSCGM™ BulletKit® (PT-3001) was obtained from Lonza Walkersville Inc. (Walkersville, USA), stored at 4°C and used according to manufacturer's guidelines.

2.1.7.5. hMSC differentiation media

Bulletkits® were bought from Lonza Walkersville Inc. for induction of hMSC osteogenesis (PT-3004) and chondrogenesis (PT-3003), and used according to the manufacturer's guidelines. Chondrogenic medium supplement TGF-β3 (R&D Systems, Minneapolis, USA) was stored in 5 µl aliquots at -20°C and added fresh, at 10 ng/ml, to medium when required.

2.2. Methods

2.2.1. Cell Culture

2.2.1.1. Preparation of 0.1% (w/v) gelatin solution

0.1% (w/v) porcine gelatin solution was used to coat dishes and cover slips for cell culture. To prepare, 1 g porcine gelatin (Sigma) was added to 1 L distilled water, and then autoclaved to sterilise.

2.2.1.2. Routine mESC culture

E14 mESCs were routinely maintained in 60 mm tissue culture dishes (Nunc, New York, USA) coated with 0.1% (w/v) porcine gelatin and 10% (v/v) FCS. Three ml 0.1% (w/v) gelatin was added to each culture dish and incubated at room temperature for 15 min then replaced with 10%

FCS for a further 15 min. The 10% FCS solution was aspirated and then washed once with PBS before seeding cells in dish.

For routine maintenance, mESCs were cultured in serum-free mESC medium (2.1.7.1) and sub-cultured 1:4 every 3 to 4 days using the following procedure: the culture medium was removed and cells washed once with PBS. PBS was replaced with 1x trypsin-EDTA solution (Sigma) and incubated at 37°C for 3-5 min. Trypsinized cells were then transferred to a 15 ml falcon tube containing 9 ml DMEM (Invitrogen) and centrifuged at 900 x g for 3 min in a desk top centrifuge to pellet the cells. The supernatant was aspirated and the cell pellet resuspended in ESC medium. The cell suspension was then transferred into gelatin and 10% (v/v) FCS coated dishes and maintained at 37°C in a humidified 10% (v/v) CO_2 environment. Medium was changed on these cells every 3 days.

2.2.1.3. Routine mMSC and KSC culture

D1 mMSCs were routinely maintained in uncoated 60 mm culture dishes (Nunc) with mMSC medium (2.1.7.2) and sub-cultured 1:4 every 4-5 days as described in 2.2.1.2. They were incubated under conditions described in 2.2.1.2 and medium was changed every 3 days.

2.2.1.4. Routine hMSC culture

hMSCs were routinely maintained in MSCGM™ (Lonza) medium and subcultured 1:3 every 5-7 days as described in 2.2.1.3.

2.2.1.5. Preparation of frozen cell stocks

Recovery™ cell culture freezing medium (Invitrogen) was used for freezing all types of cell. Cells in mid-log growth were trypsinised and

washed as for subculture, then resuspended in the freezing medium at approximately 4 $x10^5$ cells/ml and 0.5 ml aliquots were transferred to sterile freezing vials. The cells were frozen overnight in isopropanol (Sigma) at -80°C, at the rate of 1°C every minute. Vials were then transferred for long term storage in liquid nitrogen.

2.2.1.6. Recovering frozen cells

Frozen vials were removed from liquid nitrogen and immediately thawed in a 37°C water bath. When almost all the ice had melted, the cell solution was added to 9.5 ml DMEM (Invitrogen), to wash, and then centrifuged at 900 x g for 3 min to form a pellet. Cells were subsequently resuspended and cultured in the appropriate medium.

2.2.1.7. Differentiation of mouse MSCs

The protocol was adapted from Peister et al. (2004). For osteogenesis and adipogenesis; mMSCs were seeded onto uncoated plastic culture dishes at 1 $x10^4$ cells/cm^2 in medium supplemented with 10% (v/v) FCS and allowed to attach overnight. The following day medium was replaced with the appropriate differentiation medium. Cells were incubated at 37°C in a humidified 10% (v/v) CO_2 environment for three weeks in total, with medium being changed every three days.

For chondrogenesis; 2 $x10^5$ mMSCs in 0.5 ml 10% (v/v) FCS were transferred to a 15 ml falcon tube and pelleted by centrifugation at 900x g. After one day, medium was replaced with chondrogenic medium by gentle pipetting. Cells were incubated in the 15 ml falcon tube with the top loosened at 37°C in a humidified 10% (v/v) CO_2 environment for three weeks in total, with medium being changed every three days followed by gently flicking the base of the falcon tube to dislodge the pellet.

2.2.1.8. Differentiation of human MSCs

Differentiation Bulletkits® (Lonza) were used as directed by the manufacturer. Briefly, for osteogenesis; hMSCs were seeded onto uncoated plastic culture dishes at 1 $x10^4$ cells/cm^2 in MSCGM (MSC growth medium) and allowed to attach overnight. The following day, medium was replaced with osteogenic differentiation medium. Cells were incubated at 37°C in a humidified 10% (v/v) CO_2 environment for three weeks in total, with medium being changed every three days.

For chondrogenesis; 2 $x10^5$ hMSCs in 0.5 ml complete chondrogenic medium were transferred to a 15 ml falcon tube and pelleted by centrifugation at 900x g. After one day medium was replaced with chondrogenic medium by gently pipetting, ensuring the pellet was gently dislodged. Cells were incubated in the 15 ml falcon tube with the top loosened at 37°C in a humidified 10% (v/v) CO_2 environment for four weeks in total, with medium being changed every three days.

2.2.1.9. Determining relative cell density

A small aliquot of cell suspension was taken then added to the groove of the Neubauer haemocytometer (Hausser Scientific Company, PA, USA) and allowed to spread under the cover slip by capillary action. The average number of cells per 1x 10^{-4} ml was determined under a Nikon Diaphot inverted microscope, in duplicate for each solution. The average cell number was then multiplied by 10^4 to determine the cell density per millilitre. Cell suspension was then aliquoted and diluted appropriately depending on the experiment. Cell viability was also determined for each cell type using a Trypan Blue (0.4% (v/v) Trypan Blue, in PBS, exclusion assay. Briefly, cells that had stained dark blue were counted as non-

viable and the percentage viability calculated as the number of viable cells divided by the total number of cells, multiplied by 100.

2.2.1.10. Cell culture on synthetic substrates

In all experiments, cells to be seeded were collected and washed as described in routine culture (2.2.1), with the appropriate medium. Cell numbers were then calculated from a small aliquot of the cell suspension and the suspension diluted to the required level. Cells were then seeded onto substrates in either 250 µl droplets on the top surface of the substrate, or 500 µl filling the whole well. In the case of the 250 µl droplets, the medium was topped up the following day, once cells had attached. They were then incubated at 37°C in a humidified 10% (v/v) CO_2 environment and medium was changed appropriately with cell type.

2.2.1.11. mESC cell number assay

5 x10^4 mESCs were seeded onto substrates seated in 24-well plates as 250 µl droplets in ESC medium and incubated at 37°C in a humidified 10% (v/v) CO_2 environment for 24 h or 96 h. Cells were then fixed in 4% (w/v) PFA and cells stained with 0.1% (w/v) crystal violet (Serva, Heidelburg, Germany) and analysed as described in 2.2.3.

2.2.1.12. mESC adhesion assay

1 x10^5 mESCs were seeded onto substrates seated in 24-well plates as 250 µl droplets in ESC medium and incubated for 5 h at 37°C in a humidified 10% (v/v) CO_2 environment to allow cells to attach. Medium was then aspirated and cells stained with 0.1% (w/v) crystal violet (Serva) and analysed as described in 2.2.3.

2.2.1.13. mESC migration assay

Migration of mESCs was studied both manually and with automated cell tracking.

For manual imaging, 5 x10^4 mESCs were seeded onto substrates seated in 24-well plates as 250 µl droplets in ESC medium and incubated at 37°C in a humidified 10% (v/v) CO_2 environment. The same fields of view of the mESCs were imaged live in culture under phase contrast hourly between 5 h and 9 h and then after 24 h. Samples were returned to the incubator between imaging.

For automated tracking, GFP E14 mESCs were further labelled with 5 µl/ml 484 nm Vybrant dye (Invitrogen) for 15 min, before 5 x10^4 were seeded onto substrates seated in 24-well plates as 250 µl droplets in ESC medium. Samples were then incubated at 37°C in a humidified 10% (v/v) CO_2 environment for 2 h before placing plates onto a heated stage of a Leica AOBS SP2 confocal microscope (Leica, Heidelberg, Germany) with 10% (v/v) CO_2. Two fields of view were selected per substrate, which were run in duplicate, totalling 4 fields per substrate. Time-lapse imaging was then recorded between 2 h and 4 h, recording images of the same fields of view approximately every 10 min, using Zen 2009 light edition software (Zeiss). Kinetic imaging tracker (Kinetic Imaging Ltd, UK) was then used to track the fluorescent cells.

2.2.2. Cell analysis

2.2.2.1. Fixation of cells

Cells were fixed with 4% (w/v) PFA unless otherwise stated. Cells were fixed for 10-15 min in the dark at room temperature, then washed three times in PBS and stored at 4°C ready for analysis.

2.2.2.2. Crystal violet staining

Substrates with fixed cells and blank (no-cell) substrates were incubated with freshly filtered 0.1% (w/v) crystal violet (Serva) diluted in ddH_2O for 25 min, following a protocol adapted from Gillies (1986). The staining solution was removed and samples rinsed with water until water ran clear, then water was aspirated and samples were allowed to dry at room temperature for 5 min. Stain was solubilised overnight in 500 µl 0.5% (w/v) Triton-X-100 (Sigma). The following day solutions were gently triturated and 250 µl was transferred to a 96 well plate and taken for analysis. Absorption at 595 nm was determined using a SpectraMax Plus (Molecular Devices Corp, California, USA) microplate spectrophotometer. Absorbance of blank substrates was subtracted from those with cells to remove any background signal from non-specific binding of crystal violet to the polymer substrates.

2.2.2.3. Immunostaining

Fixed cells were blocked for one hour at room temperature with 0.1% (v/v) Triton X-100 (Sigma) and 10% (v/v) serum (Sigma) in PBS. Where possible the serum used was from the same species that the secondary antibody was raised in: if this was not available, goat or bovine serum was used. Following blocking, the samples were incubated with the primary antibody solution, which contained the primary antibody, or two primary antibodies for dual staining, in 0.1% (v/v) Triton X-100 and 1% (v/v) serum in PBS. The samples were incubated overnight at 4°C. Primary antibody details are listed in Table 2-1. The following day the samples were washed three times with PBS at room temperature, then incubated for 2 h in the dark at room temperature with the secondary antibody solution, containing the secondary antibody, in 0.1% (v/v) Triton X-100 and 1% (v/v) serum in PBS. Secondary antibody details are listed

in table 2-2. Samples were then washed three times with PBS at room temperature. Blocking and antibody solutions were centrifuged prior to application at 13400x g for 6 minutes in a Microcentaur centrifuge (Sanyo Electric Co. Ltd. Osaka, Japan). To identify cell nuclei, the samples were incubated with DAPI (4',6-diamidino-2-phenylindole, dihydrochloride) (Invitrogen) 1:100,000 in PBS for 5 min in the dark at room temperature. Samples were then washed three times with PBS and either imaged immediately or mounted onto twinfrost microscope slides (76x26x0.8 mm) (VWR) in Dakocytomation fluorescent mounting medium (DAKO) and sealed with clear nail polish. In all staining a negative control, comprising a sample where the primary antibody had been omitted, was included to ensure non-specific binding of the secondary antibodies did not occur. Specificity of primary antibodies was confirmed using whole embryo sections.

Images were captured under a Leica DM2500 fluorescence microscope (Leica, Heidelberg, Germany) using a DFC350FX camera. Samples were also observed under Leica AOBS SP2 confocal microscope (Leica, Heidelberg, Germany).

Table 2-1 Primary antibodies used in this study

Antibody	Host	Specificity	Isotype	Concentration	Supplier
BrdU	Mouse	Mouse	Mono IgG1	1:200	AbCam
CIIC1	Mouse	Mouse & Human	Mono IgG2a	1:200	Hybridoma
OG1	Rabbit	Mouse	Poly IgG	1:200	Santa Cruz
Osteocalcin	Rabbit	Human	Poly IgG	1:200	Santa Cruz

Table 2-2 Secondary antibodies used in this study

Antibody	Host	Isotype	Concentration	Supplier
Anti-mouse AlexaFluor® 488	Goat	IgG	1:1000	Invitrogen
Anti-mouse AlexaFluor® 488	Goat	IgG2a	1:1000	Invitrogen
Anti-mouse AlexaFluor® 594	Goat	IgG	1:1000	Invitrogen
Anti-rabbit AlexaFluor® 488	Donkey	IgG1	1:1000	Invitrogen

2.2.2.4. Alkaline phosphatase staining

Alkaline phosphatase (AP) staining was conducted by the following protocol, adapted from Paling et al. (2004). Immediately following 4% (w/v) PFA fixation, cells were washed twice in PBS, then once in Tris-HCl pH 9.2 (2.1.4). Tris-HCl was replaced with the alkaline phosphatase solution and incubated at room temperature for 5 min to 20 minutes, until a red precipitate was visible. The staining solution was prepared by adding 2 mg (0.02% w/v) napthol AS-MX phosphate (Sigma) to 10 ml Tris-HCl pH 9.2. Once the napthol was completely dissolved, 10 mg (0.1% w/v) Fast Red TR (Sigma) was added to the solution, then mixed and immediately applied to cells. The staining solution was removed and the cells rinsed once in Tris-HCl.

2.2.2.5. BrdU assay

Live cells were pulse labelled with 5-Bromo-2-deoxyuridine (BrdU) (BD Bioscience) using the following protocol adapted from Lan (2005). Cells were incubated with 10 µM BrdU (BD Bioscience, California, USA) in 1x PBS (Sigma) for 15 min at room temperature. They were then fixed in 4% (w/v) PFA and their DNA denatured in 2 M hydrochloric acid for 1 hour at room temperature. Sodium borate buffer pH 8.5 was added for 10 min to wash and neutralise the acid. Cells were washed three times in 1x PBS,

then immunostained as described in 2.2.5. The number of positive cells was determined from 9 separate random views (x200 magnification) from each of 3 replicates.

2.2.2.6. Protein adhesion assay

Micro BCA™ protein assay kit (Thermo Scientific, Massachusettes, USA) was used to determine amounts of protein adhered to substrates according to manufacturer's guidelines. In the BCA (Bicinchoninic Acid) assay, protein amide bonds react with cupric ions (Cu^{2+}) in an alkaline environment, reducing them to cuprous ions (Cu^{1+}) which then react with BCA causing a colour change. Briefly, 0.5 ml 10% (v/v) FCS was added to wells of 24-well plate (Nunc) containing substrates and incubated at room temperature for 1 h. Medium was then aspirated and substrates were washed 3x in PBS (Sigma) before 0.5 ml BCA solution was added to each well. They were then incubated at 37°C for 2 h. Following incubation, the plate was cooled to room temperature and 250 µl taken for analysis. Absorption at 562 nm was determined using a SpectraMax Plus (Molecular Devices) microplate spectrophotometer. Standards were run alongside each assay to confirm linear relationship between optical density and protein concentration.

2.2.3. Quantitative reverse-transcriptase polymerase chain reaction (qRT-PCR)

2.2.3.1. Total RNA extraction

Total RNA was isolated from cells cultured in monolayers, aggregates, in suspension, or from tissues.

For cells in monolayers or aggregates, medium was aspirated from wells containing cells grown on culture substrates before adding 0.5 ml TRIzol® Reagent (Invitrogen) to each well and incubated for 5 min at room temperature to recover ribonucleic acids (RNAs). Samples were then triturated, ensuring cells had visibly disintegrated, and the solutions transferred to 1.5 ml microfuge tubes.

For tissues, small biopsies were taken from adult mice and placed into 1.5 ml microfuge tubes with 0.5 ml TRIzol®. Tissue was then homogenised using an electric homogeniser (Qiagen, Hilden, Germany) until most of it had disaggregated. A further 0.5 ml TRIzol® was then added.

For cells in suspension, approximately 2 $x10^5$ cells were transferred in less than 50 µl medium to 0.5 ml TRIzol® and incubated for 5 min at room temperature.

For cell aggregates in suspension and sessile drop culture, medium was gently pipetted from tubes, leaving the aggregates, and 0.5 ml TRIzol® was added. Samples were then incubated for 5 min at room temperature.

RNA extraction then proceeded as follows. One hundred µl ($1/5^{th}$ volume) chloroform was added and the tubes shaken vigorously for 15 seconds. Samples were then centrifuged at 4°C for 15 min at 12,000x g, separating into 3 distinct phases. 250 µl of the upper colourless aqueous phase, containing the RNA, was transferred to a fresh 1.5 ml microfuge tube containing 1 µl of 1µg/µl glycogen (Boehringer Mannheim GmbH, Mannheim, Germany) and 250 µl isopropanol (Sigma) added to precipitate RNAs. Tubes were inverted to mix six times and incubated overnight at -20°C to increase the yield of RNAs. Samples were then pelleted by centrifugation at 4°C for 10 minutes at 12,000x g. The supernatant was discarded and 1 ml 75% (v/v) ethanol (Sigma) in nuclease-free water (Sigma) added, and the pellet was then resettled by centrifugation at 4°C for 5 minutes at 4,000x g. Ethanol was gently

removed and pellets allowed to air dry for 3 min to ensure all ethanol was removed. The RNA pellets were then dissolved in 10 µl nuclease-free water (Sigma) and stored at -20°C.

2.2.3.2. RNA quantification

The quantity of RNA present in each sample was measured using a 1 µl aliquot in a NanoDrop™ 1000 Spectrophotometer (NanoDrop Technologies, Wilmington, USA) following the manufacturer's guidelines. The 260/280 nm absorbance ratio, reflecting RNA purity, was considered for all samples; pure samples should have values close to 2.

2.2.3.3. DNase Treatment

To avoid contamination with genomic DNA, treatment with deoxyribonuclease (DNase) was performed. One µl RQ1 DNase buffer (Promega, Madison, USA) and 1 µl DNase (Promega) were added to 8 µl RNA solution in a 0.2 ml microfuge tube and incubated at 37°C for 30 min. One µl Stop Buffer (Promega) was added and incubated for 15 min at 60°C to halt the reaction. PCR reactions were performed using DNase-treated RNA with GAPDH primers to confirm that any contaminating genomic DNA had been degraded.

2.2.3.4. cDNA synthesis

cDNA was synthesized using the Superscript III First-Strand Synthesis System for RT-PCR. Five ul RNA was transferred to a fresh 0.2 ml microfuge tube. 8 µl nuclease-free water and 200 ng/µl random hexamers (Abgene, Portsmouth, USA) were added and the samples were incubated

at 65°C for 5 min. Samples were chilled for 1 min on ice and pulse centrifuged to collect contents. 4 µl 5x 1st Strand Buffer (Invitrogen), 1 µl 100 mM DTT (dithiotheitol) (Invitrogen), 1 µl 10 mM dNTP mix (Bioline Ltd, London, UK), and 1 µl SuperScript III™ reverse transcriptase (Invitrogen) were added. Samples were incubated for 5 min at 27°C, then 50°C for 60 minutes, and finally 70°C for 15 min to inactivate the enzyme. Samples were stored at -20°C until used.

2.2.3.5. Oligonucleotide primers

All mRNA primers were ordered from Sigma. On receipt primers were suspended in 1 ml nuclease-free water (Sigma) to give concentrated stock solutions. Aliquots were stored at -20°C until needed. All primers were diluted and used at 0.2 µM.

Most primers were specifically designed for this study in-house with the aid of PerlPrimer™ v1.1.18 (Marshall 2004). Table 2-3 shows primer details and origins. The specificity of primers designed in house was checked by DNA sequencing (University of Dundee sequencing service) the products from PCR (see 2.2.4.7) using whole mouse embryo cDNA or differentiated hMSCs. For each primer set, an agarose gel electrophoresis of the PCR product was performed and the size of the amplicon was checked by running a DNA Ladder (Hyperladder IV, Bioline) (See 2.2.4.8). PCR products were cleaned up using MinElute Reaction Cleanup kits (Qiagen), following the manufacturers guidelines. DNA sequencing was performed commercially by DNA Sequencing & Services (http://www.dnaseq.co.uk) (Dundee, UK), using the forward primer of the corresponding gene. In all cases, the sequenced fragments aligned with the original NCBI database sequence of the corresponding target, confirming that the primers were targetting the correct amplicon.

Table 2-3 Oligonucleotide primers used in this study. F – forward primer; R – reverse primer.

Primer	Sequence	Size	Source	Equation	Efficiency
mOG1	F: GACCATCTTTCTGCTCACTC R: TCACTACCTTATTGCCCTCC	127 bp	In-house	10^(-0.288*CT + 9.883)	0.94
mAp	F: AGGGTACACCATGATCTCAC R: TCTCCCAGGAACATGATGAC	188 bp	In-house	10^(-0.294*CT + 10.274)	0.97
mCol2	F: CTGACCTGACCTGATGATACC R: CACCAGATAGTTCCTGTCTCC	169 bp	In-house	10^(-0.283*CT + 9.083)	0.92
mAgg	F: CTCAGTGGCTTTCCTTCTGG R: CTGCTCCCAGTCTCAACTCC	185 bp	In-house	10^(-0.356*CT + 11.942)	1.21
mFABP2	F: CATGAAAGAAGTGGGAGTGG R: TGATGCTCTTCACCTTCCTG	193 bp	In-house	10^(-0.261*CT + 7.441)	0.82
mPPARg	F: GTTATGGGTGAAACTCTGGG R: GTGGTAAAGGGCTTGATGTC	202 bp	In-house	10^(-0.279*CT + 10.284)	0.90
mWt1	F: CCAGTGTAAAACTTGTCAGCGA R: TGGGATGCTGGACTGTCT	234 bp	In-house	10^(-0.305*CT + 8.889)	1.02
mN-Cad	F: CCGTGAATGGGCAGATCACT R: TAGGCGGGATTCCATTGTCA	111 bp	Longaker 06	10^(-0.321*CT + 9.486)	1.09
mSox9	F: TACGACTGGACGCTGGTGCC R: CCGTTCTTCACCGACTTCCTCC	305 bp	Asahara 09	10^(-0.298*CT + 9.263)	0.99
mGAPDH	F: TGAAGCAGGCATCTGAGGG R: CGAAGGTGGAAGAGTGGGAG	102 bp	In-house	10^(-0.286*CT + 7.397)	0.93
hOC	F: GAAGCCCAGCGGTGCA R: CACTACCTCGCTGCCCTCC	70 bp	Born 2009	10^(-0.347*CT + 12.138)	1.07
hAP	F: CCGCTATCCTGGCTCCGTGC R: GGTGGGCTGGCAGTGGTCAG	108 bp	In-house	10^(-0.313*CT + 9.019)	1.05
hCol2	F: CAACCAGATTGAGAGCATCC R: GGTCAATCCAGTAGTCTCCA	115 bp	In-house	10^(-0.240*CT + 9.303)	0.84
hAgg	F: TCGAGGACAGCGAGGCC R: TCGAGGGTGTAGCGTGTAGAGA	85 bp	Guo 08	10^(-0.282*CT + 10.155)	0.91
hGAPDH	F: GTGGTCTCCTCTGACTTCAA R: TCTCTTCCTCTTGTGCTCTT	211 bp	In-house	10^(-0.279*CT + 9.075)	0.90

Explanations for the equation and efficiency of reaction for each primer set is included in section 2.2.3.6.

2.2.3.6. Quantitative real-time polymerase chain reaction (qPCR)

Before preparing the qPCR reactions, the cDNA samples were diluted between two and three fold depending on RNA concentration. Two technical replicates were run for each template and primer set. Reactions containing no cDNA template were routinely included in all qPCR runs to check for contamination or primer dimer. The reaction was as follows: 1 µl cDNA, 10 µl SYBR® Green Jumpstart™ Taq ReadyMix™ (Sigma), 0.25 µM forward and reverse primers, made up to a final reaction volume of 20 µl with nuclease-free water (Sigma). The reaction was carried out on a Corbett Rota Gene RG-300, and continued for 40 cycles of 95°C for 6 seconds, 58°C for 20 seconds and 72°C for 30 seconds, with an annealing temperature of 58°C for all primers.

Standard curves were first performed for each primer set to assess the linearity of the DNA amplification, in order to enable the quantification of the qPCR analyses (e.g. Figure 2-1). For this, serial dilutions of control cDNA templates were used for qPCR and results were processed using the Rotor Gene 3000 analysis software version 6.1, in order to determine the relationship between the number of copies of the mRNA in the template and the flourescence signal measured.

For each standard curve, control samples were serially diluted 1:5 (v/v) with nuclease-free water, giving dilutions of 1, 1/5, 1/25, 1/125, 1/625 and 1/3125. These dilutions were given arbitrary copy numbers from 1000 to 0.32. Following the qPCR reaction, thresholds were established during the exponential phase of the reaction and threshold cycle number (Ct) values were calculated. The theorical copy number was plotted against the Ct value to build standard curves for each primer set and the equations of these curves were used to calculate the relative number of copies of each mRNA in the template. Equations for the relationship were calculated, as shown below.

$$\text{Concentration} = 10^{\wedge}(Ct*m^{-1} + c*m^{-1})$$

Where m is equal to the slope and c is equal to the intercept. The reaction efficiency was also calculated using the slope of this relationship, and it represents the fraction of copies made per cycle, which should ideally be close to one. These equations were calculated from standard curves for each of the primer sets and used in analysis of the qPCR data. Equations and efficiencies for each primer set are included in Table 2-3.

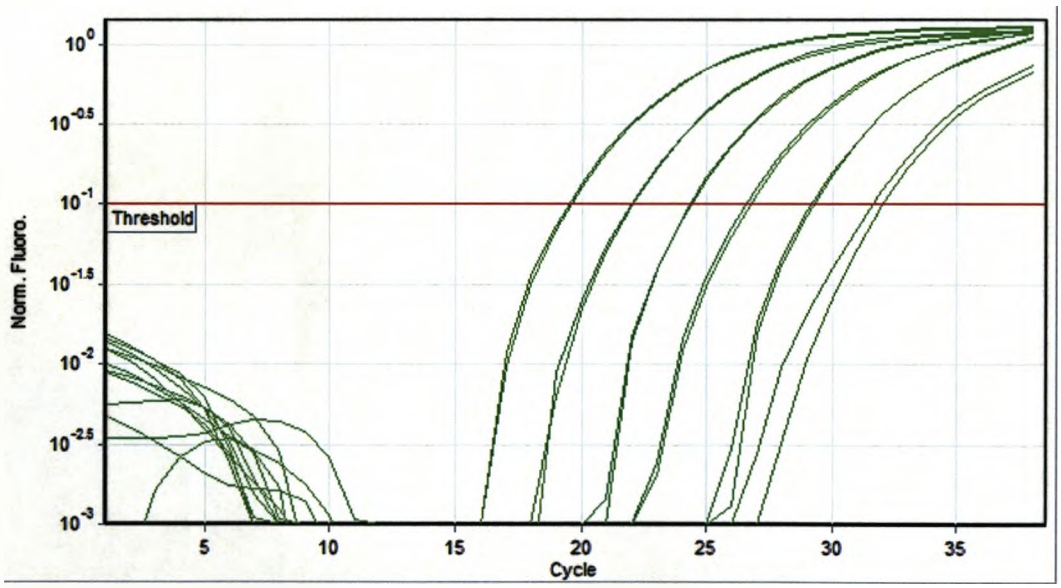

Figure 2-1 Example of standard curve from amplification of mouse collagen II. qPCR of 1:5 serial dilutions of control mouse cartilage tissue template. Standard curve was built by plotting the arbitrary copy number against the Ct at the point of crossing the threshold.

Following each qPCR run, a melting curve was performed to confirm the amplification of the same amplicon for all samples and replicates (e.g. Figure 2-2). To generate the melt curves, the change in fluorescence was measured whilst the temperature was increased gradually, rising 1°C every 5 sec, from 75°C to 98°C. Peaks will occur at the temperature the double stranded DNA is dissociated, dependent on their length and

cytosine/guanine content. Amplicons of the same size and nucleotide composition demonstrate a common peak.

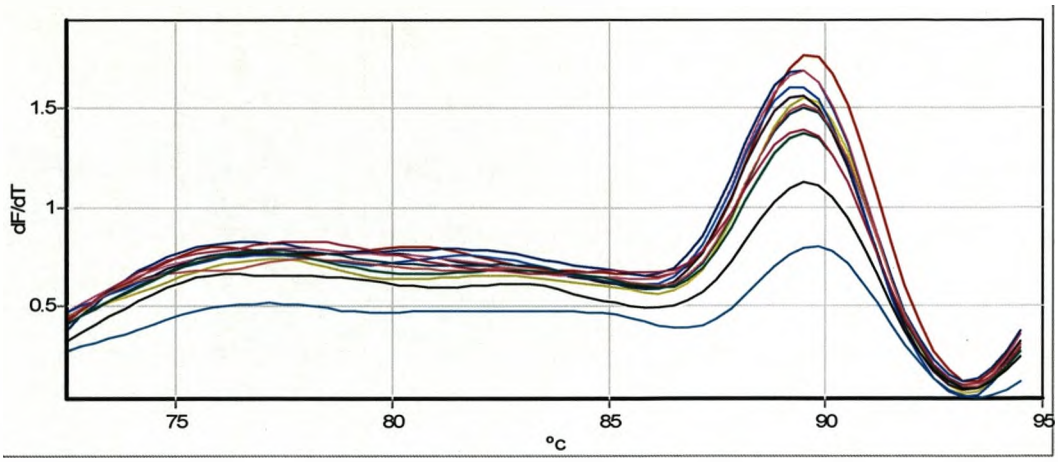

Figure 2-2 Example of melt curve from amplification of mouse collagen II. qPCR of 1:5 serial dilutions of control mouse cartilage tissue template. To validate the specificity of the primers and the amplification, melt curves were performed for each sample. Reduction in fluorescence was measured whilst the temperature increased by 1°C every 5 sec. Curves were generated by plotting fluorescence against temperature. The mouse collagen II melt curves demonstrate a single peak at 89.5oC.

All qPCR results were normalised to the expression of the house keeping gene glyceraldehyde 3-phosphate dehydrogenase (GAPDH), which is involved in glycolysis and is constitutively expressed at high levels in all cells. Two technical replicates were run for each template and three biological replicates were included for each primer set. Statistical significance was determined using ANOVA, and pairwise comparisons were conducted with the Tukey post hoc test ($P<0.05$).

2.2.3.7. Polymerase chain reaction (PCR)

The 20 µl PCR reaction contained the following; 0.5 µl cDNA, 0.8 µl forward and reverse primers, 14.4 µl nuclease-free water (Sigma), 2 µl 10x NH_4 Buffer (Mg^{2+} free), 0.5 µl $MgCl_2$ (50mM), 0.5 µl dNTP mix (10mM stock), 0.5 µl Taq DNA polymerase (all from Bioline). The reaction was conducted on an Applied Biosciences 2720 thermal cycler as follows; 3

min at 94°C, followed by 38 cycles of 94°C for 30 seconds, 58°C for 30 seconds and 72°C for 45 seconds, and finally an extension of 72°C for 10 min.

2.2.3.8. Gel electrophoresis

Gel electrophoresis was conducted in a 2% (w/v) agarose (Bioline) gel in 1x TAE, with 0.5 µg/ml ethidium bromide solution (Sigma). One µl 6x loading buffer [6x DNA glycerol loading buffer: 5 ml sterile distilled water, 1.5 ml glycerol, 0.25% (w/v) bromophenol blue, 5 µl 0.5 M EDTA] was added per 5 µl sample, and the samples were run for 30 min at 100 V. The gel was visualised with a UV transilluminator (ChemiImager 4400, Alpha Innotech Corp., CA, USA).

2.2.4. Polyacrylate substrate preparation

Accelerate™ polyacrylate samples were prepared in the form of 13 mm glass discs, using a simple dip coating procedure. Glass cover slips (r 7.5 mm, SA 1.8 cm^2, Borosilicate Glass Co. UK) were routinely coated at the Runcorn site of BTL. The cover slips were submerged just over halfway into the polymer solution (2-4% w/v in DMF) then removed and dried in a drying oven at 90 °C before coating the second side. Cover slips were dipped at a speed of 1 mm/s, with 15 minutes drying time in between. A small section of the middle of each cover slip (1-2 mm) overlapped the coatings and dried in an amorphous arrangement. This was recognised and considered when analyzing the substrates. Substrates were sterilised prior to cell culture with one cycle of ultra violet light (265 nm) lasting 30 min. Nine mm glass cover slips were coated for X-ray photoelectron spectroscopy (XPS) analysis and 20x20 mm covers slips were dipped once for dynamic contact angle measurements.

2.2.5. Substrate analysis

2.2.5.1. Contact angle measurement

The Willhelmy method was used to determine dynamic contact angle (DCA) of substrates. This was recorded using a Cahn DCA322 microbalance and analysis software WinDCA32 (Thermo Cahn, USA), calculating the advancing and receding contact angle for each sample in distilled water (72.6 dynes/cm). Counter weights were used to balance 1/5 of test sample weight.

2.2.5.2. X-ray photoelectron spectroscopy

XPS was conducted under the direction of G. Beamson at the Daresbury laboratory using the NCESS ESCA300 XPS spectrometer (VG Scienta, Uppsala, Sweden). Survey, valence, C1s, O1s and N1s spectra were analysed at take off angles of 45° and 15° at 150 eV, 0.8 mm slit, 1.8 kW. Spectra curves were analysed by curve fitting, conducted using CasaXPS (Casa software ltd.) and OriginPro 7.5 SR6 (OriginLab Corporation, MA, USA).

2.2.5.3. Polymer hydration assay

The hydration assay was conducted using approximately 1 x 1 cm squares of a 1 mm thick film of BTL15. Squares were weighed (approx 0.1 g), using a microbalance (Sartorius), before immersing them in ddH_2O for set periods of time. Samples were removed from water, dried on tissue and weighed to detect any uptake of water. Samples were then dehydrated in a drying oven at 60°C for 30 min and weighed to check for degradation of the polymer.

2.2.5.4. Scanning Ion Conductance Microscopy

Scanning ion conductance microscopy (SICM) was conducted using the ICnano® (Ionscope Ltd, UK) under the direction of Dr Filippi and Dr Fields (Ionscope Ltd) (Novak 2009). Briefly, substrates were imaged under PBS in hopping mode to determine surface roughness.

2.2.5.5. Amine detection assay

The relative amine content of substrates was measured using sulfo-NHS-Biotin (Thermo) to bind to surface amines, followed by streptavidin-horse radish peroxidase (Bioscience) to generate a colorimetric enzyme assay using TMB (Sigma) as a substrate. Specificity was confirmed by pre-treatment with NHS-acetate (Thermo), under the same conditions, to first block amine binding sites.

The assay was performed on 13 mm coated cover slips placed in 24-well plates. A half ml of fresh 1 mg/ml sulfo-NHS-biotin in PBS was added per well and incubated in the dark on a rocking table at room temperature for 1 h. Samples were then washed once in 50 mM glycine in PBS, to quench NHS, and washed 3x in PBS. A half ml 10 mM Streptavidin-HRP (Sigma) in PBS was then added to each well and incubated in the dark on a rocking table at room temperature for 30 min. Samples were then washed 3x in PBS and transferred to wells containing 0.5 ml PBS in a fresh plate and washed once more with PBS. PBS was aspirated and 0.5 ml TMB solution (Sigma) was added to each well, then incubated in the dark on a rocking table at room temperature for 15 min, after which blue coloration was evident. Reaction was halted by adding 250 µl of 1 N hydrochloric acid to each well, causing visible colour change to yellow. 250 µl of the solution was then transferred to a 96 well plate and OD was read immediately at 450 nm. Simultaneously, this protocol was performed without the treatment with sulfo-NHS-biotin, the resulting absorbance was

deducted from final absorbance to ensure no non-specific binding of the streptavidin-HRP was measured.

3. Polyacrylate biomaterials

3.1. Introduction

A biomaterial is a synthetic or natural material used to replace part of a living system or to function in intimate contact with living tissue. These include a wide range of biocompatible polymers whose properties can be easily modified and tailored to the specific use. They can provide a defined and controlled surface to contact living tissue and can be tailored with specific properties in response to tissue and environmental properties or requirements. In recent years, understanding of the value of biomaterials has advanced and they have become a key area of research, with applications across the fields of research and medical industries. Biomaterial applications can be extremely varied, and can be used wherever living cells and tissues are present.

In stem cell research, synthetic substrates may have roles in derivation and maintenance, but also in directing the differentiation of the cells. As previously described (1.1.4, 1.2.5), the role of substrate chemistry, and in particular of functional groups, in stem cell culture is beginning to be revealed (Curran 2006; Neuss 2008; Phillips 2009).

In this study, polyacrylate substrates (Nickson 2008) were developed to investigate their potential for regulating stem cell behaviour. The

polyacrylate substrates were designed to present a range of surface chemistries, differing in functional group composition and distribution. In this chapter, physicochemical properties of a range of polyacrylate substrates were investigated in order to determine which substrates would be most suitable for regulating the behaviour of embryonic stem cells (Chapter 4) and mesenchymal stem cells (Chapter 5).

3.1.1. Confidentiality agreement

Due to the nature of the polyacrylate materials, their pre-patent status and the BTL proprietary fabrication techniques, reporting of detailed compositional data was prohibited by BTL. In addition, investigation of the specific substrate formula and components was not permitted.
Therefore, the substrate analysis presented here aimed to investigate the surface properties of the substrates, and in subsequent chapters the substrates were further characterised by the cell response to them.

3.1.2. Substrate analysis techniques

The polyacrylate substrates were characterised using dynamic contact angle measurement (DCA), X-ray photo-electron spectroscopy (XPS), an amine detection assay and scanning ion conductance microsopy (SICM). The uptake of water by poly-acrylates under aqueous conditions was also investigated.

Dynamic Contact Angle

Contact angle is the angle between the surface and the tangent to the curve of a droplet as it meets the surface (Young 1805; Wang 1994). When using water, a polar liquid, the contact angle of a surface indicates its wettability. The more hydrophobic a surface, the higher the contact angle, whereas the more hydrophilic a surface, the lower the contact angle. The dynamic contact angle differentiates between hydrophobic (advancing angle, θ_A) and hydrophillic (receding angle, θ_R) interactions of a surface (Figure 3-1). Hysteresis is measured as the difference between the advancing and receding angles. A higher value suggests an increased heterogeneity of regions across the surface, possibly caused by phase separation in the polymer giving rise to distinct, unevenly distributed regions of varying hydrophilicity. Low hysteresis suggests a more homogeneous surface, either through even distribution of alternative groups or reduced variety of groups (Chen 1991).

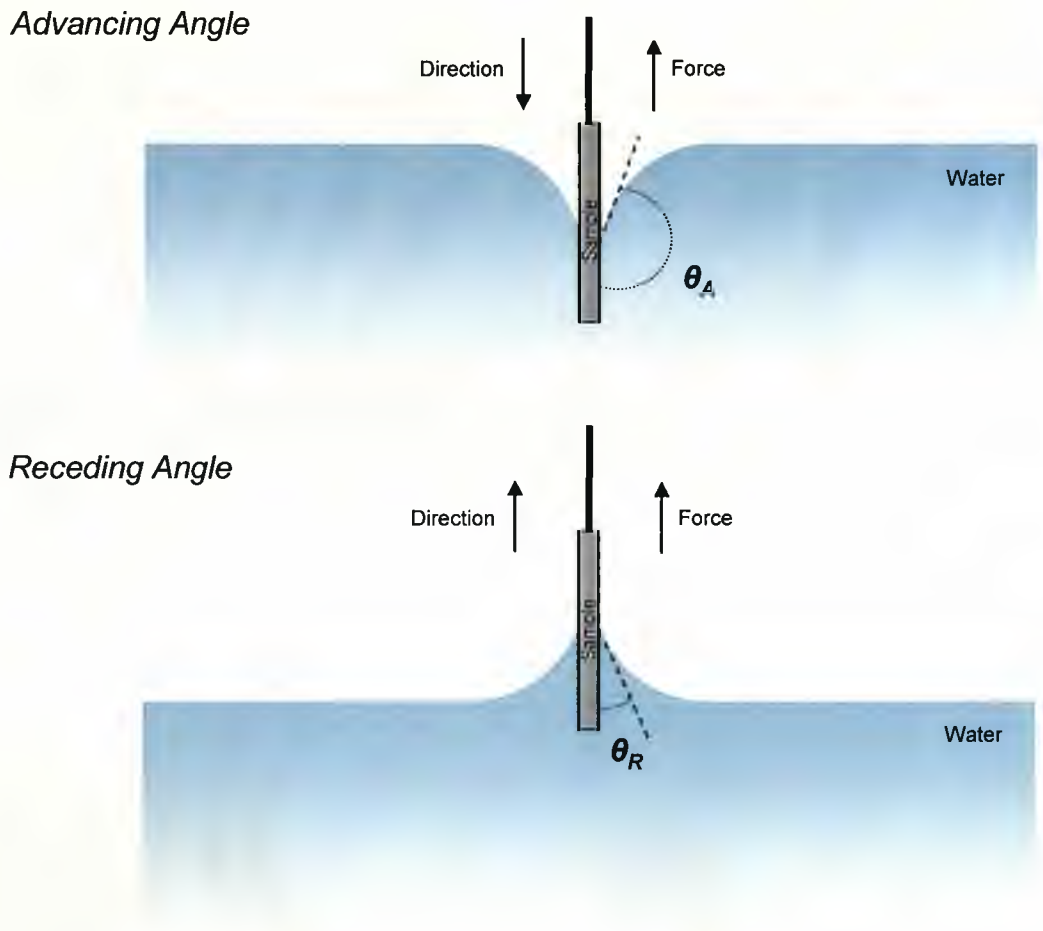

Figure 3-1 Wilhelmy technique for measuring DCA. The contact angle is measured during immersion (θA) and emersion (θR) in water.

X-Ray Photoelectron Spectroscopy

XPS is a tool for analysing the surface chemistry of a sample, specifically at nanometre depths of the surface (Beamson 2004). This technique involves irradiating the sample with x-rays and then detecting the numbers and kinetic energy (E_k) of emitted electrons (Figure 3-2). This energy is specific to the electrons in the orbitals of atoms and the frequency of electrons will be proportional to the amount of that element within the surface region of the sample. The binding energy of electrons (E_b), specific to atoms, can be calculated from the energy of the X-rays

used (E_p), the detected kinetic energy (E_k) of emitted electrons and the work function of the spectrophotometer (ø).

$$E_b = E_p - (E_k + \phi)$$

The take off angle (TOA) can be altered to analyse different thicknesses of the surface. As the TOA is reduced, fewer electrons are able to escape from deeper into the substrate without colliding with other atoms, and, therefore, a higher proportion of those electrons which are detected come from closer to the surface.

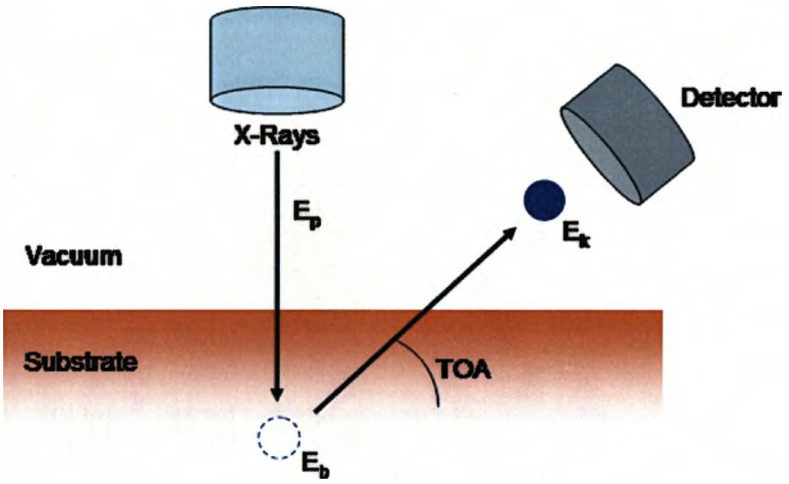

Figure 3-2 Principles of XPS. The kinetic energy (E_k) of electrons emitted from the substrate is detected and deducted from the X-ray energy (E_p) to calculate its binding energy (E_b) and identify its origin. Binding energies are specific to elements and covalent associations.

Amine Detection Assay

N-hydroxysulfosuccinimide (NHS) reacts with primary amines to form an amide bond and is commonly used to label proteins. In this chapter Sulfo-

NHS-Biotin was used to detect amines present on the surface of the polyacrylate substrates. Streptavidin-HRP (horseradish peroxidase) was used to detect bound biotin and provide a colorimetric assay to compare the amount of amines at the surface of each substrate. The Streptavidin proteins size (52.8 kDa and diameter ~5.5 nm), makes it likely that only surface amines are detected using this approach.

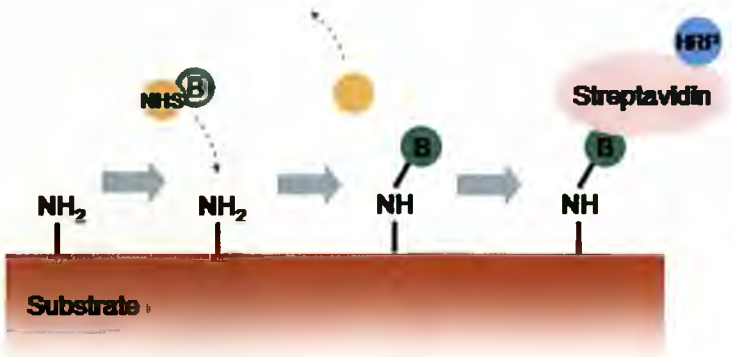

Figure 3-3 Amine detection assay. NHS reacts with primary amines labelling them with Biotin (B). Streptavidin-HRP binds to the Biotin, labelling the amines with an HRP enzyme.

Scanning Ion Conductance Microscopy

SICM can be used to generate a topographical map of a surface (Novak 2009). SICM is performed using an electrically charged glass pipette filled with electrolyte. The probe is lowered towards the sample, and, as it approaches the surface, the current decreases as the gap reduces in size. The current, and therefore the gap, is kept constant by altering the

pitch of the probe, and as the probe moves across the surface, these movements build a topographical image of the surface. Roughness is typically measured as the average vertical deviation from the mean and can be displayed as the arithmetic average of absolute values (R_a), calculated from the changes in height recorded across a substrate.

Polymer Hydration

A simple mechanism for changing the structure of a polymer is uptake of water under aqueous conditions. Additional steric effects may become apparent only under culture conditions and these could lead to re-orientation of functionality over time, changing the surface presented to cells. Many polymers are known to uptake water from their environment, in some cases forming hydrogels (Kroupova 2006; Li 2006; Mi 2006; Ashton 2007), which may lead to reorganisation and reorientation of functional groups.

3.1.3. Aims

(i) Design and fabricate a range of polyacrylate substrates, using the BTL proprietary technology, with combinations of densities and distributions of surface functional groups which mimic those of the extracellular environment and ECM protein domains, such as the RGD integrin-binding motif.

(ii) Characterise polyacrylate substrates to confirm generation of discrete surface characteristics between polymers, and demonstrate the role of steric hindrance in modulating surface properties.

3.2. Basic polymer properties

The synthetic **ac**celerate™ polymeric coatings synthesised by BTL were all polyacrylates. These polyacrylates, or acrylics, are polymers constructed from multiple acrylate monomers and share the general properties of transparency, toughness and elasticity (Nickson 2008). The **ac**celerate™ coatings were manufactured using monomers presenting amine, carboxylic acid, hydroxyl, ethyl and butyl side groups, and spacer monomers. These polyacrylates were synthesised using the BTL proprietary technology, creating statistical polymers with monomers distributed randomly within them. Only the outermost surface layer of the substrate interacts with the cell layer at the molecular level, therefore, surface properties are key to controlling that interaction (Roach 2007). The basic formula for acrylate monomers is shown below (Figure 3-4), followed by the polyacrylate formula. R^1 and R^2 denote interchangeable side groups.

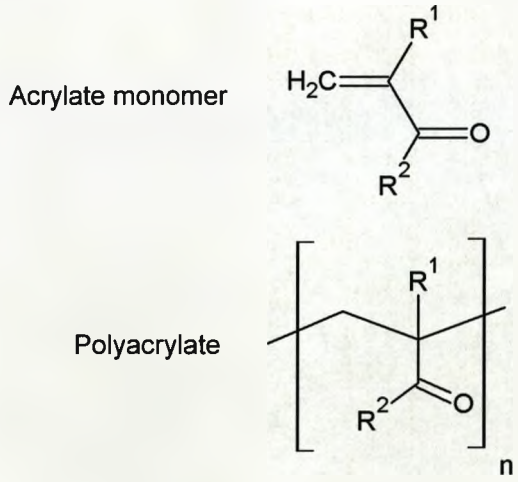

Figure 3-4 Chemical structure of acrylate materials. Acrylate monomer and polyacrylate formulae are shown. R^1 and R^2 denote potential side groups (NH_2, COOH, OH, C_2H_5 & C_4H_9).

Polyacrylate polymers were designated BTL (Biomer Technology Limited) or ESP (Embryonic Stem Cell Polymer) followed by their designation five-digit number, e.g. BTL01008. Throughout this thesis the polyacrylate substrates are referred to as their prefix designation followed by their shortened two digit number, e.g. BTL08, or in some cases simply by their shortened two-digit number, e.g. 08. There were no common number designations between BTL and ESP polymers used, therefore, no conflicts appear with this terminology.

Theoretically, each polymer differs in its distribution and presentation of discrete functionality, through modification of monomer concentrations. An overview of the theoretical polymer properties, provided by BTL, is included in Table 3-1; however, detailed chemical properties of the polymers remain confidential.

Table 3-1 BTL theoretical polymer properties

Property	*Polymer Trend*
Amine Content	08=09=15=16<01<03<02<04=07<06
Carboxylic Acid Content	07<04<08=09=15=16=03<02<01<06
Hydroxyl Content	03=04=06<07<08=09=15=16<02<01
Steric Hindrance	06<08<15=03=04=07<09<02<01<16
Glass Transition Temperature	08<15<03<07<04<09<01<02<16<06

Initial polymers (BTL08, 09, 15) were selected for their discrete capacity to support the attachment and proliferation of bovine aortic endothelial cells, bovine smooth muscle cells, human aortic endothelial cells and human coronary artery smooth muscle cells (Nickson 2008). A further polymer, BTL16, was introduced during the study with increased steric hindrance. The primary difference between these initial polymers was the proportion of larger interfering side groups, which would increase steric hindrance in the polymer chains (Kowalewska 1999). The steric hindrance was controlled by the balance between smaller ethyl and larger butyl alkyl side groups, with the total alkyl group density remaining constant.

The range of substrates was later expanded to include 5 additional polyacrylates: ESP01, ESP02, ESP03, ESP04, ESP06 and ESP07. These polymers were inspired by the functional composition of the common ECM components fibronectin (Fn) and laminin (Ln), incorporating hydroxyl, amine and carboxyl functional groups, as described below (3.3). ESP03 and ESP04 contained amine and carboxyl functional groups, and were more specifically designed to crudely mimic the functional composition and distribution of the arginine-glycine-aspartic acid (RGD) integrin binding site common to fibronectin and other ECM proteins.

3.3. ESP polymer development

As described above, the BTL designated polyacrylates differed in their degree of steric hindrance and were selected from an existing line of polymers previously shown to influence cell adhesion and growth (Nickson 2008). The ESP line of polyacrylates was developed throughout the course of this study, and the proportions of functional groups in the polymers were modified to present alternative proportions and distributions of functionality to the cells, again utilising the BTL proprietary synthesis technology.

The ESP polyacrylates were developed in numerical order. ESP01 and ESP02 were incorporated similar functional composition and proportion to Fn (NCBI accession number: AAD00019.1) and Ln (NCBI accession numbers: NP_005550, P07942, P11047) respectively. Both of these proteins play an important role in cell adhesion in vitro (Amit 2004; Ludwig 2006). Presentation of surface functionality was assessed by viewing the 3-D structure of the proteins using Cn3D (NCBI), a 3-D structure viewer. These substrates contained a combination of hydroxyl, amine and carboxyl groups at higher density than the initial BTL polymers.

ESP03 and ESP04 were more specifically attempting to mimic on the functional group composition and distribution found within the RGD integrin-binding site, common to multiple ECM attachment proteins.

Figure 3-5 demonstrates the 3-D structure of the RGD sequence within the tenth type III domain of Fn (PDB:1TTF) (Main 1992; Wang 2007). Figure 3-6 shows a model of the RGD peptide, created using Chemsketch© (ACDlabs), demonstrating the carboxyl and complex guanidinium groups and their spacing. The RGD peptide itself has been demonstrated to support cell attachment and self renewal in human (Li 2006) and primate ESCs (Sato 2007) and attachment of many other cell types (Fischer 2007).

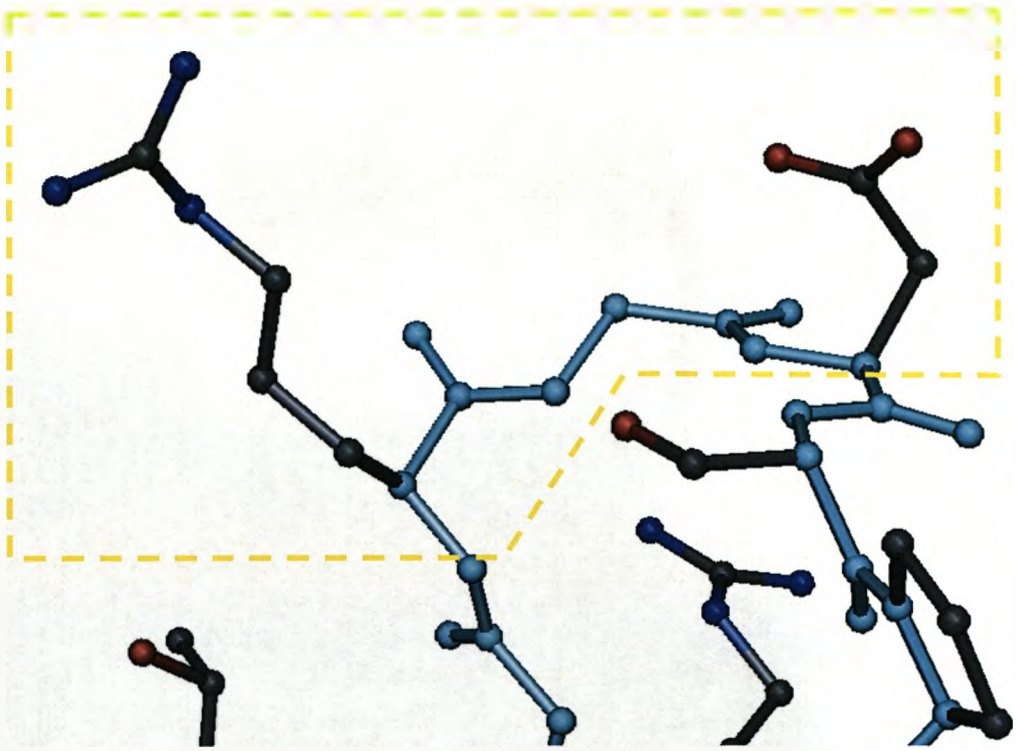

Figure 3-5 Stick and ball representation highlighting RGD sequence within Fn. The 3-D structure of RGD within the tenth type III domain of Fn is marked (yellow border). The protein backbone is marked (light blue) and side chains containing carbon (black), oxygen (red) and nitrogen (dark blue) atoms are shown. Image captured using Cn3D (NCBI).

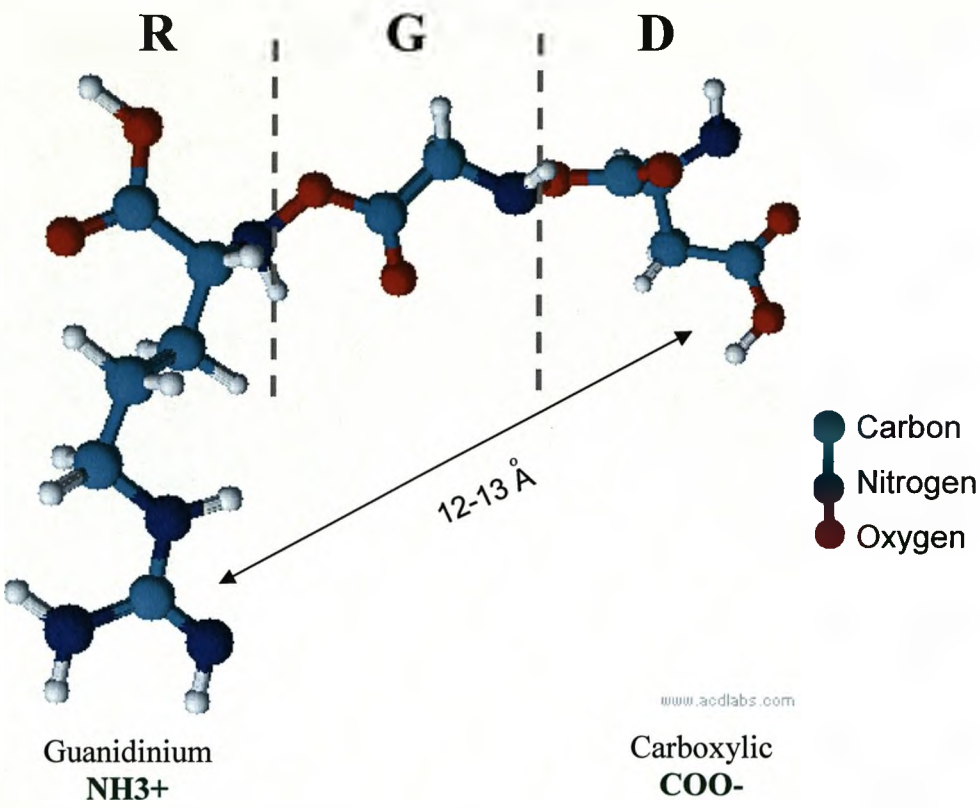

Figure 3-6 Stick and ball model of the RGD peptide. Functional groups mimicking RGD functionality and separation are shown in green.

Peptide sequences found to aid in cell attachment by other groups (Li 2006; Derda 2007; Fischer 2007; Mochizuki 2007) were assessed for specific functional presentation. Peptide sequences that encouraged cell attachment typically contained similar sequences to the RGD peptide in functional group arrangement, containing nitrogen rich regions and carboxyl groups with similar spacing. For example, Derda *et al.* (2007) screened 18 different laminin peptide fragments for support of hESC attachment and proliferation, and found several peptide sequences that promoted both adhesion and proliferation. Analysing chemical structures of the most successful peptide sequences demonstrated that they often contained RGD-like components in similar distributions, such as the

peptide sequence DIRVTLNRL (Figure 3-7 A), where DIR is similar to RGD, containing both arginine and aspartic acid at a similar spacing, however, the sequence is inverted and peptide sequences have polarity, meaning the reversed sequence will not be equal, though in some instances it may substitute. Furthermore, this combination and distribution of functional groups was typically not found in those sequences which did not support attachment, such as LGTIPG (Figure 3-7 B).

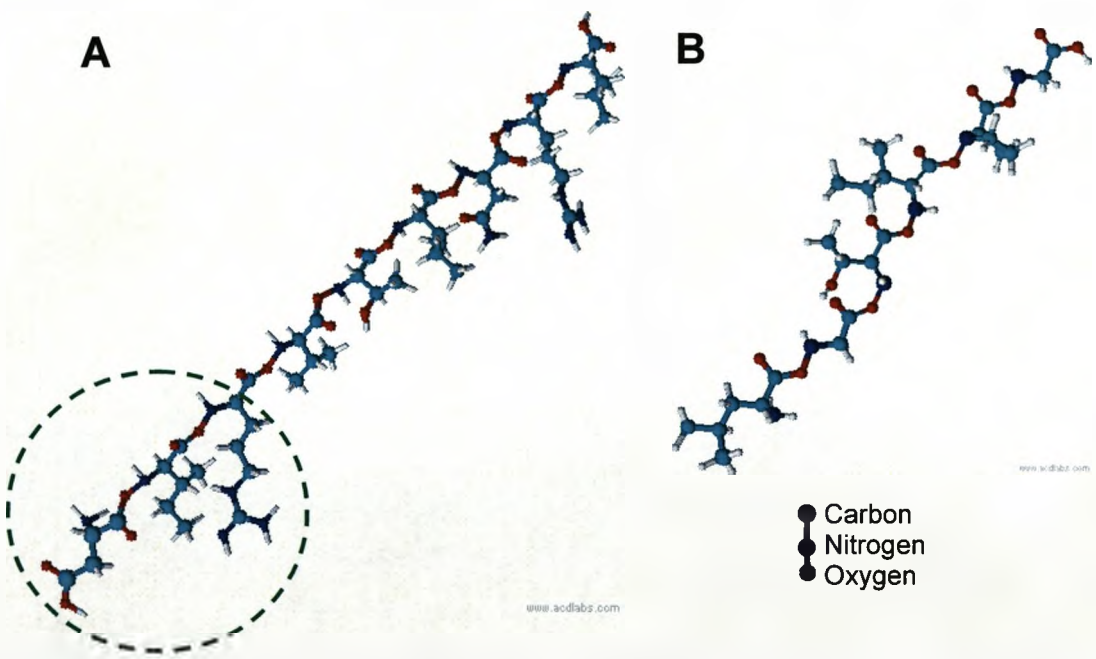

Figure 3-7 Stick and ball model of laminin peptides. 3-D models of the attachment promoting peptide sequence, DIRVTLNRL (A), and a peptide sequence that does not promote attachment, LGTIPG (B). DIR is highlighted (green).

ESP03 and ESP04 very simply modelled on the RGD peptide in that they contained only carboxyl and amine functional groups at two different proportions. These polyacrylates included a C7 spacer monomer, to

establish spacing between the other monomer units. They were also designed with intermediate steric hindrance, similar to BTL15. ESP06 further developed this line of materials by drastically increasing both amine and carboxyl functional group density over ESP03 and ESP04. ESP07 was designed to contain hydroxyl and amine side groups, with the intention of a comparison with ESP04, where carboxyl and amine side groups were present. However, ESP06 and ESP07 were developed late in the study and were unavailable for XPS characterisation.

3.4. Results

3.4.1. Dynamic contact angle

The BTL substrates demonstrated a large range of discrete dynamic contact angles (Figure 3-8). Most of the polyacrylates demonstrated significantly different advancing and receding angles from each other ($p<0.05$, Tukey model), the only substrates which showed no significant difference between advancing or receding angles were ESP03 with ESP07 or BTL08, and BTL09 with ESP06. Hysteresis was high across all polyacrylate samples, but again discrete differences were detected between substrates, implicating heterogeneity in distribution of charge and functionality at the surface of each substrate (Figure 3-9) (Chen 1991). The hydrophobic Poly-L-Lactic acid substrate and the comparatively hydrophilic plain glass were included as controls. PLLA has been used extensively as a substrate for cell culture, and it contains only a single monomer unit (Zhu 2004; Paragkumar 2006; Hanson 2007).

Of the substrates which differed by the degree of steric hindrance (BTL08, BTL09, BTL15 and BTL16) (Table 3-1), the most hydrophillic substrates contained the least steric hindrance, with a higher proportion of the smaller ethyl to butyl side groups. However, the most hydrophilic substrate was BTL15, with intermediate steric hindrance, and not the substrate with the least steric hindrance, BTL08, which had the second

lowest receding angle, although no significant difference was determined between them ($p=0.055$, Tukey model). The receding angles of BTL08 and BTL15 were significantly lower than BTL09 and BTL16 ($p<0.05$, Tukey model), with BTL09 having a significantly lower receding angle than BTL16 ($p<0.05$, Tukey model). The trend between these substrates for hydrophillicity was as follows:

BTL16<BTL09<BTL08<BTL15

Interestingly, when measuring the hydrophobic regions of these substrates, using the advancing angle, a different pattern emerges, with BTL15 having the lowest advancing angle, but BTL08 the highest. Each of these substrate's advancing angle was significantly different from the others ($p<0.05$, Tukey model). The trend between these substrates for hydrophobicity was as follows:

BTL15<BTL09<BTL16<BTL08

Aside from BTL08, both receding and advancing angles follow the trend for steric hindrance, with more hydrophilic and less hydrophobic interactions with decreasing steric hindrance. Examining hysteresis on these substrates demonstrated that hysteresis for these polyacrylates also followed this trend, where the lowest hysteresis was found with the highest steric hindrance, and substrates with lower steric hindrance had higher hysteresis. Hysteresis on BTL08 and BTL15 was not significantly

different, but both substrates demonstrated significantly higher hysteresis than BTL09, which was significantly higher than BTL16 ($p<0.05$, Tukey model).

BTL15 remained one of the most hydrophilic substrates when all of the polyacrylates were considered. BTL15 had a significantly lower receding angle ($22.2^{o} \pm 1.8$) than most of the polyacrylates ($p<0.05$, Tukey model), however, it was not significantly different from BTL08, ESP02 and ESP04 ($p>0.05$, Tukey model). BTL15 also had the lowest advancing angle ($85.3^{o} \pm 0.3$) which was significantly lower than most polyacrylates ($p<0.05$, Tukey model), and was only not significant from ESP06 ($85.5^{o} \pm 2.4$). The lowest hysteresis was on BTL16 ($46.5^{o} \pm 0.4$), which was significantly lower than all other polyacrylates ($p<0.05$, Tukey model), and corresponded with the highest proportion of more sterically hindering groups. Plain glass and PLLA substrates demonstrated significantly lower hysteresis than all of the polyacrylates, suggesting that they presented more homogeneous surfaces.

ESP04 was similar to ESP03, with the difference of increased amine and decreased carboxyl functional groups. Advancing and receding angles were significantly lower on ESP04 than ESP03 ($p<0.05$, Tukey model), and hysteresis did not significantly change ($p>0.05$, Tukey model). ESP07 was similar to ESP04, with hydroxyl groups replacing carboxyl groups, and advancing and receding angles were significantly increased whilst hysteresis decreased ($p<0.05$, Tukey model). ESP06 contained

highly increased proportions of amine and carboxyl functional groups over both ESP03 and ESP04, and also contained very few sterically hindering hydrocarbon side groups (Table 3-1). ESP06 demonstrated significantly higher receding angle than ESP03 and ESP04 ($p<0.05$, Tukey model), and a significantly lower advancing angle then ESP03 ($p<0.05$, Tukey model). The advancing angle of ESP06 was lower than that of ESP04, but this was not significant ($p=0.095$, Tukey model). Hysteresis was also significantly reduced on ESP06 compared to ESP03 and ESP04 suggesting a more homogeneous distribution of functional groups. BTL15 incorporated similar levels of steric hindrance as ESP03 and ESP04, and hysteresis was not significantly different between them ($p>0.05$, Tukey model). In contrast to the polyacrylate substrates, the hysteresis across the hydrophobic single-monomer polymer, PLLA, was much lower.

Interestingly, the hydrophobic PLLA substrate demonstrated one of the lowest advancing angles ($86^{\circ} \pm 0.4$). This was significantly lower than several of the polyacrylate substrates (BTL08, ESP01, ESP02, ESP03 and ESP07), suggesting that regions on the polyacrylates were more hydrophobic than PLLA. However, as expected, the receding angle of PLLA ($62^{\circ} \pm 1$) was much higher than all polyacrylates ($p<0.05$, Tukey model), confirming that regions of the polyacrylates were more hydrophilic than PLLA.

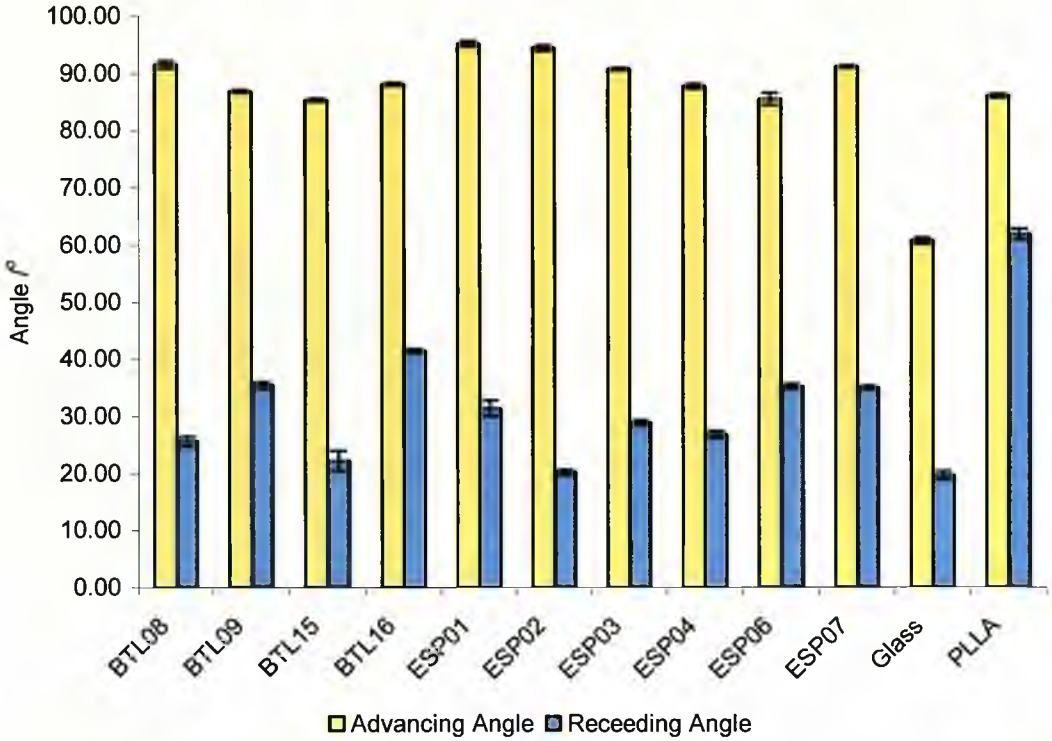

Figure 3-8 DCA measurements from polyacrylate substrates. BTL polymers were coated on to 22 x 22 mm cover slips and analysed in distilled water. Results represent the mean from a minimum of 5 replicates ± S.E.M. Most coatings displayed significantly different hydrophilicity and hydrophobicity from each other ($p<0.05$, Tukey model). The only combinations with no significant differences between both advancing and receding angles were ESP03 with ESP07 or BTL08, and BTL09 with ESP06.

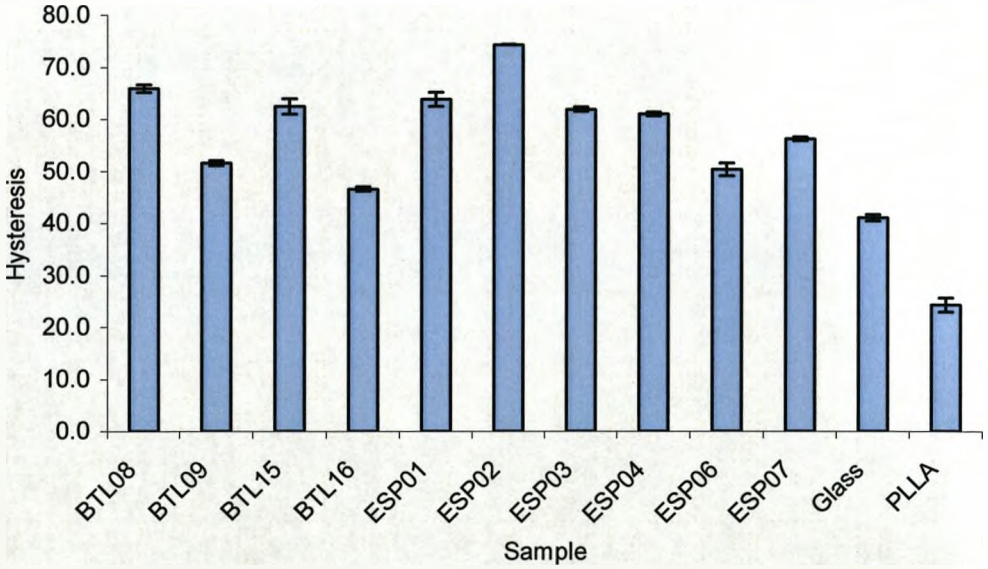

Figure 3-9 Contact angle hysteresis of polyacrylate substrates. Hysteresis was calculated as the difference between mean advancing and receding angles on each substrate. Results represent the mean from a minimum of 5 replicates ± S.E.M.

3.4.2. X-ray photoelectron spectroscopy

Surfaces of the polyacrylates were analysed at take-off angles of 15 and 45 degrees. This corresponded to penetration depths of approximately 2 and 6 nm into the substrates. Whilst these penetration depths are far too large to detect only the surface atoms, the smaller depth will favour the surface groups more and, therefore, comparison of these two results can suggest if a preference for the presentation of functional groups at the surface of the substrates exists.

Table 3-2 illustrates the XPS-determined and theoretical elemental composition (provided by BTL) of the tested polyacrylates in terms of percentage carbon, oxygen and nitrogen. The theoretical compositions were calculated from monomer concentrations, and values are included for several substrates which were unavailable for XPS analysis. Carbon and oxygen are present in the acrylate polymer backbone, as well as in functional groups, but nitrogen should only appear in amine functional groups. The accuracy of XPS-determined atomic concentrations is typically thought to be 10%, with rare atoms typically being underrepresented.

Table 3-2 XPS-analysed and theoretical atomic concentrations of polyacrylate substrates. The % composition of C, N and O are shown. Theoretical values were provided by BTL from monomer concentrations used at polymerisation.

Substrate	Angle	C	N	O
BTL08	45	75.9	1.0	23.1
BTL08	15	77.1	0.7	22.1
BTL08	Theoretical	72.69	1.12	26.18
BTL15	45	77.8	0.6	21.6
BTL15	15	78.3	0.6	21.1
BTL15	Theoretical	74.14	1.06	24.79
BTL16	45	81.0	0.5	18.6
BTL16	15	81.6	0.3	18.1
BTL16	Theoretical	76.92	0.95	22.13
ESP03	45	82.0	1.5	16.8
ESP03	15	78.5	1.3	20.0
ESP03	Theoretical	74.88	1.64	23.47
ESP04	45	80.7	1.7	17.3
ESP04	15	77.1	1.6	20.4
ESP04	Theoretical	75.11	2.05	22.83
ESP06	Theoretical	71.33	4.73	23.94
ESP07	Theoretical	74.73	2.18	23.09

The theoretical differences between the "BTLXX" designated polymers were small, with the intention of changing only the property of steric hindrance, and therefore fell within the expected noise of the technique. However, small differences were detected in nitrogen and oxygen concentrations, both decreasing slightly with increasing steric hindrance, agreeing with the trend from the predicted values. In addition, the C1s spectra (Figure 3-10) demonstrated a slight reduction in the proportion of C-O and C=O bonds, in comparison to C-C bonds, with increasing steric hindrance. Little difference was observed in the O1s spectra (Figure 3-11), corresponding to single and double bound oxygen atoms, maintaining approximately a 50:50 balance throughout all of the polyacrylates.

The XPS calculations for the "ESPXX" designated polymers also detected minor changes in polymer compositions, in line with predictions. Nitrogen content was slightly increased in ESP03 and ESP04, up to approximately two and three times that of the BTL designated polyacrylates, respectively. Whilst this was roughly in line with predictions, underrepresentation of rarer elements might contribute to an exaggerated difference.

Several polymers demonstrated a minor reduction in functional group elements closer to the surface. Less oxygen and nitrogen were typically found using a 15° TOA compared to the 45° TOA. This might suggest a preference for amine, carboxyl and hydroxyl groups to turn away from the surface of the polyacrylates, although again, this falls within the expected experimental noise. ESP03 and ESP04 also saw a 3 % rise in oxygen in the thinner section, which might suggest an increased presence of carboxylic groups at the surface.

These XPS results suggest differences between the polymers, in line with predictions, however, due to the accuracy of this technique, no conclusive evidence for distinction between the polyacrylates can be provided by this technique alone. It is also important to note that any differences in surface properties implied by these results are likely to lie within the experimental noise of the technique. Furthermore, as the polymers were analysed in a dry state under vacuum, they may not necessarily represent the substrates under culture conditions.

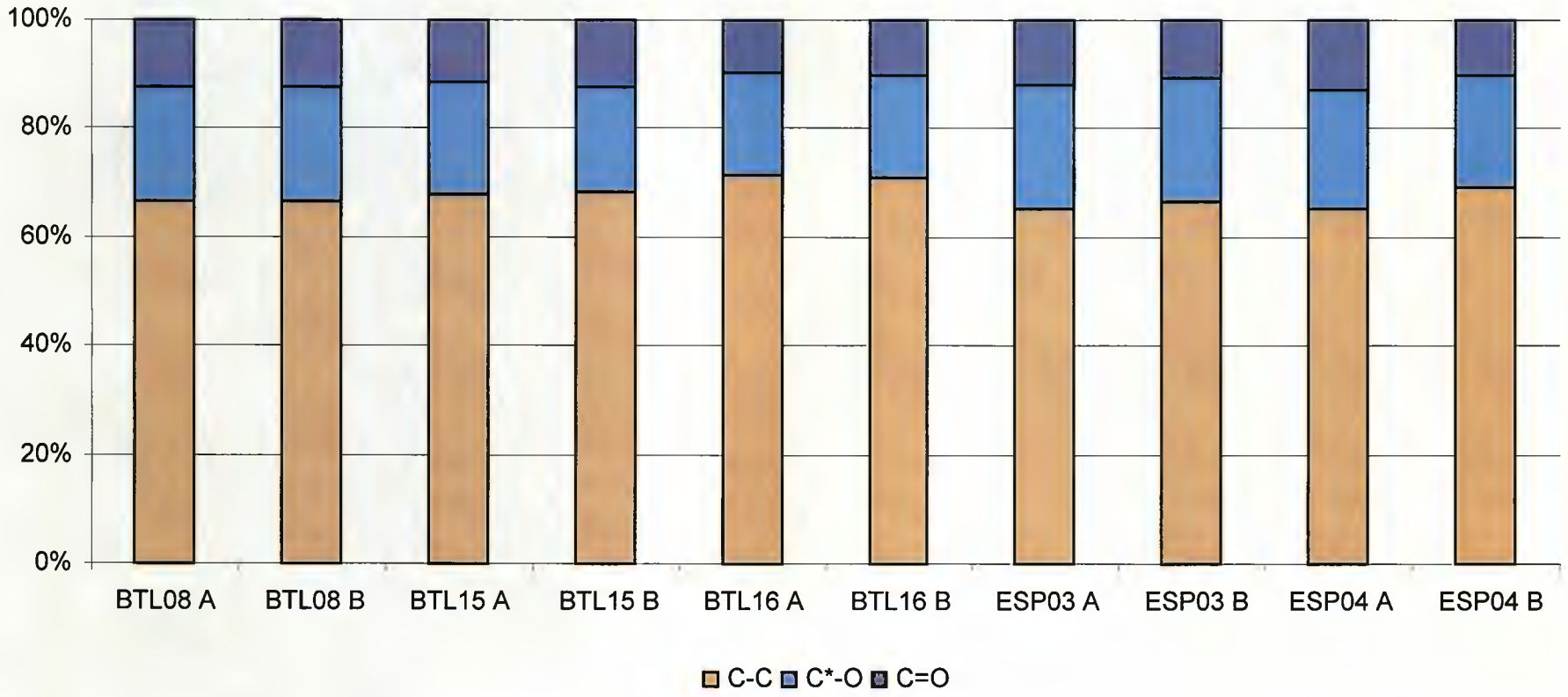

Figure 3-10 XPS surface analysis of polyacrylate substrates indicating carbon atom arrangement. Each polymer was examined at 15° (A) and 45° (B) angles to the surface corresponding to 2 and 6 nm depths. Proportions of carbon-carbon (C-C) and carbon-oxygen, single (C-O) and double (C=O) bound were calculated by curve fitting analysis of C1s spectra and displayed as a percentage of totals.

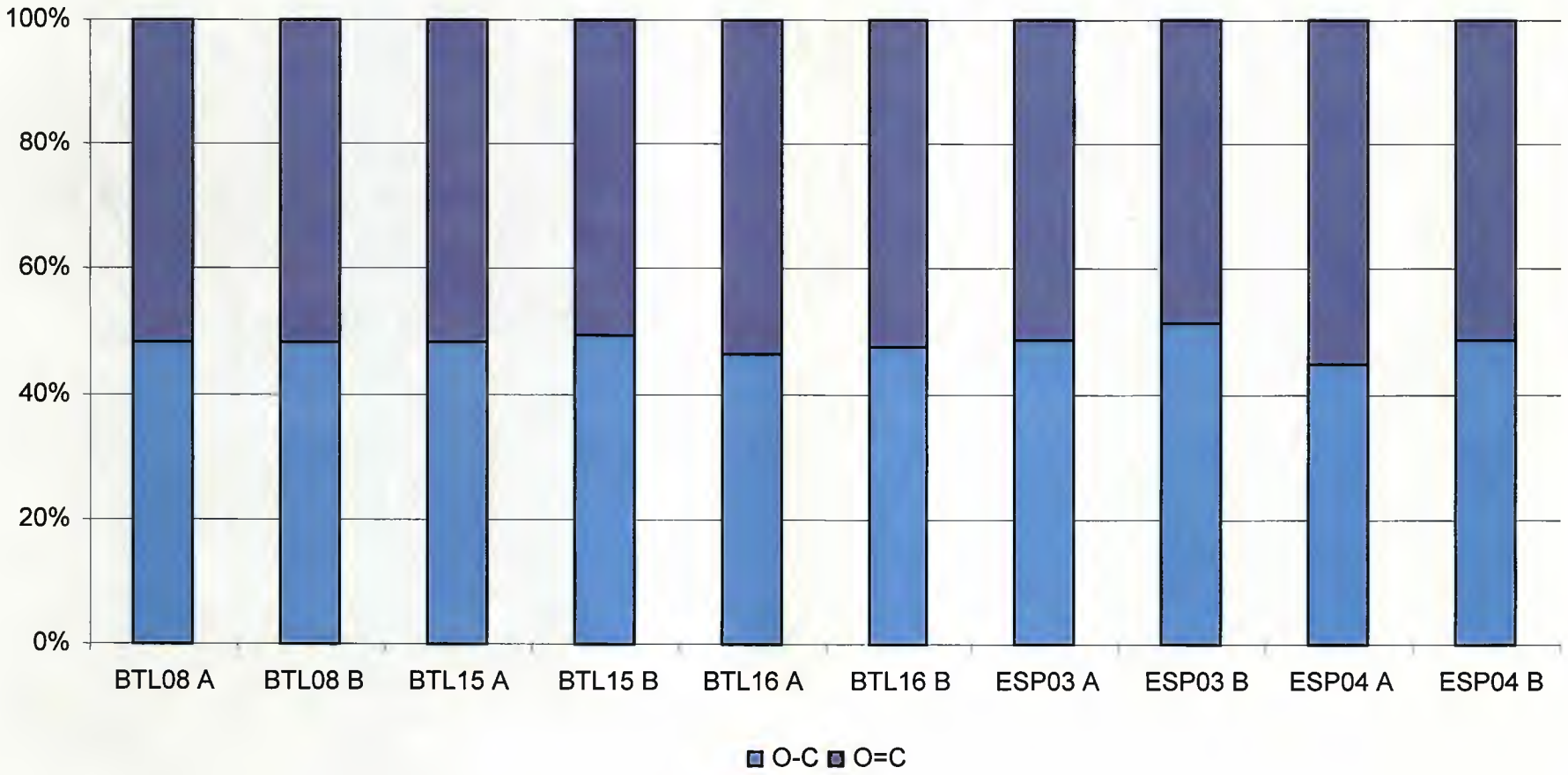

Figure 3-11 XPS surface analysis of polyacrylate substrates indicating oxygen atom arrangement. Each polymer was examined at 15° (A) and 45° (B) angles to the surface corresponding to 2 and 6 nm depths. Proportions of single (O-C) and double (O=C) oxygen were calculated by curve fitting analysis of O1s spectra and displayed as a percentage of totals.

3.4.3. Amine detection assay

To further examine the differences in surface chemistry of the polyacrylate substrates, an NHS-based amine detection assay was utilised to demonstrate the relative densities of amine functional groups at the surface of each substrate.

Significantly more amines were detected on the surface of the polyacrylate substrates ESP04, ESP06 and ESP07 (Figure 3-12) ($p<0.05$, Tukey model), and pre-treatment with NHS-acetate almost completely abolished these signals (Figure 3-13), confirming the specificity of the assay. ESP06 had a significantly higher signal than the rest of the substrates, in line with predictions (Table 3-1), followed by ESP07 then ESP04 ($p<0.05$, Tukey model). ESP07 had a significantly higher signal than ESP04 ($p<0.05$, Tukey model), despite similar theoretical amine monomer concentrations.

None of the other polyacrylates (BTL08, BTL15, BTL16 and ESP03) demonstrated a signal significantly greater than their background signal. Increasing the length of the enzymatic reaction did not further differentiate between the polymers. Signals remained indistinguishable from background even after extended periods of 30 min and 1 h with the TMB substrate. This may suggest that amines were unavailable for interaction with sulfo-NHS-biotin, or that none of these substrates contained a high enough surface density of amines to be detected using this assay.

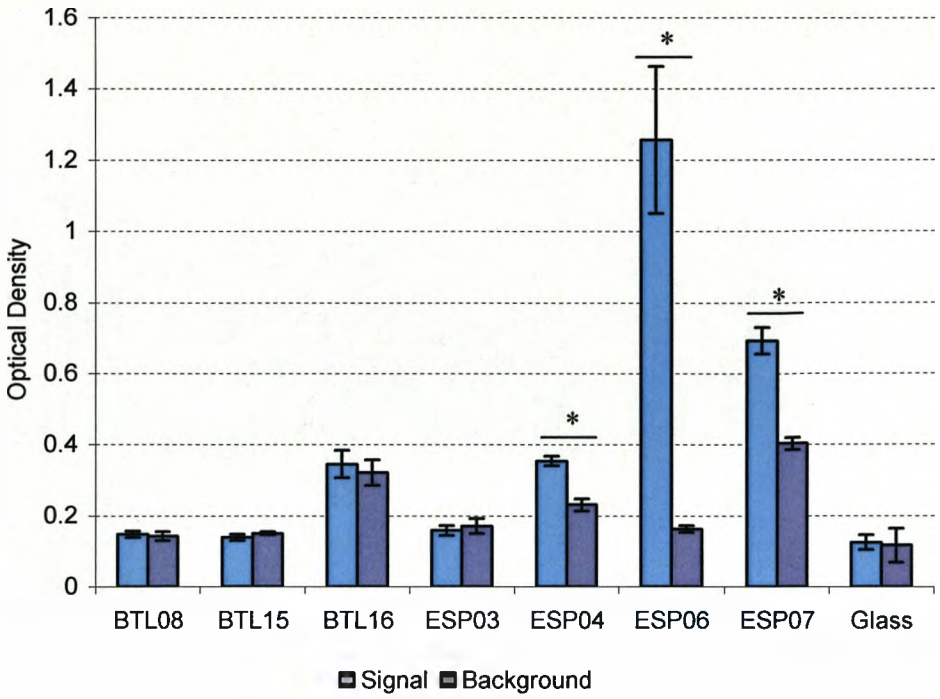

Figure 3-12 Relative amine concentrations on polyacrylate surfaces. Substrates were treated with sulfo-NHS-biotin and then streptavidin-HRP. Colorimetric enzyme assay was conducted by reacting with a TMB substrate for 15 min. Reactions were quenched with acid and read at 450 nm. For each substrate the results were compared to background readings. Results represent the mean of 3 replicates ± S.E.M. Asterisk indicates significant increase in signal over background ($p<0.05$, Tukey model).

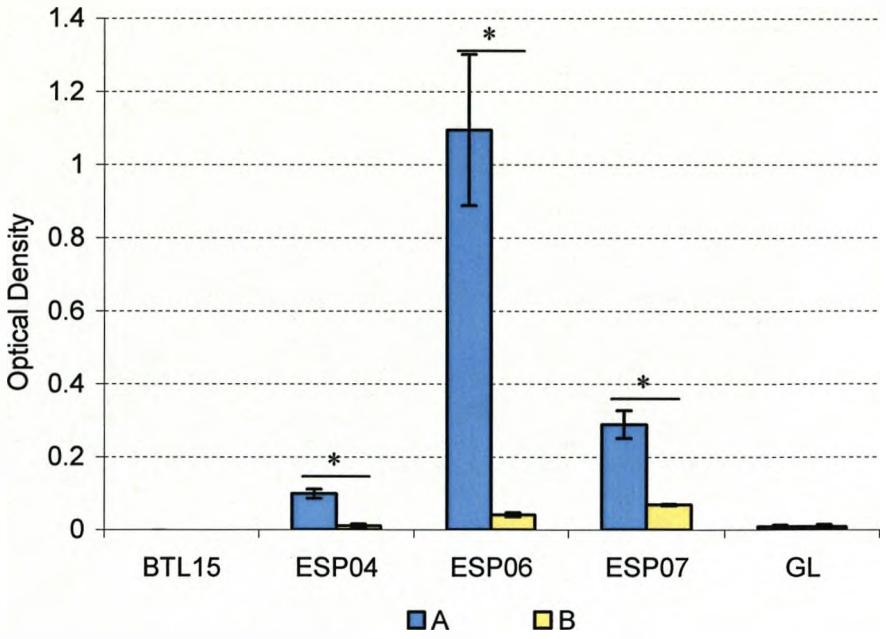

Figure 3-13 NHS-acetate blocking of amines on polyacrylates. Substrates were either treated normally (A) or with sulfo-NHS-acetate (B), followed by sulfo-NHS-biotin, followed by streptavidin-HRP. Colorimetric enzyme assay was conducted by reacting with a TMB substrate for 15 min. Reactions were quenched with acid and read at 450 nm. For each substrate the mean of triplicate background readings was subtracted from the end result, this was equal to 0.1 ± 0.05 for all except ESP07 which was 0.2. Results represent the mean of 3 replicates ± S.E.M. Asterisk indicates significant knockdown of signal ($p<0.05$, Tukey model).

3.4.4. Polyacrylate roughness

SICM was primarily used to image stem cells on the polyacrylate substrates, but also detected information about the topography of the polyacrylate surfaces. One polyacrylate from each line was chosen and compared to serum-coated glass. Interestingly, SICM demonstrated an innate roughness to the polyacrylate coatings. On analysis, this indicated that the polyacrylate coatings displayed a significantly higher surface roughness than serum-coated glass (Tukey model, $p<0.05$), with tested substrates following the trend: ESP03>BTL15>Glass (Figure 3-14).

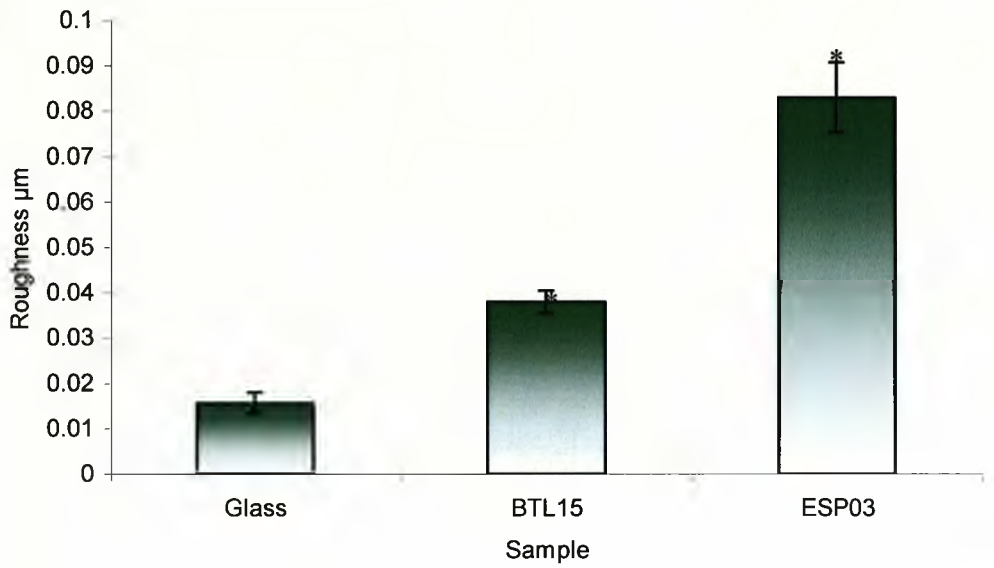

Figure 3-14 Roughness calculations from polyacrylate and control substrates. Average roughness was calculated from ionscope data using ScanIC Image software (Ionscope ltd). Results represent the mean of 10 replicates ± S.E.M. Asterisk indicates statistical significance from serum-coated glass control ($p<0.05$, Tukey model).

3.4.5. Polyacrylate hydration

Polymer swelling, due to water uptake, was investigated by immersing substrates in water for up to 24 h, followed by weighing to detect an increase in mass. Initially, polyacrylates were analysed as coatings on glass cover slips; however, no significant differences were found using these thin layers (data not shown). This may indicate that no significant uptake of water occurs in the polymer coatings, or that water uptake was undetectable in these thin samples using this technique.

To provide a larger sample of polyacrylate for hydration, sections of film (provided by BTL) were used; however, only BTL15 was available in this

form. Therefore, a thick film of BTL15 was prepared and analysed to model polyacrylate hydration, although it is important to note that the properties of the poly-acrylate film, including uptake of water, may differ from when it is bound to a glass cover slip.

Results indicated that significant swelling of the BTL15 film occurred under aqueous conditions (Figure 3-15). Peak hydration was achieved between 2 and 4 hours post-submergence with no further gain at subsequent time points. BTL15 demonstrated approximately 20% increase in weight due to hydration, suggesting that surface properties of the film may be altered under aqueous conditions. No significant reduction in mass of the polymer was detected following dehydration, demonstrating the lack of polymer degradation in BTL15.

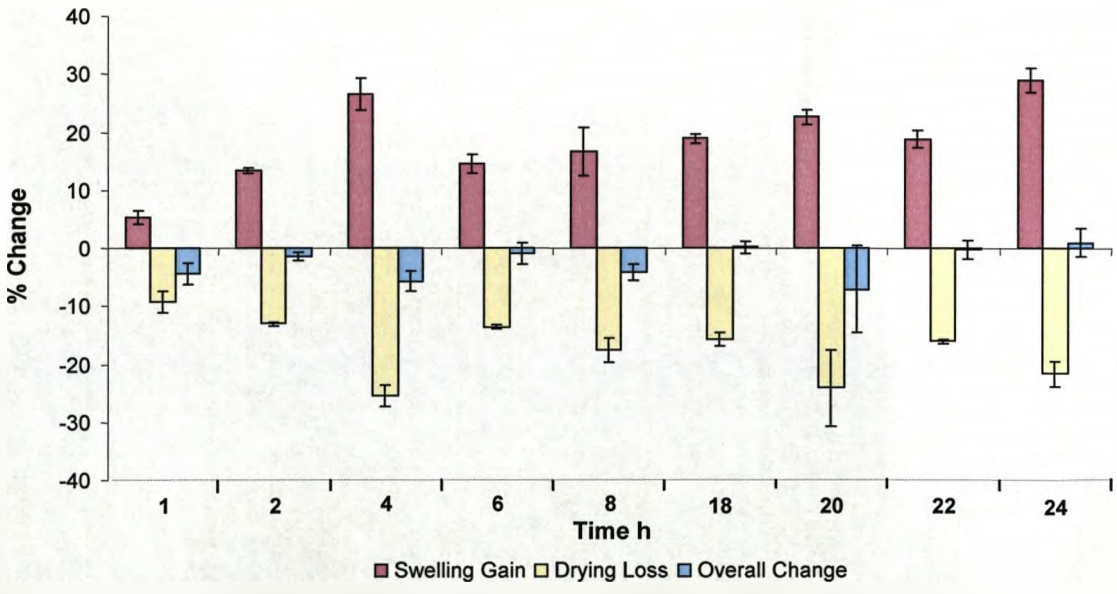

Figure 3-15 Hydration of polyacrylate BTL15 under aqueous conditions. Sections of polymer film were hydrated in water for up to 24 h. Samples were removed from water, touch dried and weighed. Dehydration of polymer film overnight at 60 °C confirmed no significant degradation. Results represent the mean of 3 replicates ± S.E.M. At all time points a significant increase in film weight indicated swelling of BTL15 ($p<0.05$, Tukey model). No significant degradation of the polymer was detected.

3.5. Discussion

In this chapter, the polyacrylate substrates were characterised with a range of surface analysis techniques to identify differences in the physicochemical properties of each surface, and how these related to their theoretical compositions. These differences were further analysed in subsequent chapters by the response of stem cells to culture in contact with them.

Whilst little change was demonstrated in the elemental composition, following theoretical values, significant differences were demonstrated between the polyacrylate substrates in dynamic contact angle and surface amine content. This demonstrated that simple alterations in polymer chemistry, effected through the BTL proprietary technology, could generate polyacrylate coatings with discrete surface properties, which in turn might influence their suitability as a culture substrate for stem cells.

3.5.1. Dynamic contact angle

Previous work has shown that the degree of steric hindrance in synthetic polymers can affect surface properties, through restricting chain rotation and obscuring functionality (Kowalewska 1999; Safa 2004). Therefore, it is likely that steric hindrance affected the surface properties of the BTL

substrates by altering the combined presentation of carboxylic acid, amine and hydroxyl functional groups. Furthermore, alkyl side groups are hydrophobic and the presence of larger alkyl groups, in the polyacrylates with higher steric hindrance, may have made the surfaces more hydrophobic directly.

Steric hindrance is expected to both prevent the orientation of functional groups to the surface of the substrate and to mask functional groups at the surface, in the case of the polyacrylate substrates, this would inhibit the interaction of amine, carboxyl and hydroxyl groups with water, making the polymers more hydrophobic. Alkyl groups are hydrophobic and will reduce wettability, whereas amine, carboxyl and hydroxyl groups will interact with water through hydrogen bonding and increase wettability. The results from this chapter suggest that steric hindrance negatively influences wettability of the polyacrylate substrates.

However, the most hydrophilic substrate, BTL15, contained intermediate steric hindrance, suggesting that the hindering side chains may also have a role in orientating functional groups to the surface. Furthermore, an increase in the hydrocarbon content, when ethyl groups are replaced with butyl, may also contribute to a more hydrophobic substrate. Surprisingly, the most hydrophilic of all the polyacrylates was again BTL15, despite higher theoretical proportions of amine, hydroxyl and carboxyl groups in some of the other polymers (e.g. ESP01, ESP02, & ESP06) (Table 3-1). There are conflicting accounts of the influence of surface wettability on

the behaviour of cells cultured in contact with them. Some studies indicate a correlation between wettability and cell attachment, likely mediated via enhanced serum protein adsorption (Harrison 2004; Zhu 2004; Hanson 2007), whereas others suggest no correlation exists, or that the specific nature of the functional group is the governing attribute (Ma 2003; Neuss 2008). One explanation could be that common charged functional groups, such as amine and carboxyl groups, promote cell attachment to varying degrees and, therefore, increasing these components enhances cell attachment, whereas increased wettability is a derived consequence. If wettability does correlate with cell attachment, BTL15 would be expected to perform the best out of the polyacrylate substrates. In contrast, plain glass demonstrated significantly higher hydrophilicity than all polyacrylate substrates.

The high hysteresis on all polyacrylate substrates suggests distinct regions of hydrophilic and of hydrophobic behaviour. This causes pinning of the water, as it either sticks to or avoids particular sections on the substrate. This may indicate heterogeneous distribution of functional groups across the polyacrylate surfaces, perhaps with clustering of the functional groups. Hysteresis also shows some positive correlation with steric hindrance, as well as negative correlation with wettability. This may suggest that steric hindrance has an alternative role in localising surface functionality. Functional groups are known to reorganise at the solid-liquid interface of a polymer surface under aqueous conditions, and this can be indicated by contact angle hysteresis (Chen 1991). Steric hindrance

effects should work to reduce this reorganisation, which is inferred by the reduced hysteresis on BTL substrates with high steric hindrance.

ESP03 had a similar theoretical composition to BTL15, but with an increased proportion of amine groups, no hydroxyl groups, and the same proportion of carboxyl groups. This resulted in an increase in advancing and receding angles, a decrease in wettability, which was likely indicative of reduced overall presence of hydrophilic side groups. Increasing amine content and reducing carboxyl content in ESP04, relative to ESP03, resulted in a decrease in advancing and receding angles. Theoretically, amine content increased equivalent to the carboxyl content decrease, and so overall change in hydrophilic functional groups should not have changed, therefore, amine groups would appear to make the polyacrylates more hydrophilic. Alternatively, changes to side group composition may alter the manner in which the polyacrylate displays surface functionality. as described below.

An important consideration when discussing surface properties is the influence of polymer reorganisation and the interactions between functional groups. The structure of a polymer is governed by many interactions, both with itself and its environment. Hydrophobic regions within biological polymers, such as proteins, influence their secondary structures. The hydrophobic regions will group together when in a polar environment, such as water, and influence protein folding such that they are positioned inside the structure and thus minimise their interaction with

the water. In a similar way the polyacrylate substrates when in an aqueous environment, as in cell culture, may reorganise the surface structure such that the hydrophobic functional groups rotate to beneath the surface and the hydrophilic regions remain at the surface. However the ability of the surface to reorganise will depend on the interactions of the functional groups within the surface of the polymer and steric hindrance limiting chain mobility. Within the polyacrylates hydrogen bonding will occur between polar groups, such as hydroxyl and amine, on the same chain and different chains, resulting in a tangle of folded polymer chains. Under aqueous conditions hydrogen bonding can also occur between these groups at the surface and the surrounding water molecules, though in general H-bonding between groups in the polymer will be favoured entropically. This is particularly true if H-bonding to water results in water molecules being trapped and losing their ability to freely exchange with bulk water. So the actual surface presented to the cells will be dependent on the interfacial energetic.

3.5.2. X-ray photoelectron spectroscopy

The XPS results demonstrated very little difference in elemental composition between the tested polyacrylate substrates. In particular few discernable differences were detected between types of bond in the C1s and O1s spectra. The detected percentages of the less common nitrogen and oxygen elements were lower than theoretical values, as was expected with this technique. Little conclusive evidence could be gleaned

from these data, due to the minimal changes in composition, typically less than one percent. However, minor differences in composition were suggested between the polyacrylate substrates, indicating that each substrate was chemically distinct, although surface contaminants could have contributed to these differences.

Those polyacrylates designed to differ solely by the degree of steric hindrance within polymer chains (BTL08, BTL15 and BTL16) demonstrated small decreases in oxygen and nitrogen content in line with increases in steric hindrance. These findings somewhat follow a trend in the theoretical values, where the relative oxygen and nitrogen percentage is reduced, as the size of the alkyl side group is increased, although detected differences are larger than those predicted. These findings might fit with increases in the size of alkyl side groups, but could also point to steric hindrance masking and turning functionality away from the surface (Kowalewska 1999). However, results from DCA indicated that BTL15 was the most hydrophilic substrate, which would be expected to coincide with highest nitrogen and oxygen content near the surface, corresponding to amine, carboxyl and hydroxyl groups. BTL16 demonstrates the least nitrogen and oxygen percentage content, which follows DCA findings that it was the most hydrophobic of the three.

XPS is a surface sensitive technique, providing elemental and molecular information of approximately the outmost 10 atomic layers in an ultra high vacuum (UHV) environment. Angle resolved XPS can help to reduce the

analysis depth with lower angles providing information from closer to the surface than larger angles. This can help to provide some information on the concentrating of specific elements or molecules at the surface. It should be remembered, however, that XPS is only semi-quantitative with a sensitivity of approximately ±10%. Therefore, the XPS data must be interpreted taking these considerations into account. Furthermore, in an UHV environment, as in the XPS, the driving force for reorganisation will be different and so it is likely that the surface chemistry will not reflect that presented to the cells in aqueous solution. Direct comparison of the wettability and XPS results are, therefore, difficult.

3.5.3. Amine content

One of the key distinctions between these polyacrylates was amine content and this result confirms a significant increase in amine content on these substrates. In comparison to the XPS results, the NHS-based amine detection assay demonstrated some far more evident differences between the polyacrylates. Many of the polyacrylates (BTL08, BLTL15, BTL16, ESP03) demonstrated no significant presence of surface amines, which might indicate a high minimum detection range in the assay. Surface amine content on the polyacrylates ESP04, ESP06 and ESP07 rose above the detection threshold, whereas the concentration of surface amines on other polyacrylate substrates may have been insufficient to register in this assay. Amine groups were present in all the polyacrylates tested, as confirmed by XPS nitrogen detection (3.4.2), therefore, if they

are not detected at the surface they may be unavailable, due to non-covalent bonding with neighbouring groups, or they may simply not be present at the surface of those polyacrylates. As described above (3.5.1), polymer organisation is complex and several interactions can occur that might restrict the availability of amine at the surface.

ESP06 had by far the highest surface amine content, which was approximately ten times the signal detected on ESP04, and four times that on ESP07. The theoretical change in amine content between ESP06 and these polyacrylates was a little over doubling. Furthermore, ESP07 demonstrated significantly higher surface amine presentation than ESP04, despite similar theoretical amine monomer concentrations. These results highlight the significance between polymer composition and surface properties. The changes to polymer composition have altered the availability of groups at the surface of these polyacrylates. Hydrogen bonding may be reduced when carboxyl groups, in ESP04, are replaced with hydroxyl, in ESP07, resulting in an increase in available amine groups at the surface. Steric hindrance may also be altered in this case, as hydroxyl groups are smaller than carboxyl, which may in itself lead to changes in organisation of the polyacrylate and changes to functional group availability at the surface.

3.5.4. Roughness

An unexpected result was the increased roughness detected on some polyacrylate substrates. ESP03 demonstrated significantly higher surface roughness than BTL15, which in turn was significantly higher than glass. However, it was difficult to ascertain what contribution the coating method made, and whether there were differences in polymer structure that were also influencing roughness. Furthermore, no specific measures were present in the coating method to control for the evenness of coatings.

In this study, a negative relationship between surface roughness and wettability is suggested, where the roughest substrate, ESP03, has the lowest wettability, whereas the least rough, glass, has the highest wettability. However, differences in surface chemistry will also contribute to changes in wettability. The testing of additional polyacrylates would be necessary before any trends between roughness and other surface properties could be reliably established.

Roughness may contribute to other surface properties, such as wettability, but also to how cells and proteins interact with the surface, and ultimately, the behaviour of cells in contact with that surface. Several studies have shown substrate roughness influencing cell behaviours, including adhesion and differentiation (Dalby 2006; Kommireddy 2006; Silva 2009).

3.5.5. Polyacrylate hydration

The culture environment is by nature aqueous, therefore the interactions of a polymer substrate with water will be vital in identifying its suitability as a culture substrate. These findings demonstrated that a film of the polyacrylate BTL15 swelled under aqueous conditions, to approximately 120 % of dry weight. Theoretical differences between the polyacrylate substrates were small, therefore it is likely that all of the polyacrylates would act similarly and uptake some water, possibly to a greater or lesser extent.

Peak swelling of BTL15 was recorded at four hours, after which the wet weight plateaued, suggesting that uptake of water into the polymer was ongoing for several hours after immersion. This might indicate a lengthy (2-4 h) equilibrating period in which the polymer structure may change. The absorption of water by BTL15 demonstrates the importance of the aqueous environment in determining the properties of any culture substrate. Water penetration into the polyacrylates will be accompanied by further hydrogen bonding, charge-charge interactions and subsequent reorganisation of polymer chains. However, both the degree of interaction with water and the ability of water to penetrate into the surface will be dependent upon the composition of the polymer. The use of hydrogels as culture substrates is common (Fisher 2010), and the degree of water uptake is likely to affect substrate properties. Water uptake may alter dynamics in polymers, enabling chain rotation and possibly facilitating

additional steric effects, but may also alter physical properties of the substrates such as stiffness, which can affect the behaviour of cells cultured on them (Evans 2009).

3.5.6. Conclusion

The substrate characterisation carried out in this chapter suggests that the polyacrylates differ very slightly in composition and surface properties. Consolidating data from the techniques used confirms that despite very similar chemical composition, demonstrated by XPS analysis (3.4.2), each polyacrylate displayed unique surface properties, including wettability (3.4.1) and functional group composition (3.4.3). The organisation of polymers is complex, involving many separate interactions, and may be altered in an environment dependent manner. The composition will ultimately dictate the surface properties, however, with each alteration to the polyacrylates, both the available functionality and the consequence to polymer organisation must be considered.

A further caveat is reorganisation of the polymer due to the influence of protein and cell contact, therefore, none of the conditions used to analyse the polyacrylates might reflect their surface properties under cell culture conditions. The definitive test for these substrates will be how cells respond to them in culture. The following chapters document the response of embryonic (Chapter 4) and mesenchymal (Chapter 5) stem cells to culture on BTL polyacrylate culture substrates. The behaviour of

cells cultured on the polyacrylate substrates was considered to be an additional surface characteristic.

4. The ability of polyacrylate substrates to support the growth of mESCs

4.1. Introduction

Despite recent progress in understanding the mechanisms behind ESC self-renewal, much remains unknown. One significant obstacle is the ability to culture ESCs under defined conditions. Typical culture techniques require the presence of serum, which raises concerns about exposure to animal components, as well as the consistency of conditions (Martin 2005). Whilst some progress has been made in developing defined growth medium for ESC maintenance, culture substrates remain ill-defined (Ludwig 2006; Tsuji 2008).

Little is known of the role of cell-substrate interactions in regulating mESC behaviour. Elucidating the mechanisms is made difficult by commonly used substrates consisting of poorly defined mixtures of ECM proteins and growth factors. Recent work has shown that mESCs can be maintained in the short-term, under serum-free conditions, on defined synthetic substrates comprising specific concentrations of carboxyl functional groups (Wells 2009). In the long-term, the mESCs remained undifferentiated, but the degree of population expansion was significantly reduced compared to controls, possibly due to cell detachment (Wells

2009). Some support of hESC culture under defined conditions has also been demonstrated recently with a synthetic polymer coating, however, analysis of the substrates surface properties is lacking (Villa-Diaz 2010).

Several artificial substrates have been shown to successfully support self-renewal of mouse and human ESCs over short-term culture (Harrison 2004; Newman 2004; Kroupova 2006; Li 2006; Willenberg 2006; Villa-Diaz 2010). However, the study of combinations of functional groups on mESC behaviour under defined conditions is much less studied, and little support for subsequent passaging and longer-term self-renewal has been shown.

4.1.1. The use of polyacrylate substrates for mESC culture

Novel synthetic **ac**cele**r**ate™ polymeric coatings, manufactured by Biomer Technology Limited, are an ideal substrate to study the effects of combined functional groups on mESC behaviour. These polymers have previously been demonstrated, through extensive *in vitro* studies, to significantly promote the growth of endothelial cells versus traditional tissue culture substrates (Nickson 2008). Acrylate polymers have also been studied as mESC culture substrates by other groups demonstrating their biocompatibility (Horak 2004; Kroupova 2006), though maintenance of self-renewal was not demonstrated.

The **ac**celer**a**te™ polymer is comprised of a multi-monomeric acrylic based polymer containing hydroxyl, amine and carboxyl functional groups. Controlled synthetic procedures ensure that these functional groups are evenly distributed throughout the polymeric backbone and that the appropriate stereochemistry will present these groups at the surface following application of the coating. Substrate analysis in the previous chapter (3.4) has demonstrated distinctions between the polyacrylate substrates, and substantiated some of their theoretical properties.

There are several advantages to using these substrates to present chemically defined surfaces for stem cell culture. Firstly, the functional group proportions and distributions can be accurately controlled to present defined combinations of functional groups at the surface. Furthermore the polymers can be easily handled and are simple and cheap to produce.

The approach taken in this study has been to assay polyacrylate biomaterials, which had previously demonstrated discrete capacity to support the colonization and growth of human aortic endothelial and smooth muscle cells (Nickson 2008). These polyacrylates differed in the degree of steric hindrance present within their polymer chains, which influenced the presentation of hydroxyl, carboxyl and amine functional groups at the surface of the substrates. Further development of the polyacrylates aimed to imitate typical cell contacts, with similar functional group composition and distribution of ECM proteins and attachment

motifs, by modulating proportions of hydroxyl, carboxyl and amine side groups as well as size of spacer monomers within the polymer chains. As described in the previous chapter (3.3), some of the polyacrylates were designed with similar functional composition of fibronectin and laminin, and others more specifically of the RGD integrin-binding motif.

The aim of the work described in this chapter was to design synthetic substrates capable of supporting mESC self-renewal under defined culture conditions. In the subsequent chapter, the ability of these substrates to regulate the behaviour of mesenchymal cell types will be investigated.

4.1.2. Aims

(i) Determine the ability of the novel polyacrylate substrates to support short-term mESC population expansion.

(ii) Establish the effect of polyacrylate substrates on mESC behaviours, including self-renewal, proliferation and attachment.

(iii) Determine the ability of polyacrylate substrates to support long-term culture of mESC populations.

4.2. Results

4.2.1. The ability of chemically defined polyacrylate substrates to support short-term growth of mESCs under serum free conditions

The initial substrates screened for support of mESC culture were previously found to demonstrate differing levels of support for colonisation and growth of human endothelial cells (Nickson 2008). In order to assay the ability of polyacrylate substrates to support mESC colonisation and growth E14 mESCs were seeded onto substrates for four days in serum-free medium in the presence of LIF and cell growth was quantified with crystal violet end-point assays.

Crystal violet bound to DNA and was then solubilised using a detergent. The optical density of the solution was linearly related to cell number and was therefore used as a representation of cell number to be compared between controls and other samples. It was found that BTL09, ESP01 and ESP02 conferred very high background crystal violet staining and visual assessment (data not shown) confirmed little support of mESC culture on these substrates. They were therefore excluded from further analysis.

The crystal violet assay following 96 h culture demonstrated that, in most cases, the polyacrylate substrates supported significantly higher levels of

cell growth than plain glass (Figure 4-1). It was determined that BTL15 was best able to support mESC growth, performing significantly better than other polyacrylates with relative cell numbers that were more than 2-fold higher than plain glass controls. Some correlation with wettability, recorded in chapter 3 (3.4.1), was apparent, with BTL15, the most hydrophilic polyacrylate, being the most successful. However, the plain glass substrates were the most hydrophilic substrates tested, but they also performed significantly worse than most of the polyacrylate substrates. Furthermore, the enhanced amine content in ESP03 and ESP04 did not improve mESC growth and may have reduced their ability to support mESC culture. However, the serum coated positive control in all cases performed significantly better than polyacrylate substrates.

The lower mESC expansion observed on polyacrylate substrates compared to the serum coated controls may be due to one or more of the following: (i) differentiation, resulting in extended population doubling time; (ii) absence of ECM, and associated growth factors; (iii) reduced rate of proliferation; (iv) increased cell death; (v) reduced cell attachment. These factors were, therefore, investigated to determine which reduced the effectiveness of, and may, therefore, provide the focus of further development of, the synthetic substrates.

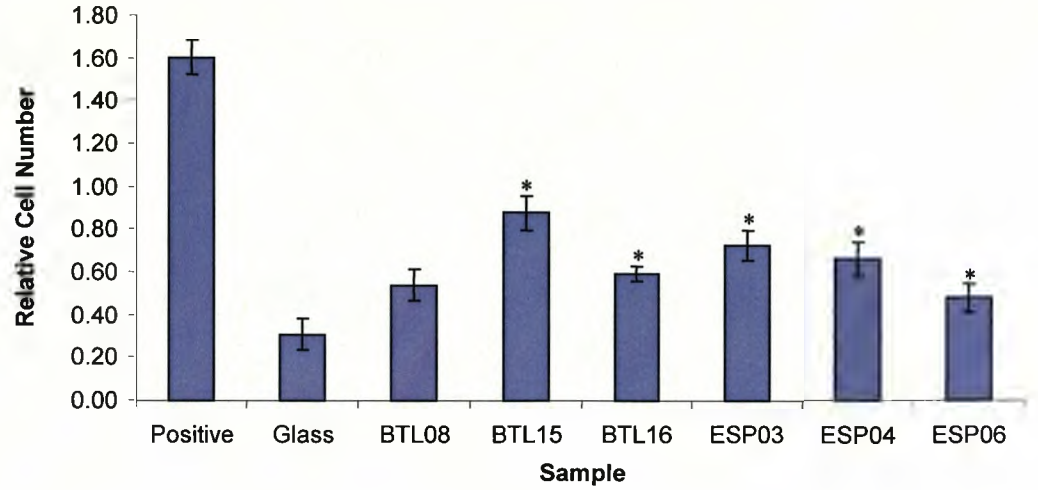

Figure 4-1 Crystal violet staining of mESCs cultured for 96 h on BTL substrates in serum free conditions. Cells were seeded onto substrates at $5x10^4$ per well. Gelatin + 10% FCS-coated and plain glass cover slips were used as positive and negative control substrates. OD was recorded at 595 nm and used to compare relative cell density. Cell numbers on BTL substrates were significantly lower than on positive control (Tukey model, $p<0.05$). Asterisk indicates BTL substrates where OD was significantly higher than the negative control ($p<0.05$, Tukey model). Results represent the mean of 3 biological replicates ± S.E.M. Background staining on substrates was within 0.2 ± 0.1.

4.2.2. The effect of polyacrylate substrates on mESC self-renewal

The differentiation status of the mESCs cultured in contact with polyacrylate substrates was assessed morphologically and with AP staining following 96 h culture. Normal mESC colony morphology was observed on the positive control substrate (Figure 4-2); these colonies were well rounded, compact and multi-layered. On substrates BTL15, BTL16, ESP03 and ESP04, the majority of colonies also had ESC-like characteristics; however, they were typically smaller and often irregularly shaped. Cells cultured on BTL08 formed colonies of similar sizes to other BTL substrates, but they were less compact and the cells were typically spread as a monolayer. The condition of colonies on ESP06 indicated that mESCs were growing atypically and were unhealthy: these colonies

appeared fragmented and dispersed, and were more similar to loose aggregates of cells than ESC colonies.

Strong AP activity was detected in all of the large rounded colonies present on BTL15, BTL16, ESP03 and ESP04, demonstrating that cells cultured on these substrates remained undifferentiated (Figure 4-3) and supporting the morphological analysis. AP was also detected in the smaller colonies on the negative control substrate of plain glass. In the less compact colonies, such as found on substrate BTL08, the stain for AP activity appears slightly reduced, however, a lack of multilayering in these colonies may also have contributed to this. The mESCs on substrate ESP06 were often present as single cells rather than colonies. AP activity was detected, but again appears slightly reduced, possibly due to lack of multilayering.

AP activity detection indicated that the mESCs were not differentiating on polyacrylate substrates over short-term culture. Morphological analysis indicated that mESCs on BTL08 and ESP06 were forming atypical colonies (Figure 4-2), which might suggest differentiation, however, AP activity was detected in these cells, indicating that they remained undifferentiated following 96 h culture. On the majority of polyacrylate substrates; BTL15, BTL16, ESP03 and ESP04, colonies were ESC-like and remained undifferentiated. Therefore, the reduced mESC growth on these polyacrylate substrates did not appear to be caused by differentiation of the mESCs.

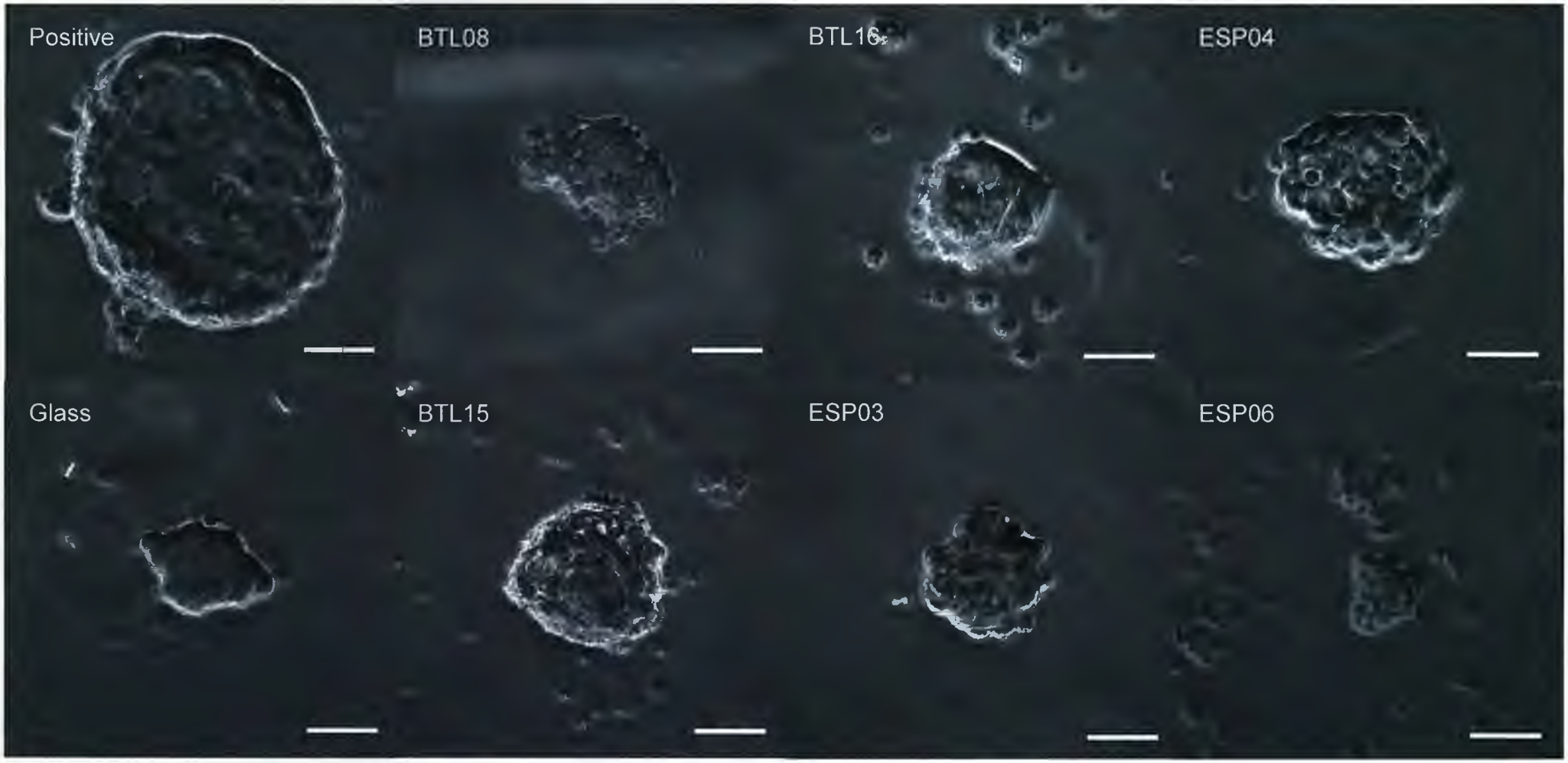

Figure 4-2 Phase contrast images demonstrating differences in E14 mESC colony size and morphology when cultured on BTL substrates. E14 mESCs were fixed in 4 % (w/v) PFA and imaged under bright field following 4 day culture in ESC medium. Cells were seeded onto substrates at 5x104 per well. Gelatin + 10% (v/v) FCS coated and plain glass cover slips were used as positive and negative control substrates. Following 96 h culture, cells were fixed and imaged under bright-field microscopy. Three field of view were examined from each of three replicate substrates were examined. Scale bar 50 µm.

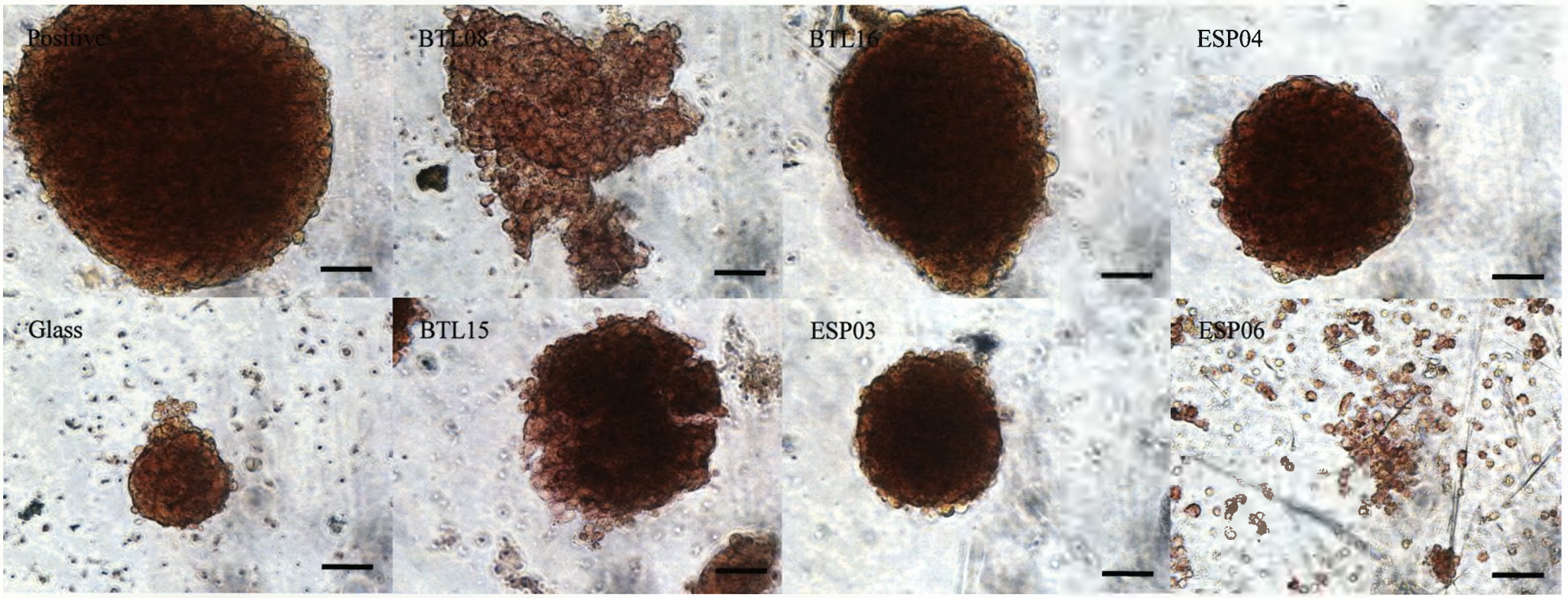

Figure 4-3 Bright field images demonstrating differentiation status of mESCs cultured on polyacrylate substrates. E14 mESCs were stained for AP activity after 96 h in ESC medium. Cells were seeded onto substrates at 5x104 per well. Gelatin + 10% (v/v) FCS coated and plain glass cover slips were used as positive and negative control substrates. The majority of polyacrylate substrates stain strongly for alkaline phosphatase activity, indicating self-renewal of these mESCs. Apparently lower AP activity at the periphery of colonies is typical and is likely due to the colony having a depth of fewer cells. Glass, BTL08 and ESP06 may demonstrate slightly reduced AP activity, however reduced multilayering may also contribute. Three field of view were examined from each of three replicate substrates were examined. Scale bar 50 µm.

4.2.3. The effect of polyacrylate substrates on mESC proliferation

To investigate the effect of the polyacrylate substrates on mESC proliferation, a BrdU uptake assay was used. The mESCs were pulse labelled for 15 min following 24 h culture on substrates (2.2.2.7). BrdU uptake was then detected by antibodies and the proportion of BrdU positive cells determined by comparison with DAPI (Figure 4-4).

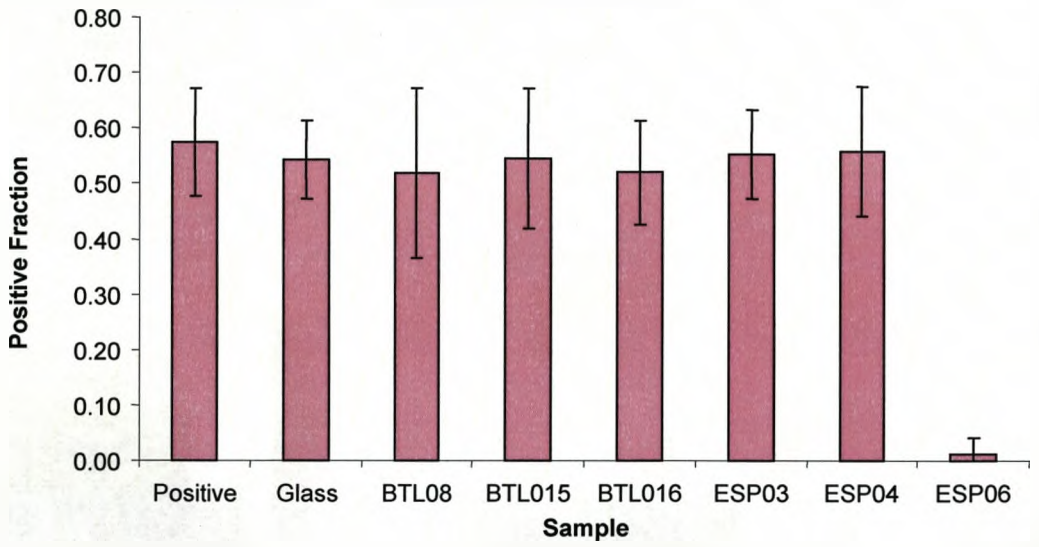

Figure 4-4 BrdU uptake in E14 mESCs cultured overnight on BTL substrates and pulse labelled for 15 minutes. Gelatin + 10% (v/v) FCS coated and plain glass cover slips were used as positive and negative control substrates respectively. Only ESP06 demonstrated a significant difference from other substrates. Results represent the mean of 9 separate fields of view across 3 replicate substrates ± S.E.M.

No significant difference was found between any of the controls and the polyacrylate substrates, excluding ESP06 (Tukey model $p>0.05$, Figure 4-4), with approximately half the mESCs observed staining positive for BrdU. Most commonly it was cells on the edges of colonies that were dividing (Figure 4-5). The mESCs on ESP06 were found to be barely proliferating at all, and only a pair of BrdU positive cells was found across

all of the replicates. DAPI staining showed very little multilayering and few colonies on ESP06 (Figure 4-5).

4.2.4. The ability of polyacrylate substrates to support the short-term growth of mESCs in the presence of serum

In routine culture, mESCs are maintained on serum coated tissue culture plastic in ESC medium. To investigate if reduced growth of mESCs on polyacrylate substrates was due to the absence of serum proteins, cells were cultured on polyacrylate substrates coated with serum and the degree of population expansion was determined after four days.

The results showed that coating the polyacrylate substrates with serum had little effect on mESC growth (Figure 4-7). The mean cell number was increased on BTL08 and BTL15 in the presence of serum, but the increase was not significant (Tukey model, $p>0.05$). Unlike the polyacrylates, coating plain glass substrates with serum resulted in a significant increase in cell number. Surprisingly, the mean cell number on ESP04 and ESP06 was significantly lower following serum coating (Tukey model, $p<0.05$) (Figure 4-6). The inability of the polyacrylate substrates to support mESC growth when coated with serum suggested that either proteins necessary for cell attachment were not attaching to the polyacrylate substrates, or that protein conformation on the substrates was unable to support mESC attachment.

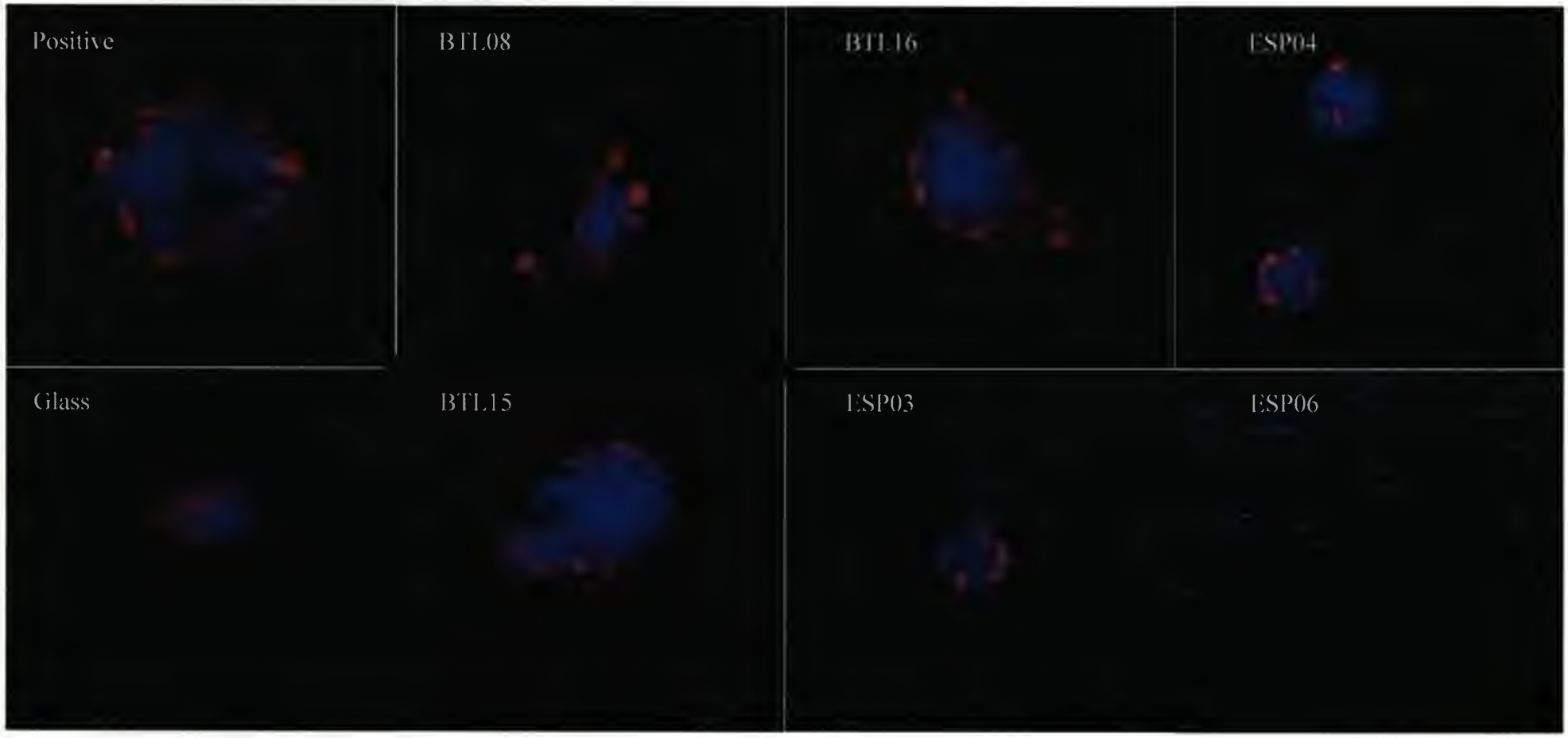

Figure 4-5 Representative images of BrdU uptake in colonies on BTL substrates. E14 mESCs were cultured for 24 h in ESC medium before 15 min pulse labelling with BrdU. Samples were stained for BrdU (red) and counterstained with Dapi (blue).

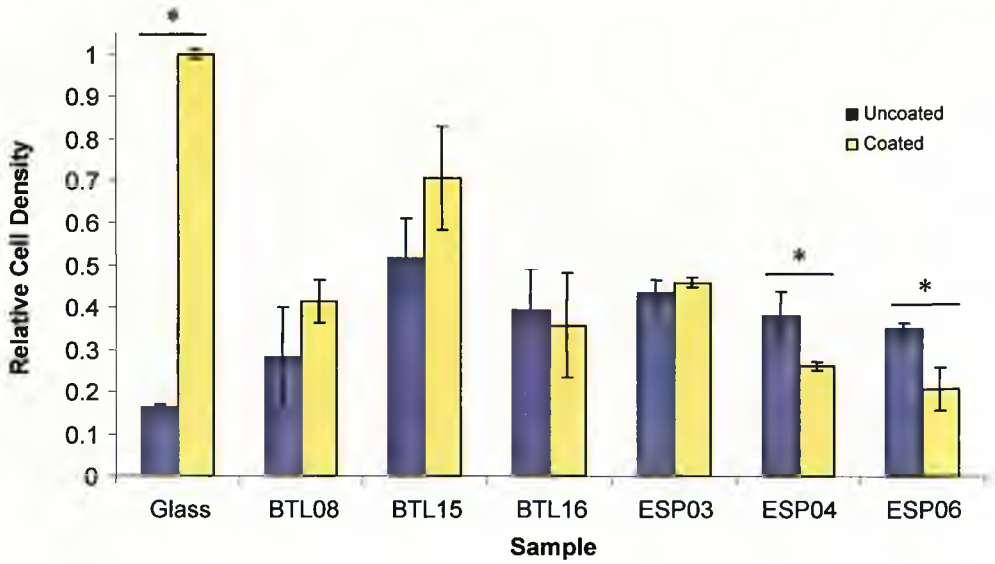

Figure 4-6 The effect of serum coating on mESC growth on polyacrylate substrates. Cells were seeded at $5x10^4$ per well and cultured for 96 h in ESC medium. Plain glass was used for controls. Values were normalised to serum coated glass. Coating glass substrates with serum resulted in a significant increase in cell numbers, whereas on polyacrylate substrates, serum coating resulted in no significant increase ($p<0.05$, Tukey model). Asterisk indicates significant difference between uncoated and serum-coated substrates ($p<0.05$, Tukey model). Results represent the mean of 3 biological replicates ± S.E.M.

To assess if serum coating was ineffective due to a lack of serum protein adsorption to polyacrylate substrates, a protein adsorption assay was conducted using bicinchoninic acid (BCA). Substrates were coated with 10% (v/v) FCS, and then screened for total adsorbed protein. The assay showed that there were no significant differences between protein adsorption on any of the polyacrylate substrates or controls (Figure 4-7). The polyacrylate substrates demonstrated a slight increase, but this was not significant. This demonstrated that insufficient protein adsorption to polyacrylate substrates was not contributing to reduced mESC growth. However, nothing was inferred about either the species of adsorbed proteins or the conformation and orientation of adsorbed proteins.

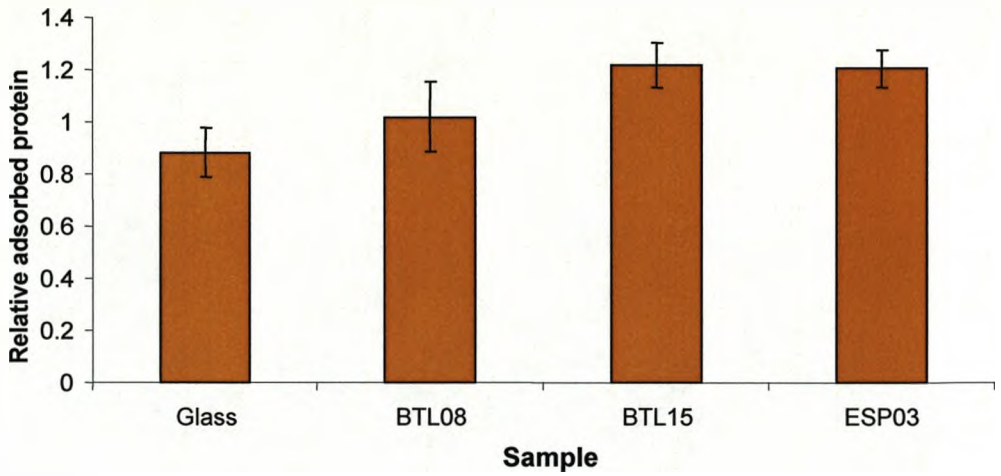

Figure 4-7 Protein adsorption to polyacrylate substrates. Substrates were coated with FCS and then assayed with BCA solution. Background staining was deducted for each substrate. Plain glass substrates were used as controls. No significance was found between adsorption on each substrate. Results represent the mean of 3 biological replicates ± S.E.M.

4.2.5. The ability of mESCs to attach to and colonise polyacrylate substrates

Whilst mESC population expansion was significantly reduced on polyacrylate substrates, compared with control substrates, compact and healthy colonies were present following 96 h culture. Given that the reduced growth did not appear to be due to differentiation or low proliferation rate, it was possible that low cell attachment to the polyacrylate substrates could have been responsible for the lack of mESC growth on polyacrylate substrates compared with controls. One scenario could be that fewer cells initially attach. To investigate the ability of polyacrylate substrates to support mESC attachment, mESC populations were examined soon after seeding. An attachment assay was initially conducted on control substrates to observe typical mESC

attachment dynamics and determine a suitable time-frame for studying mESC attachment. An attachment curve was generated (Figure 4-9) between 5 h and 24 h post-seeding. Following 5 h culture approximately half the plateau optical density was achieved, and then following 24 h the cell population had reached the plateau, indicating that maximum attachment had likely been achieved. Therefore, these times were selected for assessment of mESC attachment to polyacrylate substrates. A similar curve was generated from counts of viable unattached cells at each time point, confirming that cells were not becoming non-viable during the attachment period.

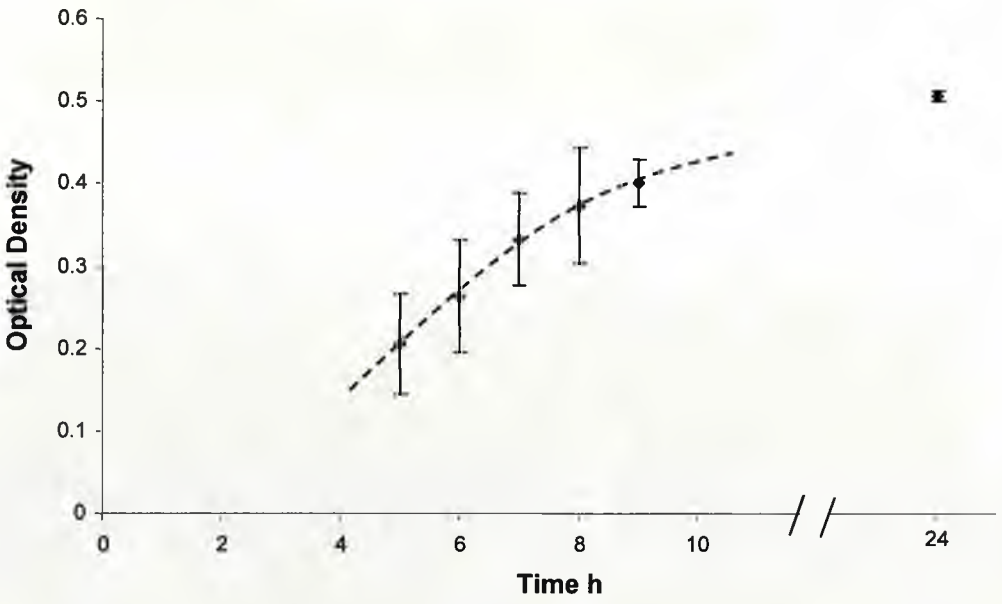

Figure 4-8 E14 mESC attachment curve. Cells were seeded onto control 0.1% (w/v) gelatin and 10% (v/v) FCS coated plastic substrates at $5x10^4$ per well and allowed to attach for various periods between 5 h and 24 h. Results represent the mean of 3 biological replicates ± S.E.M.

Following 24 h culture mESC growth on all BTL substrates was significantly lower than positive controls, but higher than plain glass

(Tukey model, $p<0.05$) (Figure 4-9), except ESP06. This suggested that reduced attachment of mESCs to the polyacrylate substrates could have contributed to reduced cell number at the 96 h time point. Indeed, on calculating the degree of population expansion from 24 h to 96 h (Figure 4-10), it was found that population expansion on BTL15, ESP03, ESP04 and ESP06 was not significantly different than on the control substrate.

Observation of mESCs following 24 h culture found that small colonies of mESCs were present on all substrates (Figure 4-11). These colonies were much larger than could be expected from single cells following 24 h growth. The mESC attachment curve (Figure 4-9) demonstrates that the majority of increases in cell number over the first 24 h is due to the seeded cells attaching. This suggested that aggregation of cells was probably occurring. Morphological analysis identified that early colonies on most polyacrylates were ESC-like (Figure 4-11). They were typically large, compact and rounded; however, unlike colonies present on control substrates, on polyacrylate substrates most exhibited uneven colony edges, similar to 96 h cultures. Therefore, even at this early stage, there was disparity between mESC colonies on controls and polyacrylate substrates. Observations also indicated that more colonies were present on all substrates after 24 h culture compared to 96 h culture, possibly indicating merging or loss of colonies between 24 h and 96 h culture, though this was also observed on control substrates.

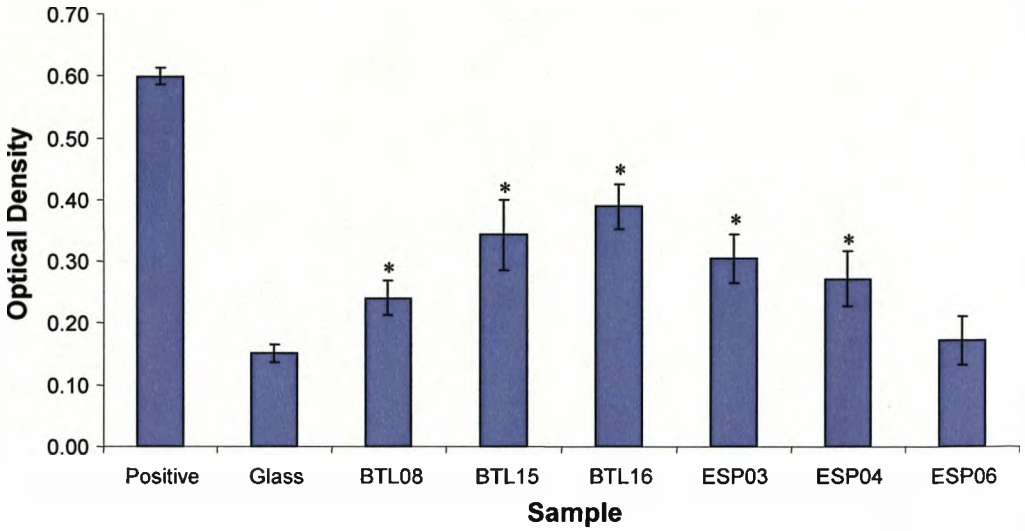

Figure 4-9 Ability of polyacrylate substrates to support E14 mESC attachment following 24 h culture under serum free conditions. Cells were seeded onto substrates at $5x10^4$ per well and cultured for 24 h in ESC media. 0.1% (w/v) gelatin and 10% (v/v) FCS coated and plain glass cover slips were used as positive and negative control substrates. The optical density, representing cell numbers, on all substrates were significantly lower than positive controls ($p<0.05$, Tukey model). Asterisk indicates statistical significance from the negative control ($p<0.05$, Tukey model). Results represent the mean of 3 biological replicates ± S.E.M.

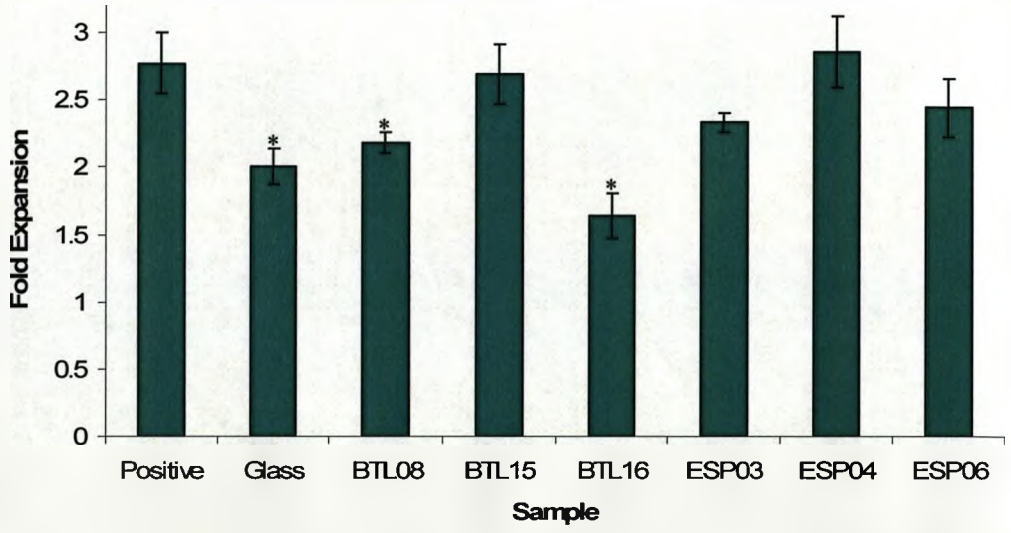

Figure 4-10 Degree of population expansion over 72 h calculated from 24 h and 96 h assays. Asterisk indicates statistical significance from positive control ($p<0.05$, Tukey model). Results represent the mean of 3 biological replicates ± S.E.M.

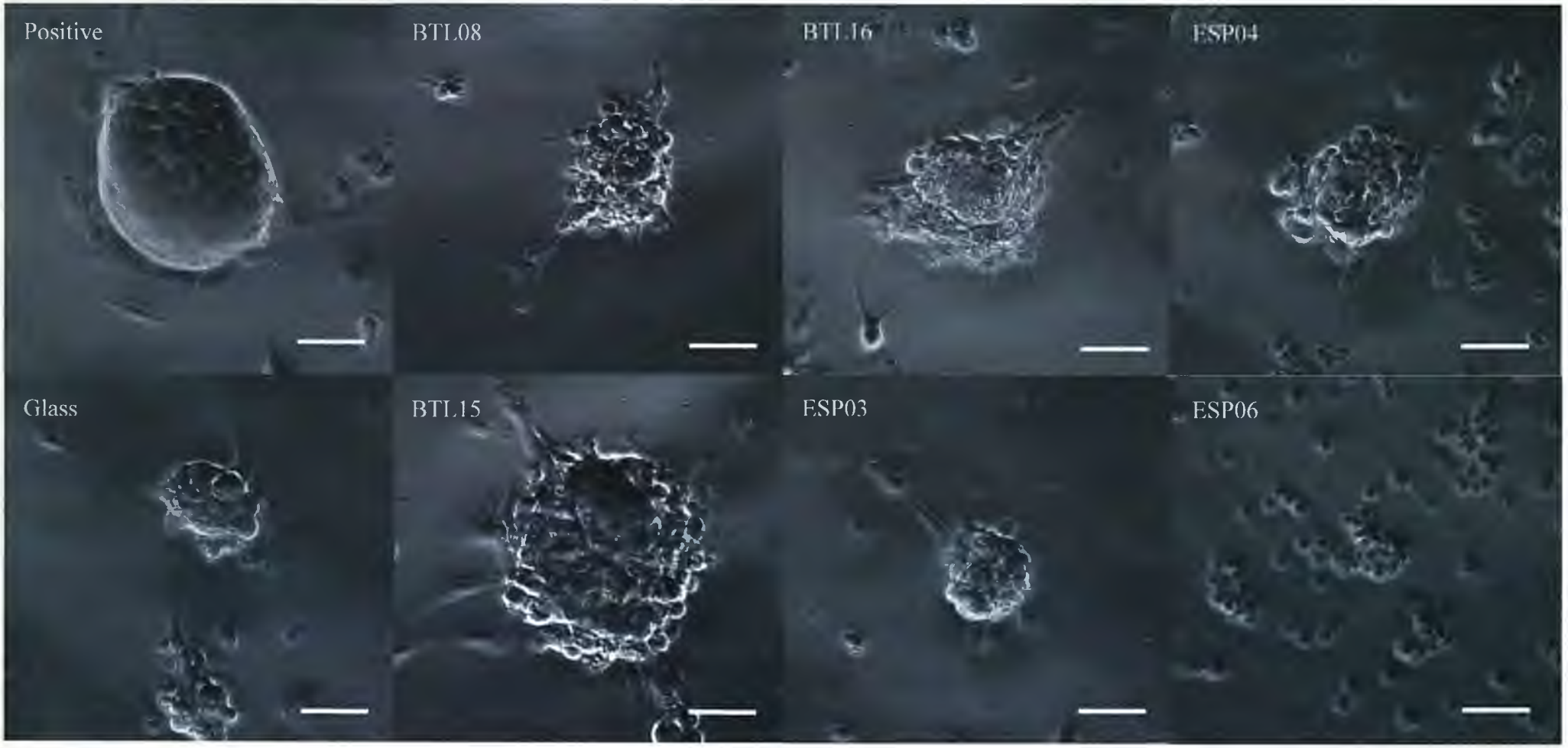

Figure 4-11 Variation in colony size and morphology of E14 mESCs following 24 h culture on polyacrylates under serum free conditions. E14 mESCs were fixed in 4% (w/v) PFA and imaged under bright field following 24 h culture in ESC media. Cells were seeded onto substrates at $5x10^4$ per well. Gelatin + 10% (v/v) FCS coated and plain glass cover slips were used as positive and negative control substrates. Uneven colony edges are visible on polyacrylate substrates. Scale bar 50 µm.

Given that differences in mESC attachment between polyacrylate substrates and positive controls were apparent by 24 h, the degree of attachment at 5 h was investigated. At this time point, on control substrates, a detectable number of cells had attached (Figure 4-8). When mESC attachment was examined following 5 h culture on polyacrylate substrates, mESC numbers were significantly lower than on positive controls (Figure 4-12). BTL15 remained the most successful polyacrylate with approximately 70% of the positive control value, and was significantly higher than that of plain glass (Tukey model, $p<0.05$). However, the relative cell number attached to BTL15 was significantly lower than that on the positive control (Tukey model, $p<0.05$). Other polyacrylate substrates performed similarly, however only BTL15 and BTL16 demonstrated significantly increased mESC attachment compared to the glass control. Interestingly, the negative control displayed similar mESC attachment, which was not significantly different to many polyacrylate substrates (Tukey model, $p>0.05$) (Figure 4-12).

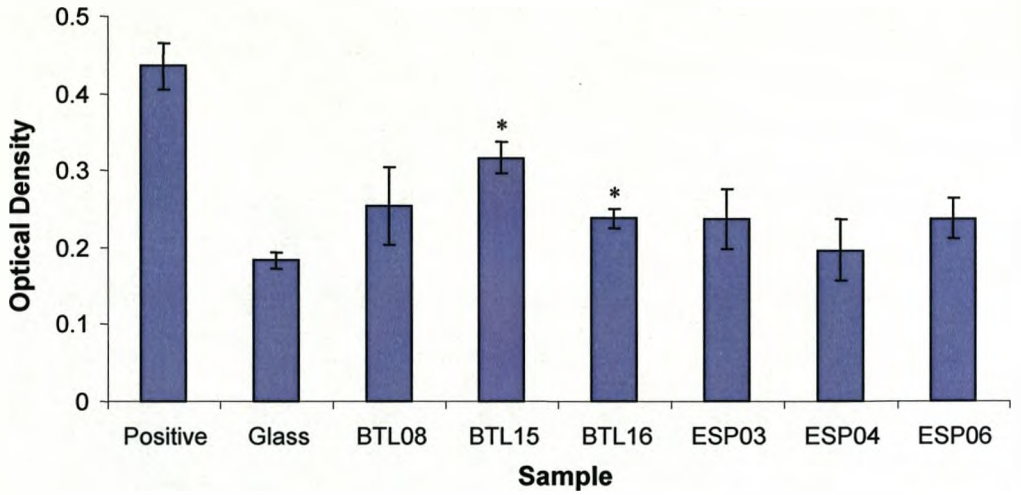

Figure 4-12 Ability of polyacrylate substrates to support E14 mESC attachment following 5 h culture under serum free conditions. Cells were initially seeded at $1x10^5$ per well. Following 5 h incubation substrates were rinsed in PBS and cell numbers quantified using crystal violet assay. Results represent the mean of 3 biological replicates ± S.E.M. Asterisk indicates statistical significance from plain glass control ($p<0.05$, Tukey model).

Data from all three time points (5 h, 24 h, 96 h) were normalised to positive controls and compared to assess their performance (Figure 4-13). The data show that, relative to the positive control substrate, the greatest reduction on plain glass, BTL08, BTL15 and ESP06 occurred between 5 h and 24 h. On BTL15, the change in cell number relative to controls between 24 h and 96 h was minimal. This suggested that, although the number of cells initially attaching was lower on these substrates, at the 5 h time point, another reason for reduced population expansion was likely due to lower attachment between 5 and 24 h. With ESP03 and ESP04, although the cell numbers were much lower than controls, the relative number remained fairly constant throughout the culture period. Therefore, reduced cell numbers on these substrates was most likely due to poor attachment at the 5 h time point.

Whilst these results demonstrate initial mESC attachment was significantly reduced on the polyacrylate substrates, they also show that on some polyacrylate substrates, this problem is compounded following attachment by reduced population expansion. Following 24 h and 96 h culture cell numbers on the positive control increased distinctly more than polyacrylate substrates (Figure 4-14, Figure 4-15). On the most successful polyacrylate, BTL15, the mESC population went from 72% of that on positive controls after 5 h to 57% after 24 h and then 54% after 96 h, which was a significant decrease (Tukey model, $p<0.05$). Interestingly, normalised mESC population on ESP03 and ESP04 did not significantly differ at progressive time points, which may indicate improved maintenance of mESCs on these substrates, though initial attachment remains reduced. Data from all three time points was further combined to model mESC growth curves on each polyacrylate substrate and controls, highlighting the differences in mESC growth between polyacrylate substrates and controls (Figure 4-16). Whilst the gradient is steepest between 5 h and 24 h, this is contributed to by continued cell attachment. The true shape of the curve is likely an inverse sigmoid, with cell attachment contributing to increasing cell numbers over the first 24 h, as demonstrated in Figure 4-8, and then exponential growth continuing following 24 h.

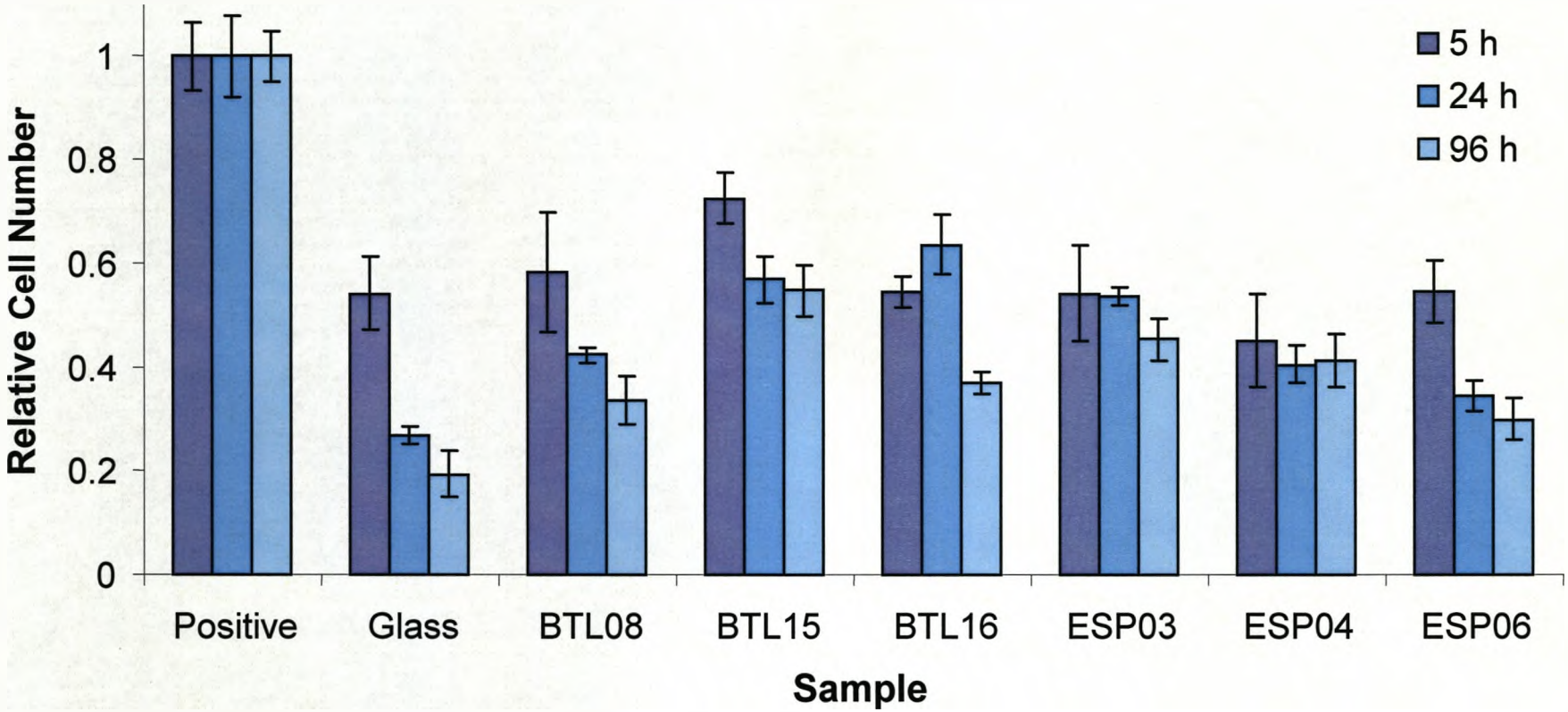

Figure 4-13 Comparison of normalised relative cell numbers assays at 3 distinct time points. Each data series was normalised to its respective positive control. $5x10^4$ and $1x10^5$ E14 mESCs were seeded onto substrates for 96 h, 24 h and 5 h, after which, relative cell numbers were quantified using crystal violet assay. Results represent the mean of 3 biological replicates ± S.E.M.

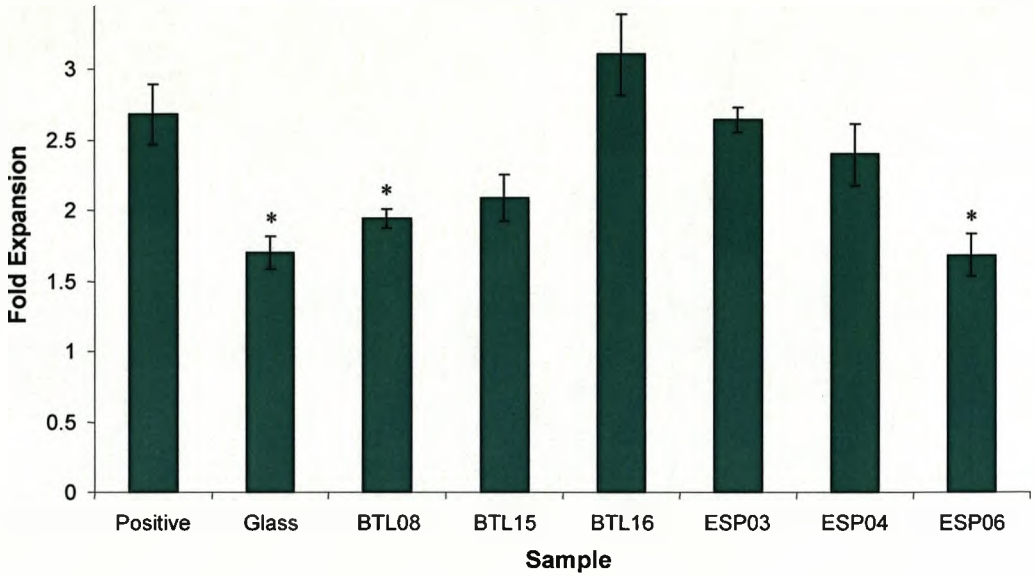

Figure 4-14 Population expansion between 5 and 24 h culture. Asterisk indicates statistically significant difference from positive control ($p<0.05$, Tukey model). Results represent the mean of 3 biological replicates ± S.E.M.

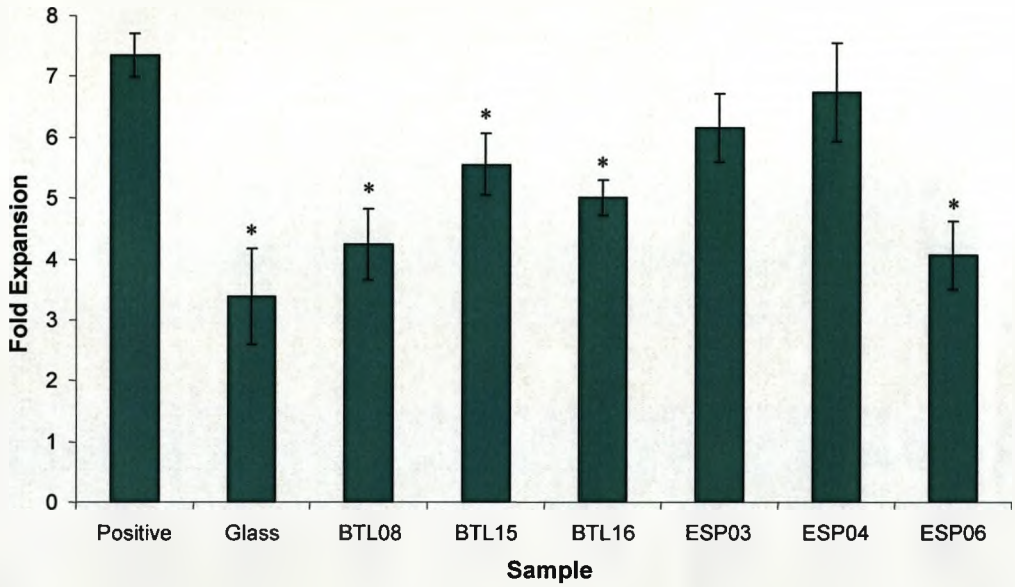

Figure 4-15 Population expansion between 5 and 96 h culture. Asterisk indicates statistically significant difference from positive control ($p<0.05$, Tukey model). Results represent the mean of 3 biological replicates ± S.E.M.

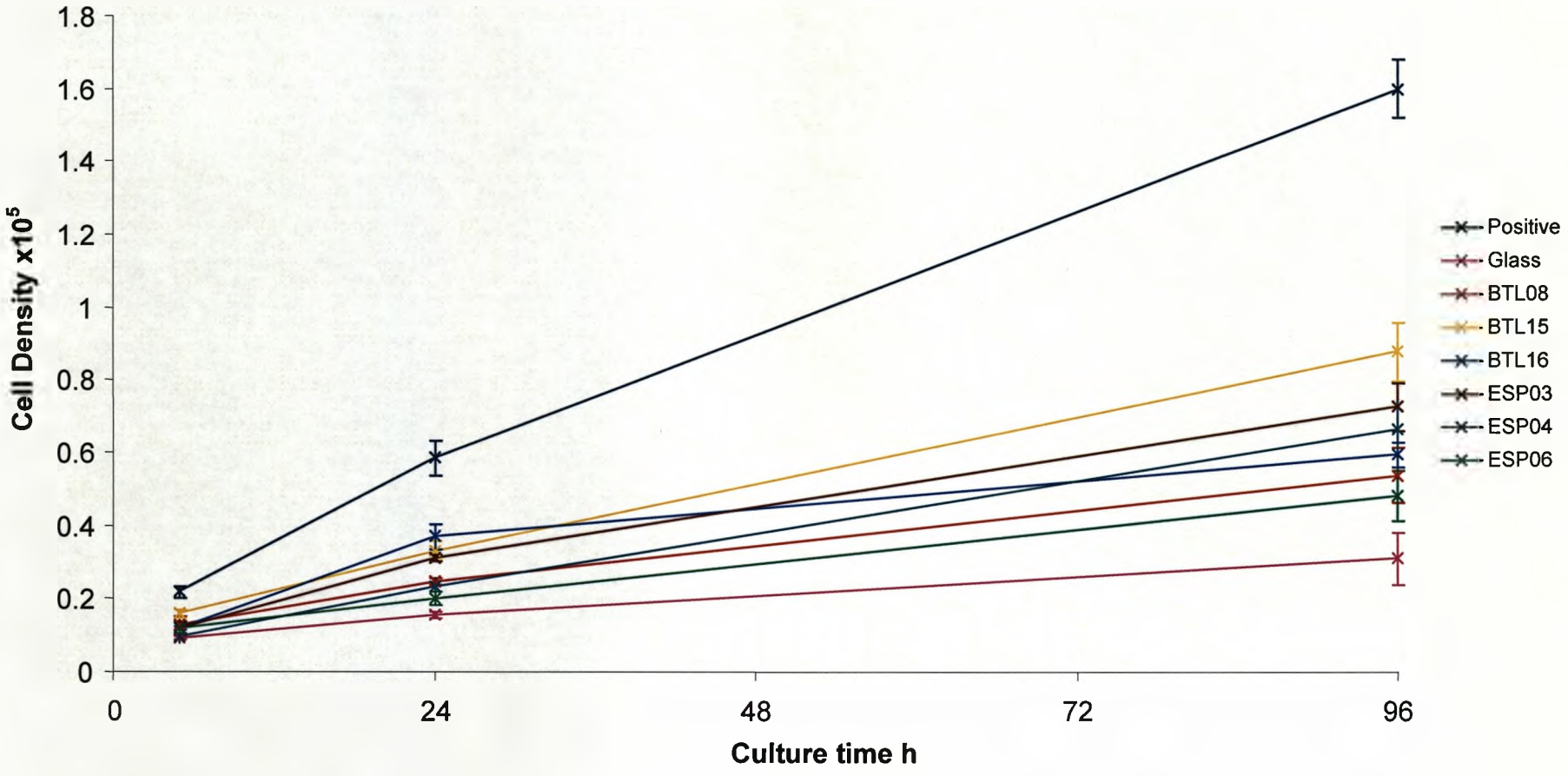

Figure 4-16 Growth curves of E14 mESCs cultured on BTL substrates generated from 5 h, 24 h and 96 h crystal violet assays. Points represent the mean of 3 biological replicates ± S.E.M.

4.2.6. Analysis of mESC attachment to polyacrylate substrates

Attachment of mESCs to a substrate is a critical step in culture. Results from this chapter indicated that problems with initial attachment were contributing to reduced population expansion on the polyacrylate substrates. Therefore, mESC initial attachment and behaviour was further studied to attempt to identify why the polyacrylate substrates were less successful in this respect.

Taken together, the results indicated that problems with initial attachment were likely to be a major factor in failure of polyacrylate substrates to support efficient population expansion of mESCs compared to serum coated glass. Further examination of the behaviour of mESCs following attachment was conducted by observing them in culture on the polyacrylate substrates.

Manual tracking of cells over the first 24 h post-seeding was conducted. These cell tracking experiments demonstrated that nearly all of the mESCs observed were aggregating (Figure 4-19). Over 5-9 h culture on BTL15 and control substrates, individual cells appeared to be spreading slightly and extending filopodia in the direction of travel (Figure 4-19, Figure 4-20). As early as 5 h into culture, clumps of cells were observed; significant reorientation of these clumps was also apparent and the cells were seen to steadily form progressively larger aggregates. Interestingly, initial qualitative observations indicated that mESC aggregation was most

prominent on the gelatin and FCS coated substrate, followed by polyacrylates, and least on glass. This order correlated well with observed population expansion on each of the substrates and indicated that reduction in cell aggregation, possibly due to changes in attachment mechanisms, might contribute to the poor capacity of the polyacrylate substrates to support mESC expansion. Though equally this might suggest poor initial attachment inhibits aggregation.

Furthermore, between 9 h and 24 h in culture, early aggregates continued to re-arrange extensively (Figure 4-19, Figure 4-20). Also, between 7 h and 24 h in culture, many aggregates were found to detach from the BTL15 substrates, but not from positive controls, and aggregates were found in suspension. Reduced growth on the polyacrylate substrates is likely due to a combination of poor initial attachment and subsequent detachment from the substrates. However, the reduced effect of serum coating on the polyacrylate substrates (4.3.4) might indicate proteins important for aggregation are either not adsorbed or adopt conformations on the substrates that might inhibit cell aggregation.

Aggregation of mESCs appeared to be important for colonisation, however, its cause in these cases is unclear. If survival was increased by closer proximity to other cells, this might indicate why polyacrylates were less successful than positive controls. Analysis of mESC migration was conducted with time-lapse imaging from 2-6 h in culture, recording images every 10 min (Figure 4-21). Analysis of cell tracking data found no

significant differences in the mean migration distance of mESCs on polyacrylate substrates and controls, over this earlier period (Tukey model, $p>0.05$) (Figure 4-22). All substrates were found to support mean mESC migration of approximately 50-60 μm over 4 h, though floating cells, which had either not fully attached or that had detached may have biased the result. However, it is also possible that only later migration, after 5 h, is inhibited on the polyacrylate substrates.

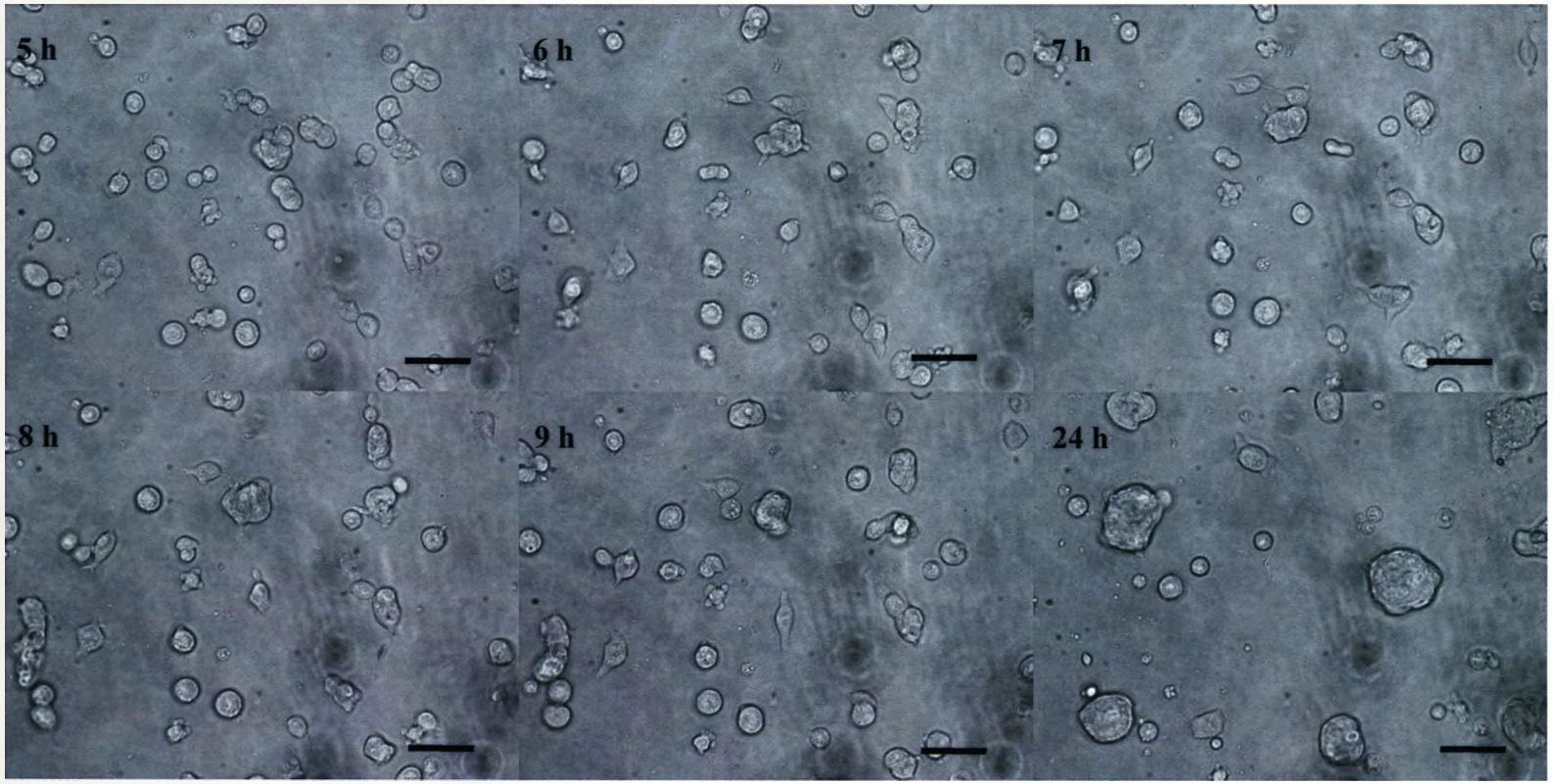

Figure 4-17 E14 mESC migration on 0.1% (w/v) gelatin + 10% (v/v) FCS coated glass. E14 mESCs were cultured for 24 h in ESC medium and observed in culture. Migration and reorientation significantly alters the arrangement of cells. Images were obtained from 5 h, 6 h, 7 h, 8 h, 9 h and 24 h from the same field of view. Scale bar 50 µm.

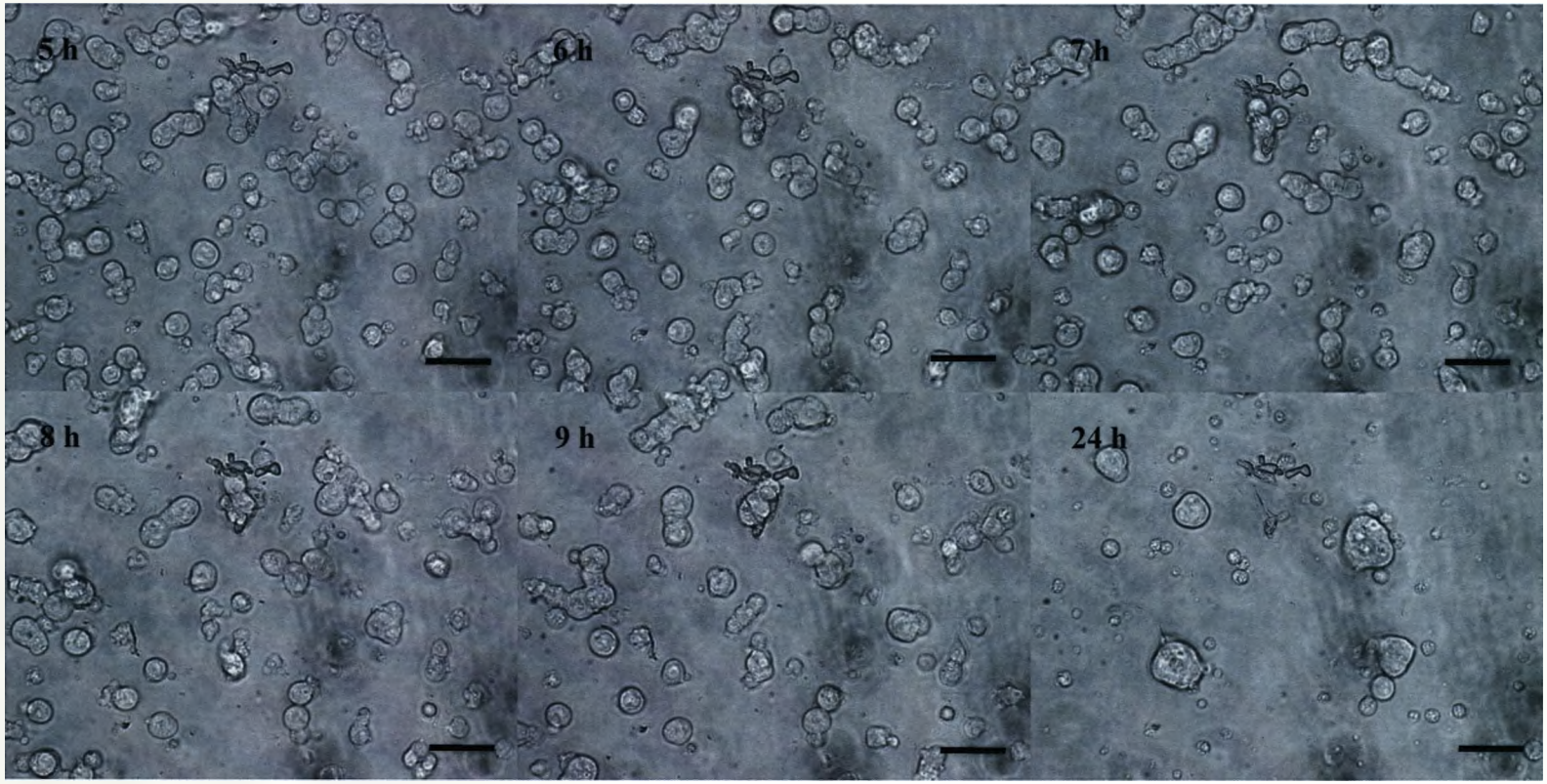

Figure 4-18 E14 mESC migration on BTL15 polyacrylate substrate. E14 mESCs were cultured for 24 h in ESC medium and observed in culture. Migration and reorientation significantly alters the arrangement of cells. From 5-24 h significant cell loss is observed. Images were obtained from 5 h, 6 h, 7 h, 8 h, 9 h and 24 h from the same field of view. Scale bar 50 μm.

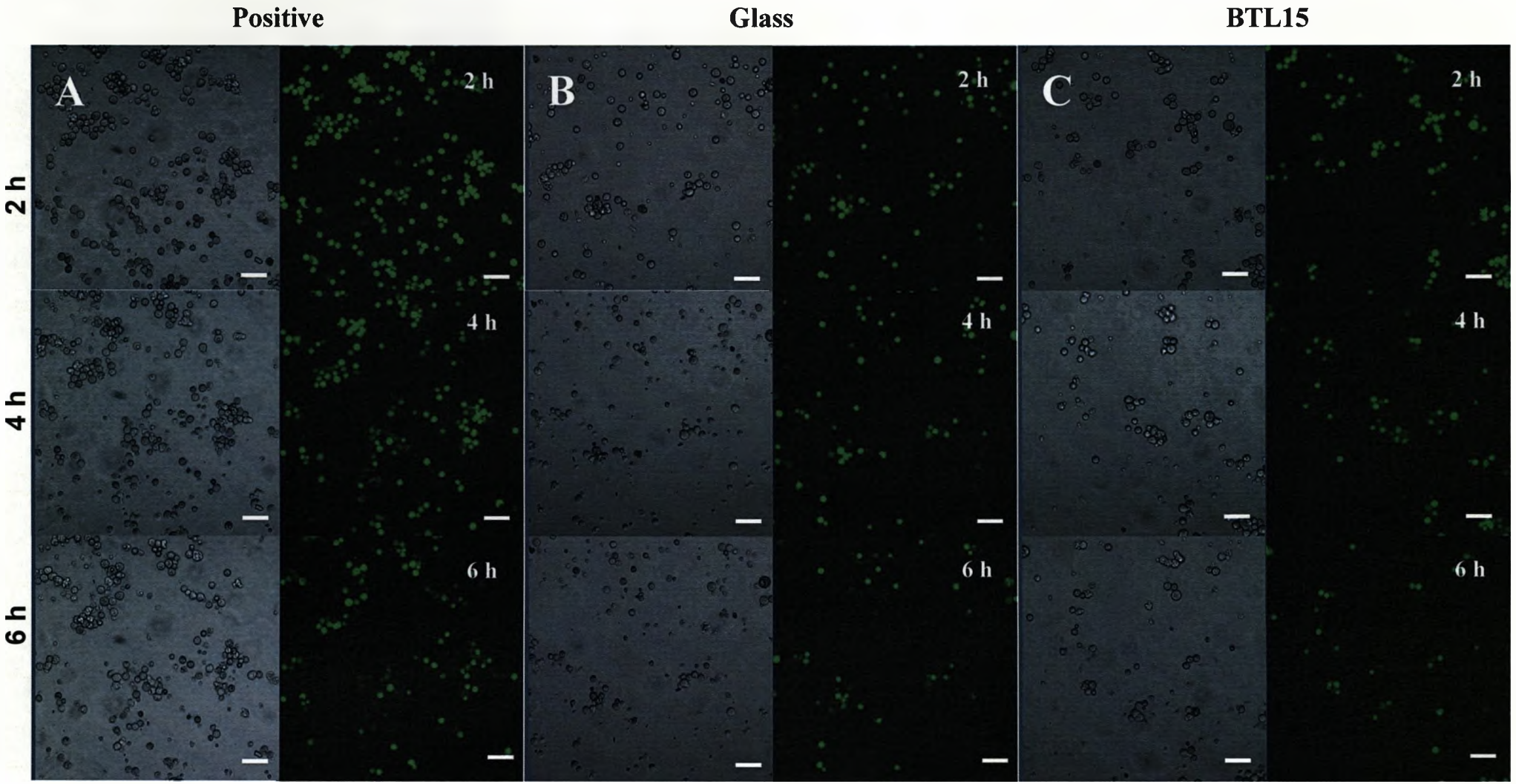

Figure 4-19 Confocal time-lapse imaging on BTL15 and controls. E14 mESCs were labelled with Vybrant and imaged from 2-6 h. Vybrant dye allowed identification and tracking of viable mESCs with fluorescence. Representative images of mESCs cultured on 0.1% (w/v) Gelatin + 10% (v/v) FCS (A), Glass (B) and BTL15 (C) at 2 h, 4 h and 6 h. Scale bar 50 µm.

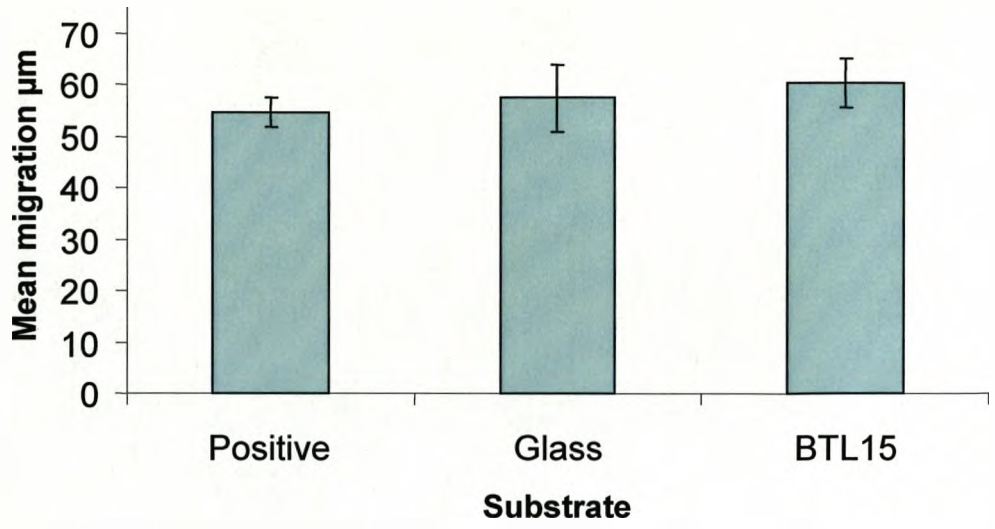

Figure 4-20 Mean mESC migration distance. The displacement of mESCs was summed across all steps from 2 h to 6 h, and the mean calculated. No statistically significant differences were demonstrated between BTL15 and control substrates ($p>0.05$). Results represent the mean of 4 replicates ± S.E.M.

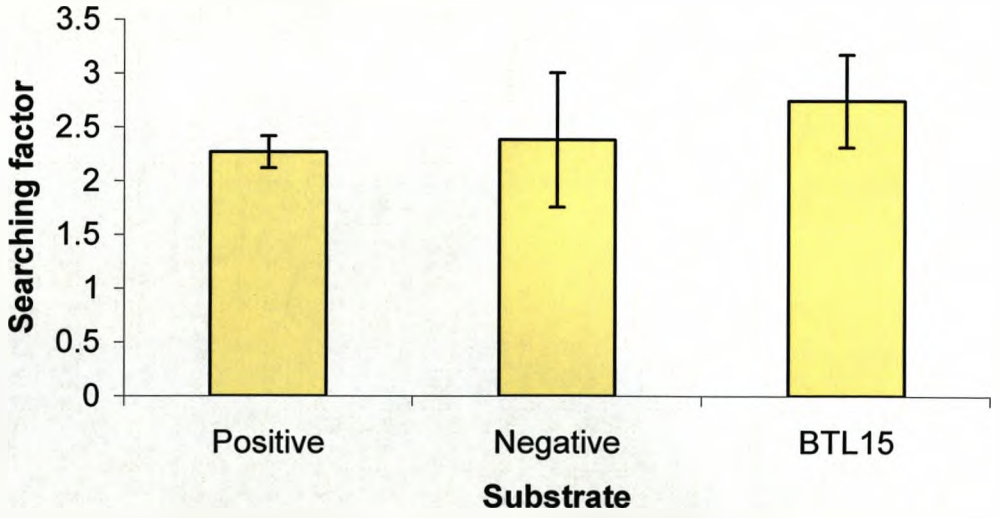

Figure 4-21 Comparison of mESC searching factors. The ratio of mean migration distance to final displacement was calculated to represent a searching factor of the mESCs. No statistically significant differences were demonstrated between BTL15 and control substrates ($p>0.05$). Results represent the mean of 4 replicates ± S.E.M.

A searching factor was calculated as the ratio of mean total migration distance to mean final displacement. Again, no significant differences were found between the substrates, suggesting that there were no differences between any directional cues for mESC migration on these substrates.

The distribution of step lengths was also analysed, using each 10 minute interval as a data point and calculating the displacement of mESCs between them. The average mean and median displacement per interval was very similar between control and BTL15 substrates, and no significant differences were demonstrated between them (Tukey model, $p>0.05$) (Table 4-1). Furthermore, positive skew was found for all substrates and all at similar values, with no significant differences between them (Tukey model, $p>0.05$). Positive skew indicates that the tail of the distribution is longer to the right, and that the majority of values lie to the left of the mean. On all substrates the median was less than the mean, which can also be implied by positive skew, and this was also implied by the percentage of displacements per interval of less than 5 μm (>50%). Finally, no significant differences were determined between the percentage of displacements per interval of less than 5 μm or less than 10 μm (Tukey model, $p>0.05$), suggesting that the range of displacements was very similar on control and BTL15 substrates.

Table 4-1 Nearest neighbour analysis of BTL15 and control substrates

	Mean µm	SE	Median µm	SE	Skew	SE	<5 µm	SE	<10 µm	SE
Positive	5.9	0.4	3.1	0.0	2.2	0.2	66.5%	2.1	81.9%	2.3
Negative	5.2	0.8	3.1	0.2	2.6	0.5	69.7%	4.7	85.0%	4.3
BTL15	5.9	0.5	3.8	0.3	2.2	0.4	60.4%	4.8	80.6%	3.3

Nearest neighbour analysis was also conducted on static fluorescence images at 2 h and 4 h to determine if clumping of mESCs was occurring, and if this differed between substrates. Fluorescently labelled cells were identified within a 500 x 500 µm area and nearest neighbour analysis conducted using WinDRP (HHMI/Masland Lab) software. The nearest neighbour distances were then compared to randomly distributed samples to adjust for cell number differences between samples. A random distribution of cells will have a regularity ratio of one, whereas clumping will result in a value less than one, as cells would be closer to their neighbours than expected by chance, and a regular pattern will result in a value greater than one, as cells would be further from their neighbours than would be expected by chance.

Following 2 h culture, the regularity ratios on control and BTL15 substrates were all less than one, indicating that clustering of mESCs was occurring. No significant difference was detected between the regularity ratios for either control substrate or BTL15 (Tukey model, $p>0.05$). However, following 4 h culture both BTL15 and the positive control had significantly lower regularity ratios than the plain glass negative control (Tukey model, $p<0.05$). No significant differences were found between regularity ratios of BTL15 and positive control substrates

at either time (Tukey model, $p>0.05$). Furthermore, BTL15 and the positive control both demonstrated a significant decrease in their regularity ratio between 2 h and 4 h (Tukey model, $p<0.05$)(Figure 4-24). This suggested that the mESCs, on these substrates, were becoming increasingly more clumped together than would be expected from a random distribution of cells.

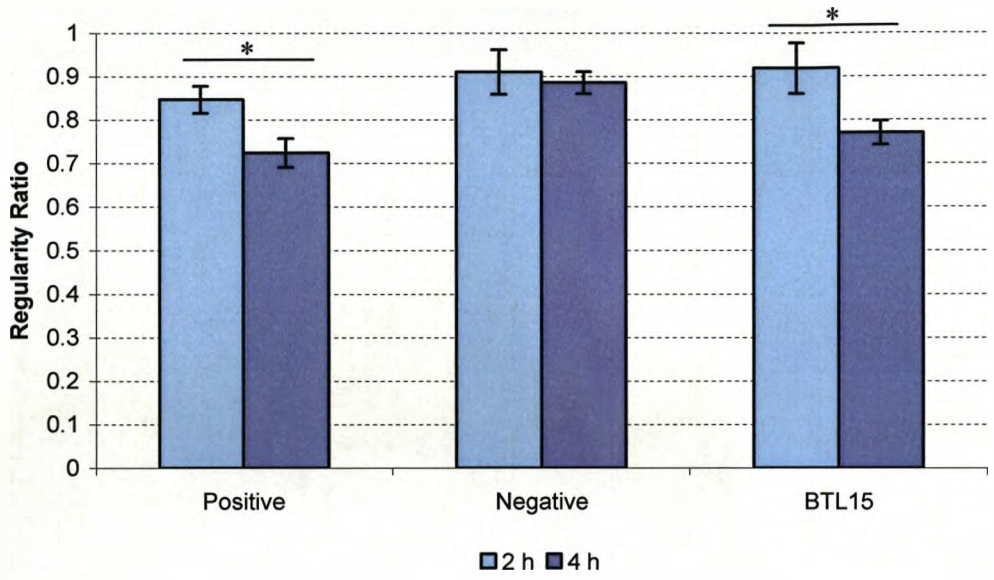

Figure 4-22 Nearest neighbour regularity ratios from control and BTL15 substrates. No difference was found between substrates at 2 h, however the positive control and BTL15 were significantly lower than the negative control at 4 h ($p<0.05$). Asterisk indicates statistically significant difference between 2 h and 4 h regularity ratios ($p<0.05$). Results represent the mean of 4 replicates ± S.E.M.

Comparison of the change in regularity index between 2 h and 4 h found a similar level on BTL15 and positive controls, which showed a decrease, and little change on the plain glass negative control (Figure 4-25). However, these measurements were not statistically significant different from each other (Tukey model, $p>0.05$), which might be due to a large range of values and small sample size, and may become significant with a larger sample size.

Examination of the static fluorescence images at 2 h and 4 h determined that the number of fluorescent cells per image typically fell. Analysis of these numbers demonstrated that, at 4 h, the number of detected mESCs fell to between eighty and ninety percent of the numbers at 2 h. However, there was no significant difference between substrates (Tukey model, $p>0.05$)(Figure 4-26), suggesting that this was typical of the mESCs in culture. The loss of fluorescence may have been contributed to by: photobleaching over prolonged exposure; dilution of the dye during proliferation, although the time period was only 2 h in this instance; migration of cells from the plane of view; cell death or detachment. However, no additional cells were able to attach during the experiments as the cell suspension was removed and replaced with fresh medium prior to the start of time-lapse imaging.

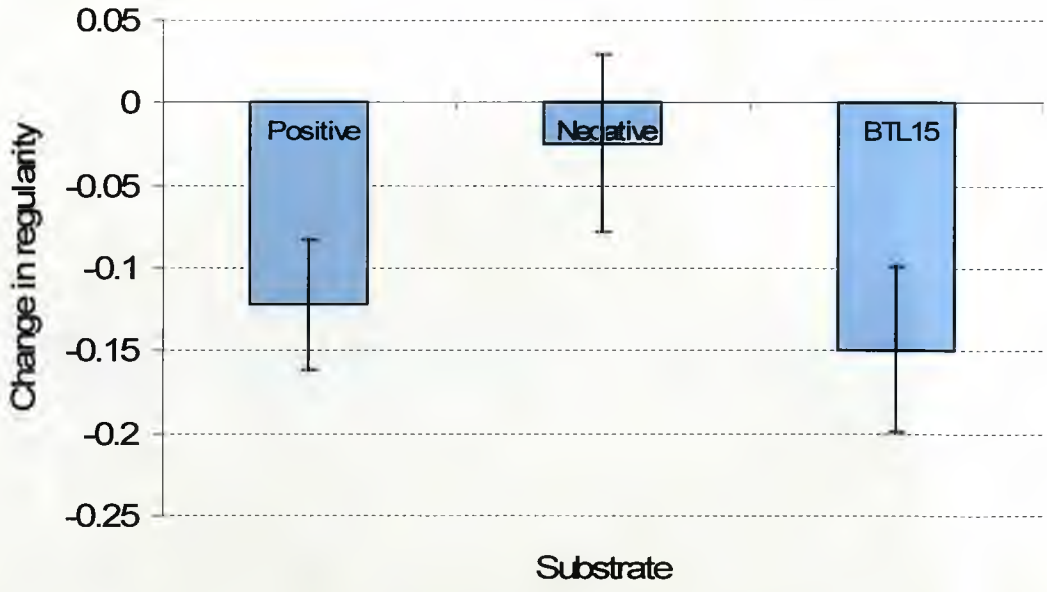

Figure 4-23 Change in regularity ratio between 2 h and 4 h on BTL15 and control substrates. The difference between the regularity ratio at 2 h and 4 h was calculated and the mean taken. Both the positive control and BTL15 demonstrated a decrease in regularity ratio, of comparable value, whereas the negative control demonstrates little change. However, these differences were not statistically significant from each other ($p>0.05$). Results represent the mean of 4 replicates ± S.E.M.

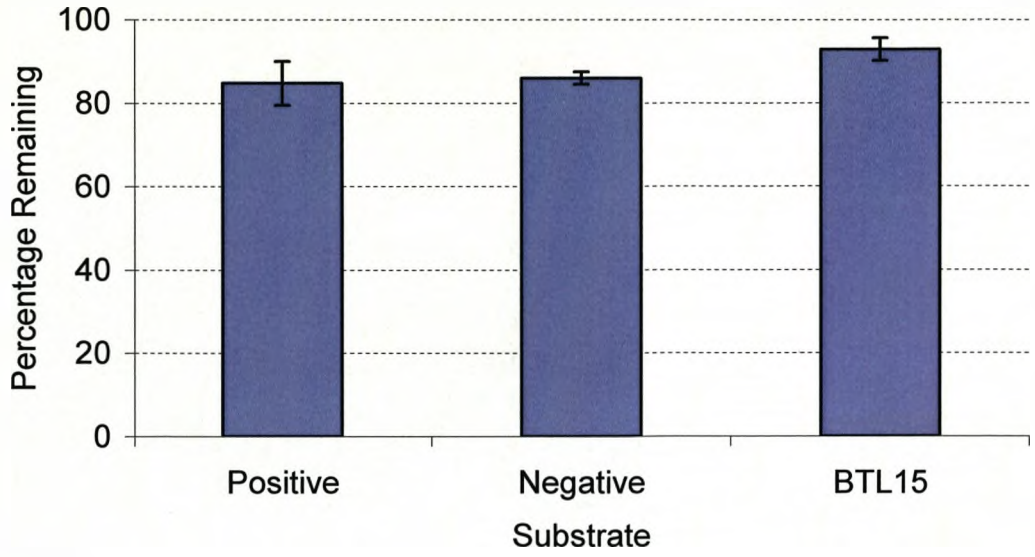

Figure 4-24 Percentage mESCs remaining from 2 h to 4 h in culture. No statistically significant differences were demonstrated between BTL15 and control substrates ($p>0.05$). Results represent the mean of 4 replicates ± S.E.M.

4.2.7. The ability of polyacrylate substrates to support long-term culture of mESCs in serum free conditions

Whilst mESC growth was significantly lower than controls on all polyacrylate substrates, expansion of mESC populations did occur, for example a 2-fold increase in relative cell number was demonstrated on BTL15 between 24 h and 96 h in culture (Figure 4-14). In addition, undifferentiated mESC colonies were observed on most of the polyacrylate substrates following 96 h culture. Further assays were performed on selected polyacrylate substrates to determine if mESCs could be maintained in longer-term culture on polyacrylate substrates, particularly following passaging. E14 mESCs were cultured for 2 days, then dissociated and re-seeded for a further 4 days on polyacrylate

substrates. All of the polyacrylate substrates gave low harvested cell numbers following 2 day culture, this was compensated for by normalising all second passage seeding densities to 3 x 10^4 viable mESCs.

The results showed that, following secondary passaging, little mESC growth was occurring on polyacrylates. However, the optical density of the eluted crystal violet stain was significantly higher than that from glass on BTL15, ESP03 and ESP06 ($p<0.05$, Tukey model)(Figure 4-27). Inspection of the substrates under bright-field microscopy found that few colonies were present. The colonies that were observed displayed absent or low AP activity, indicating loss of self-renewal (Figure 4-29). Therefore, polyacrylate substrates were unable to maintain self-renewal of mESCs over prolonged culture, and so under these conditions, were not suitable for long-term mESC culture. However, although typical mESC growth was observed on positive controls, the reduced seeding density could have contributed to reduced growth and self renewal on polyacrylate substrates.

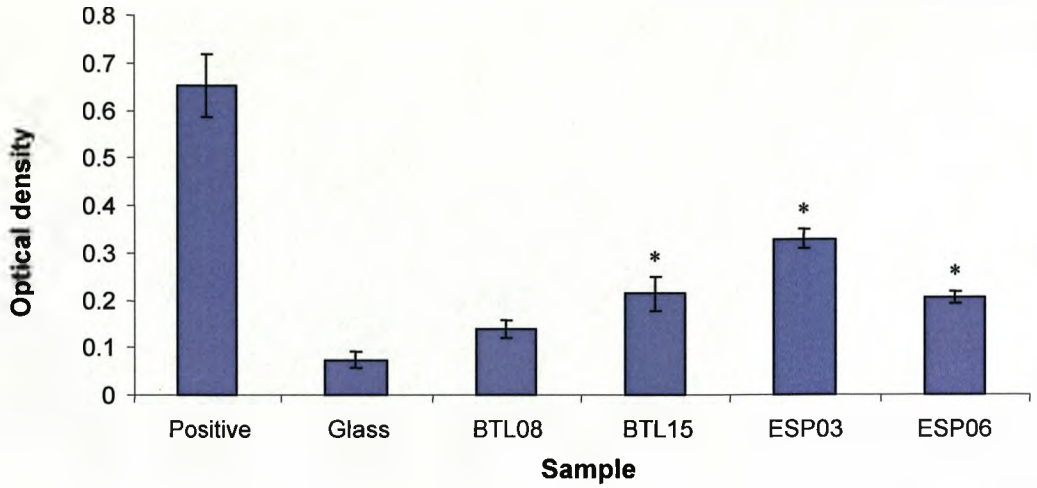

Figure 4-25 Long term culture ability of E14 mESCs on BTL substrates under serum free conditions. Cells were initially seeded at $5x10^4$ per well, cultured for 48 h, then sub-cultured to fresh substrates at approximately $3x10^4$ per well for 96h. Gelatin + 10% (v/v) FCS coated and plain glass cover slips used as positive and negative controls. Cell numbers on all substrates were significantly lower than positive control ($p<0.05$, Tukey model). Asterisk indicates statistical significance to the negative control ($p<0.05$, Tukey model). Results represent the mean of 3 biological replicates ± S.E.M.

Comparison of relative mESC numbers following first and second passages demonstrated that on most polyacrylate substrates and glass a significant decrease occurred. The substrates glass, BTL08, BTL15 and ESP06 all showed a significant decrease relative to the positive control ($p<0.05$, Tukey model)(Figure 4-28). However, the polyacrylate substrate ESP03 showed no significant difference between first and second passages ($p>0.05$, Tukey model), suggesting that this substrate might be more functional for prolonged culture of mESCs. Furthermore, the AP staining demonstrated strong positive staining in mESC colonies on ESP03 (Figure 4-29), and mESCs were able to form loose colonies on ESP06 substrates following secondary passaging, and these were also weakly positive for AP activity (Figure 4-27). However, a quantitative

assay would be required to determine whether AP activity differed between substrates.

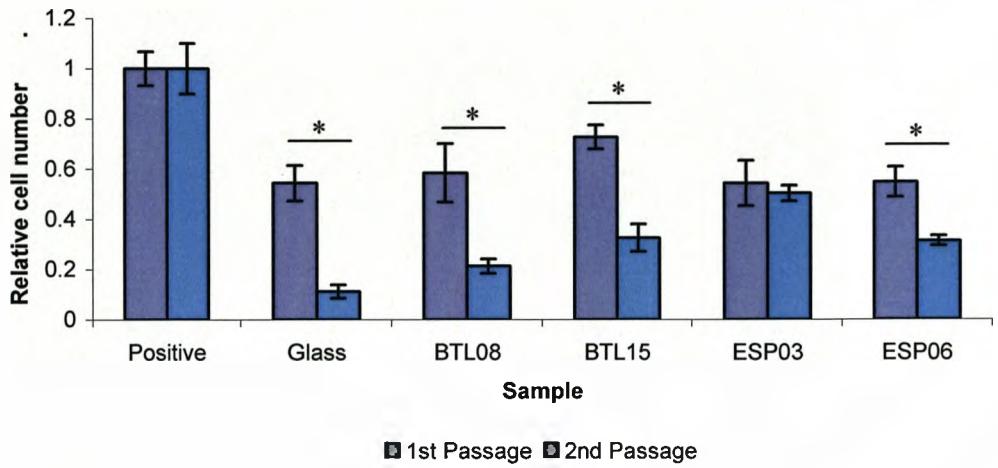

Figure 4-26 Comparison of relative mESC numbers following first and second passages. Cells were initially seeded at $5x10^4$ per well, cultured for 48 h, then either fixed and stained or sub-cultured to fresh substrates at approximately $3x10^4$ per well for 96h. Gelatin + 10% (v/v) FCS coated and plain glass cover slips used as positive and negative controls. All substrates except ESP03 demonstrated significant decreases in relative cell number to the positive control ($p<0.05$, Tukey model). Asterisk indicates statistical significance between first and second passage ($p<0.05$, Tukey model). Results represent the mean of 3 biological replicates ± S.E.M.

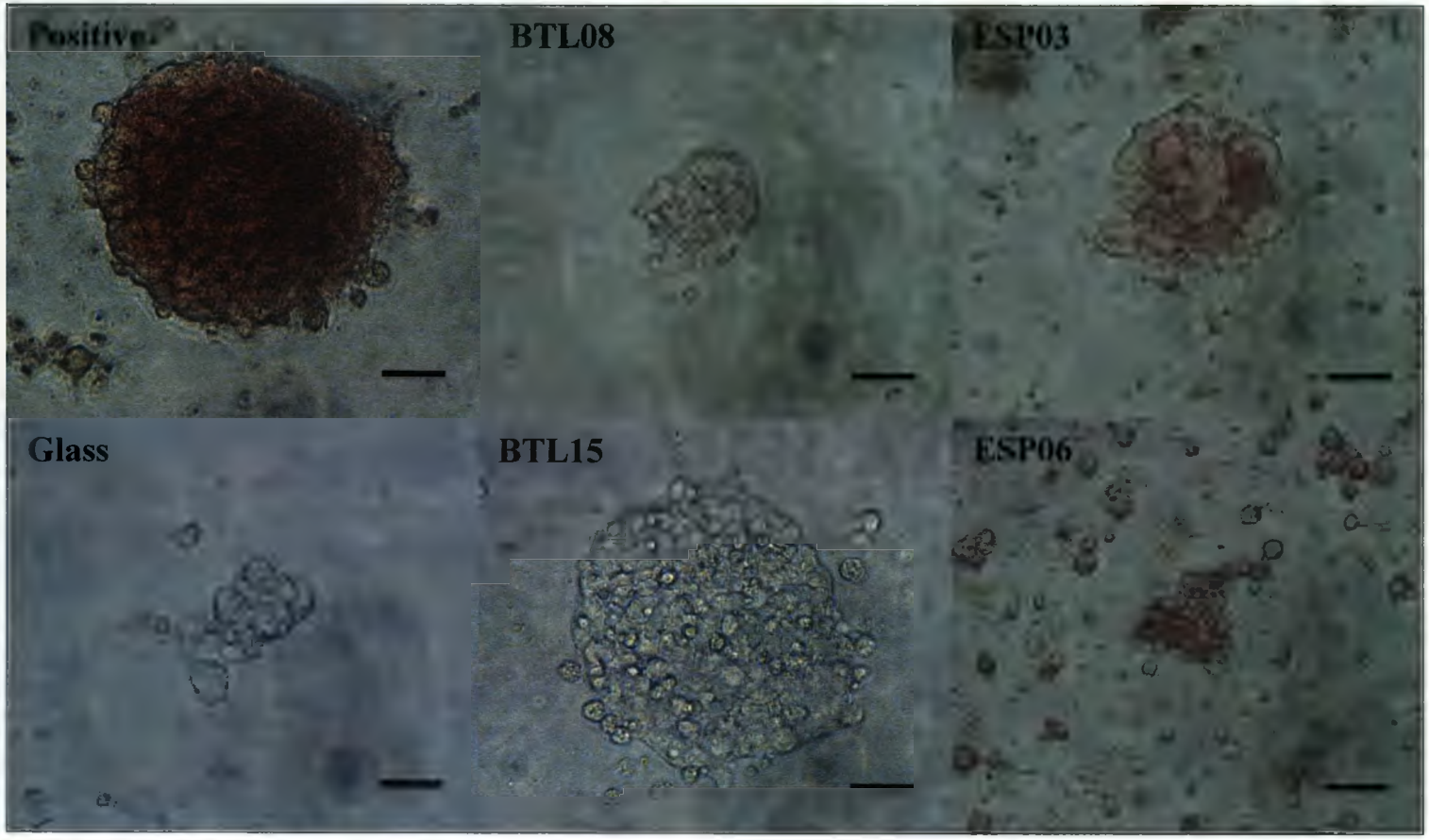

Figure 4-27 Long term maintenance of E14 mESC colonies on BTL substrates. E14 mESCs were dissociated after 2 days and re-seeded for a further 4 days culture. They were then fixed and stained for the pluripotency marker AP. Cells were seeded onto substrates at 5x104 per well and then 3x104 per well. Gelatin + 10% FCS coated and plain glass cover slips were used as positive and negative control substrates. Scale bar 50 µm.

To investigate if mESC growth following passaging could be improved by the addition of serum to the culture medium, cells were cultured for 2 days, then dissociated and re-plated for a further 4 days on polyacrylate substrates in the presence of 2% (v/v) FCS. However, the presence of serum did not significantly affect cell growth on any of the polyacrylate substrates (Tukey model, $p>0.05$) (Figure 4-30), and only plain glass demonstrated a large increase in cell density under serum conditions.

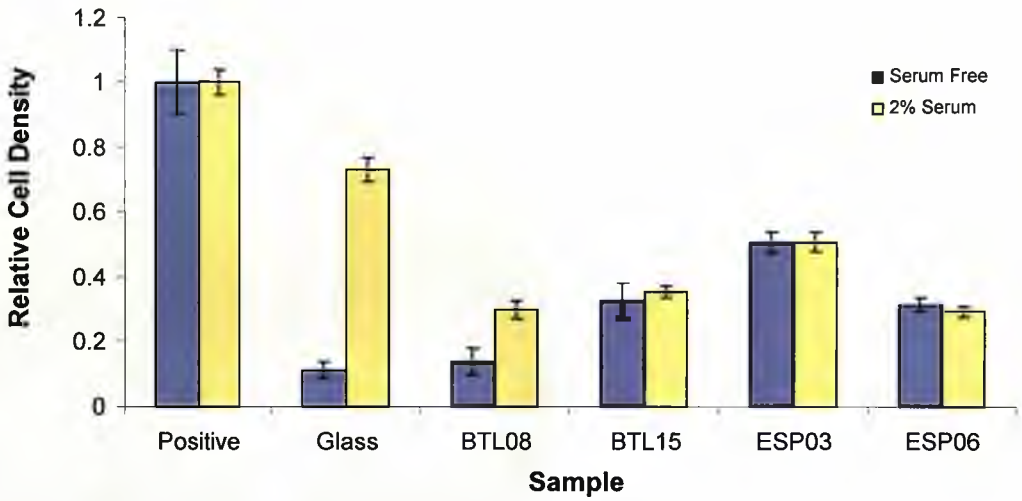

Figure 4-28 Normalised mESC numbers following passaging in serum-free and 2% (v/v) serum conditions. Cells were seeded at $5x10^4$ per well, then re-seeded after 48 h at $3x10^4$ per well. Gelatin + 10% (v/v) FCS coated and plain glass cover slips were used as positive and negative control substrates respectively. Values were normalised to positive controls. All BTL substrates showed significant difference in cell numbers from positive control (Tukey model, $p<0.05$). Results represent the mean of 3 biological replicates ± S.E.M.

4.3. Discussion

In this chapter, polyacrylate substrates were assessed for their ability to support mESC population expansion under serum-free conditions. The purpose of this study was two-fold. Firstly, to demonstrate that simple alterations in polymer chemistry, effected through the BTL proprietary techniques, could generate polyacrylate coatings with discrete surface properties, which in turn would demonstrate control over mESC behaviour. Secondly, this was ultimately to aid in the design of novel artificial substrates for mESC expansion and maintenance under serum-free conditions.

This study found that the polyacrylate substrate BTL15 could support short-term culture of undifferentiated mESCs. However, the population expansion was significantly lower than that observed on positive control substrates (gelatin and FCS coated plastic or glass). The reduction in population expansion observed during short-term culture on the polyacrylate substrates was found to be likely due to altered cell attachment to the substrates.

Further to this, differences in mESC behaviour were observed across the range of polyacrylate substrates. The three substrates whose polymer chains differed solely by the proportions of larger more sterically hindering groups (BTL08, BTL15 & BTL16) demonstrated significant disparity in maintenance and expansion of the mESC populations,

despite minimal detectable change in surface element composition. This demonstrates that the cells are able to detect and respond to changes between substrates which were largely undetectable by surface analysis techniques, such as XPS. The most successful polyacrylate substrate, BTL15, comprised intermediate levels of steric hindrance, whereas higher levels of steric hindrance resulted in a similar, but less successful substrate, BTL16. BTL08, which had lower levels of steric hindrance, demonstrated significantly reduced cell growth, compared to BTL15 and BTL16. Additionally, the polyacrylates ESP03 and ESP04, which contained amine and carboxylic acid functional groups inspired by the RGD integrin-binding peptide, typically demonstrated more numerous, but smaller mESC colonies than comparable polyacrylates, with short-term growth similar to BTL15, but better longer-term growth of mESCs accompanied with maintenance of self renewal.

4.3.1. The role of surface properties and steric hindrance in modulating mESC response to polyacrylate substrates

Previous work has shown that the degree of steric hindrance in synthetic polymers can affect surface properties, through restricting chain rotation and obscuring functionality (Kowalewska 1999; Safa 2004). Therefore, it is likely that steric hindrance affected the surface properties of the BTL substrates by altering the combined presentation of carboxylic acid, amine and hydroxyl functional groups, which in turn likely influenced the behaviour of the mESCs cultured in contact with them. In this study it was

found that BTL15, which had intermediate levels of steric hindrance and was the most hydrophilic of the polyacrylates, was better able to support mESC growth than BTL08 or BTL16, which had low and high degrees of steric hindrance, respectively, and were more hydrophobic. A similar study using human aortic endothelial cells also showed that increasing steric hindrance in polyacrylate substrates enhanced population growth (Nickson 2008). However, data from this chapter demonstrates that further enhancement of steric hindrance from the level in BTL15 was to the detriment of the capability to support mESC expansion on the substrate, as demonstrated by lower observed growth on BTL16. Therefore, intermediate levels of steric hindrance appeared to be the most beneficial for mESC growth.

In addition to steric hindrance, polyacrylate substrates were developed to exhibit alternate proportions of functional group presentation. Analysis of the substrates, as recorded in Chapter three, suggested differences in composition and physio-chemical properties of the polyacrylate substrates, indicating the presence of differing proportions and presentations of hydroxyl, amine and carboxyl functional groups. However, little correlation between surface properties and mESC behaviour has been observed. A likely explanation is that cells recognise nano-scale features, whilst standard surface analysis techniques examine average properties across large areas of the surface. Therefore, no direct surface characterisation is provided that might be used to predict behaviour of the cells.

Many studies have demonstrated cell responses to varying surface properties (Keselowsky 2004; Curran 2006; Pompe 2007). However, in most cases, studies were performed in the presence of serum or knockout serum replacement (a defined cocktail of growth factors and serum proteins), and the observed effects could likely be due to differential binding and presentation of ECM molecules, as well as through direct interaction of cells with the artificial substrates (Garcia 1999; Keselowsky 2004). However, Ren et al. (2009) recently postulated the direct interaction of rat neural stem cells with surface chemical groups under serum free conditions, possibly via integrin interactions. Whilst this mechanism is difficult to demonstrate, due in part to endogenous ECM production, this would be the model for interaction of polyacrylate substrates with mESCs under serum-free conditions in this chapter. When mESCs are seeded onto a substrate some form of interaction must occur to, at least initially, anchor them to the substrate and enable the generation of ECM.

Anderson et al. (2004) characterised hESC response to combinations of acrylate monomers presenting a range of hydroxyl, carboxyl, fluro and alkenyl groups, in the presence of serum, but found no clear trends in cell attachment and growth. These materials were likely very similar to the polyacrylates used in the current study, and similarly, no clear trends have been identified with functional group composition. Another group has demonstrated that a range of photo-immobilised polymers with

differing electrostatic charge influenced mESC behaviour; they found that more negatively charged surfaces reduced cell attachment and led to embryoid body formation (Konno 2006). Whilst detachment of mESCs from polyacrylate substrates was observed during culture in this chapter, no differences were noted between the polyacrylate substrates or a correlation identified with substrate properties. However, anionic carboxyl groups were present in all polyacrylates, which could have contributed to cell detachment. Konno et al. (2006) also found that mESCs attached to positively charged polyallylamine surfaces, which contained amine functional groups, however, aggregation was inhibited and they did not form colonies. These findings might implicate the role of amine functional groups in mESC response to ESP06, where colony formation was inhibited and the highest amounts of surface accessible amine was present (Figure 3-12).

Harrison et al. (2004) found alkali treatment of poly(α-hydroxyesters) significantly increased mESC proliferation over 48 h, in the presence of serum, on gelatin coated substrates. Alkali treatment cleaves the polyester backbone of these polymers to present carboxyl and hydroxyl groups, which increased wettability, however, the roughness of the substrates was also increased by the treatment. Harrison et al. (2004) also showed that population expansion was highest on moderately hydrophilic substrates, likely due to preferential adsorption of ECM proteins. This is similar to results with the BTL polymers in this chapter, where high wettability, and intermediate steric hindrance, appears to be

most successful. Mahlstedt et al. (2009) used oxygen plasma etched tissue culture plastic to culture hESCs using mouse embryonic fibroblast (MEF) conditioned medium. Plasma etching increased the levels of oxygen and nitrogen in the surface elemental composition, and the substrates became highly hydrophilic. The plasma etched substrates were able to support undifferentiated hESC culture with conditioned media, which was largely attributed to improved adsorption kinetics. However, when using a defined medium, the oxygen plasma etched tissue culture plastic was unable to support hESC culture, and prior coating of the substrates with MEF conditioned medium was insufficient to maintain culture of hESCs. This indicates that both adsorbed proteins and soluble factors from MEF conditioned medium were necessary for the culture of hESCs on these substrates, making them unsuitable for a defined culture system, which is what this chapter was working towards. Furthermore, the culture of hESCs on untreated tissue culture plastic using human fibroblast conditioned medium has previously been shown (Bigdeli 2008).

A study by Neuss et al. (2008) tested a number of synthetic and biological substrates, including poly-l-lactic acid (PLLA), polycaprolactone (PCL), collagen and hyaluronic acid, for their ability to support mESC growth, but found no significant relationship to the chemical or physical substrate properties. A second high-throughput study by Anderson et al. (2004) characterised hESC response to combinations of acrylate monomers. In total 576 combinations of 25 different acrylate monomers on a layer of

poly(hydroxethyl methacrylate) (pHEMA) were tested. These substrates also demonstrated differences in hESC growth in response to substrate chemistry, but again no specific relationships were established over short-term culture.

Other stem cell types have also been found to respond to specific functional groups. Ren et al. (2009) found that hydroxyl, sulfonic, amine, carboxylic acid, mercapto and methyl groups influenced rat neural stem cell (NSC) adhesion, migration and differentiation under serum-free conditions, with no association to the contact angle of the substrates. For example, carboxyl and sulfonic surfaces had similar hydrophilicity, but NSC migration, viability and cell elongation was significantly higher on carboxyl surfaces. Conversely, the hydrophilicity of carboxyl surfaces were significantly lower than thiol surfaces, but the amount of cell migration was similar. Ren et al. (2009) suggest that cell adhesion depends on functional group species rather than general surface properties such as hydrophilicity, however, properties such as charge density and hydrogen bonding differ between functional groups, which might better correlate with cell behaviour. Studies with MSCs have also shown that functional groups can affect MSC differentiation (Curran 2006; Benoit 2008). The study by Benoit et al. (2008) specifically demonstrated hMSC response to tethered small-molecule chemical functional groups when encapsulated in hydrogels, preventing changes in cell morphology (Benoit 2008). They found phosphate and t-butyl groups to promote

adipogenesis and osteogenesis, respectively, in the presence of serum, leading to pathway specific matrix production.

The studies discussed above demonstrate differing cell responses to specific functional group chemistries. However, they also demonstrate that no overall trends in substrate properties for controlling cell behaviour, particularly in ESCs, have yet been forthcoming. More complex substrates, with combinations of functional groups are likely necessary to properly simulate the in vivo environment and control stem cell behaviour.

4.3.2. The ability of polyacrylate substrates to support mESC growth

Cell growth on polyacrylate substrates was consistently significantly higher than on plain glass controls. This suggests that the surface properties of the polyacrylate substrates are significantly more conducive to mESC culture than the relatively hydrophilic, homogenous and negatively charged glass. However, cell growth on all polyacrylate substrates was significantly less than observed on serum-coated tissue culture plastic controls. To determine the causes of the reduced cell growth on the artificial substrates, their differentiation status, proliferation rate and degree of attachment to the surfaces were assessed.

Differentiation was not found to be occurring on most polyacrylate substrates, as shown by morphological analysis and the presence of AP activity in mESC colonies, suggesting that these polyacrylates could

maintain mESC self-renewal. The polyacrylates BTL08 and ESP06 were exceptions, where mESCs appeared more spread, colonies were irregular and AP activity appeared diminished, although reduced multilayering of mESCs on these substrates may be a simple explanation for the apparently lower density of staining observed in these instances.

Morphological analysis of colonies on BTL08 showed a higher degree of spreading compared to those on the other substrates. It is likely that this promoted differentiation, as a recent study has shown that increased spreading of mESC can induce differentiation even in the presence of LIF (Wells 2009). BTL08 incorporated the highest levels of steric hindrance of the polyacrylates, which should reduce the surface presentation of functionality, confirmed by being the most hydrophobic of the BTL designated substrates (Section 3.4.1). Spreading of mESCs in response to BTL08 may occur via reduced surface presentation of functional groups, or via altered affinity of endogenous ECM protein binding. Studies have shown positive correlation between hydrophilicity and both mESC growth and self-renewal (Harrison 2004), but also that highly increased hydrophilicity can promote differentiation via strong attachment and spreading (Wells 2009). A third possibility could be enhanced spreading of mESCs in response to substrate stiffness. Increasing steric hindrance also increases the stiffness of the polyacrylates, which has been shown to increase spreading and promote differentiation in mESCs (Evans 2009).

The mESC colonies on ESP06 may have been less healthy, since high levels of cell debris was observed in the culture medium (data not shown), suggesting that any loss of AP might likely be due to the cells losing viability. ESP06 had much higher concentrations of amine and carboxyl functional groups than the other polymers tested. Wells et al. demonstrated spreading and differentiation of mESCs cultured on high concentrations of carboxyl groups (Wells 2009). This might suggest very strong attachment is occurring on ESP06, which might explain why cell debris remains attached. Strong attachment can promote spreading and differentiation, but may also promote cell death (Roach 2007).

The findings of the BrdU assay, to compare proliferation, were surprising. Nearly all the polyacrylate substrates and controls showed no significant differences in proliferation rate following 24 h culture. Considering the large differences in relative cell numbers between substrates following 24 h and 96 h culture (Figure 4-1, Figure 4-9), this was an unexpected result. However, rates of attachment and detachment appear to play a significant role in the observed differences in relative cell numbers between substrates, and may perhaps be the main source, which supports the idea that the polyacrylates have little impact on proliferation rates. Furthermore, at 24 h, the mESCs may not have had time to adapt to their new substrates and, therefore, similar proliferation rates might be expected. Interestingly, ESP06 demonstrated a substantial decrease in proliferation rate in comparison to the other polyacrylate substrates and controls. Almost none of the mESCs on ESP06 were labelled positive in

the BrdU assay, suggesting that very little proliferation was occurring, yet population expansion was observed (Figure 4-10). One explanation might be that mESCs take longer to adapt and begin proliferating on ESP06 substrates or that strong attachment and differentiation are contributing.

4.3.3. The ability of polyacrylate substrates to support mESC growth in the presence of serum

The addition of serum to the mESC culture environment made no significant improvement in mESC population expansion on the polyacrylate substrates. This result was surprising considering the impact of serum coating on the plain glass substrates, which revealed large increases in mESC expansion. In addition, on the polyacrylate substrates ESP04 and ESP06, population expansion actually appeared reduced following serum coating, suggesting that serum proteins may in fact inhibit or interfere with growth on these substrates. Other studies have demonstrated short-term mESC culture on artificial substrates only under serum conditions (Harrison 2004; Melville 2006), suggesting that an underlying layer of ECM proteins is necessary for ideal attachment and growth of mESCs. In two studies using other cell types, surfaces with specific chemical functionalities were pre-coated with fibronectin and changes in proliferation were effected via alterations in integrin binding to adsorbed fibronectin (Garcia 1999; Lan 2005), suggesting fibronectin presentation can be controlled by surface chemistry.

The protein adsorption assay indicated that similar quantities of protein were adsorbing to both the polyacrylate and plain glass substrates. This may indicate incorrect adsorption of serum proteins to the polyacrylates, either through their orientation or conformation, which has been demonstrated in several studies (Underwood 1993; Michael 2003; Keselowsky 2004). It is important to note, however, that the assay did not distinguish between specific proteins present in the serum. Therefore, the adsorption of albumin, or other serum proteins not involved in attachment could differ between substrates, altering the proportions of ECM proteins present.

From these results it appears that the lack of an adsorbed serum protein layer on polyacrylate substrates did not cause the reduced mESC population expansion. This was likely due to either adsorbed ECM protein not being a limiting factor in mESC culture on polyacrylate substrates, or orientation and conformational changes preventing adsorbed proteins from fulfilling their roles in cell attachment and signalling. Alternatively, polyacrylate substrates might preferential adsorb serum proteins not involved in cell adhesion, as protein species was not differentiated between in this assay. A final possibility is that an alternate attachment mechanism to the typical cell-protein-substrate model is occurring, where direct interaction of the substrate and cell leads to adhesion and growth of mESCs, which has been suggested in other cell types (Ren 2009).

These polyacrylates have high proportions of functionality and are in this respect more similar chemically to the surfaces of proteins than glass. The ESP line of polyacrylates was specifically developed to crudely mimic the functional group composition of the RGD integrin binding site present in attachment proteins. Several studies have shown enhancement of cell adhesion by artificial peptide ligands derived from ECM proteins (Derda 2007; Fischer 2007; Kalaskar 2008). The RGD peptide in particular has been shown to increase cell attachment when presented on a surface (Alvarez-Barreto 2007; Sato 2007). Only recently, Kolhar et al. (2010) have demonstrated long-term maintenance of hESCs, for several months, on cyclic RGD peptide surfaces in conditioned medium, and short-term maintenance using serum-free conditions. However, mimicking the functional composition of the RGD peptide has not enhanced cell adhesion in the present study. Furthermore, Melkoumian et al. (2010) demonstrated maintenance of hESC self-renewal on RGD containing peptide-acrylate surfaces derived from vitronectin and bone sialoprotein.

Fibronectin adsorption from serum has been shown to vary among copolymers with different compositions of hydroxyethyl methacrylate and ethylmethacrylate (Horbett 1988). This demonstrates that surface chemistry can affect quantities of protein adsorption, despite no observable differences on the polyacrylates in this chapter. In addition, several studies using monoclonal antibodies have indicated differences in the conformation of fibronectin and vitronectin adsorbed to chemically distinct substrates (Underwood 1993; Steele 1995; Garcia 1999; Michael

2003) and this has also been observed with other serum proteins (Lan 2005; Roach 2005). This may correlate with results described in this chapter, where coating with serum proteins does not significantly affect mESC growth. If attached proteins undergo changes in conformation due to adsorption to the substrates, their ability to support cell attachment and signalling may be diminished. Therefore, coating with serum would not confer improved mESC attachment and growth. Pompe et al. (2007) found that poly(hydroxybutyrate) films, which had been plasma treated to enhance amine and carboxyl functionalities, altered fibronectin anchorage strength and its subsequent rearrangement by endothelial cells. A second study by Lan et al. (2005) demonstrated similar alterations in fibronectin remodelling by mouse myoblasts on alkanethiol SAMs presenting methyl, hydroxyl, carboxyl and amine functionalities. These may suggest a second mechanism for inhibiting serum protein mediated mESC growth, if proteins are adsorbed to the substrates, but are unable to be rearranged as might be required by the mESCs.

These findings may implicate a mechanism behind reduced attachment and growth of mESCs in serum-free conditions on polyacrylate substrates; if endogenous ECM proteins are secreted by the cells, but then undergo conformation changes induced by interaction with the substrates, they may no longer support mESC attachment and growth. This result leads to the question of how were mESCs interacting with the polyacrylate substrates under serum-free conditions and why there is no change when serum was added. The mESCs were able to form colonies

and grow on the polyacrylate substrates, suggesting interaction with the substrates. If the substrates were having a detrimental effect on adsorbed proteins, but the proteins remained a component of attachment, then some increase in mESC growth would be expected. As this was not the case, the observed attachment and growth of mESCs was perhaps more likely orchestrated by direct interaction with the substrates, which could possibly be regulated by charge interactions, hydrogen bonding or cell adhesion molecules. However, the exact mechanism of cell-substrate interaction remains to be identified.

4.3.4. The ability of polyacrylate substrates to support mESC attachment

Study of the early interaction, at 5 h, between mESCs and the polyacrylate substrates determined that initial attachment is reduced. Furthermore, following 24 h, there was an even greater reduction in the degree of attachment to most of the polyacrylate substrates compared to controls. Given that proliferation and self-renewal were similar on the polyacrylate substrates compared to controls, the attachment study suggests that the main reason for the lack of population expansion on the polyacrylate substrates is likely due to mESCs being unable to attach adequately.

Analysis of mESC growth curves from each polyacrylate substrate indicated that the largest change in proportion of cell numbers compared

to controls was between 5 h and 24 h post-seeding. Further investigation showed that mESCs might be detaching from the substrates, causing the lower than expected relative cell number determined at later times, and the subsequent apparent lower population expansion. A study by Konno et al. (2006) found reduced attachment of 129SV mESCs on negatively charged substrates, which led to increased embryoid body formation. A successful substrate requires cell attachment, however, it is important to consider related factors such as attachment strength and cell shape, which have been shown to affect mESC behaviour (Evans 2009; Wells 2009). Whilst attachment may be deficient on polyacrylate substrates, short-term maintenance of undifferentiated mESCs was achieved on most of these substrates. Recent studies have devised novel approaches for the use of non-cell-adhesive materials, such as control of mESC aggregate size with patterned cell-adhesive and non-cell-adhesive regions (Sasaki 2009). Polyacrylates present highly customisable substrate materials, which can be combined to generate convergent influences on cell behaviour. Results from this chapter show significant differences in mESC behaviour, including attachment, from relatively minor changes in substrate properties, indicating that more extreme responses may be generated with additional modifications.

4.3.5. The role of migration in mESC colonisation of polyacrylates

Whilst no significant differences were found in migration distance of cells between BTL15 and control substrates, there was some disparity in

clumping behaviour. On BTL15 and positive control substrates the nearest neighbour regularity ratio significantly decreased between 2 h and 4 h, identifying aggregating behaviour (Figure 4-24). Whilst the mean regularity ratio on the plain glass negative controls also decreased, it was very slight and not statistically significant. Therefore, mESC migration on BTL15 appears to behave similarly to the positive control, whereas little or no clumping occurs on the negative control, despite similar migration rates. Furthermore, no significant difference was demonstrated in the searching factor between BTL15 and positive and negative controls, which might again suggest similar migration behaviour. One explanation could be that mESCs on BTL15 and positive controls recognise the substrate as suitable, possibly for anchorage, and, therefore, when the cells come into contact they remain together and form a colony, whereas on plain glass the cells will continue to migrate separately as no such signalling is activated. Little is currently known about the role of migration in ESC colony formation, however, in embryo development many processes require the migration or aggregation of cells and it has, so far, been better studied in adult stem cells.

A study by Webb et al. (2000), using mouse MC3T3-E1 osteoblast-like cells, found significant differences in migration rate when cultured on serum-coated model silane surfaces, including amine, quaternary amine, methyl and thiol groups. They found that MC3T3-E1 cells migration was dependent on the surface functional groups, and the degree of surface wettability had no effect, with surfaces demonstrating the highest

migration rates on highly hydrophobic (Θ_c=90°) methyl surfaces. However, the less hydrophobic (Θ_c=60°) thiol surfaces demonstrated the highest cell attachment, and the lowest migration rate. Lauffenburger's group, and others, found that migration rate is a function of cell-substrate adhesion strength, with maximum migration levels at intermediate attachment strength (DiMilla 1993; Webb 2000). This suggests that weak attachment should be accompanied by low migration rate in mESCs on the polyacrylates. As no differences in migration rates were demonstrated between controls and BTL15 in this chapter, this might suggest that the strength of attachment is also similar.

A surprising finding was the scale of mESC migration observed on polyacrylate substrates, which has not been well described in ESCs. Aggregation of cells was generating large colonies quickly, and analysis of substrates under time-lapse imaging demonstrated nearly all mESCs were migrating a considerable distance. In mESCs the chemo-attractant stromal derived factor-1 (SDF-1) and its receptor CXCR4 are both expressed (Ying 2005). A study by Ying et al (2005) also found that SDF-1 increased survival of E14 mESCs. Therefore, aggregation might promote survival of mESCs, and will be an important consideration for artificial substrates. However, E-cadherin null mESCs have been found to survive well and maintain self renewal, despite a lack of colony formation (Soncin 2009). Furthermore, E-cadherin substrates have been shown to inhibit colony formation in embryonal carcinoma cells (Nagaoka 2008).

Ren et al. (2009) examined migration of rat neural stem cells from neurospheres on functional group surfaces in serum-free conditions. They found amine surfaces to promote significantly higher relative migration of cells than carboxyl, hydroxyl and methyl surfaces, and carboxyl significantly higher than hydroxyl and methyl. BTL15 theoretically contained amine, carboxyl and hydroxyl groups and the substrate analysis confirms that some functional groups must be presented at the surface and that amine groups are likely present due to nitrogen content. Therefore, some of these functional groups, or a combination of them, may be promoting aggregation of mESCs compared to plain glass.

4.3.6. The ability of polyacrylate substrates to support long-term culture of undifferentiated mESCs

Polyacrylate substrates were unsuccessful at maintaining mESC self-renewal and population expansion over successive passaging. Following the second passage, mESC numbers significantly decreased on most substrates relative to positive controls. In the presence of serum this trend was not changed. This mimics results over 96 h culture in the presence of serum (4.3.4), suggesting that the lack of mESC maintenance demonstrated by polyacrylates substrates was not due to progressive loss of ECM components during subculture. The contribution of differentiation to the reduced growth is unclear, as mESCs typically remained undifferentiated following 96 h culture. Furthermore, the

lowered seeding density may have impacted on the ability of mESCs to remain undifferentiated and proliferate, as mESCs are known to commonly exhibit reduced survival with low cell density. Although positive controls behaved normally, the polyacrylate substrates may have required a higher threshold seeding density, due to additional pressures, and as such, self-renewal and growth may have been reduced. Due to the use of passaging methods appropriate for the positive control.

Whilst the present batch of polyacrylates demonstrated little support for long-term culture, there was discrimination in success between them. The polyacrylate substrate ESP03 demonstrated improved maintenance of both long-term mESC growth and self-renewal over other polyacrylates and negative controls, though this was still reduced compared to positive controls. These results are similar to earlier findings where ESP03, and the similar polyacrylate ESP04, demonstrated improved maintenance of mESC culture relative to positive controls (Figure 4-13) and no significant difference in short-term population expansion compared with positive controls (Figure 4-14, Figure 4-15). This indicates that tailoring of polymer properties could improve the substrate's ability to support long-term culture of mESCs.

5. The ability of polyacrylate substrates to support mouse and human MSC chondrogenesis

5.1. Introduction

Articular cartilage is found in joints, where it provides both a cushion for shock-absorbing, and a smooth surface for ease of movement. However, cartilage tissue is distinctive in that it is unable to repair itself following injury (Newman 1998). Thus, cartilage damage can be debilitating, and often leads to osteoarthritis. The NHS estimates that osteoarthritis affects more than 8 million people in the UK, and at present there are few options available for its treatment. Current treatments aim to manage the condition; mild symptoms can often be alleviated through exercise and physiotherapy, but in more severe cases, joint replacement surgery may be the only option. However, the ability of stem cells, such as MSCs, to differentiate *in vitro* to chondrocytes (cartilaginous matrix producing cells) has opened the possibility of generating de novo cartilage tissue for treatment of osteoarthritis, and other cartilage damage-related conditions (Csaki 2008).

5.1.1. Induction of MSC chondrogenesis

The *in vitro* induction of chondrogenesis in MSCs typically requires the presence of expensive growth factors, such as TGF-βs, and a complex 3-D environment (Mackay 1998). These requirements are problematic, as the use of micro-mass culture systems is not user-friendly and the required growth factors can be expensive, making scale-up to the quantities of cells needed for treatments difficult. Therefore, over recent years, several groups have attempted to develop biomaterial solutions for the differentiation of MSCs to chondrocytes, without the need of micro-mass culture and expensive growth factors. However, whilst surface chemistry and peptide ligands have demonstrated the ability to promote chondrogenesis, in all cases they still require the presence of expensive growth factors (Curran 2006; Guo 2008; Shao Qiong 2009; Re'em 2010).

Typically, chondrogenesis is initiated in the limb bud, during embryo development, by the condensation of mesenchymal cells into tightly packed aggregates. TGF-β is thought to be the earliest activator of chondrogenesis, and promotes the expression of Sox9, the master regulator of chondrogenesis (Chimal-Monroy 1999; Akiyama 2002). The cell-cell adhesion molecules N-cadherin and N-CAM are expressed early in chondrogenesis, and are primarily involved in the aggregation of the mesenchymal cells (Tavella 1994; DeLise 2002). Fibronectin expression is also promoted by TGF-β signalling, and is essential for condensation (Chimal-Monroy 1999; White 2003). Following condensation, expression

of LSox5 and Sox6 is induced by Sox9, and then co-operate with it to promote expression of mature chondrocyte markers, including collagen II and aggrecan (Smits 2001; Chimal-Monroy 2003). This process is largely mimicked by *in vitro* chondrogenesis techniques, with micro-mass culture and chondrogenic induction conditions, predominantly TGF-β (Sekiya 2002; Mackay 1998).

5.1.2. The role of substrates in induction of chondrogenesis

Whilst some success has been achieved in promoting chondrogenesis using defined substrates, the substrate alone has yet been unable to induce chondrogenesis in MSCs (Phillips 2009; Re'em 2010). In particular the RGD integrin-binding motif, common to several ECM proteins, has demonstrated the capacity for enhancing chondrogenesis (Salinas 2008; Tigli 2008; Shao Qiong 2009; Liu 2010). The RGD/$\beta_1\alpha_5$ integrin interaction is known to be critical in initiation of condensation and chondrogenesis in the limb bud (White 2003). Therefore, altering substrate chemistry to mimic the RGD integrin binding motif may enable cell-substrate signalling pathways to promote chondrogenesis.

This chapter investigates the ability of polyacrylate substrates modelled on the RGD-integrin binding motif to induce chondrogenesis in MSCs. These substrates attempt to model the guanidinium and carboxyl groups and their spacing simply, using amine and carboxyl side groups distributed along a polyacrylate backbone. If successful, these substrates

would provide a cheap, simple and easily modifiable alternative to peptide sequences. Furthermore, if 2-D substrates can be designed that promote the initial steps of aggregation and condensation in MSCs, subsequent steps of chondrogenesis may be autonomously regulated by the differentiating MSCs.

5.1.3. Aims

I. Investigate effect of polyacrylate substrates modelled on the functional group distributions found in the RGD-integrin binding motif on differentiation of mMSCs.
    (i) Analyse morphological changes to mMSCs in response to polyacrylate substrates.
    (ii) Conduct immuno-assays for chondrocyte and osteoblst-specific markers.
    (iii) Conduct qPCR analysis to determine the expression levels of chondrocyte and osteoblast-specific genes in mMSCs cultured on polyacrylate substrates.

II. Investigate effect of polyacrylate substrates on mouse kidney-derived mesenchymal-like stem cells and mouse limb bud cells, to corroborate findings with mMSCs.

III. Investigate if polyacrylate substrates that are capable of promoting mMSC chondrogenesis are also able to promote chondrogenesis of hMSCs.

5.2. Results

5.2.1. Effect of polyacrylate substrates on mMSC morphology

D1 mMSCs were initially cultured on selected polyacrylate substrates and control substrates for 10 days to assess the effect of the substrates on cell morphology. The substrates used here were the two polyacrylates whose amine and carboxyl content were modelled on the RGD integrin binding site (ESP03 & ESP04), a third polyacrylate presenting an even distribution of hydroxyl, carboxyl and amine functional groups (BTL15), tissue culture plastic and plain glass control substrates.

Following a 10 day culture period in MSC medium (2.1.7.2), the mMSCs grew to form a monolayer on control substrates and the polyacrylate substrate BTL15 (Figure 5-1), and the cells displayed a typical spindle-shaped morphology, demonstrating maintenance of the undifferentiated mMSC phenotype on this unadapted polyacrylate. However, the mMSCs cultured on the RGD-mimicking polyacrylate substrates were found to have formed aggregates attached to the substrates (Figure 5-1). The mMSCs cultured on ESP03 formed a combination of cell monolayers with a few large aggregates being present, whereas on ESP04, the vast majority of the cells formed condensed multi-layered aggregates, with very few remaining in monolayer.

The mechanisms of this aggregation were further investigated by daily observation of the cells in culture. Figure 5-1 shows representative images of mMSCs following 1, 3, 5, 7 and 10 days in culture. Cells were seeded as a single cell suspension. On tissue culture plastic, glass and BTL15, the morphology of mMSCs was similar throughout the culture period, and by day ten a confluent monolayer was present. On ESP03 the mMSCs formed a monolayer by the first week of culture, following which, tears appeared in the monolayer and some of the mMSCs compacted to form large multilayered aggregates (Figure 5-2), indicating enhancement of cell-cell adhesion and/or reduced cell-substrate affinity. Following aggregate formation, further monolayer outgrowth of mMSCs was observed from the aggregates.

On ESP04, after approximately three days, small aggregates of mMSCs were visible across the substrates. At this stage no multi-layering was apparent, however, at successive time points, aggregates grew in size and developed into compact multi-layers. After 10 days in culture nearly all mMSCs were found in these compact aggregates. The main body of the aggregate consisted of a compact ball of cells, however, those cells still in contact with the substrates typically retained a well spread morphology, extending from underneath the aggregates, and appeared to anchor the aggregates to their substrates.

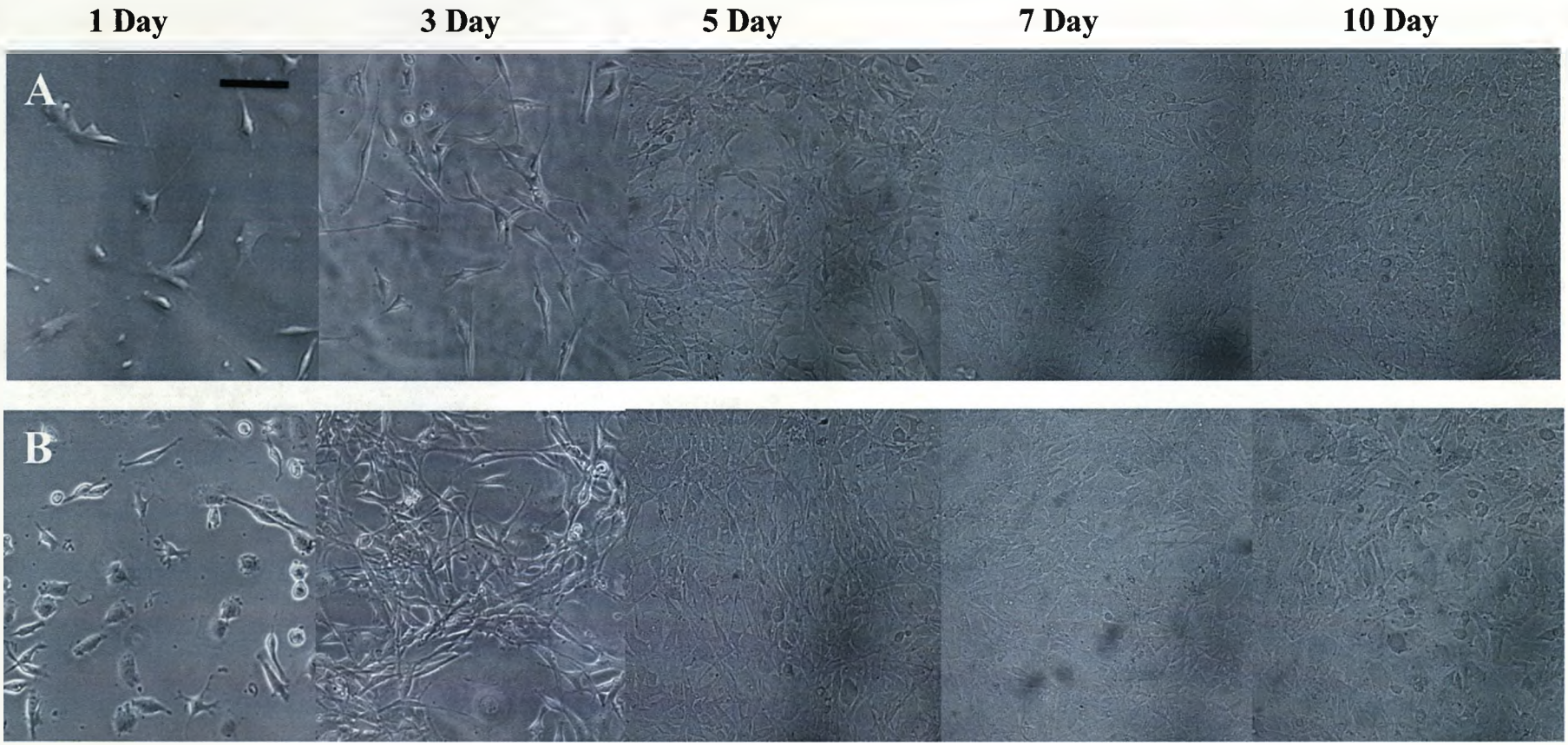

Figure 5-1 D1 mMSC behaviour on polyacrylate substrates. D1 mMSCs were seeded at $1x10^4$ cells per well, cultured for 10 days in MSC medium and observed in culture on tissue culture plastic (A), plain glass (B), BTL15 (C), ESP03 (D), and ESP04 (E). Images were obtained daily. Cells attached and grew into evenly distributed monolayers on plastic, glass and BTL15. Cells on ESP03 initially grew as a monolayer, then partially compacted to form large aggregates distributed within the monolayer. On ESP04 cells aggregated quickly in culture, condensed and grew to form tightly packed multi-layered aggregates. Representative images are shown, D and E demonstrate typical aggregate formation. Scale bar 100 µm.

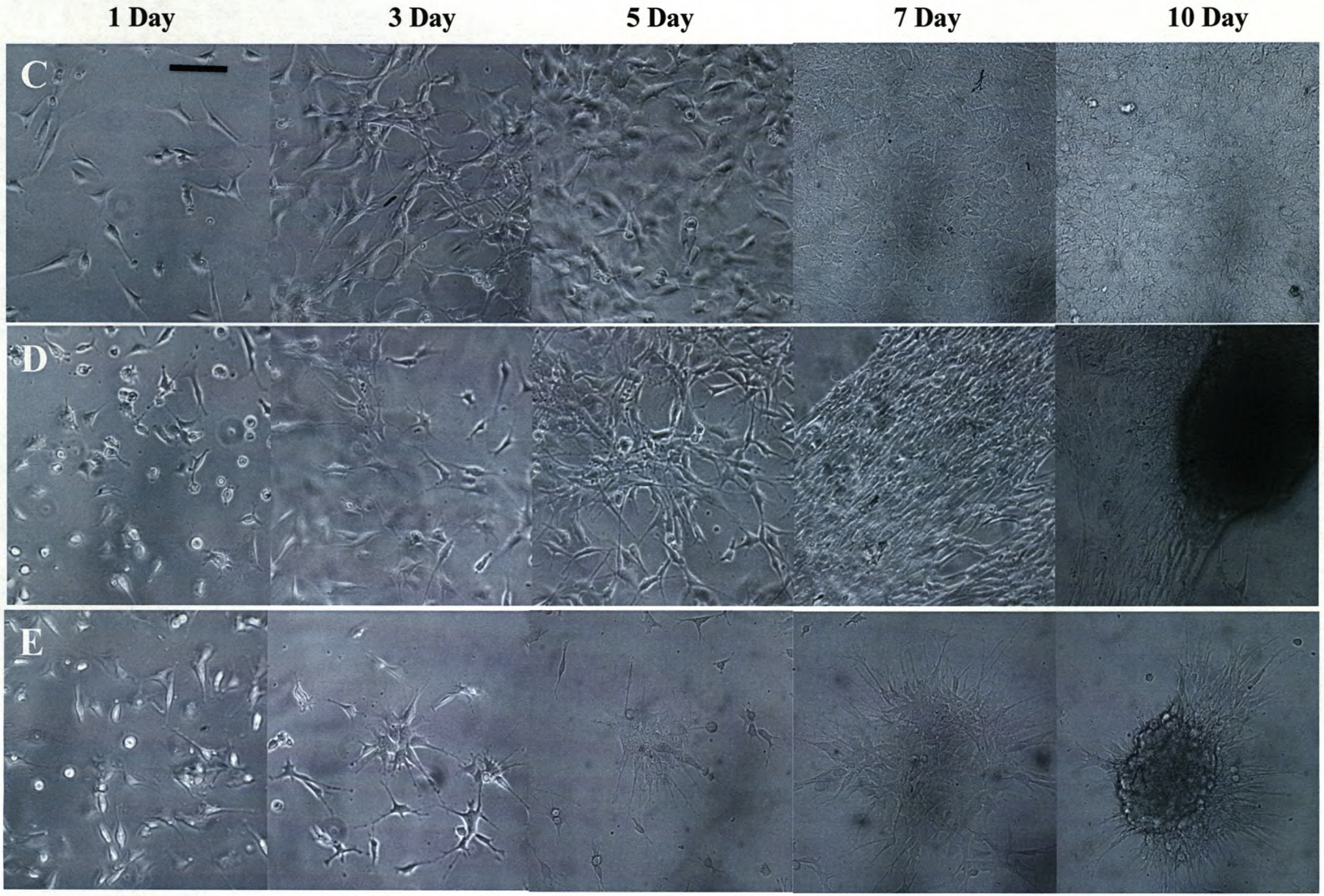

Figure 5-1 continued

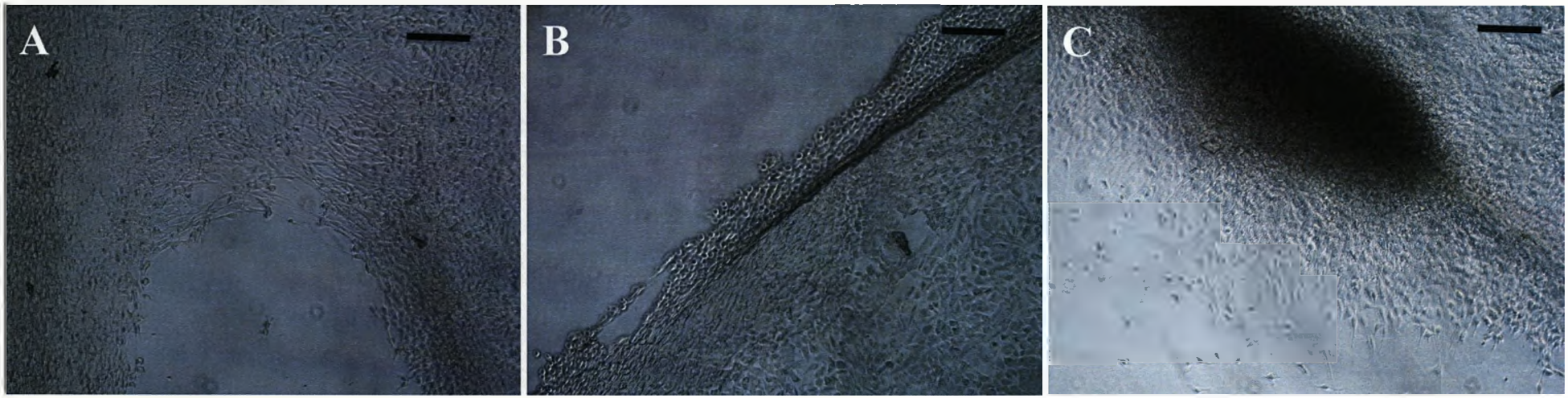

Figure 5-2 Phase contrast images demonstrating mMSCs behaviour in culture on polyacrylate substrate ESP03. D1 mMSCs were imaged following 4 (A), 6 (B) and 8 (C) day culture in MSC medium. Cells were seeded onto substrates at $1x10^4$ per well. Monolayer growth was initially observed followed by tearing (A), compaction (B) and aggregate formation and outgrowth (C). Scale bar 100 µm.

5.2.2. The effect of RGD-modelled polyacrylate substrates on mMSC differentiation

Whilst morphology of mMSCs on plastic, glass and BTL15 substrates appeared similar, on RGD-modelled polyacrylates, ESP03 and ESP04, mMSCs formed aggregates. Aggregation of cells suggested that differentiation of cells may have been occurring, particularly chondrogenesis, which is typically associated with cell compaction (see 4.1.2.1). Therefore, the mMSC aggregates were further analysed by immunostaining for differentiation markers; collagen II for chondrogenesis and osteocalcin for osteogenesis. Adipogenesis was discounted due to negative preliminary staining and the absence of characteristic fat droplets in the mMSCs. Controlled induction of differentiation in the D1 mMSC line into adipocytes, osteoblasts and chondrocytes had previously been demonstrated (Kuzma-Kuzniarska, UoL Stem Cell Group, unpublished).

5.2.2.1. mMSC differentiation detected by immuno-assays

To investigate the effect of the polyacrylate substrates on mMSC differentiation, following 10 day culture, mMSCs were immunostained for markers of osteoblasts and chondrocytes. Since plastic, glass and BTL15 substrates demonstrated similar monolayer growth, solely glass was used

as a representative control; however, similar staining was observed on plastic and BTL15. Strong collagen II staining was detected in all the aggregates on the ESP04 substrate (Figure 5-3). This suggested that chondrogenesis was indeed occurring within these mMSC aggregates. Furthermore, the DAPI nuclei stain confirmed multi-layering and compaction of mMSCs within the aggregates, with higher compaction in aggregates on ESP04 compared to ESP03. Staining was weak in aggregates on ESP03, possibly due to the different mechanism of later aggregation observed in culture, since less compaction and multi-layering was observed. No positive staining was found in cells cultured on glass or the monolayer areas on ESP03 substrates. Interestingly, osteocalcin was also detected in the mMSC aggregates, possibly suggesting a mechanism of co-differentiation. However, the collagen II and osteocalcin stains overlapped significantly, which could also indicate bleed-through between channels, therefore, confocal imaging was conducted to confirm their presence.

Confocal imaging confirmed the presence of collagen II and osteocalcin within aggregates on the ESP04 substrate and demonstrated their three dimensional distribution. Osteocalcin staining was typically localised to the periphery of aggregates, whereas collagen II was localised to the centre, but was also present at the periphery, overlapping with the osteocalcin staining (Figure 5-4). This suggested localised co-differentiation within these aggregates.

5.2.2.2. Investigation of mMSC differentiation by qPCR analysis

Quantitative PCR was conducted to investigate the effect of the substrates on the expression of chondrogenic and osteogenic genes. For chondrogenesis, expression of collagen II and aggrecan were assayed. For osteogenesis, expression of osteocalcin and alkaline phosphatase (AP) were assayed. In all cases expression levels were recorded relative to GAPDH levels. qPCR analysis was conducted following culture for ten days, once mMSCs had formed multi-layered aggregates (Figure 5-1), and eighteen days, when immunostaining demonstrated high levels of collagen II expression from differentiated cells within aggregates (Figure 5-3).

qPCR data demonstrated similar findings to the immunostaining results. Collagen II demonstrated significantly increased expression after 10 day culture on ESP04 (Tukey, $p<0.05$), compared to mMSCs cultured on plastic (Figure 5-5). However, it was not significantly different to glass substrates, suggesting that some degree of spontaneous chondrogenesis was occurring on the glass substrate. Following 18 day culture on ESP04, there was a significant increase in the expression of the chondrocyte markers collagen II and aggrecan, compared to both plastic and glass substrates, indicating progression of chondrogenesis (Figure 5-6). In micromass cultures, following 21 day culture, expression of collagen II and aggrecan was significantly increased over controls (Tukey, $p<0.05$). In comparison to ESP04, the micromass cultures demonstrated a

significant increase in collagen II expression (Tukey, $p<0.05$), however, an increase in expression of aggrecan was not significantly different to ESP04 (Tukey, $p>0.05$). Osteocalcin expression was also significantly increased on ESP04 and ESP03 following 18 day culture; however, AP expression did not appear to increase. Furthermore, expression of osteocalcin and AP was not significantly increased in micromass cultures compared to most controls (Tukey, $p>0.05$), only AP expression compared to tissue culture plastic controls showed a small significant increase (Tukey, $p<0.05$). Whilst up-regulation of chondrogenesis markers was observed following 10 day culture, statistically significant increases in expression were not detected until after 18 days culture. This is not surprising, however, as *in vitro* chondrogenesis typically requires several weeks culture before markers can be detected (Mackay 1998).

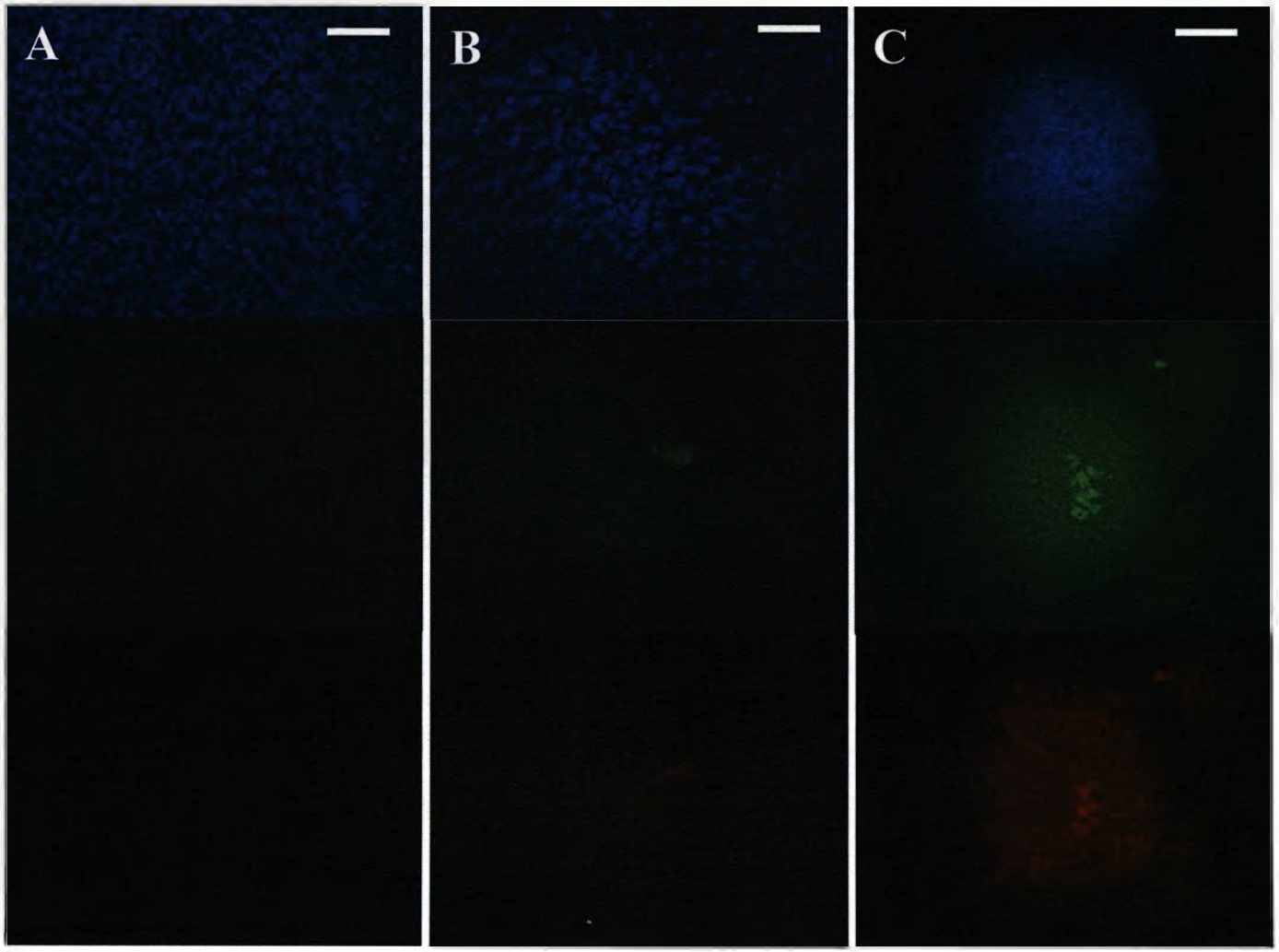

Figure 5-3 Markers for chondrogenesis and osteogenesis detected in mMSCs cultured on polyacrylate substrates. MSCs were grown on Glass (A), EPS03 (B) and ESP04 (C) for 18 days. Cells were fixed and stained for collagen II (green), osteocalcin (red) and nuclei were stained with DAPI (blue). Collagen II and osteocalcin were detected within mMSC aggregates on ESP04. Scale bars represent 200 µm.

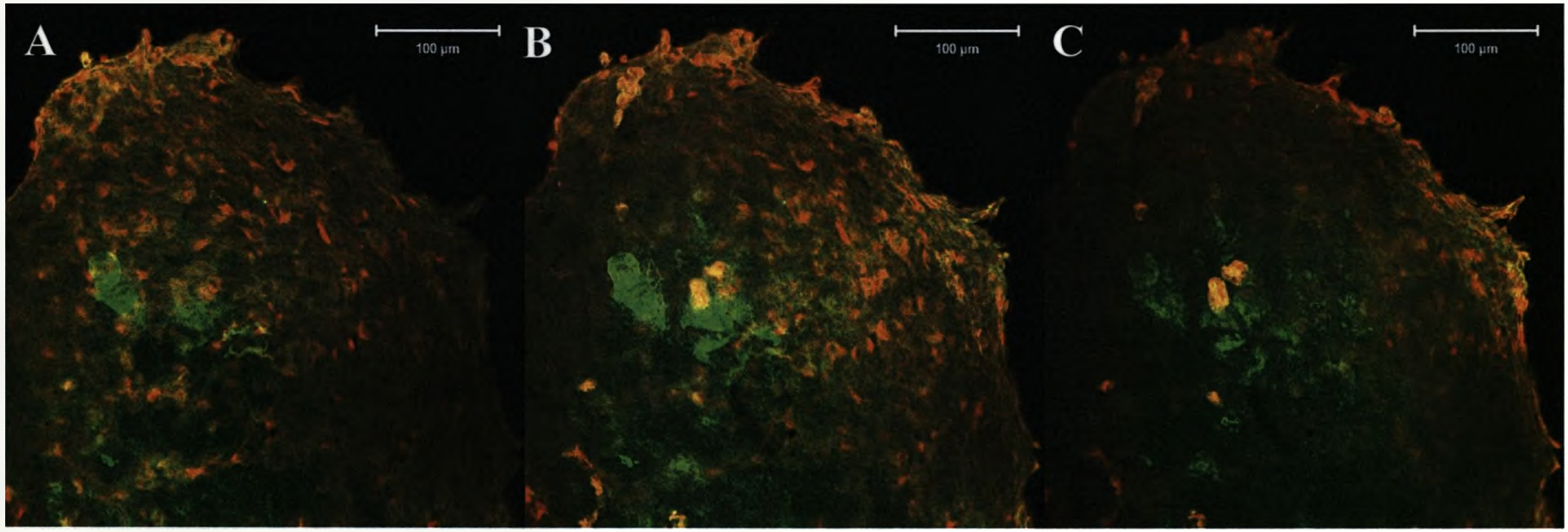

Figure 5-4 Confocal imaging of an mMSC aggregate on ESP04. Confocal microscopy was used to image progressive slices at 2.65 µm increments. Images shown are from Top (A), Middle (B), and Bottom (C) of a single 18 day aggregate. Positive osteocalcin staining (red) is demonstrated in cells at the periphery of the aggregates, whereas collagen II (green) is expressed by cells throughout the aggregates. Images shown are representative of aggregates found on ESP04. Scale bar 100 µm.

5.2.3. Investigating if chondrogenesis precedes or follows aggregation of mMSCs

Following confirmation of chondrocyte differentiation in mMSCs cultured on ESP04, the mechanisms behind this process were further investigated by determining the expression levels of genes required for the induction of chondrogenesis, namely, Sox9 and N-Cadherin. Following 10 and 18 day culture no change in Sox9 or N-cadherin was detected in mMSCs (data not shown). However, this wasn't too surprising, as it is known that these genes tend to be down-regulated following induction of chondrogenesis. Therefore, to investigate expression at earlier time points, the expression of Sox9 and N-cadherin were assayed by qPCR following 2 day culture, prior to aggregate formation. The aim was to identify if substrates were directly inducing chondrogenesis pathways, following which, the cells were induced to aggregate, or alternatively, if the substrates were promoting aggregation, and this was the trigger for chondrogenesis.

Following 2 day culture, mMSCs attached to ESP04 were not spread, but were more rounded compared to cells on the control surface and ESP03 (Figure 5-7). qPCR analysis demonstrated significantly increased expression of the early chondrogenesis marker Sox9 by mMSCs adhered to ESP03 and ESP04 (Tukey model, $p<0.05$)(Figure 5-8). This suggests the Sox9 pathway may be directly induced by the defined substrate chemistry of these substrates. In particular, up-regulation of Sox9 in

mMSCs on ESP03, despite normal spread morphology and lack of early aggregation, suggests promotion of chondrogenesis by this combination and distribution of functional groups. N-cadherin was found to be significantly increased in mMSCs adhered to ESP04 but not ESP03 ($p<0.05$) (Figure 5-8). This suggests that expression of N-cadherin might be induced by the substrate chemistry of ESP04, and once expressed, is likely to promote cell-cell adhesion.

Expression of Sox9 and N-cadherin in mouse E11.5 embryonic limb bud cells (LBCs) was included as a positive control. Both Sox9 and N-cadherin expression was highly increased over typical mMSCs cultured on plastic or glass (Tukey model, $p<0.05$). However, both also demonstrated significantly higher expression than mMSCs cultured on ESP03 and ESP04 substrates (Tukey model, $p<0.05$). In the LBCs, expression of Sox9 was only slightly higher than mMSCs on ESP04, whereas expression of N-cadherin was more than five-fold higher in LBCs.

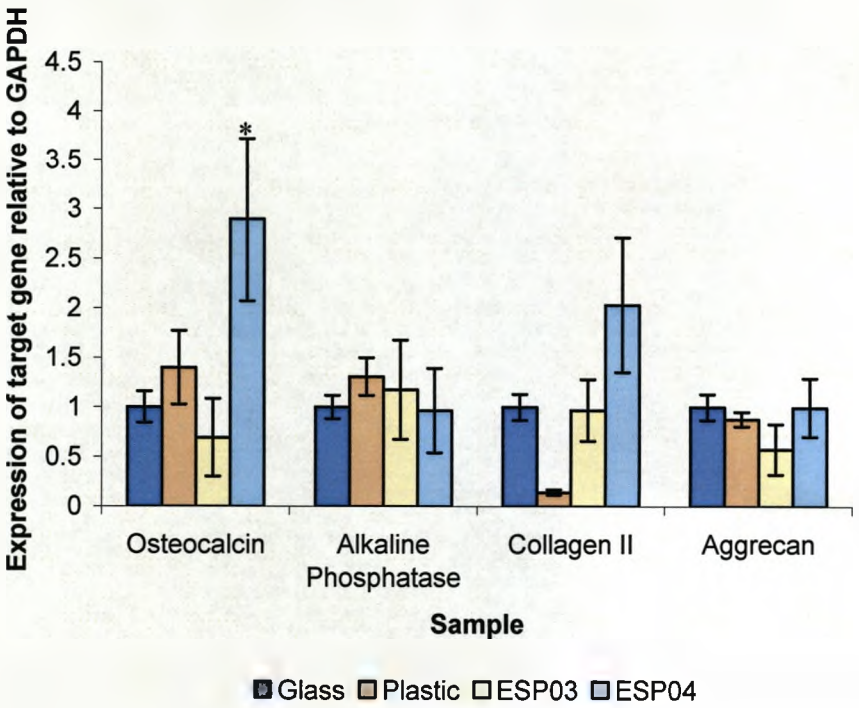

Figure 5-5 PCR analysis of mRNA extracted from mMSCs following 10 day culture. Samples were assayed for osteogenesis markers (osteocalcin & alkaline phosphatase) and chondrogenesis markers (collagen II & aggrecan). Data were normalised to expression on glass substrate. Osteocalcin was significantly upregulated on ESP04. Collagen II demonstrated a slight increase on ESP04. No other statistical significance from controls was demonstrated ($p<0.05$, Tukey model). Results represent the mean of 3 biological replicates ± S.E.M.

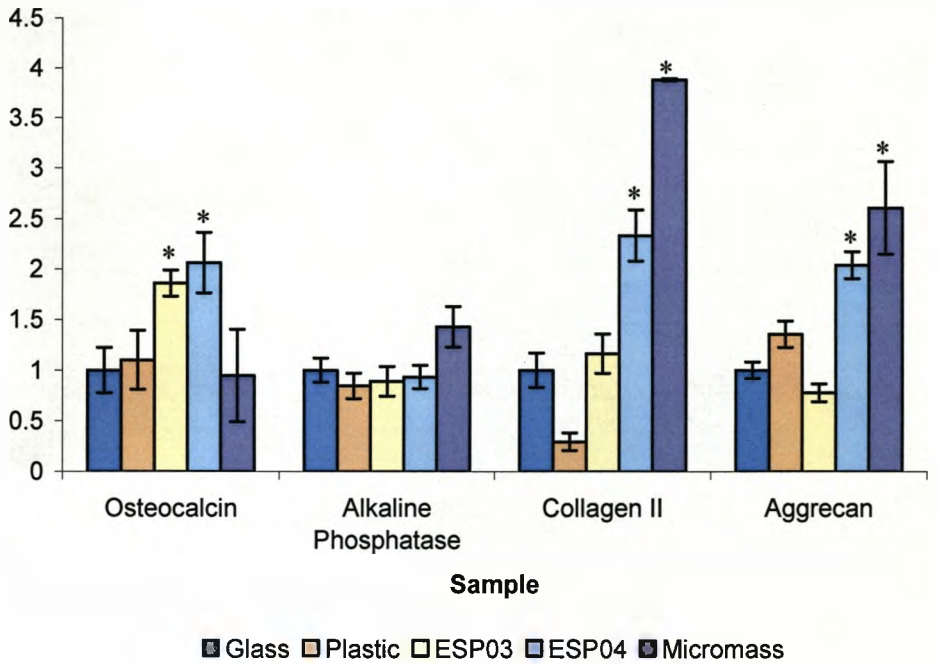

Figure 5-6 PCR analysis of mRNA extracted from mMSCs following 18 day culture. Samples were assayed for osteogenesis markers (osteocalcin & alkaline phosphatase) and chondrogenesis markers (collagen II & aggrecan). Data were normalised to expression on glass substrate. Chondrogenesis markers were significantly upregulated in mMSCs cultured on ESP04. Osteocalcin was significantly upregualted on ESP03 & ESP04. Asterisk indicates data points which are statistically significant from controls ($p<0.05$, Tukey model). Results represent the mean of 3 biological replicates ± S.E.M. except micromass culture which was 2 replicates.

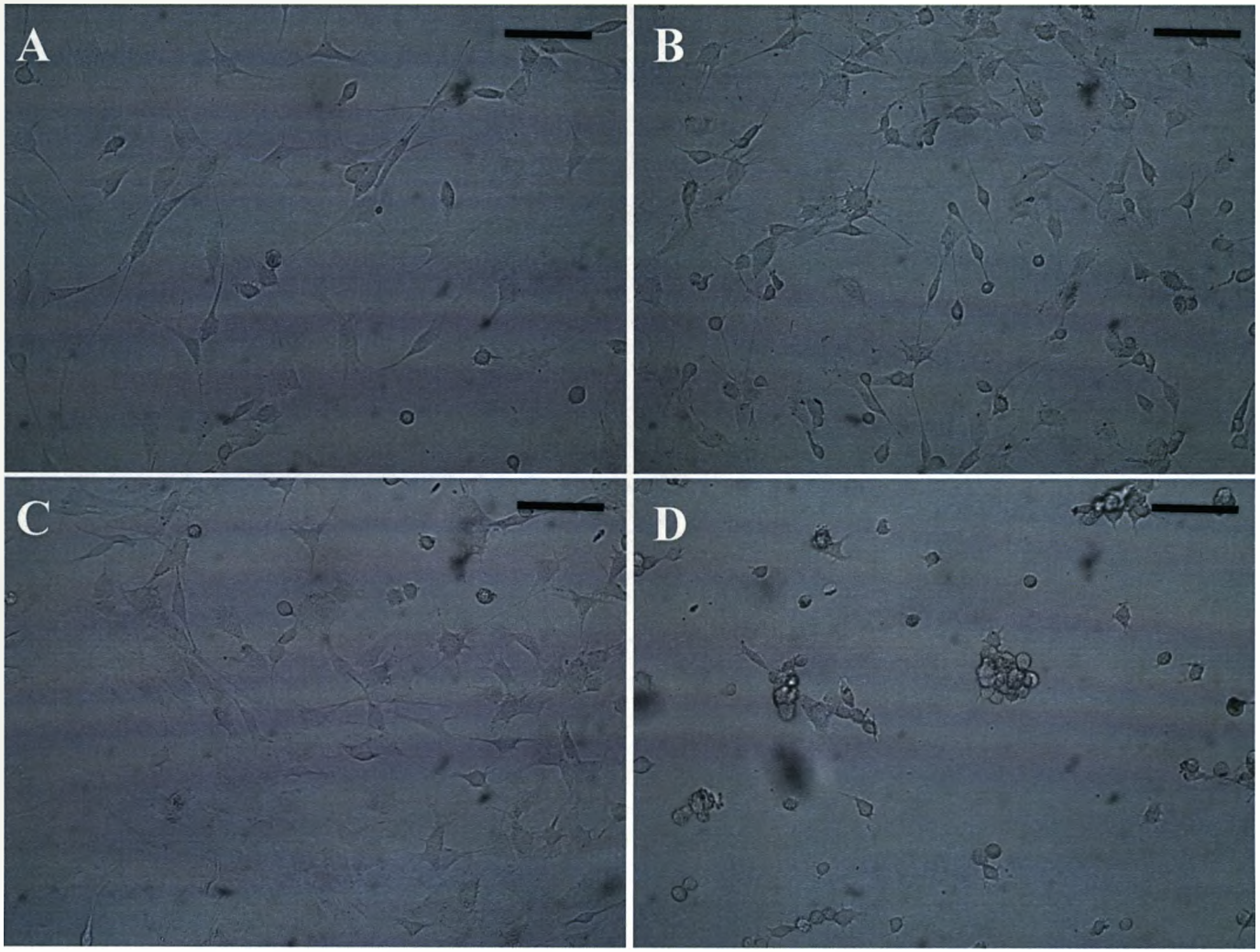

Figure 5-7 Phase contrast of MSCs following 2 day culture on control and polyacrylate substrates. D1 mMSCs were seeded on to plastic (A), glass (B), ESP03 (C) and ESP04 (D) substrates at $1x10^4$ cells per well. Following 2 day culture mMSCs were imaged before RNA extraction. Scale bars represent 50 µm.

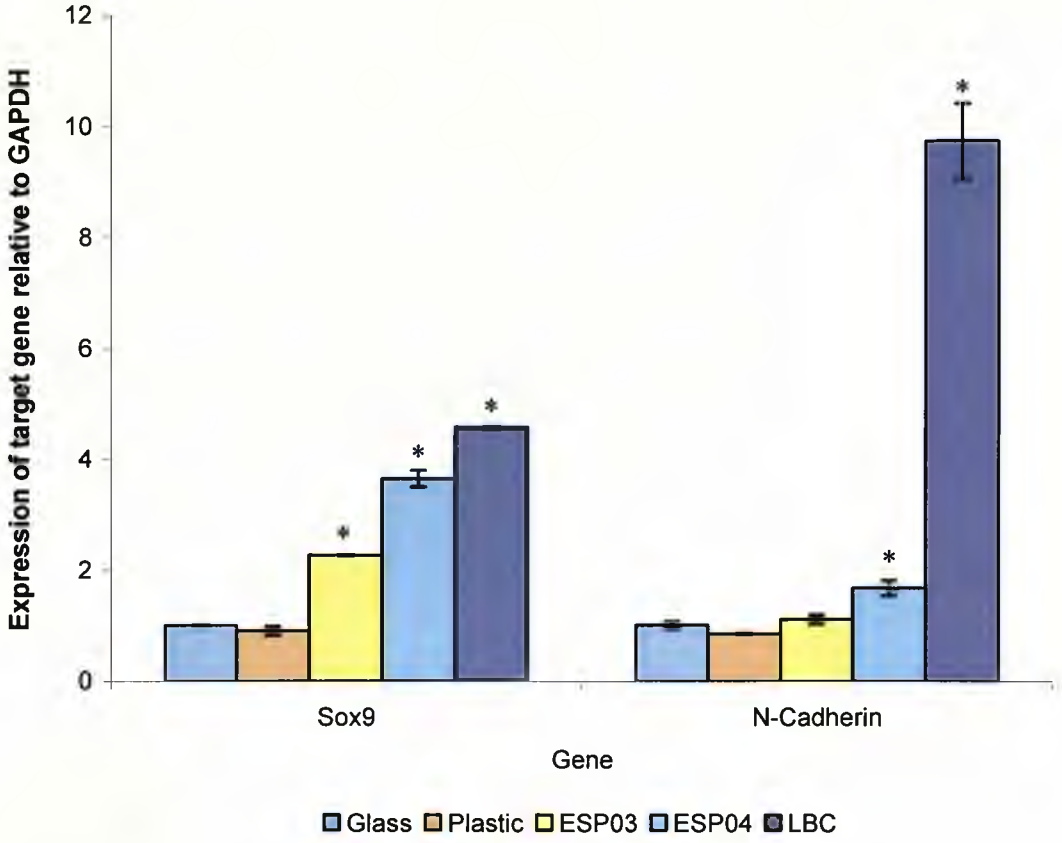

Figure 5-8 qPCR analysis of early mMSC chondrogenesis markers on polyacrylate substrates. Samples were assayed for the early chondrogenesis marker Sox9 and the cell-cell adhesion molecule N-cadherin. Data were normalised to expression on glass substrates. Sox9 was significantly up-regulated in mMSCs adhered to ESP04 and ESP03. N-cadherin was significantly up-regulated on ESP04. Sox9 and N-cadherin expression were significantly higher in E11.5 mouse embryonic limb bud cells. Asterisk indicates data points which are statistically significant from controls ($p<0.05$, Tukey model). Results represent the mean of 3 biological replicates ± S.E.M.

5.2.4. Investigating response of mMSCs to amine substrates

Previous studies had demonstrated that amine substrates were capable of promoting MSC aggregation and chondrogenesis, albeit in the presence of TGF-βs (Curran 2006; Guo 2008). This raised the possibility that the chondrogenic response observed on ESP04 might simply have

resulted from the high degree of amine functionality in this substrate. To test this, the mMSCs were cultured on amine surfaces generated by plasma polymerisation, supplied by Dr. Vasilev (Mawson Institute, University of South Australia) (Losic 2008), and their behaviour compared to mMSCs cultured on ESP04.

Following both one and two week culture, mMSCs demonstrated no aggregating behaviour on amine plasma modified substrates (Figure 5-9). Monolayer growth was observed on low and high amine substrates and was indistinguishable from growth on tissue culture plastic controls. Aggregate formation proceeded as expected on ESP04. This suggested that the chondrogenic response in mMSCs was due to the combination and distribution of amine and carboxyl functional groups within the polyacrylate substrate ESP04.

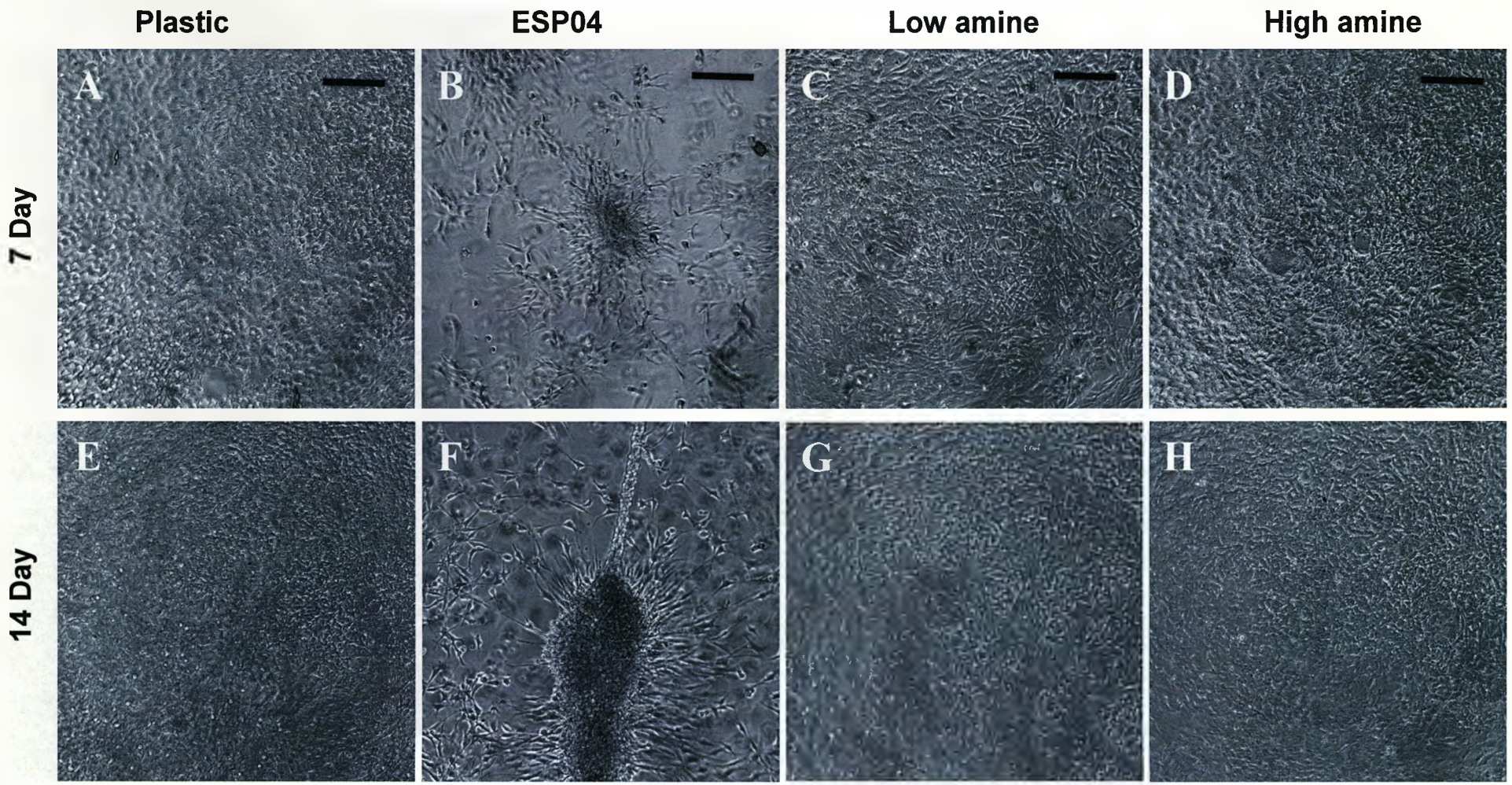

Figure 5-9 Phase contrast images of mMSCs cultured on ESP04 and amine substrates. D1 mMSCs were seeded on to plastic (A&E), ESP04 (B&F), low amine (C&G) and high amine (D&H) substrates at $1x10^4$ cells per well. Representative images were obtained following 7 day (A-D) and 14 day (E-H) culture. Scale bar 100 µm.

5.2.5. Transfer of technology to multiple mesenchymal cell types

To confirm if the aggregating behaviour and chondrogenesis in response to RGD-modelled polyacrylate substrates was common to other MSC-like cells, mouse kidney-derived stem cells (KSCs) and limb bud cells (LBCs) were cultured on the chondrogenesis-inducing polyacrylate substrate ESP04 and assayed for chondrogenesis. Furthermore, mouse embryonic fibroblasts, which have been shown to differentiate to chondrocytes (Lengner 2004), were found not to aggregate when cultured on the polyacrylate substrates (data not shown), suggesting the aggregating response is specific to chondrogenesis in MSCs and MSC-like cells.

5.2.5.1. Ability of RGD-modelled polyacrylate substrates to promote chondrogenesis in KSCs

The H6 KSC line was originally derived by Cristina Fuente Mora (UoL Stem Cell Group) from a population of KSCs isolated from 2-6 day old CD1 mice. These KSCs have demonstrated MSC-like properties and can differentiate to form a number of mesenchymal cell lineages, including adipocytes and osteoblasts (Fuente Mora, UoL Stem Cell Group) (Fuente-Mora 2009). Therefore, it was reasonable to predict they would have the capacity to undergo chondrogenesis via similar mechanisms to mMSCs. Cell morphology was observed throughout the culture period and following 14 day culture, cells were immunostained for the

chondrocyte-specific marker collagen II, and the osteoblast-specific marker osteocalcin. Furthermore, qPCR was performed to determine expression levels of chondrocyte specific genes, collagen II and aggrecan, and osteoblast-specific genes, osteocalcin and AP.

The KSCs began aggregating soon after seeding on to the ESP04 substrate (Figure 5-10), similar to behaviour observed with the mMSCs, whereas cells on control substrates grew in monolayers, as expected. Immunostaining suggested the presence of collagen II and osteocalcin within the KSC aggregates, however, it was unclear if bleed-through may have contributed to the fluorescence (Figure 5-11). Confocal images confirmed the presence and discrete distribution of collagen II and osteocalcin (Figure 5-12). Osteocalcin demonstrated some expression close to the periphery of aggregates, whereas collagen II was expressed throughout most of the aggregates, with a somewhat stronger apparent staining towards the centre. Increased expression of chondrogenesis and osteogenesis markers was demonstrated by qPCR (Figure 5-13), and down-regulation of the kidney-specific marker Wt1 was demonstrated in KSCs on ESP04, confirming loss of the kidney cell phenotype. Therefore, the induction of chondrogenesis in these KSCs replicated that observed with the mMSC line.

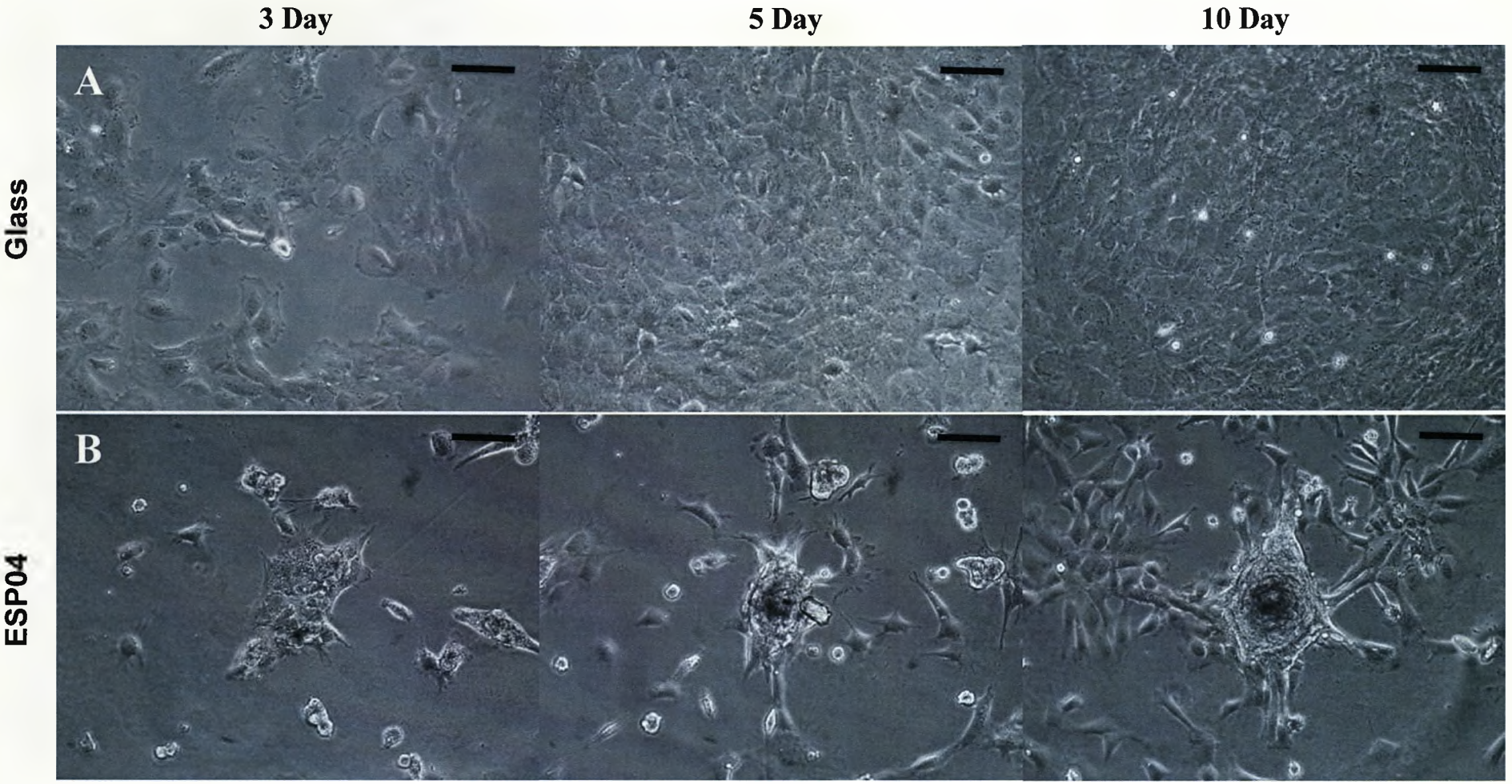

Figure 5-10 KSC behaviour on glass and ESP04 substrates. H6 KSCs were seeded at $1x10^4$ cells, cultured for 14 days in MSC medium and observed in culture on glass (A) and ESP04 (B). Images were obtained daily, shown above are representative images at 3, 5 and 10 days. Cells attached and grew into evenly distributed monolayers on glass. On ESP04 cells aggregated quickly in culture, condensed and grew to form tightly packed multi-layered aggregates. Scale bar 100 µm.

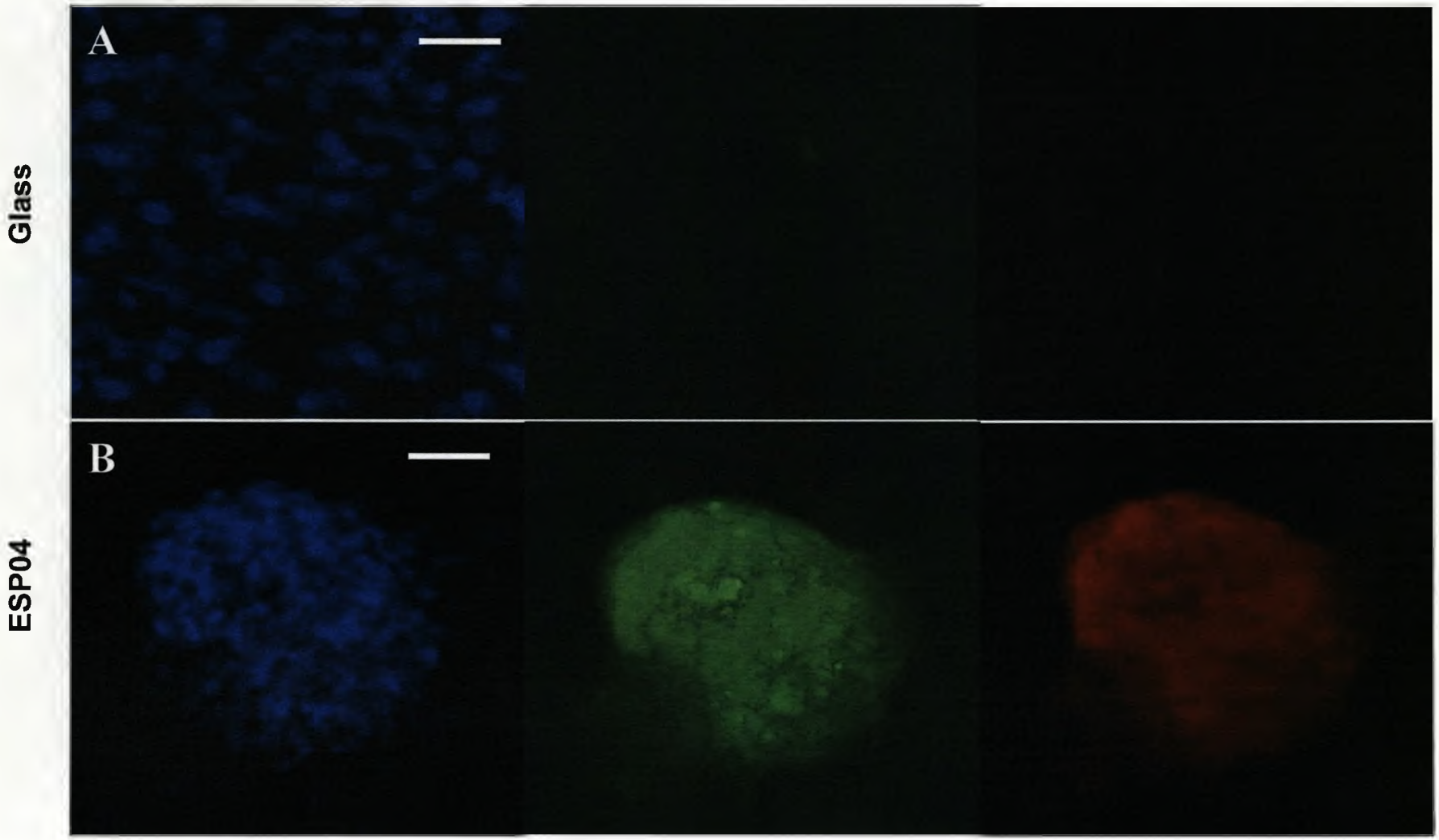

Figure 5-11 Markers for chondrogenesis and osteogenesis detected in KSCs cultured on glass and ESP04 substrates. KSCs were grown on glass (A) and ESP04 (B) in MSC medium for 14 days. Cells were fixed and stained for collagen II (green), osteocalcin (red) and nuclei were stained with DAPI (blue). Scale bars represent 100 μm.

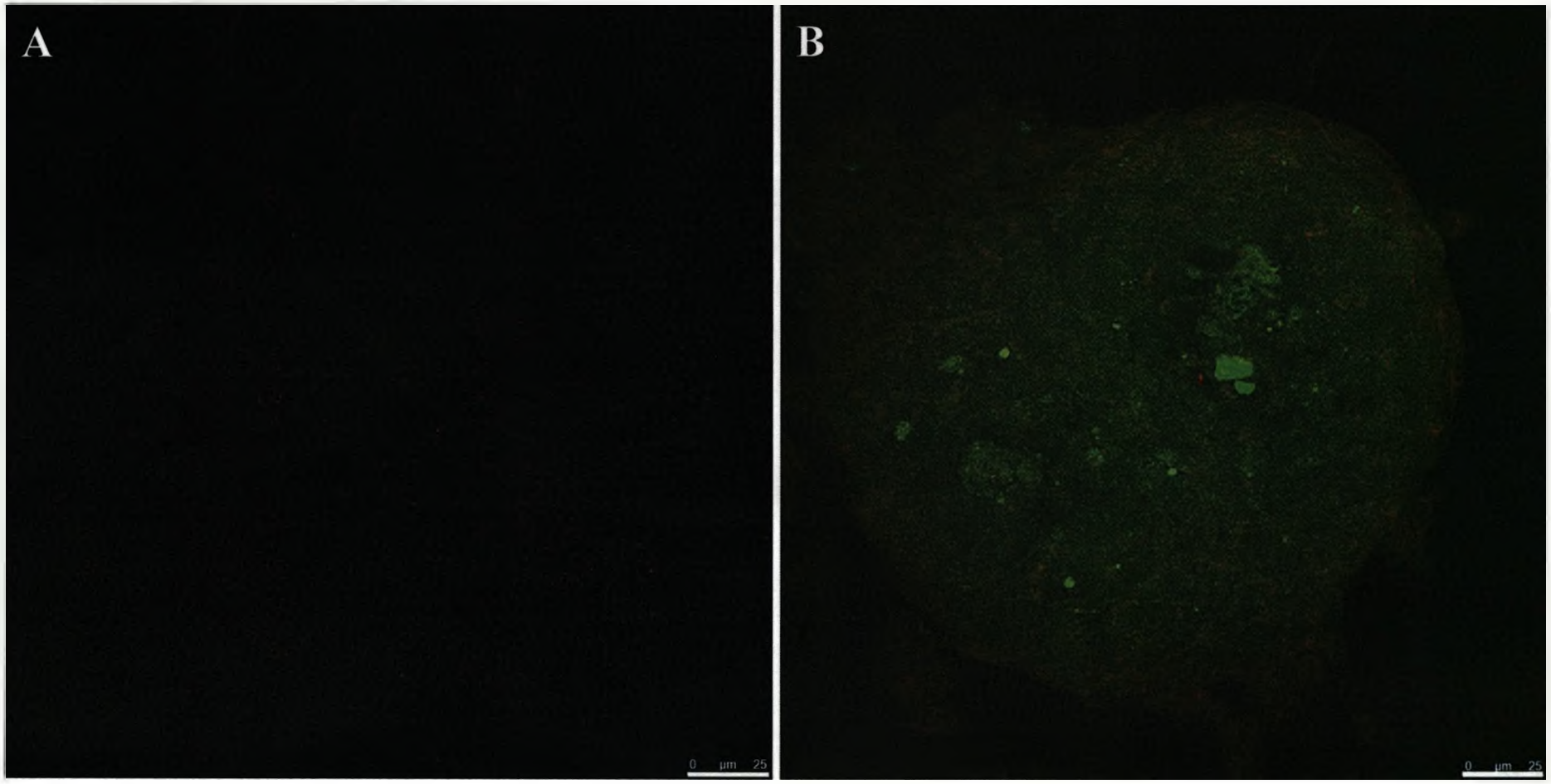

Figure 5-12 Confocal images of KSCs cultured on glass and ESP04 substrates. KSCs were grown on glass (A) and ESP04 (B) in MSC medium for 14 days. Cells were fixed and stained for collagen II (green) and osteocalcin (red). Immunostaining for osteocalcin demonstrates some expression close to the periphery of aggregates, whereas collagen II is stronger towards the centre of the aggregates. Scale bars represent 25 µm.

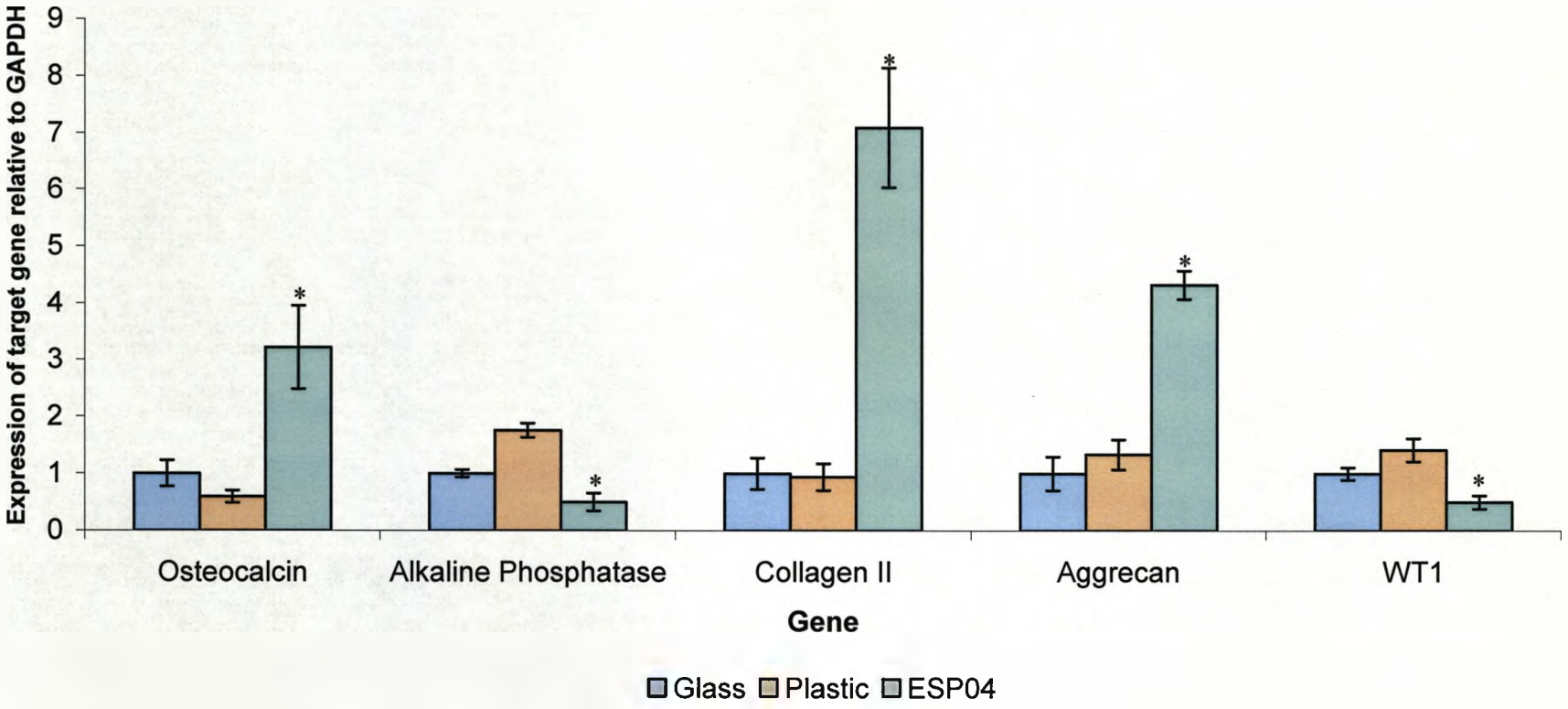

Figure 5-13 PCR analysis of mRNA extracted from KSCs following 14 day culture. Samples were assayed for osteogenesis markers (osteocalcin & alkaline phosphatase), chondrogenesis markers (collagen II & aggrecan), and a kidney marker (Wt1). Data was normalised to expression on glass substrate. Chondrogenesis markers were significantly up-regulated in KSCs cultured on ESP04. Osteocalcin was significantly up-regulated on ESP04. Wt1 and AP (kidney markers) were down-regulated in differentiating cells. Asterisk indicates statistical significance from controls ($p<0.05$, Tukey model). Results represent the mean of 3 biological replicates ± S.E.M.

5.2.5.2. Ability of RGD-modelled polyacrylate substrates to promote chondrogenesis in LBCs

LBCs were obtained by dissociating E11.5 mouse embryo limb buds, and were immediately seeded onto test substrates. This population of cells should have contained the condensing undifferentiated mesenchymal cells responsible for cartilage and bone formation in the limb bud, and it was predicted that culturing on ESP04 could induce them to aggregate and undergo chondrogenesis similar to the D1 mMSC and H6 KSC line.

Aggregation again began soon after seeding the LBCs onto ESP04, and was observed as early as day 6 (Figure 5-14). Collagen II was detected within aggregates, however, osteocalcin was very weak in the LBC aggregates on ESP04 (Figure 5-15). qPCR demonstrated significantly higher expression of chondrogenic markers on ESP04 compared with control substrates (Tukey model, $p<0.01$) (Figure 5-16), with only a slight increase in osteocalcin (Tukey model, $p<0.05$). However, the second marker for osteogenesis, AP was also significantly higher (Tukey model, $p<0.01$).

qPCR data from RNA extracted from freshly isolated LBCs demonstrated high expression of chondrogenesis markers and AP (Figure 5-16), suggesting that chondrocytes were already present within the LBC population. Expression of collagen II, aggrecan and AP was significantly lower in LBCs after 14 day culture on glass and plastic substrates (Tukey

model, $p<0.05$), possibly indicating dedifferentiation of the LBC-derived chondrocytes. Expression of chondrogenesis markers in cells cultured for 14 days on ESP04 were more similar to freshly isolated LBCs, suggesting that LBCs are able to maintain a chondrogenic phenotype when cultured on ESP04, whereas dedifferentiation takes place on control substrates.

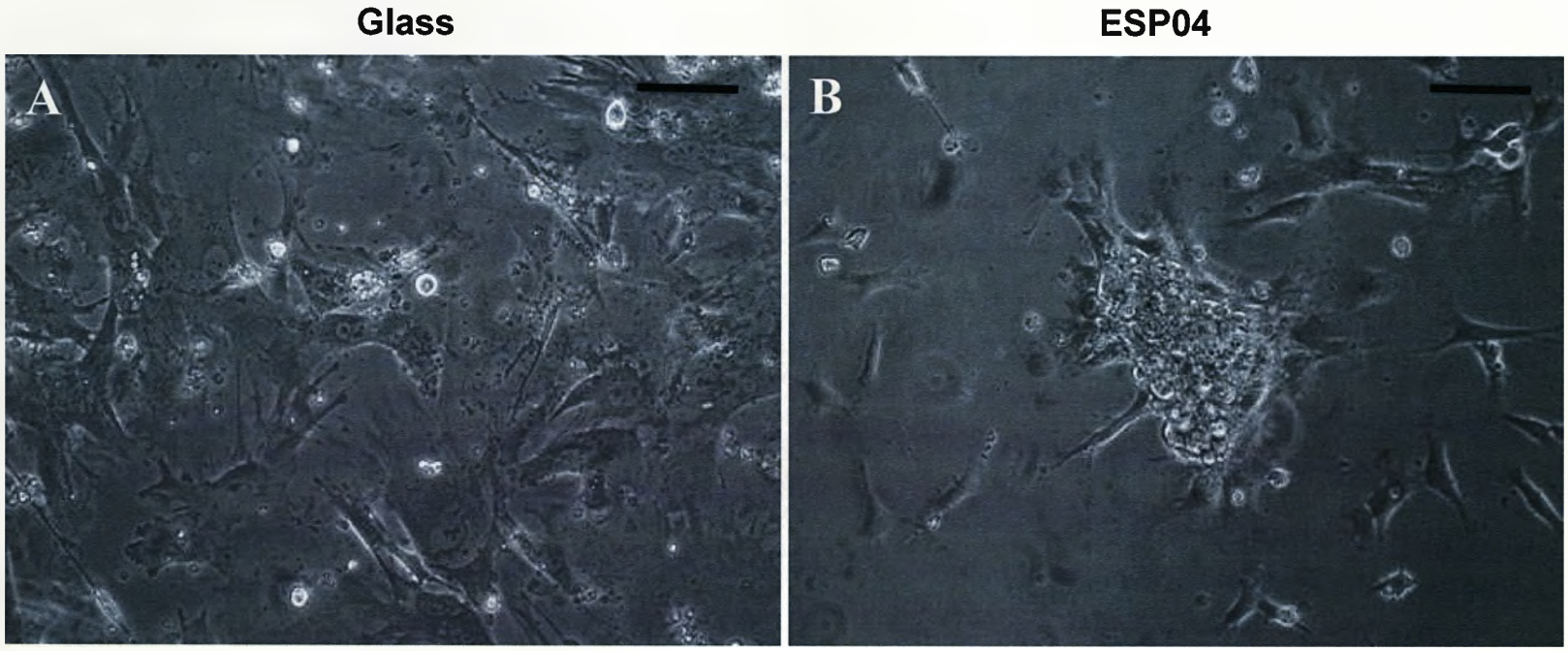

Figure 5-14 LBC behaviour on glass and ESP04 substrates. LBCs were seeded at $1x10^5$ cells, and cultured for 6 days in MSC medium and observed in culture on glass (A) and ESP04 (B). Representative images of LBC growth following 6 day culture are shown. Cells attached and grew into evenly distributed monolayers on glass. On ESP04 cells aggregated quickly in culture, condensed and grew to form tightly packed multi-layered aggregates. Scale bar 100 μm.

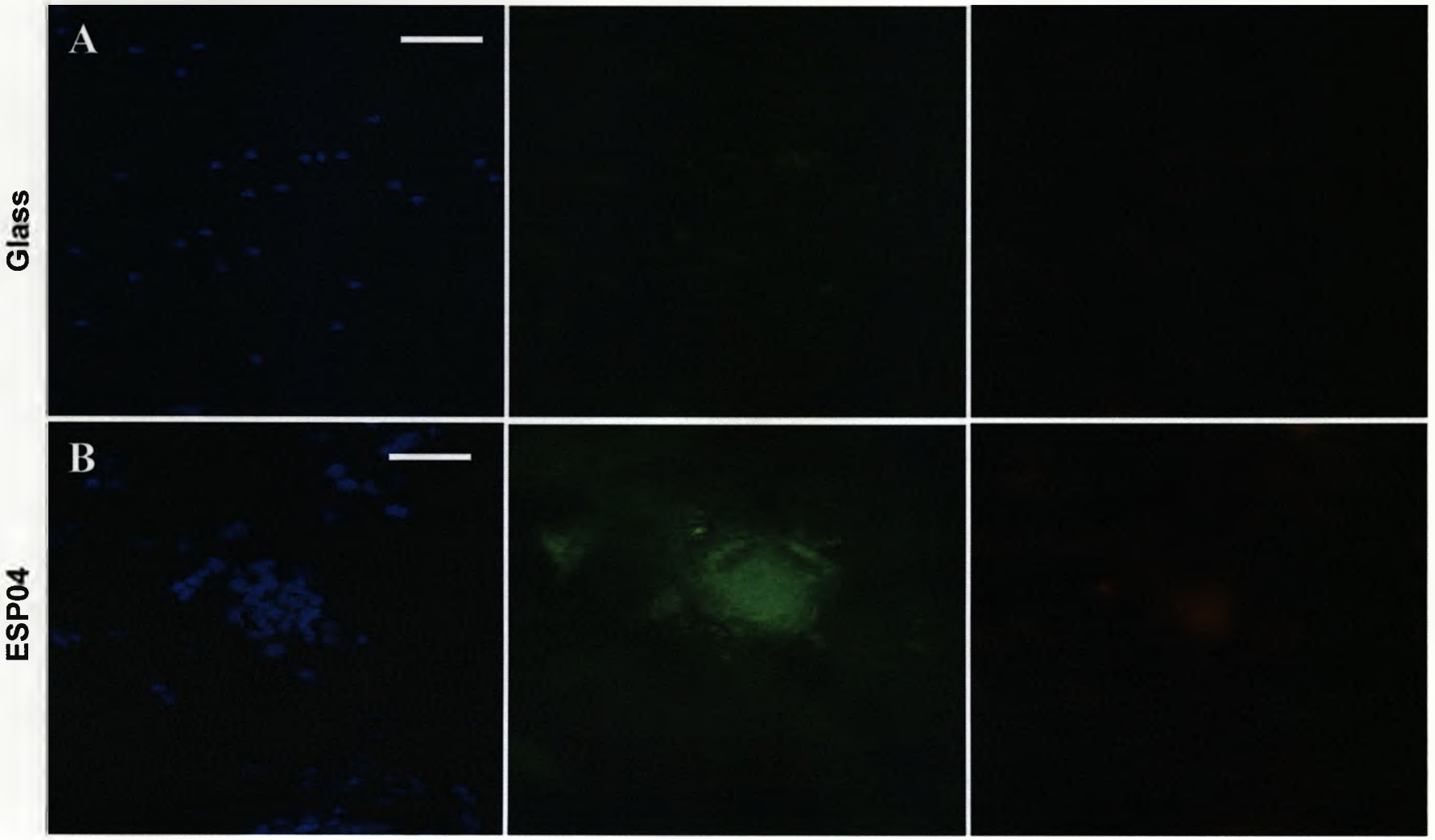

Figure 5-15 Markers for chondrogenesis and osteogenesis detected in LBCs cultured on glass and ESP04 substrates. LBCs were grown on ESP04 in MSC medium for 14 days. Cells were fixed and stained for collagen II (green), osteocalcin (red) and nuclei were stained with DAPI (blue). Immunostaining for collagen II demonstrates expression within the aggregates, whereas osteocalcin is lower. Scale bars represent 100 μm.

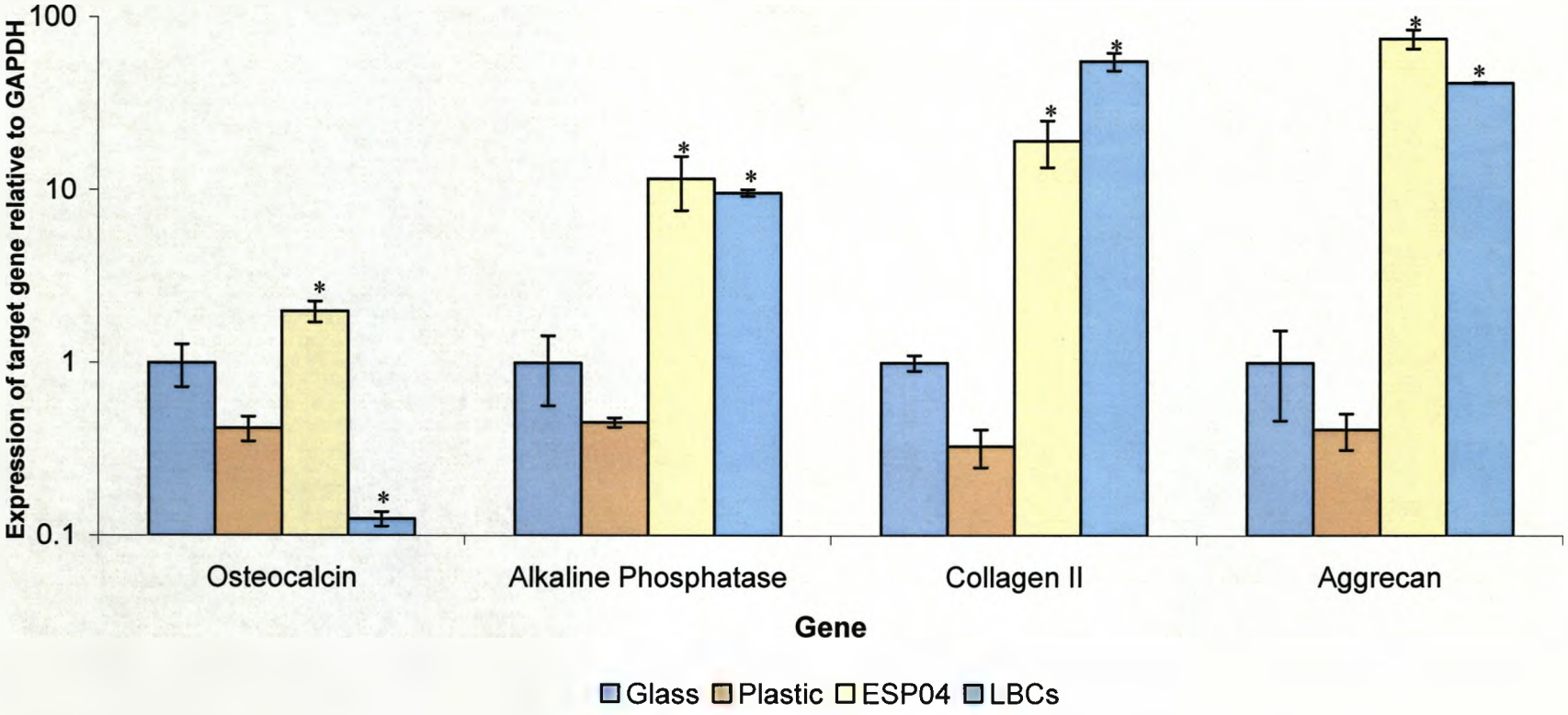

Figure 5-16 PCR analysis of mRNA extracted from LBCs following 14 day culture. Samples were assayed for osteogenesis markers (osteocalcin & alkaline phosphatase) and chondrogenesis markers (collagen II & aggrecan). Data was normalised to expression on glass substrate. Data from freshly isolated E11.5 mouse embryonic limb bud cells was included for comparison. Expression of chondrogenesis markers was significantly higher in LBCs cultured on ESP04 compared with plastic or glass. Osteocalcin and AP were significantly higher on ESP04. Asterisk indicates statistical significance from controls ($p<0.05$, Tukey model). Results represent the mean of 3 biological replicates ± S.E.M.

5.2.6. Ability of RGD-mimicking polyacrylate substrates to promote chondrogenesis in hMSCs

Results from this chapter demonstrated induction of chondrogenesis in different mouse mesenchymal cell types in response to the polyacrylate substrates mimicking the functional composition and distribution of RGD, principally ESP04. Transfer of this technology to human cells was the next challenge of this study. Primary hMSCs were, therefore, cultured on polyacrylate substrates under similar conditions to the mMSCs. Cell behaviour was followed in culture for 20 days, after which the hMSCs were assayed for chondrogenesis with qPCR and immunostaining protocols. ESP07 was a new polyacrylate designed for this study and based on ESP04, but deviating from the RGD-inspired functionality by having enhanced hydroxyl content. The ESP07 substrate was tested alongside ESP03 and ESP04 for support of hMSC chondrogenesis.

Aggregation proceeded similar to that observed with mMSCs. Following seeding as a single cell suspension, the hMSCs were found to attach evenly across all substrates. Aggregation was observed on ESP03, ESP04 and ESP07 soon after attachment, and after 3 days the cells had clearly aggregated (Figure 5-17). However, on ESP03 and ESP04 compaction was less pronounced and aggregates remained more spread with less multi-layering than had been previously observed with mMSCs. On ESP03, aggregate development proceeded similar to ESP04 and a clear progression in the extent of aggregation was demonstrated between

ESP03 and ESP04 substrates, which correlated positively with rising amine content.

Fluorescence imaging confirmed the lack of multi-layering and compaction within aggregates on ESP03 and ESP04 by DAPI imaging of nuclei (Figure 5-18). Collagen II and osteocalcin immunostaining was very weak on ESP03 and ESP04, suggesting little differentiation of the hMSCs (Figure 5-18). In addition, qPCR analysis demonstrated no significant increase in expression of differentiation markers on ESP03 and ESP04 (Tukey model, $p>0.05$), apart from SOX9, the early chondrogenesis marker, which was significantly up-regulated in hMSCs cultured on ESP04 (Tukey model, $p<0.05$) (Figure 5-20).

Enhancement of multi-layering and compaction was observed on ESP07 substrates after a week in culture (Figure 5-17). Following 20 day culture, tightly packed aggregates were observed on the ESP07 substrates, and the differentiation markers collagen II and osteocalcin were detected by immunostaining (Figure 5-18). Confocal imaging demonstrated the compaction of cells and nuclei within aggregates. Confocal imaging also confirmed the presence of collagen II and osteocalcin (Figure 5-19), demonstrating a similar distribution to that observed with mMSCs (Figure 5-4) and KSCs (Figure 5-12). Osteocalcin was detected in the most peripheral cells of the aggregates, whereas collagen II was expressed throughout, with a trend to somewhat stronger staining towards the centre of aggregates. qPCR data demonstrated significant increases in

expression of chondrogenesis markers in hMSCs cultured on ESP07 compared to other polyacrylates and controls (Tukey model, $p<0.05$) (Figure 5-20). Expression of collagen II, aggrecan and SOX9 was significantly increased on ESP07 compared to controls (Tukey model, $p<0.05$), and collagen II and aggrecan were significantly increased on ESP07 compared to the other polyacrylates, ESP03 and ESP04 (Tukey model, $p<0.05$).

Standard micromass chondrogenesis of hMSCs was conducted and analysed by qPCR to compare with aggregate culture on the polyacrylate substrates (Figure 5-20). Micromass differentiated hMSCs demonstrated similar collagen II and aggrecan expression (Tukey model, $p>0.05$) and significantly higher SOX9 expression (Tukey model, $p<0.05$) in comparison to hMSCs cultured on ESP07. However, expression of osteocalcin was significantly lower than in hMSCs cultured on ESP07 (Tukey model, $p<0.05$), indicating that no osteogenesis was occurring. Furthermore, in hMSCs differentiated by micromass culture, expression of aggrecan and osteocalcin were not significantly different from cells cultured on the plain glass and tissue culture plastic control substrates (Tukey model, $p>0.05$).

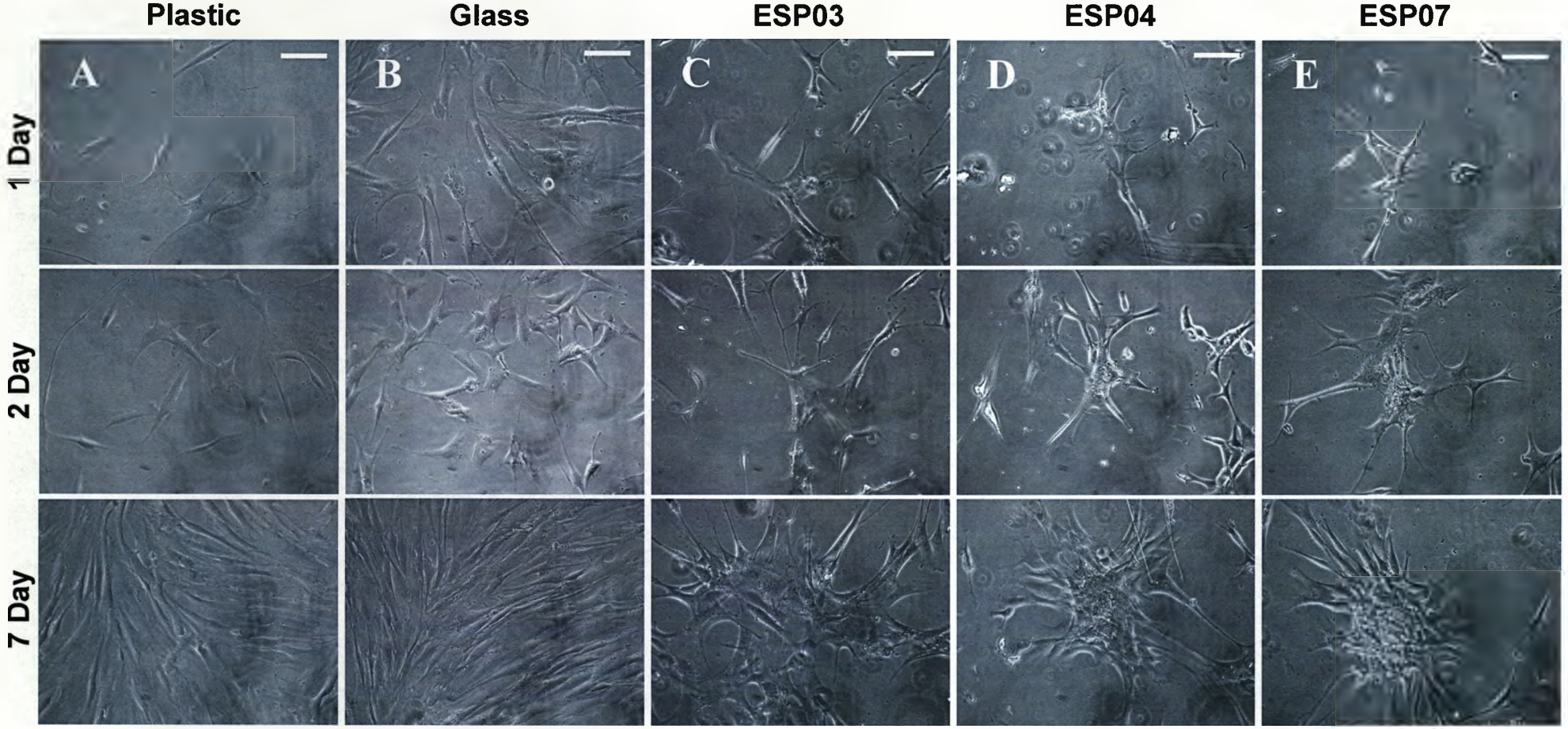

Figure 5-17 Primary hMSC behaviour on polyacrylate and control substrates. hMSCs were cultured for 20 days in hMSC medium and observed in culture on tissue culture plastic (A), glass (B), ESP03 (C), ESP04 (D) and ESP07 (E). Images were obtained daily, shown above are representative images at 1, 2 and 7 days. Cells attached and grew into evenly distributed monolayers on glass. On ESP03, ESP04 and ESP07 cells aggregated soon after culture, however, considerably greater condensation and multi-layering was observed on ESP07. Scale bar 200 µm.

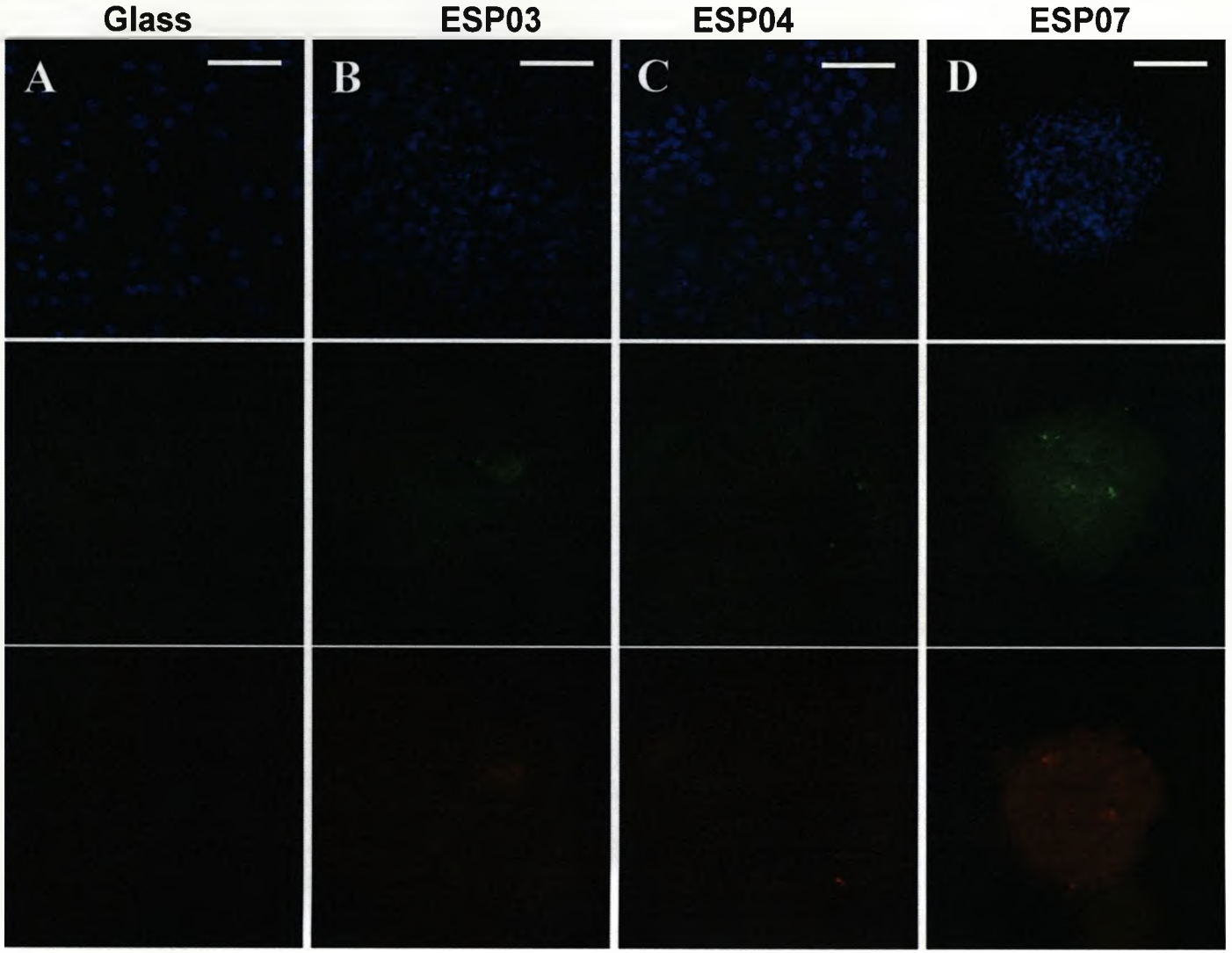

Figure 5-18 Primary hMSC differentiation on polyacrylate and control substrates. hMSCs were cultured for 20 days in hMSC medium on glass (A), ESP03 (B), ESP04 (C) and ESP07 (D). Cells were fixed and stained collagen II (green) osteocalcin (red) and nuclei were stained with DAPI (blue). Enhanced aggregation, compaction and multi-layering was observed on ESP07. Scale bar 200 µm.

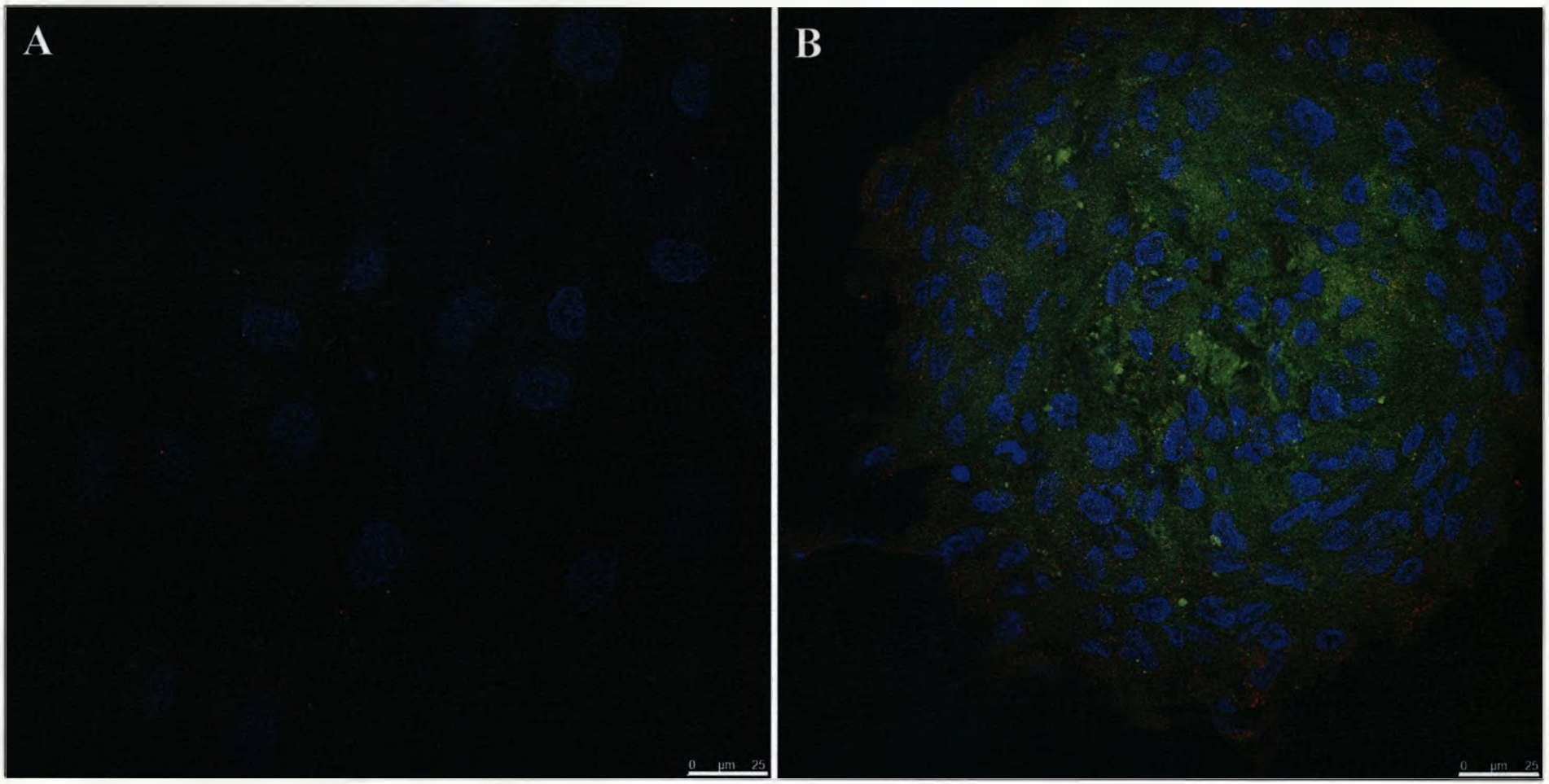

Figure 5-19 Confocal images of hMSCs cultured on glass and ESP04 substrates. hMSCs were grown on glass (A) and ESP04 (B) in hMSC medium for 14 days. Cells were fixed and stained for collagen II (green), osteocalcin (red) and nuclei were stained with DAPI (blue). Immunostaining for osteocalcin demonstrates some expression close to the periphery of aggregates, whereas collagen II staining was observed throughout, with a trend to stronger central staining. Scale bars represent 25 µm.

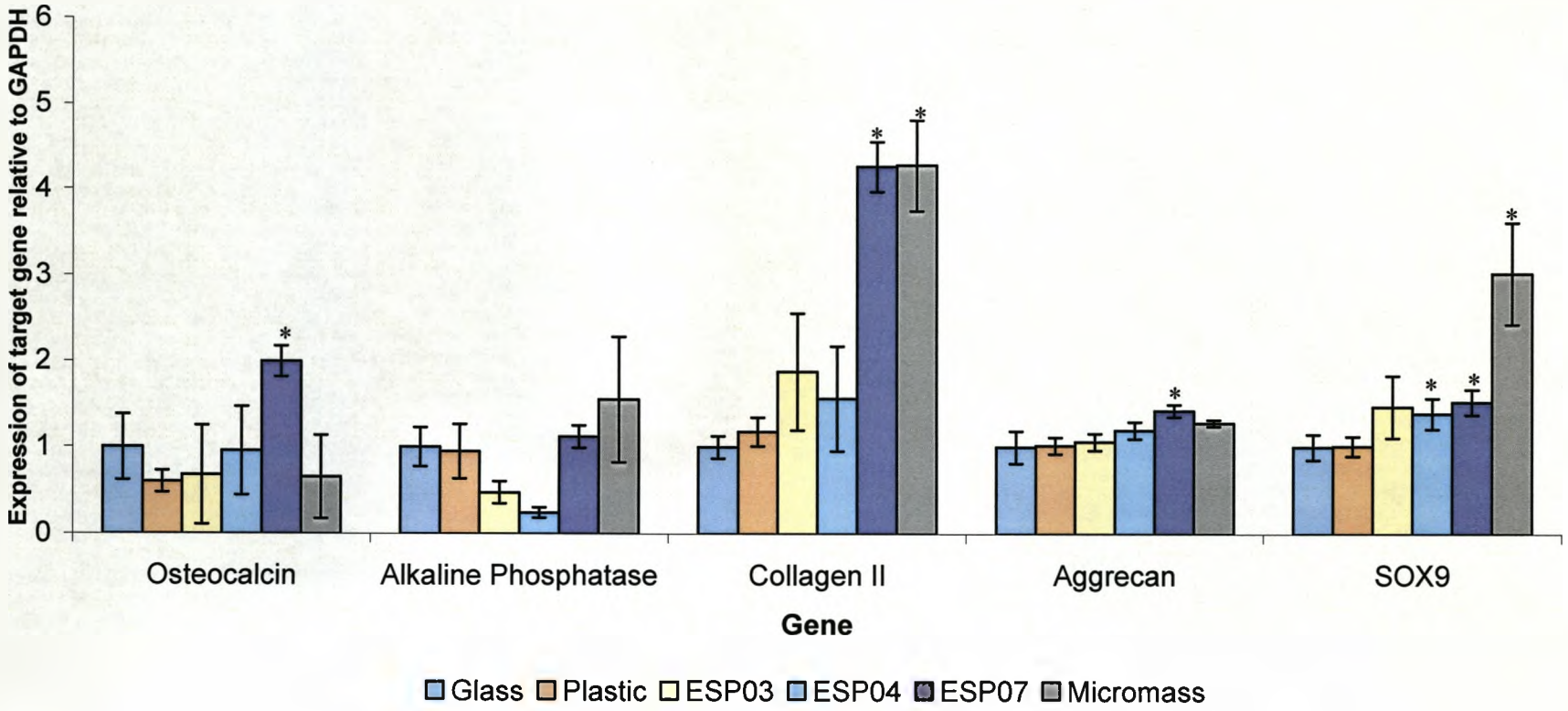

Figure 5-20 PCR analysis of mRNA extracted from primary hMSCs cultured on polyacrylate substrates. $1x10^4$ hMSCs were cultured for 20 days in hMSC medium. Samples were assayed for osteogenesis markers (osteocalcin & alkaline phosphatase) and chondrogenesis markers (collagen II, aggrecan & SOX9). Data were normalised to expression on glass substrate. Collagen II, aggrecan, SOX9 and osteocalcin were significantly up-regulated on ESP07. PCR data from micromass chondrogenesis was included for comparison. Asterisk indicates statistical significance from controls ($p<0.05$, Tukey model). Results represent the mean of 3 biological replicates ± S.E.M. except micromass culture which was 2 replicates.

5.2.6.1. The ability of RGD-mimicking polyacrylates to support chondrogenesis of hMSCs under chondrogenic conditions

Whilst aggregation of hMSCs was clearly demonstrated on ESP03 and ESP04, chondrogenesis on these substrates was severely diminished compared to the results obtained with mMSCs. However, some positive immunostaining for collagen II was found and SOX9 was upregulated following culture on ESP04, suggesting chondrogenesis was progressing, but more slowly than in the mMSCs. In micro-mass culture both compaction of the hMSCs into aggregates and addition of factors, particularly TGF-β3, are essential for chondrogenesis. Therefore, hMSCs were cultured on the polyacrylate substrate ESP04 whilst exposed to chondrogenic medium, to see if chondrogenesis would be promoted under these conditions.

Preliminary tests found greatly enhanced aggregation and compaction of hMSCs under chondrogenic conditions (Figure 5-21), whilst little change was observed on control substrates. However, the tightly packed aggregates were observed lifting off from the polyacrylate substrates following one to two weeks in culture. Therefore, the procedure was altered to allow hMSCs to attach and grow in normal medium for one week, and then cultured under chondrogenic conditions for one week. Following culture under chondrogenic conditions hMSCs were examined using immunostaining and qPCR techniques.

Results from the modified procedure demonstrated enhanced aggregation and compaction on ESP04 under chondrogenic conditions (Figure 5-22). Following 7 days exposure to chondrogenic medium, aggregates appeared multi-layered and highly condensed, but remained adhered to the surface. Immunostaining detected the presence of compact multi-layered aggregates and of chondrogenesis within these aggregates (Figure 5-23). This was supported by qPCR analysis which demonstrated significant up-regulation of chondrogenic markers (Collagen II & SOX9) on ESP04 under chondrogenic conditions ($p<0.05$, Tukey model). Aggrecan appears increased on ESP04 with and without chondrogenic conditions, however, it was not significantly higher than controls ($p>0.05$, Tukey model) (Figure 5-24).

Whilst osteocalcin was detected by immunostaining (Figure 5-23), qPCR demonstrated no significant increase in osteocalcin expression (Figure 5-24), which suggests that bleed-through of the collagen II signal was responsible for the immunostaining observed in this case. AP expression was significantly increased on ESP04 under chondrogenic conditions ($p<0.05$, Tukey model), whereas, using hMSC medium AP expression was significantly lower than controls ($p<0.05$, Tukey model). On plain glass, under chondrogenic conditions, only collagen II expression was significantly increased ($p<0.05$, Tukey model), however, this was less than half the level of expression on ESP04 under chondrogenic conditions. In comparison to results after 20 day culture on ESP04 (Figure 5-20) AP expression was again significantly lower than controls

($p<0.05$, Tukey model) and osteocalcin, collagen II and aggrecan were not significantly different ($p>0.05$, Tukey model). However, SOX9 expression was not significantly different from controls ($p>0.05$, Tukey model), which could be attributed to the shorter, 14 day, culture length.

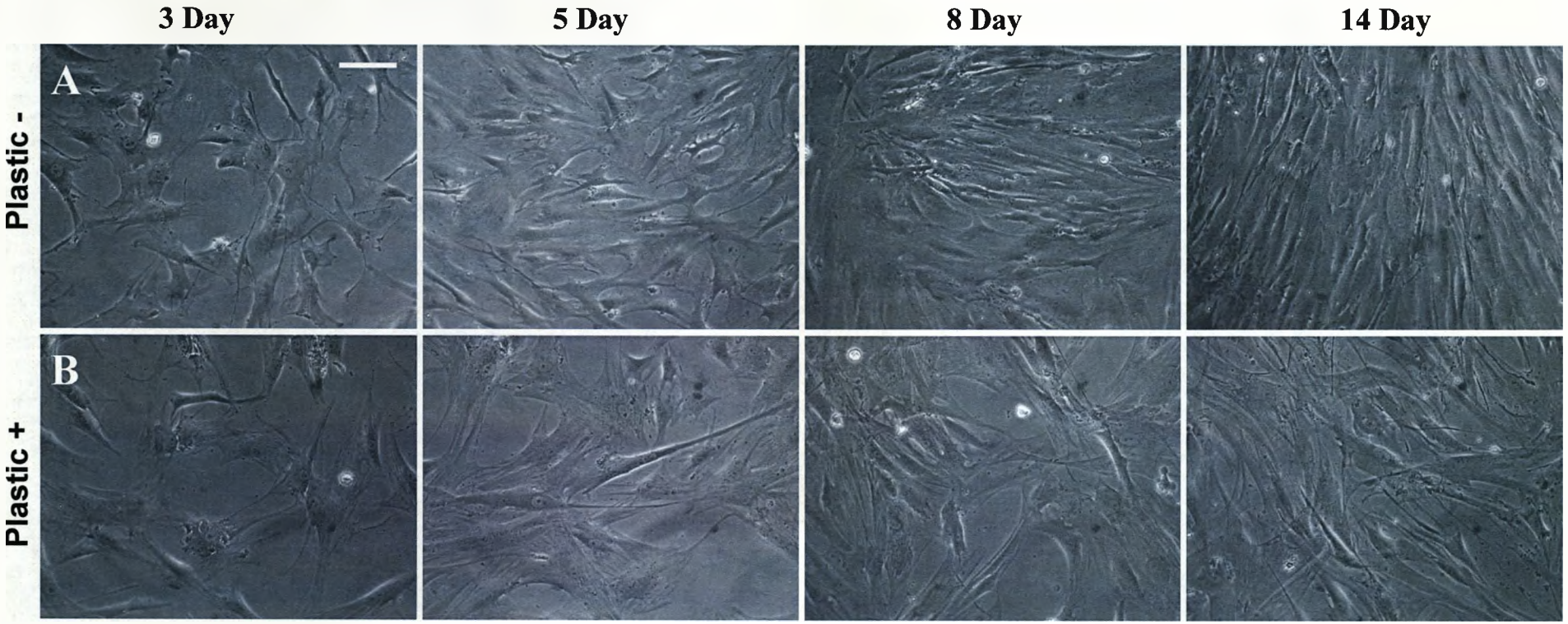

Figure 5-21 Primary hMSC behaviour on polyacrylate and control substrates under chondrogenic conditions. hMSCs were cultured for 14 days in hMSC (-) and chondrogenic (+) medium and observed in culture on tissue culture plastic (A&B), glass (C&D) and ESP04 (E&F). Images were obtained daily, shown above are representative images at 3, 5, 8 and 14 days. Cells attached and grew into evenly distributed monolayers on controls. On ESP04 cells aggregation was enhanced under chondrogenic conditions, however following 7-14 day culture detachment of tightly packed aggregates was observed. Scale bar 200 µm.

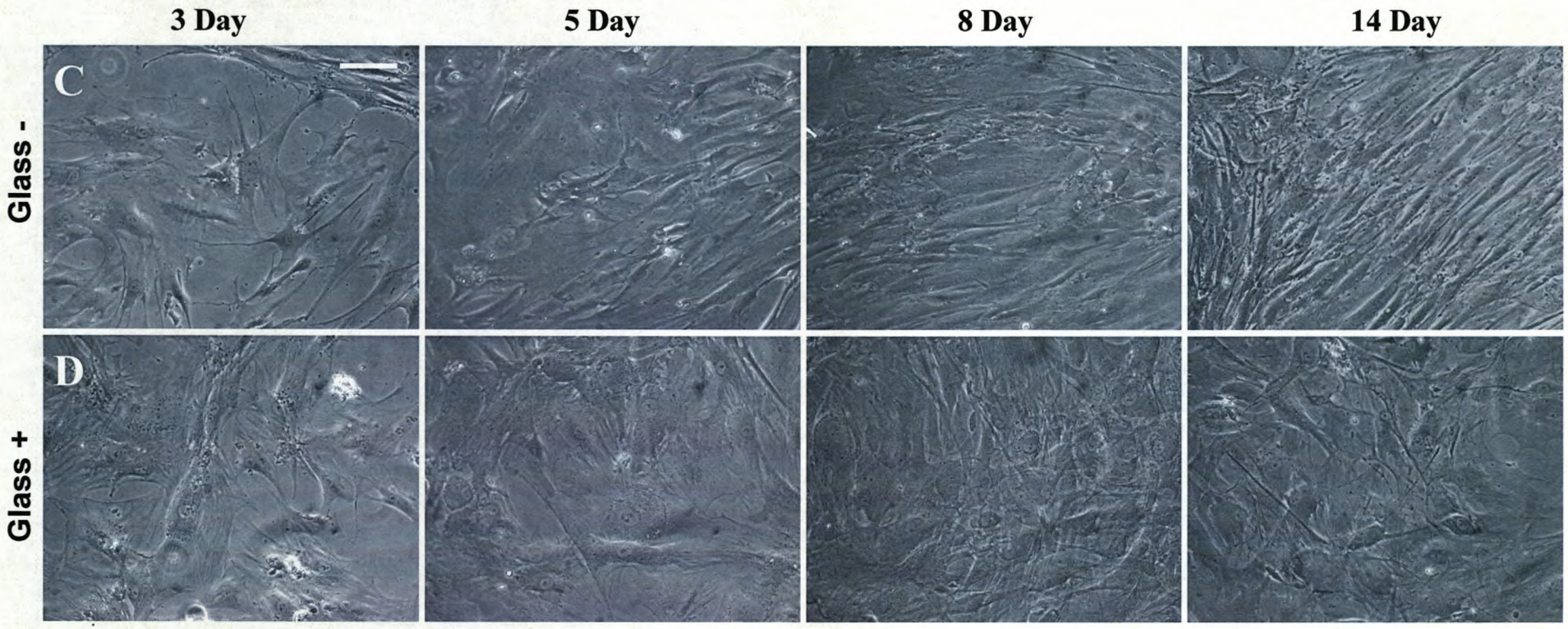

Figure 5-21 continued

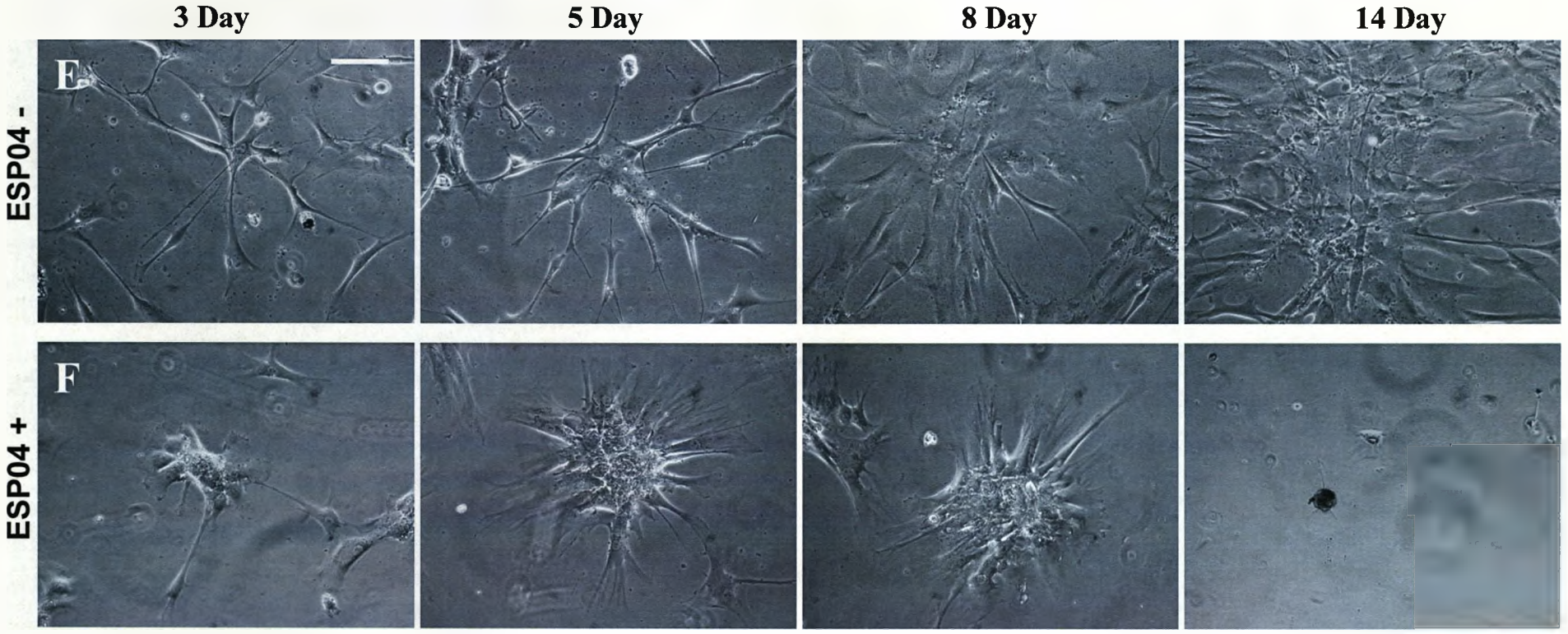

Figure 5-21 continued

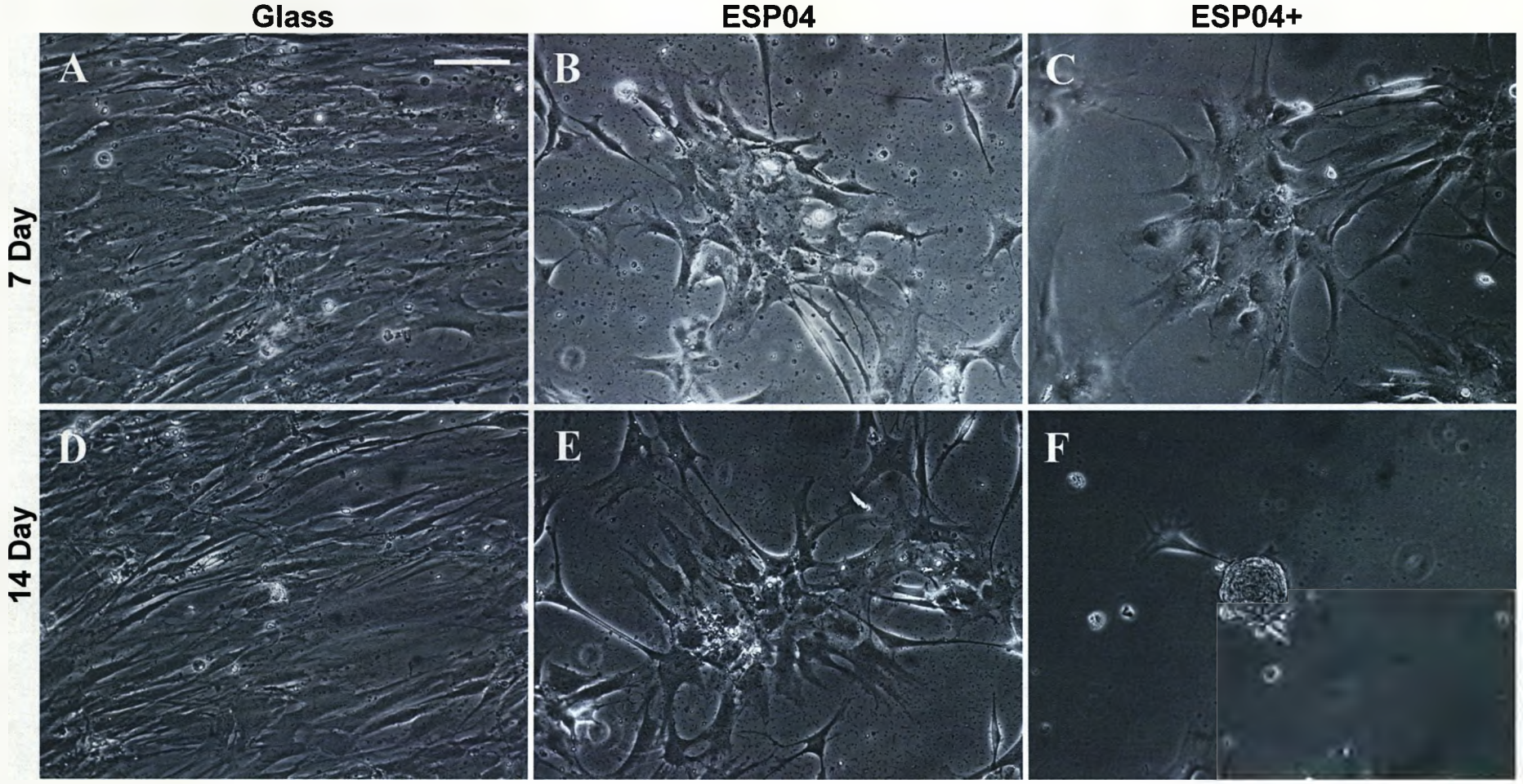

Figure 5-22 Primary hMSC behaviour on polyacrylate and control substrates under chondrogenic conditions. hMSCs were cultured for 14 days in hMSC medium (Glass & ESP04) or 7 days in hMSC medium then 7 days in chondrogenic medium (ESP04+). Representative images are shown following each 7 day period. hMSCs grew as monolayer on glass (A&D), as normal aggregates on ESP04 in hMSC medium (B&E), and with enhanced compaction in chondrogenic medium (C&F). Scale bar 200 μm.

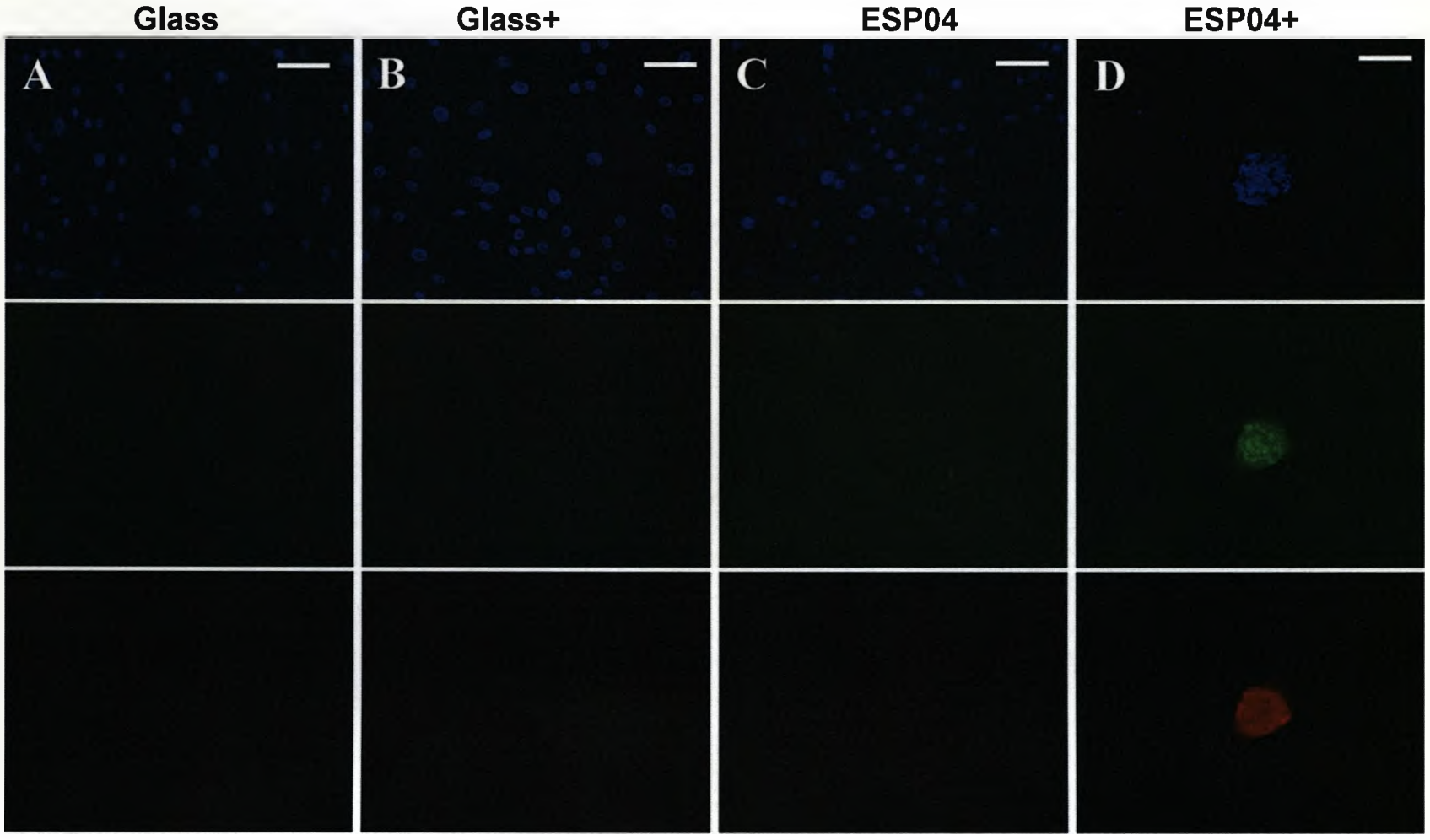

Figure 5-23 Primary hMSC differentiation on polyacrylate and control substrates under chondrogenic conditions. $1x10^4$ hMSCs were cultured for 14 days in hMSC medium on glass (A) & ESP04 (C) or 7 days in hMSC medium then 7 days in chondrogenic medium (+) on Glass (B) & ESP04 (D). Cells were fixed and stained for DAPI (blue), collagen II (green) and osteocalcin (red). Tightly compacted aggregates with significant multi-layering were observed on ESP04 under chondrogenic conditions (D), and these stained strongly for chondrogenesis and osteogenesis markers. Scale bar 200 μm.

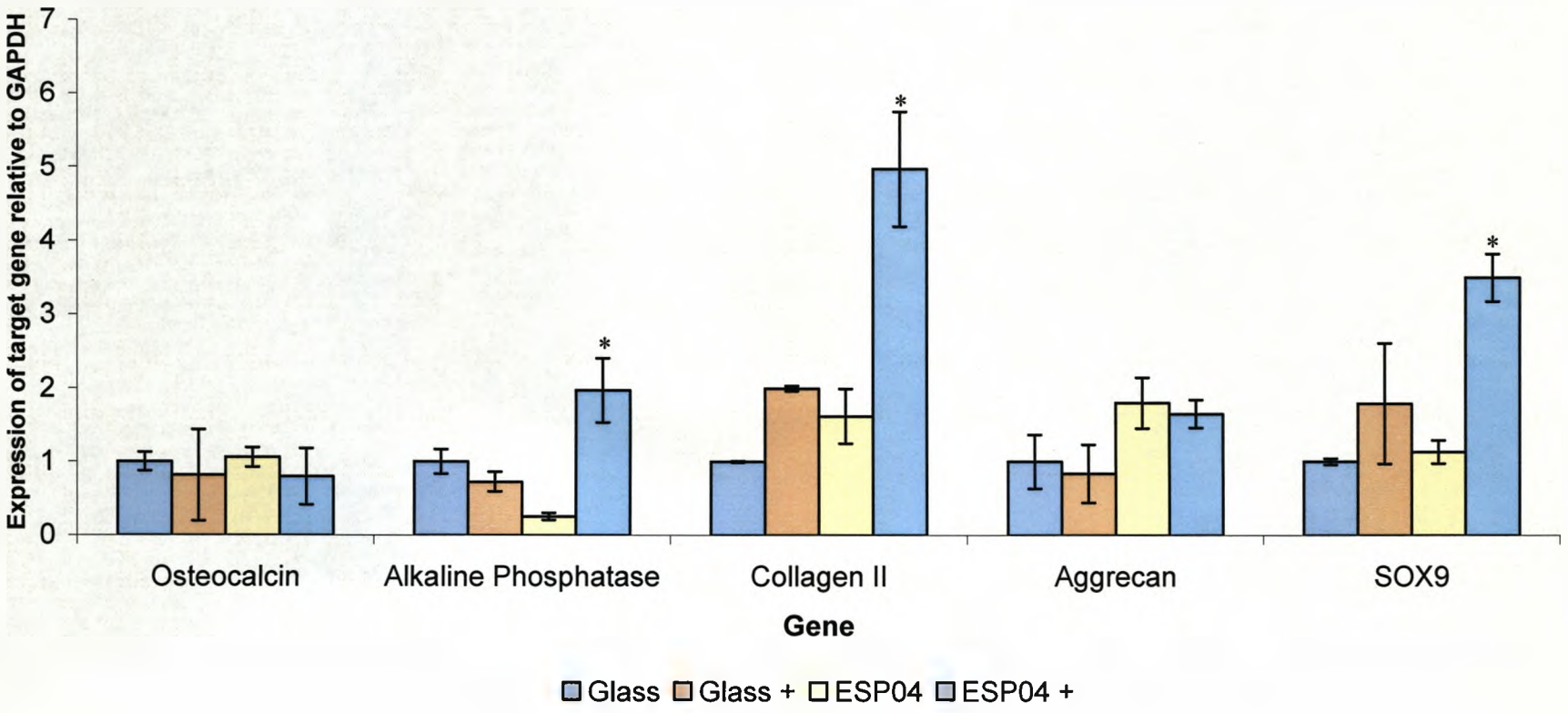

Figure 5-24 PCR analysis of mRNA extracted from primary hMSCs under chondrogenic conditions. $1x10^4$ hMSCs were cultured for 14 days in hMSC medium (Glass & ESP04) or 7 days in hMSC medium then 7 days in chondrogenic medium (Glass+ & ESP04+). Samples were assayed for osteogenesis markers (osteocalcin & alkaline phosphatase) and chondrogenesis markers (collagen II, aggrecan & SOX9). Data was normalised to expression on glass substrate. Collagen II and SOX9 were significantly up-regulated on ESP04 under chondrogenic conditions. Asterisk indicates significant increase over controls ($p<0.05$, Tukey model). Results represent the mean of 3 biological replicates ± S.E.M.

5.3. Discussion

In this chapter polyacrylate substrates were assessed for their ability to support chondrogenesis of mouse and human mesenchymal stem cells. The purpose was to investigate if specific surface chemistries, designed to mimic the functional group composition and distribution of the common RGD integrin-binding motif, were able to induce MSC chondrogenesis. The ultimate purpose was to remove the need for complex micro-mass culture procedures and expensive growth factors, which are typically required for chondrogenesis, and to improve scale up, thereby developing a simple and cheap solution for the mass culture and differentiation of chondrocytes.

This study found that the polyacrylate substrate, ESP04, could induce chondrogenesis in mMSCs under normal culture conditions, without exogenous growth factor supplements, within self-formed aggregates attached to the substrate, and this result was replicated with two other mesenchymal-like cell types. Aggregation appears to be associated with chondrogenesis on these substrates, and is reminiscent of mesenchymal cells condensation and subsequent chondrogenesis in early limb-bud formation (1.2.3). Chondrogenesis of MSCs in response to the polyacrylate surface chemistry appears to have strong parallels with fibronectin-RGD induction of chondrogenesis via α5β1 integrin signalling (White 2003). Aggregation and condensation of MSCs may have been promoted by the up-regulation of the cell-cell adhesion molecule N-

cadherin, alongside the key chondrogenic transcription factor Sox9 (Akiyama 2002; Delise 2002; Modarresi 2005; Woods 2007).

However, despite similar aggregating behaviour in culture, ESP04 could only induce significant chondrogenesis in hMSCs in the presence of chondrogenic medium, primarily the addition of TGF-β3. This was likely due to reduced compaction and multi-layering of aggregates observed with the hMSCs. In the absence of chondrogenic factors, these hMSCs appeared to differentiate more slowly, expressing only early markers of chondrogenesis. An additional polyacrylate designed during this study, ESP07, was found to enhance aggregation and promote chondrogenesis in hMSCs under basal culture conditions, without the need for exogenous TGF-β3 supplementation. This demonstrates the potential for customising polyacrylates for a specific role.

Polyacrylate substrates were designed to mimic the RGD integrin-binding motif due to its established role in chondrogenesis (Salinas 2008; Chang 2009; Re'em 2010). However, whilst the RGD-mimicking polyacrylates were found to promote chondrogenesis, it is not clear from this study if this was due to α5β1 integrin signalling via RGD-like interactions, as has been shown on substrates utilising RGD peptides (Chang 2009).

5.3.1. The ability of defined polyacrylate substrates to control MSC behaviour

This study demonstrated that polyacrylate substrates could be designed to promote aggregation and differentiation of mMSCs and hMSCs. The polyacrylate substrates designed to mimic the RGD integrin binding motif promoted aggregation of MSCs cultured in contact with them. All mouse and human mesenchymal-like cells tested aggregated in response to ESP03, ESP04 and ESP07. Importantly, changing the functional group composition and distribution of the polyacrylate (BTL15) negated this effect, demonstrating the response is specific to ESP03, ESP04 and ESP07. Furthermore, these polyacrylates were only able to induce aggregation and chondrogenesis in mesenchymal cells, for no response was observed in mouse fibroblasts.

Study of mMSCs during culture demonstrated that the mechanism of aggregate formation differed between ESP03 and ESP04. Whilst on control and BTL15 substrates, mMSCs attached evenly and grew into well distributed monolayers, whereas on ESP03, mMSCs initially grew similarly, with minimal aggregation, but then monolayers appeared to split and contract, pulling cells together into large multi-layered aggregates within the monolayers. However, on ESP04 aggregation of mMSCs was observed as early as 3 days into culture and the cells continued to form tightly packed multilayered aggregates across the surface, with no areas of monolayer visible. Furthermore, the aggregation mechanisms

appeared more similar in hMSC culture. Both ESP03 and ESP04 demonstrated aggregate formation early in culture, with tighter aggregation on ESP04, but minimal compaction and multi-layering occurred under normal medium conditions. On ESP07, hMSC aggregation was further enhanced, with obvious compaction and multi-layering consistently observed within a week of culture, even in the absence of TGF-β3.

These results suggest a stronger induction of aggregation on the ESP04 rather than the ESP03 surfaces. However, qPCR analysis demonstrates up-regulation of the chondrogenesis markers in mMSCs early in culture on both ESP03 and ESP04, with significantly higher expression on ESP04. This suggests that the aggregation inducing signal is weaker on ESP03, where less amine and more carboxyl functional groups were present. This later aggregation may be caused by slower up-regulation of the chondrogenesis markers, particularly N-cadherin, which was not significantly up-regulated in mMSCs on ESP03 after 2 days. Critically, the lack of N-cadherin up-regulation was associated with a lack of aggregate formation on the ESP03 substrate. If cell-cell interactions increased more gradually in mMSCs cultured on ESP03, the cells may initially grow as a monolayer before N-cadherin directed cell-cell adhesion causes the mMSCs to pull together and compact, and the monolayer is then seen to contract into an aggregate. On ESP04, up-regulation occurs more quickly, and mMSCs aggregate and compact before they are able to grow into a monolayer, indicating that the substrate may be inducing

chondrogenic pathways. Still, on ESP04, aggregates remain in a single layer until approximately a week into culture, suggesting a delay in the ability of the mMSCs to multilayer, and after that the majority of growth is in the z-plane. In hMSCs, SOX9 was again up-regulated on polyacrylate substrates. The aggregation mechanism appears to be similar, but stronger on ESP07, where SOX9 was significantly up-regulated compared to ESP04 and ESP03, correlating with the observed enhancements in aggregation and compaction of hMSCs.

An important question arising from these studies is whether aggregation of MSCs on the RGD-mimicking polyacrylate substrates is the trigger for chondrogenesis, or if chondrogenesis is triggered by the substrates, and this in turn initiates aggregation; the results from this chapter suggest the latter. Early markers of chondrogenesis were expressed in mMSCs after only 2 days culture on both ESP03 and ESP04. Whilst aggregation may already be occurring on ESP04, mMSCs on ESP03 appeared similar to controls, yet expression of Sox9 was significantly increased. Therefore, markers for chondrogenesis were being expressed long before any aggregation was observed. Furthermore, N-cadherin was not significantly up-regulated at that time on ESP03, suggesting that its expression is downstream of initiation of chondrogenesis. However, aggregation appears to be required for progression of chondrogenesis in this environment, as demonstrated by the lack of chondrogenesis in hMSCs which, while aggregating to some extent, did not condense and form multilayers. In contrast, studies by Re'em et al. (2010) and Shao Qiong et

al. (2009), showed chondrogenesis occurring in scaffolds and hydrogels in the absence of aggregation. These studies were performed under chondrogenic conditions, with TGF-β supplementation, suggesting that, with the appropriate artificial environment and access to factors, aggregate formation is not necessary for chondrogenesis.

Interestingly, mouse LBCs cultured in monolayers on control substrates were found to dedifferentiate, reducing expression of chondrogenesis markers collagen II and aggrecan, whereas on ESP04, aggregates were formed and a more chondrogenic phenotype was maintained (4.2.5.2). These findings agree with a study by Lin et al. (2008), where chondrocytes were shown to dedifferentiate during monolayer culture, and again highlights the importance of aggregate formation for chondrogenesis on 2D polyacrylate substrates.

The migration of MSCs has previously been demonstrated in response to multiple chemotactic factors *in vitro* (Son 2006; Herrera 2007; Ponte 2007). The growth factors platelet-derived growth factor-AB, insulin-like growth factor-1, epidermal growth factor and hepatocyte growth factor/scatter factor (HGF/SF) and the chemokines chemokine ligand 5, macrophage-derived chemokine and stromal-derived factor-1 (SDF-1) demonstrate significant chemotactic activity in hMSCs (Ponte 2007). The pro-migratory signals driving limb-bud condensation are still unidentified. However, other *in vivo* MSC migration models are better understood, such as in wound healing, where MSCs migrate to the site of damaged

tissue. In this case it is known that hMSCs respond to the chemo-attractants SDF-1 and HGF/SF, which are up-regulated at sites of tissue damage, via the CXCR4 and c-MET receptors, respectively (Son 2006). Furthermore, in mMSCs, CD44 was found to enhance migration by chemotaxis towards its ligand hyaluronic acid (HA), both *in vivo*, towards damaged kidneys, and *in vitro* (Herrera 2007). Interestingly, HA is a component of human articular cartilage (Holmes 1988) and has been shown to promote cartilage nodule formation in chick limb mesenchyme cells when bound to a substrate (Kujawa 1986). Several cytokines and chemokines, along with their receptors, are expressed endogenously by MSCs (Ponte 2007), suggesting that up-regulation of these factors could contribute to the observed aggregation on ESP03, ESP04 and ESP07 polyacrylate substrates.

As previously described, the aggregation of mMSCs observed in this chapter, whilst not required for the induction of chondrogenesis, appears to be necessary for the progression of chondrogenesis. Aggregation also appears to play a significant role in chondrogenesis in the developing limb bud (Oberlender 1994; DeLise 2002). In this case, MSCs migrate into the limb bud at the earliest stage of formation, before condensing into a tightly packed mass and undergoing chondrogenesis. The precartilagenous condensation process itself is thought to be regulated by cell-cell and cell-matrix interactions, mediated through the ECM. Fibronectin has been shown to be critical in migration and aggregation of MSCs, and its absence inhibits condensation (Downie 1995; Gehris 1997;

White 2003). Serum conditions were used in all MSC experiments in this chapter, providing a source of fibronectin (Steele 1995); however, the RGD-like substrates may be promoting a similar interaction. This would indicate why they differ in chondrogenic capacity (ESP04>ESP03), if some substrates activate fibronectin-like RGD-integrin signalling better than others. The cell adhesion molecules N-cadherin and neural cell adhesion molecule (N-CAM) are also important in aggregating and compacting MSCs during condensation (Tavella 1994; Chimal-Monroy 1999). However, expression of fibronectin and these adhesion molecules is decreased as cells become chondrogenic (Tavella 1994), which may suggest cross-talk in their regulation. The molecular mechanisms of this process are yet to be elucidated; however, TGF-βs are some of the earliest genes to be expressed during chondrogenesis and are known to up-regulate the expression of N-cadherin, N-CAM, fibronectin and Sox9 (Chimal-Monroy 1999).

Migration and aggregation was also investigated in mESCs cultured on polyacrylates substrates in chapter four (4.3.6). Whilst few differences were observed in migration of mESCs on polyacrylate or control substrates, aggregation was greater on positive control and BTL15 substrates compared to plain glass controls. This implies that, under serum free conditions, BTL15 better mimicked the serum coated control than plain glass. Furthermore, aggregation was clearly important for colony formation. However, comparisons between migration and

aggregation of mESCs on other polyacrylate substrates were not conducted.

As previously described, aggregation and condensation of MSCs is critical for progression of both limb bud and *in vitro* chondrogenesis. In addition to the importance of cell-cell interactions in this process, studies have shown cell shape can also regulate chondrogenesis (Gao 2010). In both micro-mass culture and limb bud condensation, MSCs are tightly packed within the aggregates and are thereby restricted from spreading, constricting them to a rounded cell morphology (Shum 2002). Restricting the spreading of hMSCs and enforcing a rounded morphology, has been shown to promote chondrogenesis in hMSCs, possibly by blocking Rac1 signalling via rearrangement of the cytoskeleton (Woods 2007; Kumar 2009; Gao 2010). The compaction of cells within aggregates on polyacrylate substrates was demonstrated by fluorescence and confocal images. In addition, confocal images demonstrate compaction of nuclei within aggregates (Figure 5-19), which may influence gene expression (Marshall 2003). The lack of condensation in hMSCs cultured on ESP03 and ESP04 substrates may indicate why chondrogenesis was not induced under basal medium conditions. When cultured on ESP07 or in the presence of TGF-β3, compaction and multi-layering of hMSCs was observed and chondrogenesis markers were expressed.

The RGD-like polyacrylates theoretically differed in their proportions and distributions of key functional groups found within the integrin binding

motif. ESP03 contained the least amine and most carboxyl functionality of the three polymers. ESP04 contained more amine and less carboxyl functionality than ESP03, whilst both contained no hydroxyl side groups. Therefore, the enhancement of aggregation on ESP04 appears to be due to the altered balance of amine and carboxyl groups, though importantly, the amine functionality appears to be key, which agrees with findings by other groups (Curran 2006; Guo 2008; Phillips 2009). In most cases, aggregation in response to substrate chemistry is attributed to reduced cell adhesion to the substrate (Phillips 2009) or, on amine substrates, has been reported due to differential binding of ECM proteins (Guo 2008). However, on substrates presenting only plasma deposited amine groups, aggregation was sporadic and limited, similar to results from other studies (Curran 2006; Guo 2008; Phillips 2009). Furthermore, the increased expression of N-cadherin and SOX9 in response to substrates in this study suggests more specific signalling.

ESP07 was based on ESP04 and contained a similar amount of amine, but all carboxyl side groups were replaced with hydroxyl groups. Surprisingly, despite theoretically being less RGD-like, aggregation and chondrogenesis were further enhanced in hMSCs cultured on ESP07, again identifying amine functionality as a key component. However, the surface amine content of ESP07 was found to be significantly higher than ESP04 (3.4.3), which was itself significantly higher than ESP03, possibly pointing to surface amines as a key property for MSC aggregation and chondrogenesis on polyacrylate substrates. XPS analysis also suggested

increasing amine content from BTL15 to ESP03 to ESP04 (3.4.2), following the trend in aggregation. As described previously, Guo et al. (2007) demonstrated enhancement of hMSC aggregation and chondrogenesis, in the presence of chondrogenic medium, on amine presenting substrates (Guo 2008).

These results indicate that, whilst the amine appears essential, alone it is insufficient to promote chondrogenesis, and the combination of functionality is important for the aggregating behaviour observed in this study, and additional functional groups may cooperate or enhance the effect of the amine functionality. However, the response of hMSCs to amine substrates under chondrogenic conditions was not examined here. Importantly, without chondrogenic conditions, little aggregation or chondrogenesis has previously been demonstrated in any studies conducted by other groups (Curran 2006; Guo 2008; Phillips 2009).

5.3.2. The ability of polyacrylate substrates mimicking the RGD integrin binding motif to promote MSC chondrogenesis

This study demonstrated that chemically defined polyacrylate substrates, mimicking the RGD integrin-binding motif, common to several ECM proteins, were able to exclusively induce chondrogenesis in mMSCs and hMSCs. Analysis of mMSCs following 2 day culture demonstrated up-regulation of Sox9 and N-cadherin, two early markers for chondrogenesis, indicating immediate and direct induction of

chondrogenesis via cell-substrate interactions. Analysis of hMSCs demonstrated that, whilst aggregation proceeded similarly to mMSCs, chondrogenic induction was weaker, and only significant up-regulation of SOX9 was detected following 20 day culture on ESP04. However, addition of chondrogenic factors, particularly TGF-β3, significantly enhanced expression of chondrogenic markers on polyacrylate substrates over control substrates. Furthermore, the polyacrylate ESP07, a modification of ESP04 but with hydroxyl replacing carboxyl side groups, enhanced aggregation and condensation of hMSCs, and significantly enhanced expression of chondrogenic markers, even in the absence of TGF-β3.

Comparison of MSCs cultured on polyacrylate substrates with control micromass cultures largely demonstrated similarly enhanced expression of chondrogenesis markers. In mMSCs, expression of collagen II was significantly higher in micromass cultures than on ESP04, having approximately 3.9 and 2.3 fold higher expression of mMSCs on controls respectively, whereas, expression of aggrecan in micromass cultures was slightly higher, but not significantly so, having approximately 2- and 2.6-fold higher expression than mMSCs on controls respectively. Micromass cultures followed a typical chondrogenesis protocol (2.2.1.7) for 21 days. Therefore, micromasses were cultured for three days longer than the 18 day mMSCs on polyacrylates, which could have contributed to the increased expression detected. Furthermore, the expression of osteogenic markers was not consistently higher than in mMSCs on

controls, and expression of osteocalcin was significantly lower than in mMSCs cultured on ESP03 and ESP04, indicating that little osteogenesis occurs in typical micromass chondrogenesis.

In hMSCs, expression of chondrogenesis markers was very similar between hMSCs cultured in micromass culture and on ESP07. Expression of collagen II was not significantly different between micromass and ESP07, both having approximately 4.3-fold higher expression than hMSCs on control substrates. Expression of aggrecan was slightly higher on ESP07 compared to micromass, 1.3- and 1.4-fold higher than controls respectively. In contrast, expression of SOX9 was much higher in micromass hMSCs than on ESP07. Upregulation of SOX9 is known to be strongly linked to TGF-β exposure (Chimal-Monroy 2003; Kawakami 2006), making its increased expression expected. However, SOX9 expression is carefully controlled *in vivo*, with both over and under expression resulting in chondrodysplasia (Akiyama 2004). Furthermore, induction of chondrogenesis using TGF-β is known to lead to hypertrophic phenotypes when TGF-β is removed (Mueller 2010), which is unsuitable for treating articular cartilage defects. This indicates a possible advantage to using aggregate culture on polyacrylate substrates for autonomous hMSC chondrogenesis. These results indicate that chondrogenesis on polyacrylate substrates could give comparable results to micromass culture.

The 3-D distribution of chondrocytes and osteoblasts within the aggregates of MSCs formed on ESPO4 demonstrates strong parallels with *in vivo* limb bud formation, where mesenchymal cells migrate into the limb-bud then condense to form a tightly packed aggregate which differentiates to chondrocytes, but then begins to develop osteoblasts around the periphery (Figure 1-9). This is not surprising as MSC aggregation and condensation are occurring similarly to limb bud formation (Ornitz 2002; Goldring 2006), with the extracellular environment being generated by the MSCs themselves. Both osteoblasts and chondrocytes have been shown to share a common lineage in Sox9-expressing limb bud mesenchymal cells (Akiyama 2005). Several studies have now shown the positive impact of morphogenetic signals from chondrocytes on osteoblast differentiation (Gerstenfeld 2002; Gerstenfeld 2003; Hwang 2007; Guo 2009) and vice versa (Guo 2009), and these systems likely act through morphogenetic signals known to be released by chondrocytes and osteoblasts in culture, such as TGF-β1 (Gerstenfeld 2003; Gomes 2006; Pham 2008). Furthermore, results from this chapter indicate that both lineages will differentiate concurrently in MSC aggregate culture on ESP03 and ESP04, as markers of both lineages appeared simultaneously. These studies highlight the induction of differentiation to alternate lineages in MSCs, but also the benefits of co-culture and allowing MSCs to organize themselves to promote their own differentiation, which is a possible mechanism for the chondrogenesis occurring on polyacrylate substrates. Cartilage has an elaborate, highly ordered structure, consisting of multiple zones with different properties

(Buckwalter 1998). Differentiation via aggregate culture may allow cartilage to develop with natural in-vivo properties.

5.3.2.1. Mechanisms of substrate-cell signalling

Several studies have suggested substrate-dependent MSC differentiation is in response to differential fibronectin binding (Lan 2005; Phillips 2009). However, more recent studies have speculated over direct cell-substrate interactions (Ren 2009). In this study, polyacrylates were intentionally designed to mimic the functional group composition and distribution of a key ECM protein binding site. Whilst this does not rule out substrate chemistry-dependent differences being regulated through differential binding of ECM proteins, as described in other studies (Keselowsky 2004; Lan 2005), no comparable studies have demonstrated a similar response on defined chemical substrates. However, as noted above, serum was present in all experiments in this chapter. Therefore, culture of MSCs on ESP03, ESP04 and ESP07 under serum free conditions would be necessary to determine if serum proteins were involved in mediating cell adhesion.

In chapter four, polyacrylate substrates, including BTL15, ESP03 and ESP04, were assessed for their ability to support mESC culture under serum free and serum coated conditions (4.3.4). Coating with serum prior to culture was found to generate no significant improvement in mESC

growth. Furthermore, ESP04 demonstrated a significant decrease in mESC numbers following coating with serum. These results suggested that either serum proteins that aided cell attachment, such as fibronectin, did not adsorb to these surfaces, or that the conformation of adsorbed proteins was unable to support cell attachment. This might indicate that adsorption of serum proteins should equally not impact the growth of MSCs on polyacrylate substrates in this chapter. However, serum free culture would still be necessary to confirm this. Another possibility might be that deformation of adsorbed proteins is higher on ESP04, which reduced mESC attachment and growth under serum coated conditions, and, therefore, MSC attachment to the substrate was also reduced, encouraging aggregation. However, this would not explain increased expression of chondrogenic genes observed early in MSC culture.

A further finding with mESCs in chapter four was that the RGD-mimicking polyacrylates ESP03 and ESP04 did not demonstrate any improvement in attachment or short-term culture, as has been demonstrated with RGD peptide surfaces (Sato 2007; Kolhar 2010). However, short-term population expansion on ESP03 and ESP04 was not significantly different from positive controls (4.3.5) and longer-term culture of mESCs was significantly better on ESP03 than other polyacrylate substrates (4.3.7). These findings leave the influence of the RGD-like polyacrylates on mESC culture unclear.

Fibronectin is critical for aggregation, condensation and early chondrogenesis of MSCs (Gehris 1997; Tavella 1997; White 2003), and fibronectin substrates have been shown to promote MSC chondrogenesis *in vitro* (White 2003). Furthermore, fibronectin has long been known to be essential in migration and aggregation of multiple cell types (Fassler 1995; Palecek 1997; Carlson 2008). Cell interactions with fibronectin are typically mediated by the RGD-integrin binding motif and the $\alpha_5\beta_1$ integrin (Pulai 2002; Shakibaei 2008), but also less commonly, the $\alpha_v\beta5$ integrin, that normally binds to vitronectin (Goessler 2008; Martino 2009). Furthermore, RGD peptides have been demonstrated to promote chondrogenesis when presented on 3-D culture scaffolds (Salinas 2008; Tigli 2008; Chang 2009; Shao Qiong 2009; Liu 2010; Re'em 2010). Whilst studies have shown the importance of fibronectin and the RGD-integrin binding motif in chondrogenesis, the mechanisms of their action have yet to be fully elucidated (Li 2005; Djouad 2007; Goessler 2008). ESP03, ESP04 and ESP07 were specifically designed to mimic the RGD sequence, with the aim of eliciting an equivalent response.

Addition of TGF-β3 demonstrated enhancement of chondrogenesis in hMSCs cultured on ESP04. However, aggregates detached from the substrates with prolonged exposure to this growth factor, similar to observations in other studies (Guo 2008). Whilst the TGF-β3 could be regulated to control detachment, or solely used to induce condensation, the preferred route was to modify substrate chemistry to further promote

chondrogenesis in hMSCs, as was achieved with ESP07, which promoted hMSC chondrogenesis.

Whilst RGD peptide ligands have been shown to promote induction of chondrogenesis, there is also evidence that RGD signalling is only required for initiation and the early stages of chondrogenesis, after which the presence of RGD will actually inhibit further chondrogenesis (Connelly 2007; Salinas 2008). However, in chondrogenesis, emphasis is commonly on artificial 3-D culture environments despite the ability of MSCs to form their own ECM in micromass culture (Yoo 1998). This indicates the advantage of the 2-D culture method demonstrated in this chapter, as the MSCs are only initially in contact with the artificial substrate, which encourages aggregation and the initiation of chondrogenesis. Once chondrogenesis is progressing, attachment of cells remaining in contact with the substrate may be enhanced via RGD functionality, but later stages of chondrogenesis can proceed under the direction of cells within the multi-layered aggregates, with their endogenously generated ECM. However, later markers of chondrogenesis and chondrocyte maturation were not analysed here.

The $\alpha_5\beta_1$ is the most commonly expressed integrin in chondrocytes and is the primary receptor for fibronectin (Loeser 2002; Goessler 2008). It is also expressed in undifferentiated MSCs, and becomes up-regulated on chondrogenesis (Goessler 2008). However, little is known about the mechanisms involved in its regulation of chondrogenesis. Several studies

have suggested integrin-activated intra-cellular signalling pathways involved in MSC chondrogenesis. Foremost is focal adhesion kinase (FAK) signalling, recruited and activated by the β_1 subunit on $\alpha_5\beta_1$ integrin binding to fibronectin (Bang 2000; Jin 2007). FAK in turn associates with a number of signalling molecules, including paxillin, c-SRC and PI 3-kinase (Bang 2000; DeLise 2000). Interactions between FAK and the cytoskeleton protein paxillin are required for precartilage condensation, and interactions of FAK with the c-SRC kinase also coincide with cellular condensation (Bang 2000). Paxillin is also involved in regulating the actin cytoskeleton and cell migration (Deakin 2008), both important in MSC aggregation. In addition, FAK activation of mitogen-activated protein kinases (MAPK), such as p38 MAPK, has been shown to be necessary for MSC chondrogenesis (Nakamura 1999; Forsyth 2002). Furthermore, the extracellular-regulated kinases 1 and 2, or p42 and p44 MAPKs, are up-regulated in later chondrogenesis and regulate the switch from condensation and early chondrogenesis to chondrocyte maturation in opposition to p38, possibly through regulation of adhesion molecules, such as N-cadherin (Oh 2000; Li 2009). More recently, FAK signalling has also been implicated in suppressing chondrogenesis following condensation events, which agrees with studies involving fibronectin (Li 2005; Pala 2008). In contrast to FAK, inhibition of the integrin linked kinase by fibronectin binding to the $\alpha_5\beta_1$ integrin blocks translocation of β-catenin to the nucleus, and subsequent WNT signalling, promoting chondrogenesis (DeLise 2000; Goessler 2008). Investigation of these

pathways would be valuable in elucidating the mechanisms behind MSC chondrogenesis on the polyacrylate substrates.

6. General Discussion

The field of biomaterials in stem cell culture has seen a rapid expansion in recent years. It is now well recognised that surface properties influence the behaviour of cells cultured in contact with them, and in many cases biomaterials are cheaper and more consistent than biological substrates. Furthermore, the defined nature of biomaterial substrates will aid in the elucidation of mechanisms involved in the self-renewal and differentiation of stem cells.

In this study, the surface properties of polyacrylate substrates were altered to enact control over the self-renewal and differentiation of stem cells. The main aims of this thesis were:

1. To develop a defined substrate for the culture of mESCs.
2. To develop defined substrates for inducing chondrogenesis in mMSCs and hMSCs.

6.1. ESC self-renewal

This study showed that polyacrylate substrates could support limited mESC population expansion over the short-term. The mESCs attached to the substrates, aggregated and grew into colonies, which remained undifferentiated following 96 h culture. However, population expansion was significantly reduced compared with control substrates, and the

results showed that this was likely caused by altered attachment of cells to the substrates. This altered cell attachment could be due to changes in affinity or deformation of endogenous ECM proteins adsorbing to the surface of the substrates, and/or weak direct binding of cells to the surface of the substrates under serum-free conditions. Furthermore, self-renewal and population expansion of mESCs were not maintained on polyacrylate substrates after the first passage, indicating that additional stimuli were needed to support long-term mESC culture.

Whilst the polyacrylate substrates used in this study were not suitable for long-term culture of mESCs, ESP03 demonstrated improved long-term support over the other polyacrylates, including the most successful short-term substrate BTL15. Cell numbers were higher and AP activity was evident in second passage colonies on ESP03. This demonstrates potential for further improvement of the polyacrylates capacity to support long-term mESC growth. With further modifications to the polyacrylate side-groups, a suitable substrate for mESC culture may be found.

Steric hindrance was found to alter the surface properties of polyacrylate substrates, which in turn, modulated mESC behaviour. The most successful of the BTL substrates at supporting mESC expansion, BTL15, contained intermediate steric hindrance and wettability, suggesting that intermediate proportions of functional group presentation were best. In addition, the highest theoretical levels of functional group presentation, on

BTL08 and ESP06, appeared to have a detrimental effect on self renewal and cell survival.

6.1.1. Applications

The ultimate purpose in developing substrates to support the expansion of mESC populations is for transfer to hESC applications. For any hESC-based techniques, large numbers of undifferentiated cells are required, which must then be efficiently differentiated to the required cell types. In this study, the polyacrylate substrates have demonstrated some support of both mESC self-renewal and differentiation. Further modification of the substrate chemistry may yet provide suitable substrates for the expansion and differentiation of ESCs for use in drug discovery and regenerative therapies. However, hESCs differ from mESCs, importantly in that they are not maintained by LIF (Ginis 2004). Therefore, promotion of self-renewal via the correct substrate chemistry will be of greater importance in the progression to hESC culture. Recently, hESC culture on a synthetic polymer coating under defined conditions has been achieved, however, the beneficial surface properties of the substrate are yet to be elucidated (Villa-Diaz 2010).

Increasingly, evidence of the role of integrins in regulating cell behaviour is becoming apparent. In mESCs, multiple integrins have been implicated in the maintenance of self-renewal (Lee 2010). Recently, undifferentiated hESCs have been successfully cultured on peptide presenting surfaces,

containing the RGD motif, under serum-free medium conditions (Kolhar 2010; Melkoumian 2010). Further development of polyacrylate substrates to mimic the functional composition and distribution of integrin-binding sites found in ECM proteins may improve their ability to support ESC culture.

6.1.2. Future work

A surprising finding during this study was that serum coating did not significantly improve mESC growth on any of the polyacrylate substrates. In fact, on some polyacrylates, serum coating actually appears to have significantly reduced cell numbers. The mechanisms of mESC attachment to the polyacrylate substrates under serum-free conditions remain obscure. Whilst direct integrin binding of cells to the substrates is unlikely, due to the complexity of the biological machinery, charge-charge interactions or low affinity integrin binding may be involved, which might also indicate why attachment is reduced.

One area that requires attention is the action of serum coating on the polyacrylate substrates. The BCA assay indicated no significant differences in the presence of protein adsorbed to the surface of polyacrylate and control substrates. However, no information on the species of proteins, nor their state, was inferred by this technique. Furthermore, whilst mESC growth experiments were typically conducted

under serum-free conditions, serum proteins could have entered into the system by either carry-over, during dissociation, or endogenous production by the mESCs. Therefore, valuable information on the interaction of the mESCs with the polyacrylate substrates could be obtained not only from analysing serum components that adsorb to the substrates, but also their conformational states and orientations. Equally, investigating endogenous protein production and its interaction with the substrates might indicate the objective for further customisations to the polyacrylates composition.

6.2. MSC chondrogenesis

This study showed that polyacrylate substrates designed to mimic the functional group composition and distribution of the RGD integrin-binding motif could promote chondrogenesis in human and mouse MSCs, without the need for additional stimuli. Specifically, ESP04 and ESP07 were able to induce compaction and chondrogenesis in mMSCs and hMSCs, respectively, in the absence of chondrogenic media, which invariably contain TGF-β3, or complex culture techniques. Furthermore, the results suggest that these polyacrylate substrates were able to drive chondrogenesis through a direct mechanism, via promoting the expression of SOX9 and N-cadherin, as opposed to indirectly inducing chondrogenesis via facilitating MSC aggregation. Studies employing RGD have suggested it promotes chondrogenesis via up-regulation of SOX9

and inhibition of RhoA activity (Chang 2009; Shao Qiong 2009; Re'em 2010).

6.2.1. Future work

The mechanisms behind the induction of chondrogenesis on the polyacrylate substrates have yet to be elucidated. Whilst the RGD-mimicking polyacrylate substrates appear to illicit an RGD-like response in MSCs cultured in contact with them, serum was present in the culture medium in all experiments. Therefore, the substrates could be acting through protein adsorption, either by modulating its affinity for the types of proteins adsorbed or by altering the conformation of bound proteins and their affinity for cell binding, as have been demonstrated in other studies (Michael 2003; Roach 2005). Culturing MSCs on the polyacrylate substrates under serum-free media conditions would indicate if serum proteins were involved, whereas if induction of chondrogenesis is maintained under serum-free conditions it would confirm a direct interaction between the MSCs and the substrates. A serum-free hMSC culture system has recently been developed, using a fibronectin substrate, which might enable this analysis (Chase 2010).

Another useful extension to this study would be inhibiting $\alpha_5\beta_1$ integrin-RGD binding and determining if aggregation and chondrogenesis continued. This could be investigated using antibodies specific for binding sites on integrins or peptide sequences to block the RGD interaction. If

chondrogenesis was inhibited it would indicate a direct mode of induction mimicking integrin-RGD interactions.

6.2.2. Cartilage development

The ultimate purpose in inducing chondrogenesis in MSCs is for use in cartilage repair and regeneration. In the aggregate culture method described in this study, chondrocytes could be generated from MSCs derived from a patient, and then re-implanted at the location of cartilage damage, as an autologous implant treatment. Correct development and organisation of cartilage tissue is essential for *de novo* tissue to replicate the properties of normal cartilage, i.e., its impressive resistance to compressive and shear forces, as well as a smooth surface to reduce friction. Therefore, aggregate culture, as demonstrated in this study, might be ideal in allowing development of cartilage tissues, as only initiation of MSC chondrogenesis would be promoted by the substrates, then progression of chondrogenesis would largely be regulated via paracrine signalling within the aggregates, similar to *in vivo* chondrogenesis.

One point to keep in mind is the development of cartilage *in vivo*. As there are strong parallels between the in vitro chondrogenesis of MSCs demonstrated in this study and limb bud development, it is possible that development might continue and lead to hypertrophy of the cultured

chondrocytes, as has been seen in pellet culture with TGF-β3 (Pelttari 2006; Mueller 2010). Although TGF-β3 and dexamethasone are thought to inhibit the progression of hypertrophy in MSC cultures, they are unable to halt it completely and expression of the hypertrophic marker type X collagen has been detected following four week culture (Mueller 2010). Furthermore, ectopic implantation of chondrogenic MSC pellets has lead to vascularisation and mineralisation, indicators of endochondral ossification, in SCID mice (Pelttari 2006). However, ossification must be halted *in vivo* to leave cartilage at the joint surface, which suggests that the articular cartilage niche would include the correct signalling for this (Onyekwelu 2009).

Articular chondrocytes are thought to arise from a subpopulation of early chondrocytes, arising from a cartilaginous interzone of the anlagen, which specifies the future joint (Hyde 2007). Maturation and hypertrophy appear to be blocked in these cells, possibly by parathyroid hormone related peptide (PTHrP) or Indian hedgehog (IHH) signalling, and inhibition of RUNX2 signalling (Onyekwelu 2009). These cells express type II collagen, but do not turn on expression of matrilin-1, which is common to hypertrophic chondrocytes (Hyde 2007). In osteoarthritis a common symptom is ossification of the articular cartilage and vascularisation, under the control of vascular endothelial growth factor (VEGF) (Onyekwelu 2009). Future cartilage tissue engineering techniques will require the generation of stable hyaline cartilage, but must also consider

the definition of the osteochondral interface, normally marked by the calcified cartilage zone and its tidemark (Onyekwelu 2009).

6.2.3. Cartilage repair and regeneration

Bone marrow stimulation via penetration of subchondral bone is the oldest and most commonly used method of stimulating the regeneration of neo-cartilage. Micro-fracture, perforation or abrading techniques are used to damage the subchondral bone and disrupt the blood vessels within. Bone marrow mesenchymal stem cells can then migrate to the damaged area and be involved in regeneration of the tissue. However, results are inconsistent and the new tissue does not completely resemble hyaline cartilage, but often contains fibrocartilage (Bhosale 2008).

A second technique is autologous chondrocyte implantation (Chimal-Monroy), where chondrocytes are harvested from non-weight bearing cartilage, expanded in culture and re-implanted into the defect. However, ACI involves damaging intact areas of the patients cartilage, the size of defect that can be treated is limited, and again the new tissue is not identical to hyaline cartilage (Bajada 2008). The use of MSC-derived chondrocytes instead of autologous chondrocytes would reduce costs and the number of required surgeries, and would remove the consequence of donor-site morbidity and enable treatment of large cartilage defects. Several studies have now successfully transplanted MSC-derived chondrocytes for cartilage repair, with results comparable to

ACI (Matsumoto 2010; Nejadnik 2010). However, as with other techniques, *de novo* cartilage tissue was not identical to hyaline cartilage. These studies highlight that present strategies for the in vitro differentiation of MSCs to chondrocytes are not ideal for use in articular cartilage repair. Further investigation of cartilage development is necessary to identify the mechanisms of hyaline cartilage generation, to enable complete regeneration of articular cartilage function.

Using polyacrylate substrates to culture chondrocytes in aggregates attached to a 2-D substrate has several advantages. These include the cheap price of materials, and reduced requirements for expensive growth factors or complex culture techniques. Furthermore, chondrocytes derived from this method might be more receptive to generating articular cartilage, due to their unique derivation. One study found that collagen type X, a marker for hypertrophy, was reduced in RGD-containing scaffolds (Chang 2009). It is also possible that a cartilaginous interzone might be formed in aggregates, providing articular cartilage progenitors, which could be used in therapy. Finally, this culture technique may be useful in determining additional signalling components required for the derivation of fully functional hyaline cartilage.

The use of human chondrocytes derived from MSCs for treatment of conditions other than articular cartilage damage has also achieved some success. One major study populated a decellularised human donor trachea matrix with epithelial cells and MSC-derived chondrocytes,

cultured from cells of the patient. When transplanted into the patient, this autologous graft immediately provided a functional airway (Macchiarini 2008). This study underlines the potential use of MSC-derived chondrocytes in the treatment of conditions other than articular cartilage defects.

Bibliography

Akiyama, H., M. C. Chaboissier, R. R. Behringer, D. H. Rowitch, A. Schedl, J. A. Epstein and B. de Crombrugghe (2004). "Essential role of Sox9 in the pathway that controls formation of cardiac valves and septa." Proc Natl Acad Sci U S A101: 6502-7.

Akiyama, H., M. C. Chaboissier, J. F. Martin, A. Schedl and B. de Crombrugghe (2002). "The transcription factor Sox9 has essential roles in successive steps of the chondrocyte differentiation pathway and is required for expression of Sox5 and Sox6." Genes Dev16(21): 2813-28.

Akiyama, H., J. E. Kim, K. Nakashima, G. Balmes, N. Iwai, J. M. Deng, Z. Zhang, J. F. Martin, R. R. Behringer, T. Nakamura and B. de Crombrugghe (2005). "Osteo-chondroprogenitor cells are derived from Sox9 expressing precursors." Proc Natl Acad Sci U S A102(41): 14665-70.

Akiyama, H., J. P. Lyons, Y. Mori-Akiyama, X. Yang, R. Zhang, Z. Zhang, J. M. Deng, M. M. Taketo, T. Nakamura, R. R. Behringer, P. D. McCrea and B. de Crombrugghe (2004). "Interactions between Sox9 and beta-catenin control chondrocyte differentiation." Genes Dev18: 1072-87.

Alhadlaq, A., J. H. Elisseeff, L. Hong, C. G. Williams, A. I. Caplan, B. Sharma, R. A. Kopher, S. Tomkoria, D. P. Lennon, A. Lopez and J. J. Mao (2004). "Adult stem cell driven genesis of human-shaped articular condyle." Ann Biomed Eng32(7): 911-23.

Alvarez-Barreto, J. F., M. C. Shreve, P. L. Deangelis and V. I. Sikavitsas (2007). "Preparation of a functionally flexible, three-dimensional, biomimetic poly(L-lactic acid) scaffold with improved cell adhesion." Tissue Engineering13(6): 1205-1217.

Amit, M., C. Shariki, V. Margulets and J. Itskovitz-Eldor (2004). "Feeder Layer- and Serum-Free Culture of Human Embryonic Stem Cells." Biology of Reproduction70(3): 837-845.

Anderson, D. G., S. Levenberg and R. Langer (2004). "Nanoliter-scale synthesis of arrayed biomaterials and application to human embryonic stem cells." Nature Biotechnology22(7): 863-866.

Andressen, C., S. Arnhold, M. Puschmann, W. Bloch, J. Hescheler, R. Fassler and K. Addicks (1998). "beta 1 integrin deficiency impairs migration and differentiation of mouse embryonic stem cell derived neurons." Neuroscience Letters251(3): 165-168.

Arikawa-Hirasawa, E., H. Watanabe, H. Takami, J. R. Hassell and Y. Yamada (1999). "Perlecan is essential for cartilage and cephalic development." Nat Genet23(3): 354-8.

Ashton, R. S., A. Banerjee, S. Punyani, D. V. Schaffer and R. S. Kane (2007). "Scaffolds based on degradable alginate hydrogels and poly(lactide-co-glycolide) microspheres for stem cell culture." Biomaterials28: 5518-5525.

Bajada, S., I. Mazakova, J. B. Richardson and N. Ashammakhi (2008). "Updates on stem cells and their applications in regenerative medicine." Journal of Tissue Engineering and Regenerative Medicine2(4): 169-183.

Bang, O. S., E. J. Kim, J. G. Chung, S. R. Lee, T. K. Park and S. S. Kang (2000). "Association of focal adhesion kinase with fibronectin and paxillin is required for precartilage condensation of chick mesenchymal cells." Biochem Biophys Res Commun278(3): 522-9.

Barry, F., R. E. Boynton, B. Liu and J. M. Murphy (2001). "Chondrogenic Differentiation of Mesenchymal Stem Cells from Bone Marrow: Differentiation-Dependent Gene Expression of Matrix Components." Experimental Cell Research268(2): 189-200.

Baxter, M. A., M. V. Camarasa, N. Bates, F. Small, P. Murray, D. Edgar and S. J. Kimber (2009). "Analysis of the distinct functions of growth factors and tissue

culture substrates necessary for the long-term self-renewal of human embryonic stem cell lines." Stem Cell Research3(1): 28-38.
Beamson, G. and M. R. Alexander (2004). "Angle-resolved XPS of fluorinated and semi-fluorinated side-chain polymers." Surface and Interface Analysis36(4): 323-333.
Bell, D. M., K. K. Leung, S. C. Wheatley, L. J. Ng, S. Zhou, K. W. Ling, M. H. Sham, P. Koopman, P. P. Tam and K. S. Cheah (1997). "SOX9 directly regulates the type-II collagen gene." Nat Genet16(2): 174-8.
Benoit, D. S., M. P. Schwartz, A. R. Durney and K. S. Anseth (2008). "Small functional groups for controlled differentiation of hydrogel-encapsulated human mesenchymal stem cells." Nat Mater7(10): 816-23.
Benya, P. D. and J. D. Shaffer (1982). "Dedifferentiated chondrocytes reexpress the differentiated collagen phenotype when cultured in agarose gels." Cell30(1): 215-24.
Bhosale, A. M. and J. B. Richardson (2008). "Articular cartilage: structure, injuries and review of management." British Medical Bulletin87(1): 77-95.
Bigdeli, N., M. Andersson, R. Strehl, K. Emanuelsson, E. Kilmare, J. Hyllner and A. Lindahl (2008). "Adaptation of human embryonic stem cells to feeder-free and matrix-free culture conditions directly on plastic surfaces." Journal of Biotechnology133: 146-153.
Bosnakovski, D., M. Mizuno, G. Kim, T. Ishiguro, M. Okumura, T. Iwanaga, T. Kadosawa and T. Fujinaga (2004). "Chondrogenic differentiation of bovine bone marrow mesenchymal stem cells in pellet cultural system." Experimental Hematology32(5): 502-509.
Braam, S. R., L. Zeinstra, S. Litjens, D. Ward-van Oostwaard, S. van den Brink, L. van Laake, F. Lebrin, P. Kats, R. Hochstenbach, R. Passier, A. Sonnenberg and C. L. Mummery (2008). "Recombinant Vitronectin is a Functionally Defined Substrate that Supports Human Embryonic Stem Cell Self Renewal via {alpha}V{beta}5 Integrin." Stem Cells: 2008-0291.
Brooke, G., H. Tong, J. P. Levesque and K. Atkinson (2008). "Molecular trafficking mechanisms of multipotent mesenchymal stem cells derived from human bone marrow and placenta." Stem Cells Dev17(5): 929-40.
Buckwalter, J. A. and H. J. Mankin (1998). "Articular cartilage: tissue design and chondrocyte-matrix interactions." Instr Course Lect47: 477-86.
Buhring, H. J., V. L. Battula, S. Treml, B. Schewe, L. Kanz and W. Vogel (2007). "Novel markers for the prospective isolation of human MSC." Ann N Y Acad Sci1106: 262-71.
Burdon, T., A. Smith and P. Savatier (2002). "Signalling, cell cycle and pluripotency in embryonic stem cells." Trends Cell Biol12(9): 432-8.
Carlson, T. R., H. Q. Hu, R. Braren, Y. H. Kim and R. A. Wang (2008). "Cell-autonomous requirement for beta 1 integrin in endothelial cell adhesion, migration and survival during angiogenesis in mice." Development135(12): 2193-2202.
Carr, A. J., A. Vugler, J. Lawrence, L. L. Chen, A. Ahmado, F. K. Chen, M. Semo, C. Gias, L. da Cruz, H. D. Moore, J. Walsh and P. J. Coffey (2009). "Molecular characterization and functional analysis of phagocytosis by human embryonic stem cell-derived RPE cells using a novel human retinal assay." Mol Vis15: 283-95.
Carre, A. and V. Lacarriere (2010). "How Substrate Properties Control Cell Adhesion. A Physical-Chemical Approach." Journal of Adhesion Science and Technology24(5): 815-830.
Cartwright, P., C. McLean, A. Sheppard, D. Rivett, K. Jones and S. Dalton (2005). "LIF/STAT3 controls ES cell self-renewal and pluripotency by a Myc-dependent mechanism." Development132(5): 885-896.
Chambers, I., D. Colby, M. Robertson, J. Nichols, S. Lee, S. Tweedie and A. Smith (2003). "Functional expression cloning of Nanog, a pluripotency sustaining factor in embryonic stem cells." Cell113(5): 643-655.
Chang, J. C., S. H. Hsu and D. C. Chen (2009). "The promotion of chondrogenesis in adipose-derived adult stem cells by an RGD-chimeric protein in 3D alginate culture." Biomaterials30(31): 6265-6275.
Chapel, A., J. M. Bertho, M. Bensidhoum, L. Fouillard, R. G. Young, J. Frick, C. Demarquay, F. Cuvelier, E. Mathieu, F. Trompier, N. Dudoignon, C. Germain, C.

Mazurier, J. Aigueperse, J. Borneman, N. C. Gorin, P. Gourmelon and D. Thierry (2003). "Mesenchymal stem cells home to injured tissues when co-infused with hematopoietic cells to treat a radiation-induced multi-organ failure syndrome." J Gene Med5(12): 1028-38.

Chase, L., U. Lakshmipathy, L. Solchaga, M. Rao and M. Vemuri (2010). "A novel serum-free medium for the expansion of human mesenchymal stem cells." Stem Cell Research & Therapy1(1): 8.

Chen, S. S., W. Fitzgerald, J. Zimmerberg, H. K. Kleinman and L. Margolis (2007). "Cell-cell and cell-extracellular matrix interactions regulate embryonic stem cell differentiation." Stem Cells25(3): 553-561.

Chen, Y. L., C. A. Helm and J. N. Israelachvili (1991). "Molecular Mechanisms Associated with Adhesion and Contact-Angle Hysteresis of Monolayer Surfaces." Journal of Physical Chemistry95(26): 10736-10747.

Chimal-Monroy, J. and L. Diaz de Leon (1999). "Expression of N-cadherin, N-CAM, fibronectin and tenascin is stimulated by TGF-beta1, beta2, beta3 and beta5 during the formation of precartilage condensations." Int J Dev Biol43(1): 59-67.

Chimal-Monroy, J., J. Rodriguez-Leon, J. A. Montero, Y. Ganan, D. Macias, R. Merino and J. M. Hurle (2003). "Analysis of the molecular cascade responsible for mesodermal limb chondrogenesis: Sox genes and BMP signaling." Dev Biol257(2): 292-301.

Connelly, J. T., A. J. Garcia and M. E. Levenston (2007). "Inhibition of in vitro chondrogenesis in RGD-modified three-dimensional alginate gels." Biomaterials28(6): 1071-83.

Csaki, C., P. R. Schneider and M. Shakibaei (2008). "Mesenchymal stem cells as a potential pool for cartilage tissue engineering." Ann Anat190: 395-412.

Curran, J. M., R. Chen and J. A. Hunt (2006). "The guidance of human mesenchymal stem cell differentiation in vitro by controlled modifications to the cell substrate." Biomaterials27(27): 4783-4793.

Dalby, M. J., D. McCloy, M. Robertson, H. Agheli, D. Sutherland, S. Affrossman and R. O. C. Oreffo (2006). "Osteoprogenitor response to semi-ordered and random nanotopographies." Biomaterials27(15): 2980-2987.

Deakin, N. O. and C. E. Turner (2008). "Paxillin comes of age." J Cell Sci121(Pt 15): 2435-44.

DeLise, A. M., L. Fischer and R. S. Tuan (2000). "Cellular interactions and signaling in cartilage development." Osteoarthritis Cartilage8(5): 309-34.

DeLise, A. M. and R. S. Tuan (2002). "Alterations in the spatiotemporal expression pattern and function of N-cadherin inhibit cellular condensation and chondrogenesis of limb mesenchymal cells in vitro." J Cell Biochem87(3): 342-59.

Delise, A. M. and R. S. Tuan (2002). "Analysis of N-cadherin function in limb mesenchymal chondrogenesis in vitro." Dev Dyn225(2): 195-204.

Delon, I. and N. H. Brown (2007). "Integrins and the actin cytoskeleton." Current Opinion in Cell Biology19(1): 43-50.

Derda, R., L. Y. Li, B. P. Orner, R. L. Lewis, J. A. Thomson and L. L. Kiessling (2007). "Defined substrates for human embryonic stem cell growth identified from surface arrays." Acs Chemical Biology2(5): 347-355.

Derfoul, A., G. L. Perkins, D. J. Hall and R. S. Tuan (2006). "Glucocorticoids promote chondrogenic differentiation of adult human mesenchymal stem cells by enhancing expression of cartilage extracellular matrix genes." Stem Cells24(6): 1487-95.

DiMilla, P. A., J. A. Stone, J. A. Quinn, S. M. Albelda and D. A. Lauffenburger (1993). "Maximal migration of human smooth muscle cells on fibronectin and type IV collagen occurs at an intermediate attachment strength." J Cell Biol122(3): 729-37.

Djouad, F., B. Delorme, M. Maurice, C. Bony, F. Apparailly, P. Louis-Plence, F. Canovas, P. Charbord, D. Noel and C. Jorgensen (2007). "Microenvironmental changes during differentiation of mesenchymal stem cells towards chondrocytes." Arthritis Research & Therapy9(2).

Downie, S. A. and S. A. Newman (1995). "Different roles for fibronectin in the generation of fore and hind limb precartilage condensations." Dev Biol172(2): 519-30.

Duboc, V. and M. P. O. Logan (2009). "Building limb morphology through integration of signalling modules." Current Opinion in Genetics & Development19(5): 497-503.
Elangbam, C. S., C. W. Qualls and R. R. Dahlgren (1997). "Cell adhesion molecules - Update." Veterinary Pathology34(1): 61-73.
Ellis, S. J. and G. Tanentzapf (2009). "Integrin-mediated adhesion and stem-cell-niche interactions." Cell and tissue research339(1): 121-30.
Estes, B. T., J. M. Gimble and F. Guilak (2004). "Mechanical signals as regulators of stem cell fate." Curr Top Dev Biol60: 91-126.
Evans, N. D., C. Minelli, E. Gentleman, V. LaPointe, S. N. Patankar, M. Kallivretaki, X. Chen, C. J. Roberts and M. M. Stevens (2009). "Substrate stiffness affects early differentiation events in embryonic stem cells." Eur Cell Mater18: 1-13.
Fassler, R., M. Pfaff, J. Murphy, A. A. Noegel, S. Johansson, R. Timpl and R. Albrecht (1995). "Lack of beta 1 integrin gene in embryonic stem cells affects morphology, adhesion, and migration but not integration into the inner cell mass of blastocysts." J. Cell Biol.128(5): 979-988.
Fathi, F., T. Altiraihi, S. J. Mowla and M. Movahedin (2010). "Transplantation of retinoic acid treated murine embryonic stem cells & behavioural deficit in Parkinsonian rats." Indian Journal of Medical Research131(4): 536-544.
Fernandez-Teran, M. and M. A. Ros (2008). "The Apical Ectodermal Ridge: morphological aspects and signaling pathways." International Journal of Developmental Biology52(7): 857-871.
Fischer, S. E., X. Y. Liu, H. Q. Mao and J. L. Harden (2007). "Controlling cell adhesion to surfaces via associating bioactive triblock proteins." Biomaterials28: 3325-3337.
Fisher, O. Z., A. Khademhosseini, R. Langer and N. A. Peppas (2010). "Bioinspired Materials for Controlling Stem Cell Fate." Accounts of Chemical Research43(3): 419-428.
Forsyth, C. B., J. Pulai and R. F. Loeser (2002). "Fibronectin fragments and blocking antibodies to alpha 2 beta 1 and alpha 5 beta 1 integrins stimulate mitogen-activated protein kinase signaling and increase collagenase 3 (matrix metalloproteinase 13) production by human articular chondrocytes." Arthritis and Rheumatism46(9): 2368-2376.
Friedenstein, A. J., J. F. Gorskaja and N. N. Kulagina (1976). "Fibroblast precursors in normal and irradiated mouse hematopoietic organs." Exp Hematol4(5): 267-74.
Fuente-Mora, C. (2009). Isolation and characterization of a novel population of potential kidney stem cells from postnatal mouse kidney. School of Biological Sciences. University of Liverpool. **PhD**.
Furumatsu, T., M. Tsuda, N. Taniguchi, Y. Tajima and H. Asahara (2005). "Smad3 induces chondrogenesis through the activation of SOX9 via CREB-binding protein/p300 recruitment." Journal of Biological Chemistry280(9): 8343-8350.
Gao, L., R. McBeath and C. S. Chen (2010). "Stem cell shape regulates a chondrogenic versus myogenic fate through Rac1 and N-cadherin." Stem Cells28(3): 564-72.
Garcia, A. J., M. D. Vega and D. Boettiger (1999). "Modulation of cell proliferation and differentiation through substrate-dependent changes in fibronectin conformation." Molecular Biology of the Cell10(3): 785-798.
Gehris, A. L., E. Stringa, J. Spina, M. E. Desmond, R. S. Tuan and V. D. Bennett (1997). "The region encoded by the alternatively spliced exon IIIA in mesenchymal fibronectin appears essential for chondrogenesis at the level of cellular condensation." Dev Biol190(2): 191-205.
Gerstenfeld, L. C., G. L. Barnes, C. M. Shea and T. A. Einhorn (2003). "Osteogenic differentiation is selectively promoted by morphogenetic signals from chondrocytes and synergized by a nutrient rich growth environment." Connective Tissue Research44: 85-91.
Gerstenfeld, L. C., J. Cruceta, C. M. Shea, K. Sampath, G. L. Barnes and T. A. Einhorn (2002). "Chondrocytes provide morphogenic signals that selectively induce osteogenic differentiation of mesenchymal stem cells." J Bone Miner Res17(2): 221-30.
Gillies, R. J., N. Didier and M. Denton (1986). "Determination of Cell Number in Monolayer-Cultures." Analytical Biochemistry159(1): 109-113.

Ginis, I., Y. Luo, T. Miura, S. Thies, R. Brandenberger, S. Gerecht-Nir, M. Amit, A. Hoke, M. K. Carpenter, J. Itskovitz-Eldor and M. S. Rao (2004). "Differences between human and mouse embryonic stem cells." Developmental Biology269(2): 360-380.

Goessler, U. R., P. Bugert, K. Bieback, J. Stern-Straeter, G. Bran, K. Hormann and F. Riedel (2008). "Integrin expression in stem cells from bone marrow and adipose tissue during chondrogenic differentiation." International Journal of Molecular Medicine21(3): 271-279.

Goldring, M. B., K. Tsuchimochi and K. Ijiri (2006). "The control of chondrogenesis." J Cell Biochem97(1): 33-44.

Gomes, M. E., C. M. Bossano, C. M. Johnston, R. L. Reis and A. G. Mikos (2006). "In vitro localization of bone growth factors in constructs of biodegradable scaffolds seeded with marrow stromal cells and cultured in a flow perfusion bioreactor." Tissue Eng12(1): 177-88.

Greenlee, A. R., T. A. Kronenwetter-Koepel, S. J. Kaiser and K. Liu (2005). "Comparison of Matrigel (TM) and gelatin substrata for feeder-free culture of undifferentiated mouse embryonic stem cells for toxicity testing." Toxicology in Vitro19(3): 389-397.

Gronthos, S., S. E. Graves, S. Ohta and P. J. Simmons (1994). "The STRO-1+ fraction of adult human bone marrow contains the osteogenic precursors." Blood84(12): 4164-73.

Gumbiner, B. M. (1996). "Cell adhesion: the molecular basis of tissue architecture and morphogenesis." Cell84: 345-57.

Guo, L., N. Kawazoe, Y. Fan, Y. Ito, J. Tanaka, T. Tateishi, X. Zhang and G. Chen (2008). "Chondrogenic differentiation of human mesenchymal stem cells on photoreactive polymer-modified surfaces." Biomaterials29: 23-32.

Guo, X., H. Park, G. Liu, W. Liu, Y. Cao, Y. Tabata, F. K. Kasper and A. G. Mikos (2009). "In vitro generation of an osteochondral construct using injectable hydrogel composites encapsulating rabbit marrow mesenchymal stem cells." Biomaterials30(14): 2741-52.

Haegele, L., B. Ingold, H. Naumann, G. Tabatabai, B. Ledermann and S. Brandner (2003). "Wnt signalling inhibits neural differentiation of embryonic stem cells by controlling bone morphogenetic protein expression." Mol Cell Neurosci24(3): 696-708.

Hall, J., G. Guo, J. Wray, I. Eyres, J. Nichols, L. Grotewold, S. Morfopoulou, P. Humphreys, W. Mansfield, R. Walker, S. Tomlinson and A. Smith (2009). "Oct4 and LIF/Stat3 Additively Induce Kruppel Factors to Sustain Embryonic Stem Cell Self-Renewal." Cell Stem Cell5(6): 597-609.

Hanson, A. D., M. E. Wall, B. Pourdeyhimi and E. G. Loboa (2007). "Effects of oxygen plasma treatment on adipose-derived human mesenchymal stem cell adherence to poly(L-lactic acid) scaffolds." Journal of Biomaterials Science-Polymer Edition18: 1387-1400.

Harrison, J., S. Pattanawong, J. S. Forsythe, K. A. Gross, D. R. Nisbet, H. Beh, T. F. Scott, A. O. Trounson and R. Mollard (2004). "Colonization and maintenance of murine embryonic stem cells on poly(alpha-hydroxy esters)." Biomaterials25(20): 4963-4970.

Hatakeyama, Y., J. Nguyen, X. Wang, G. H. Nuckolls and L. Shum (2003). "Smad signaling in mesenchymal and chondroprogenitor cells." J Bone Joint Surg Am85-A Suppl 3: 13-8.

Hayashi, Y., M. K. Furue, T. Okamoto, K. Ohnuma, Y. Myoishi, Y. Fukuhara, T. Abe, J. D. Sato, R. I. Hata and M. Asashima (2007). "Integrins regulate mouse embryonic stem cell self-renewal." Stem Cells25: 3005-3015.

Herrera, M. B., B. Bussolati, S. Bruno, L. Morando, G. Mauriello-Romanazzi, F. Sanavio, I. Stamenkovic, L. Biancone and G. Camussi (2007). "Exogenous mesenchymal stem cells localize to the kidney by means of CD44 following acute tubular injury." Kidney Int72(4): 430-41.

Hersel, U., C. Dahmen and H. Kessler (2003). "RGD modified polymers: biomaterials for stimulated cell adhesion and beyond." Biomaterials24(24): 4385-4415.

Hoemann, C. D., H. El-Gabalawy and M. D. McKee (2009). "In vitro osteogenesis assays: influence of the primary cell source on alkaline phosphatase activity and mineralization." Pathol Biol (Paris)57(4): 318-23.
Holmes, M. W., M. T. Bayliss and H. Muir (1988). "Hyaluronic acid in human articular cartilage. Age-related changes in content and size." Biochem J250(2): 435-41.
Hooper, M., K. Hardy, A. Handyside, S. Hunter and M. Monk (1987). "HPRT-deficient (Lesch-Nyhan) mouse embryos derived from germline colonization by cultured cells." Nature326(6110): 292-295.
Horak, D., J. Kroupava, M. Slouf and P. Dvorak (2004). "Poly(2-hydroxyethyl methacrylate)-based slabs as a mouse embryonic stem cell support." Biomaterials25(22): 5249-5260.
Horbett, T. A. and M. B. Schway (1988). "Correlations between mouse 3T3 cell spreading and serum fibronectin adsorption on glass and hydroxyethylmethacrylate-ethylmethacrylate copolymers." J Biomed Mater Res22(9): 763-93.
Horbett, T. A., M. B. Schway and B. D. Ratner (1985). "Hrydrophilic-hydrophobic copolymers as cell substrates - effect on 3T3 cell-growth rates." Journal of Colloid and Interface Science104(1): 28-39.
Huang, S. and D. E. Ingber (2000). "Shape-dependent control of cell growth, differentiation, and apoptosis: switching between attractors in cell regulatory networks." Exp Cell Res261(1): 91-103.
Hwang, N. S., S. Varghese, C. Puleo, Z. Zhang and J. Elisseeff (2007). "Morphogenetic signals from chondrocytes promote chondrogenic and osteogenic differentiation of mesenchymal stem cells." J Cell Physiol212(2): 281-4.
Hyde, G., S. Dover, A. Aszodi, G. A. Wallis and R. P. Boot-Handford (2007). "Lineage tracing using matrilin-1 gene expression reveals that articular chondrocytes exist as the joint interzone forms." Dev Biol304: 825-33.
Hynes, R. O. (2002). "Integrins: Bidirectional, allosteric signaling machines." Cell110(6): 673-687.
Hynes, R. O. (2009). "The Extracellular Matrix: Not Just Pretty Fibrils." Science326(5957): 1216-1219.
Jin, E. J., Y. A. Choi, E. Kyun Park, O. S. Bang and S. S. Kang (2007). "MMP-2 functions as a negative regulator of chondrogenic cell condensation via down-regulation of the FAK-integrin beta1 interaction." Dev Biol308(2): 474-84.
Jinming, G., N. Laura and L. Robert (1998). "Surface hydrolysis of poly(glycolic acid) meshes increases the seeding density of vascular smooth muscle cells." Journal of Biomedical Materials Research42(3): 417-424.
Kalaskar, D. M., J. E. Gough, R. V. Ulijn, W. W. Sampson, D. J. Scurr, F. J. Rutten, M. R. Alexander, C. L. R. Merry and S. J. Eichhorn (2008). "Controlling cell morphology on amino acid-modified cellulose." Soft Matter4(5): 1059-1065.
Kamiya, N., H. Watanabe, H. Habuchi, H. Takagi, T. Shinomura, K. Shimizu and K. Kimata (2006). "Versican/PG-M regulates chondrogenesis as an extracellular matrix molecule crucial for mesenchymal condensation." J Biol Chem281(4): 2390-400.
Karabekian, Z., N. D. Gillum, E. W. P. Wong and N. Sarvazyan (2009). "Effects of N-cadherin overexpression on the adhesion properties of embryonic stem cells." Cell Adh Migr3(3): 305-10.
Kawakami, Y., J. Rodriguez-Leon and J. C. Izpisua Belmonte (2006). "The role of TGFbetas and Sox9 during limb chondrogenesis." Curr Opin Cell Biol18(6): 723-9.
Keselowsky, B. G., D. M. Collard and A. J. Garcia (2004). "Surface chemistry modulates focal adhesion composition and signaling through changes in integrin binding." Biomaterials25(28): 5947-5954.
Kilian, K. A., B. Bugarija, B. T. Lahn and M. Mrksich (2010). "Geometric cues for directing the differentiation of mesenchymal stem cells." Proceedings of the National Academy of Sciences of the United States of America107(11): 4872-4877.
Kim, J. H., D. B. Koo, H. T. Lee and K. S. Chung (1995). "Expression patterns of mRNA for members of the alkaline phosphatase family in embryonic stem and primordial germ cells of mouse." Theriogenology43(1): 248-248.

Kim, M. R., J. H. Jeong and T. G. Park (2002). "Swelling induced detachment of chondrocytes using RGD-modified poly(N-isopropylacrylamide) hydrogel beads." Biotechnol Prog18(3): 495-500.
Kleinman, H. K. and G. R. Martin (2005). "Matrigel: Basement membrane matrix with biological activity." Seminars in Cancer Biology15(5): 378-386.
Kolf, C. M., E. Cho and R. S. Tuan (2007). "Mesenchymal stromal cells. Biology of adult mesenchymal stem cells: regulation of niche, self-renewal and differentiation." Arthritis Res Ther9: 204.
Kolhar, P., V. R. Kotamraju, S. T. Hikita, D. O. Clegg and E. Ruoslahti (2010). "Synthetic surfaces for human embryonic stem cell culture." J Biotechnol146: 143-6.
Kollar, K., M. M. Cook, K. Atkinson and G. Brooke (2009). "Molecular mechanisms involved in mesenchymal stem cell migration to the site of acute myocardial infarction." Int J Cell Biol2009: 904682.
Kommireddy, D. S., S. M. Sriram, Y. M. Lvov and D. K. Mills (2006). "Stem cell attachment to layer-by-layer assembled TiO2 nanoparticle thin films." Biomaterials27(24): 4296-4303.
Konno, T., N. Kawazoe, G. P. Chen and Y. Ito (2006). "Culture of mouse embryonic stem cells on photoimmobilized polymers." Journal of Bioscience and Bioengineering102(4): 304-310.
Kowalewska, A., W. A. Stanczyk, S. Boileau, L. Lestel and J. D. Smith (1999). "Novel polymer systems with very bulky organosilicon side chain substituents." Polymer40(3): 813-818.
Kroupova, J., D. Horak, J. Pachernik, P. Dvorak and M. Slouf (2006). "Functional polymer hydrogels for embryonic stem cell support." Journal of Biomedical Materials Research Part B-Applied Biomaterials76B(2): 315-325.
Kujawa, M. J. and A. I. Caplan (1986). "Hyaluronic acid bonded to cell-culture surfaces stimulates chondrogenesis in stage 24 limb mesenchyme cell cultures." Developmental Biology114(2): 504-518.
Kumar, D. and A. B. Lassar (2009). "The transcriptional activity of Sox9 in chondrocytes is regulated by RhoA signaling and actin polymerization." Mol Cell Biol29(15): 4262-73.
Kunath, T., M. K. Saba-El-Leil, M. Almousailleakh, J. Wray, S. Meloche and A. Smith (2007). "FGF stimulation of the Erk1/2 signalling cascade triggers transition of pluripotent embryonic stem cells from self-renewal to lineage commitment." Development134(16): 2895-2902.
Lan, M. A., C. A. Gersbach, K. E. Michael, B. G. Keselowsky and A. J. Garcia (2005). "Myoblast proliferation and differentiation on fibronectin-coated self assembled monolayers presenting different surface chemistries." Biomaterials26(22): 4523-4531.
Landis, W. J. (1996). "Mineral characterization in calcifying tissues: atomic, molecular and macromolecular perspectives." Connect Tissue Res34(4): 239-46.
Larue, L., C. Antos, S. Butz, O. Huber, V. Delmas, M. Dominis and R. Kemler (1996). "A role for cadherins in tissue formation." Development122(10): 3185-3194.
Lee, S. T., J. I. Yun, Y. S. Jo, M. Mochizuki, A. J. van der Vlies, S. Kontos, J. E. Ihm, J. M. Lim and J. A. Hubbell (2010). "Engineering integrin signaling for promoting embryonic stem cell self-renewal in a precisely defined niche." Biomaterials31(6): 1219-1226.
Lefebvre, V., W. Huang, V. R. Harley, P. N. Goodfellow and B. de Crombrugghe (1997). "SOX9 is a potent activator of the chondrocyte-specific enhancer of the pro alpha1(II) collagen gene." Mol Cell Biol17(4): 2336-46.
Legate, K. R., S. A. Wickstrom and R. Fassler (2009). "Genetic and cell biological analysis of integrin outside-in signaling." Genes Dev23: 397-418.
Lengner, C. J., C. Lepper, A. J. Van Wijnen, J. L. Stein, G. S. Stein and J. B. Lian (2004). "Primary mouse embryonic fibroblasts: A model of mesenchymal cartilage formation." Journal of Cellular Physiology200(3): 327-333.
Li, J., Z. Zhao, J. Liu, N. Huang, D. Long, J. Wang, X. Li and Y. Liu (2009). "MEK/ERK and p38 MAPK regulate chondrogenesis of rat bone marrow mesenchymal stem cells through delicate interaction with TGF-beta 1/Smads pathway." Cell Proliferation43(4): 333-343.

Li, W.-G. and X.-X. Xu (2005). "The expression of N-cadherin, fibronectin during chondrogenic differentiation of MSC induced by TGF-beta(1)." Chin J Traumatol8(6): 349-51.
Li, W. J., R. Tuli, C. Okafor, A. Derfoul, K. G. Danielson, D. J. Hall and R. S. Tuan (2005). "A three-dimensional nanofibrous scaffold for cartilage tissue engineering using human mesenchymal stem cells." Biomaterials26(6): 599-609.
Li, Y. J., E. H. Chung, R. T. Rodriguez, M. T. Firpo and K. E. Healy (2006). "Hydrogels as artificial matrices for human embryonic stem cell self-renewal." Journal of Biomedical Materials Research Part A79A(1): 1-5.
Liu, F., L. Malaval and J. E. Aubin (2003). "Global amplification polymerase chain reaction reveals novel transitional stages during osteoprogenitor differentiation." J Cell Sci116(Pt 9): 1787-96.
Liu, J., X. W. He, S. A. Corbett, S. F. Lowry, A. M. Graham, R. Fassler and S. H. Li (2009). "Integrins are required for the differentiation of visceral endoderm." Journal of Cell Science122(2): 233-242.
Liu, L., W. Wu, X. Tuo, W. Geng, J. Zhao, J. Wei, X. Yan, W. Yang, L. Li and F. Chen (2010). "Novel strategy to engineer trachea cartilage graft with marrow mesenchymal stem cell macroaggregate and hydrolyzable scaffold." Artif Organs34(5): 426-33.
Liu, S. Q., Q. Tian, J. L. Hedrick, J. H. Po Hui, P. L. Rachel Ee and Y. Y. Yang (2010). "Biomimetic hydrogels for chondrogenic differentiation of human mesenchymal stem cells to neocartilage." Biomaterials.
Loeser, R. F. (2002). "Integrins and cell signaling in chondrocytes." Biorheology39(1-2): 119-124.
Lord, M. S., B. G. Cousins, P. J. Doherty, J. M. Whitelock, A. Simmons, R. L. Williams and B. K. Milthorpe (2006). "The effect of silica nanoparticulate coatings on serum protein adsorption and cellular response." Biomaterials27(28): 4856-4862.
Losic, D., M. A. Cole, B. Dollmann, K. Vasilev and H. J. Griesser (2008). "Surface modification of nanoporous alumina membranes by plasma polymerization." Nanotechnology19(24): 7.
Love, J. C., L. A. Estroff, J. K. Kriebel, R. G. Nuzzo and G. M. Whitesides (2005). "Self-assembled monolayers of thiolates on metals as a form of nanotechnology." Chemical Reviews105(4): 1103-1169.
Ludwig, T. E., M. E. Levenstein, J. M. Jones, W. T. Berggren, E. R. Mitchen, J. L. Frane, L. J. Crandall, C. A. Daigh, K. R. Conard, M. S. Piekarczyk, R. A. Llanas and J. A. Thomson (2006). "Derivation of human embryonic stem cells in defined conditions." Nature Biotechnology24(2): 185-187.
Luo, W., S. R. Jones and M. N. Yousaf (2008). "Geometric control of stem cell differentiation rate on surfaces." Langmuir24(21): 12129-33.
Luo, Y., I. Kostetskii and G. L. Radice (2005). "N-cadherin is not essential for limb mesenchymal chondrogenesis." Dev Dyn232(2): 336-44.
Ma, Z. W., C. Y. Gao, Y. H. Gong and J. C. Shen (2003). "Chondrocyte behaviors on poly-L-lactic acid (PLLA) membranes containing hydroxyl, amide or carboxyl groups." Biomaterials24(21): 3725-3730.
Macchiarini, P., P. Jungebluth, T. Go, M. A. Asnaghi, L. E. Rees, T. A. Cogan, A. Dodson, J. Martorell, S. Bellini, P. P. Parnigotto, S. C. Dickinson, A. P. Hollander, S. Mantero, M. T. Conconi and M. A. Birchall (2008). "Clinical transplantation of a tissue-engineered airway." Lancet372: 2023-30.
Mackay, A. M., S. C. Beck, J. M. Murphy, F. P. Barry, C. O. Chichester and M. F. Pittenger (1998). "Chondrogenic differentiation of cultured human mesenchymal stem cells from marrow." Tissue Eng4(4): 415-28.
Mackie, E. J., Y. A. Ahmed, L. Tatarczuch, K. S. Chen and M. Mirams (2008). "Endochondral ossification: How cartilage is converted into bone in the developing skeleton." International Journal of Biochemistry & Cell Biology40(1): 46-62.
Mahlstedt, M. M., D. Anderson, J. S. Sharp, R. McGilvray, M. D. B. Munoz, L. D. Buttery, M. R. Alexander, F. Rose and C. Denning (2009). "Maintenance of Pluripotency

in Human Embryonic Stem Cells Cultured on a Synthetic Substrate in Conditioned Medium." Biotechnology and Bioengineering105(1): 130-140.
Main, A. L., T. S. Harvey, M. Baron, J. Boyd and I. D. Campbell (1992). "The 3-dimensional structure of the 10th type-III module of fibronectin - an insight into RGD-mediated interactions." Cell71(4): 671-678.
Malaval, L., F. Liu, P. Roche and J. E. Aubin (1999). "Kinetics of osteoprogenitor proliferation and osteoblast differentiation in vitro." J Cell Biochem74(4): 616-27.
Marie, P. J. and O. Fromigue (2006). "Osteogenic differentiation of human marrow-derived mesenchymal stem cells." Regen Med1(4): 539-48.
Marom, R., I. Shur, R. Solomon and D. Benayahu (2005). "Characterization of adhesion and differentiation markers of osteogenic marrow stromal cells." J Cell Physiol202(1): 41-8.
Marshall, O. J. (2004). "PerlPrimer: cross-platform, graphical primer design for standard, bisulphite and real-time PCR." Bioinformatics20(15): 2471-2.
Marshall, W. F. (2003). "Gene expression and nuclear architecture during development and differentiation." Mechanisms of Development120: 1217-1230.
Martin, M. J., A. Muotri, F. Gage and A. Varki (2005). "Human embryonic stem cells express an immunogenic nonhuman sialic acid." Nature Medicine11(2): 228-232.
Martino, M. M., M. Mochizuki, D. A. Rothenfluh, S. A. Rempel, J. A. Hubbell and T. H. Barker (2009). "Controlling integrin specificity and stem cell differentiation in 2D and 3D environments through regulation of fibronectin domain stability." Biomaterials30(6): 1089-97.
Masui, S., Y. Nakatake, Y. Toyooka, D. Shimosato, R. Yagi, K. Takahashi, H. Okochi, A. Okuda, R. Matoba, A. A. Sharov, M. S. Ko and H. Niwa (2007). "Pluripotency governed by Sox2 via regulation of Oct3/4 expression in mouse embryonic stem cells." Nat Cell Biol9(6): 625-35.
Matsumoto, T., T. Okabe, T. Ikawa, T. Iida, H. Yasuda, H. Nakamura and S. Wakitani (2010). "Articular cartilage repair with autologous bone marrow mesenchymal cells." J Cell Physiol225(2): 291-5.
Mehlhorn, A. T., P. Niemeyer, K. Kaschte, L. Muller, G. Finkenzeller, D. Hartl, N. P. Sudkamp and H. Schmal (2007). "Differential effects of BMP-2 and TGF-beta1 on chondrogenic differentiation of adipose derived stem cells." Cell Prolif40(6): 809-23.
Meirelles Lda, S. and N. B. Nardi (2009). "Methodology, biology and clinical applications of mesenchymal stem cells." Front Biosci14: 4281-98.
Melkoumian, Z., J. L. Weber, D. M. Weber, A. G. Fadeev, Y. E. Zhou, P. Dolley-Sonneville, J. W. Yang, L. Q. Qiu, C. A. Priest, C. Shogbon, A. W. Martin, J. Nelson, P. West, J. P. Beltzer, S. Pal and R. Brandenberger (2010). "Synthetic peptide-acrylate surfaces for long-term self-renewal and cardiomyocyte differentiation of human embryonic stem cells." Nature Biotechnology28(6): 606-U95.
Melville, A. J., J. Harrison, K. A. Gross, J. S. Forsythe, A. O. Trounson and R. Mollard (2006). "Mouse embryonic stem cell colonisation of carbonated apatite surfaces." Biomaterials27(4): 615-622.
Mendler, M., S. G. Eich-Bender, L. Vaughan, K. H. Winterhalter and P. Bruckner (1989). "Cartilage contains mixed fibrils of collagen types II, IX, and XI." J Cell Biol108(1): 191-7.
Mi, L. X., S. Fischer, B. Chung, S. Sundelacruz and J. L. Harden (2006). "Self-assembling protein hydrogels with modular integrin binding domains." Biomacromolecules7(1): 38-47.
Michael, K. E., V. N. Vernekar, B. G. Keselowsky, J. C. Meredith, R. A. Latour and A. J. Garcia (2003). "Adsorption-induced conformational changes in fibronectin due to interactions with well-defined surface chemistries." Langmuir19(19): 8033-8040.
Michelini, M., V. Franceschini, S. S. Chen, S. Papini, A. Rosellini, F. Ciani, L. Margolis and R. P. Revoltella (2006). "Primate embryonic stem cells create their own niche while differentiating in three-dimensional culture systems." Cell Proliferation39(3): 217-229.

Miyabayashi, T., J. L. Teo, M. Yamamoto, M. McMillan, C. Nguyen and M. Kahn (2007). "Wnt/beta-catenin/CBP signaling maintains long-term murine embryonic stem cell pluripotency." Proc Natl Acad Sci U S A104(13): 5668-73.

Mochizuki, M., N. Yamagata, D. Philp, K. Hozumi, T. Watanabe, Y. Kikkawa, Y. Kadoya, H. K. Kleinman and M. Nomizu (2007). "Integrin-dependent cell behavior on ECM peptide-conjugated chitosan membranes." Biopolymers88(2): 122-130.

Modarresi, R., T. Lafond, J. A. Roman-Blas, K. G. Danielson, R. S. Tuan and M. R. Seghatoleslami (2005). "N-cadherin mediated distribution of beta-catenin alters MAP kinase and BMP-2 signaling on chondrogenesis-related gene expression." J Cell Biochem95(1): 53-63.

Mousa, S. A. (2008). "Cell adhesion molecules: Potential therapeutic & diagnostic implications." Molecular Biotechnology38(1): 33-40.

Mueller, M. B., M. Fischer, J. Zellner, A. Berner, T. Dienstknecht, L. Prantl, R. Kujat, M. Nerlich, R. S. Tuan and P. Angele (2010). "Hypertrophy in mesenchymal stem cell chondrogenesis: effect of TGF-beta isoforms and chondrogenic conditioning." Cells Tissues Organs192(3): 158-66.

Nagaoka, M., H. Ise, I. Harada, U. Koshimizu, A. Maruyama and T. Akaike (2008). "Embryonic undifferentiated cells show scattering activity on a surface coated with immobilized E-cadherin." Journal of Cellular Biochemistry103: 296-310.

Nakamura, K., T. Shirai, S. Morishita, S. Uchida, K. Saeki-Miura and F. Makishima (1999). "p38 mitogen-activated protein kinase functionally contributes to chondrogenesis induced by growth/differentiation factor-5 in ATDC5 cells." Exp Cell Res250(2): 351-63.

Nejadnik, H., J. H. Hui, E. P. Feng Choong, B. C. Tai and E. H. Lee (2010). "Autologous bone marrow-derived mesenchymal stem cells versus autologous chondrocyte implantation: an observational cohort study." Am J Sports Med38: 1110-6.

Neuss, S., C. Apel, P. Buttler, B. Denecke, A. Dhanasingh, X. L. Ding, D. Grafahrend, A. Groger, K. Hemmrich, A. Herr, W. Jahnen-Dechent, S. Mastitskaya, A. Perez-Bouza, S. Rosewick, J. Salber, M. Woltje and M. Zenke (2008). "Assessment of stem cell/biomaterial combinations for stem cell-based tissue engineering." Biomaterials29: 302-313.

Newman, A. P. (1998). "Articular cartilage repair." The American journal of sports medicine26(2): 309-24.

Newman, K. D. and M. W. McBurney (2004). "Poly(D,L lactic-co-glycolic acid) microspheres as biodegradable microcarriers for pluripotent stem cells." Biomaterials25(26): 5763-5771.

Nichols, J., J. Silva, M. Roode and A. Smith (2009). "Suppression of Erk signalling promotes ground state pluripotency in the mouse embryo." Development136(19): 3215-3222.

Nickson, C. M., P. J. Doherty and R. L. Williams (2008). "Novel polymeric coatings with the potential to control in-stent restenosis--an in vitro study." J Biomater Appl24(5): 437-52.

Niwa, H., T. Burdon, I. Chambers and A. Smith (1998). "Self-renewal of pluripotent embryonic stem cells is mediated via activation of STAT3." Genes Dev12(13): 2048-60.

Niwa, H., J. Miyazaki and A. G. Smith (2000). "Quantitative expression of Oct-3/4 defines differentiation, dedifferentiation or self-renewal of ES cells." Nat Genet24(4): 372-6.

Novak, P., C. Li, A. I. Shevchuk, R. Stepanyan, M. Caldwell, S. Hughes, T. G. Smart, J. Gorelik, V. P. Ostanin, M. J. Lab, G. W. Moss, G. I. Frolenkov, D. Klenerman and Y. E. Korchev (2009). "Nanoscale live-cell imaging using hopping probe ion conductance microscopy." Nat Methods6: 279-81.

Nuttelman, C. R., M. C. Tripodi and K. S. Anseth (2005). "Synthetic hydrogel niches that promote hMSC viability." Matrix Biol24(3): 208-18.

Oberlender, S. A. and R. S. Tuan (1994). "Expression and functional involvement of N-cadherin in embryonic limb chondrogenesis." Development120(1): 177-87.

Oh, C. D., S. H. Chang, Y. M. Yoon, S. J. Lee, Y. S. Lee, S. S. Kang and J. S. Chun (2000). "Opposing role of mitogen-activated protein kinase subtypes, erk-1/2 and p38, in the regulation of chondrogenesis of mesenchymes." J Biol Chem275(8): 5613-9.

Okita, K., T. Ichisaka and S. Yamanaka (2007). "Generation of germline-competent induced pluripotent stem cells." Nature448(7151): 313-U1.

Onyekwelu, I., M. B. Goldring and C. Hidaka (2009). "Chondrogenesis, joint formation, and articular cartilage regeneration." Journal of cellular biochemistry107(3): 383-92.

Ornitz, D. M. and P. J. Marie (2002). "FGF signaling pathways in endochondral and intramembranous bone development and human genetic disease." Genes & Development16(12): 1446-1465.

Ortiz, L. A., F. Gambelli, C. McBride, D. Gaupp, M. Baddoo, N. Kaminski and D. G. Phinney (2003). "Mesenchymal stem cell engraftment in lung is enhanced in response to bleomycin exposure and ameliorates its fibrotic effects." Proc Natl Acad Sci U S A100(14): 8407-11.

Pala, D., M. Kapoor, A. Woods, L. Kennedy, S. Liu, S. Chen, L. Bursell, K. M. Lyons, D. E. Carter, F. Beier and A. Leask (2008). "Focal Adhesion Kinase/Src Suppresses Early Chondrogenesis." Journal of Biological Chemistry283(14): 9239-9247.

Palecek, S. P., J. C. Loftus, M. H. Ginsberg, D. A. Lauffenburger and A. F. Horwitz (1997). "Integrin-ligand binding properties govern cell migration speed through cell-substratum adhesiveness." Nature385(6616): 537-40.

Paling, N. R. D., H. Wheadon, H. K. Bone and M. J. Welham (2004). "Regulation of embryonic stem cell self-renewal by phosphoinositide 3-kinase-dependent signaling." Journal of Biological Chemistry279(46): 48063-48070.

Palmqvist, L., C. H. Glover, L. Hsu, M. Lu, B. Bossen, J. M. Piret, R. K. Humphries and C. D. Helgason (2005). "Correlation of murine embryonic stem cell gene expression profiles with functional measures of pluripotency." Stem Cells23(5): 663-80.

Paragkumar, N. T., E. Dellacherie and J. L. Six (2006). "Surface characteristics of PLA and PLGA films." Applied Surface Science253(5): 2758-2764.

Park, J. S., H. J. Yang, D. G. Woo, H. N. Yang, K. Na and K. H. Park (2009). "Chondrogenic differentiation of mesenchymal stem cells embedded in a scaffold by long-term release of TGF-beta 3 complexed with chondroitin sulfate." Journal of Biomedical Materials Research Part A92A(2): 806-816.

Peister, A., J. A. Mellad, B. L. Larson, B. M. Hall, L. F. Gibson and D. J. Prockop (2004). "Adult stem cells from bone marrow (MSCs) isolated from different strains of inbred mice vary in surface epitopes, rates of proliferation, and differentiation potential." Blood103(5): 1662-8.

Pelham, R. J., Jr. and Y. Wang (1997). "Cell locomotion and focal adhesions are regulated by substrate flexibility." Proceedings of the National Academy of Sciences of the United States of America94(25): 13661-5.

Pelttari, K., A. Winter, E. Steck, K. Goetzke, T. Hennig, B. G. Ochs, T. Aigner and W. Richter (2006). "Premature induction of hypertrophy during in vitro chondrogenesis of human mesenchymal stem cells correlates with calcification and vascular invasion after ectopic transplantation in SCID mice." Arthritis and Rheumatism54(10): 3254-3266.

Pham, Q. P., F. Kurtis Kasper, L. Scott Baggett, R. M. Raphael, J. A. Jansen and A. G. Mikos (2008). "The influence of an in vitro generated bone-like extracellular matrix on osteoblastic gene expression of marrow stromal cells." Biomaterials29(18): 2729-2739.

Phillips, J. E., T. A. Petrie, F. P. Creighton and A. J. Garcia (2009). "Human mesenchymal stem cell differentiation on self-assembled monolayers presenting different surface chemistries." Acta Biomater6(1): 12-20.

Pittenger, M. F., A. M. Mackay, S. C. Beck, R. K. Jaiswal, R. Douglas, J. D. Mosca, M. A. Moorman, D. W. Simonetti, S. Craig and D. R. Marshak (1999). "Multilineage potential of adult human mesenchymal stem cells." Science284(5411): 143-7.

Plainfosse, M., P. V. Hatton, A. Crawford, Z. M. Jin and J. Fisher (2007). "Influence of the extracellular matrix on the frictional properties of tissue-engineered cartilage." Biochem Soc Trans35(Pt 4): 677-9.

Pompe, T., K. Keller, G. Mothes, M. Nitschke, M. Teese, R. Zimmermann and C. Werner (2007). "Surface modification of poly(hydroxybutyrate) films to control cell-matrix adhesion." Biomaterials28(1): 28-37.

Ponte, A. L., E. Marais, N. Gallay, A. Langonne, B. Delorme, O. Herault, P. Charbord and J. Domenech (2007). "The in vitro migration capacity of human bone marrow mesenchymal stem cells: comparison of chemokine and growth factor chemotactic activities." Stem Cells25(7): 1737-45.

Pulai, J. I., M. Del Carlo and R. F. Loeser (2002). "The alpha 5 beta 1 integrin provides matrix survival signals for normal and osteoarthritic human articular chondrocytes in vitro." Arthritis and Rheumatism46(6): 1528-1535.

Quintana, L., N. I. zur Nieden and C. E. Semino (2009). "Morphogenetic and regulatory mechanisms during developmental chondrogenesis: new paradigms for cartilage tissue engineering." Tissue Eng Part B Rev15(1): 29-41.

Re'em, T., O. Tsur-Gang and S. Cohen (2010). "The effect of immobilized RGD peptide in macroporous alginate scaffolds on TGFbeta1-induced chondrogenesis of human mesenchymal stem cells." Biomaterials31(26): 6746-55.

Ren, Y. J., H. Zhang, H. Huang, X. M. Wang, Z. Y. Zhou, F. Z. Cui and Y. H. An (2009). "In vitro behavior of neural stem cells in response to different chemical functional groups." Biomaterials30(6): 1036-44.

Roach, P., D. Eglin, K. Rohde and C. C. Perry (2007). "Modern biomaterials: a review-bulk properties and implications of surface modifications." Journal of Materials Science-Materials in Medicine18(7): 1263-1277.

Roach, P., D. Farrar and C. C. Perry (2005). "Interpretation of protein adsorption: Surface-induced conformational changes." Journal of the American Chemical Society127: 8168-8173.

Robertson, E. J. (1987). Embryo-derived stem cell lines. Robertson, E. J.: 71-112.

Safa, K. D., M. Babazadeh, H. Namazi, M. Mahkam and M. G. Asadi (2004). "Synthesis and characterization of new polymer systems containing very bulky tris(trimethylsilyl)methyl substituents as side chains." European Polymer Journal40(3): 459-466.

Salinas, C. N. and K. S. Anseth (2008). "The enhancement of chondrogenic differentiation of human mesenchymal stem cells by enzymatically regulated RGD functionalities." Biomaterials29(15): 2370-2377.

Santiago, L. Y., R. W. Nowak, J. Peter Rubin and K. G. Marra (2006). "Peptide-surface modification of poly(caprolactone) with laminin-derived sequences for adipose-derived stem cell applications." Biomaterials27(15): 2962-9.

Sasaki, D., T. Shimizu, S. Masuda, J. Kobayashi, K. Itoga, Y. Tsuda, J. K. Yamashita, M. Yamato and T. Okano (2009). "Mass preparation of size-controlled mouse embryonic stem cell aggregates and induction of cardiac differentiation by cell patterning method." Biomaterials30(26): 4384-4389.

Sato, H., H. Suemori, J. Toguchida and H. Iwata (2007). "Recombinant matrix protein for maintenance of undifferentiated primate embryonic stem cells." Tissue Engineering13(7): 1539-1547.

Sato, N., L. Meijer, L. Skaltsounis, P. Greengard and A. H. Brivanlou (2004). "Maintenance of pluripotency in human and mouse embryonic stem cells through activation of Wnt signaling by a pharmacological GSK-3-specific inhibitor." Nat Med10(1): 55-63.

Savatier, P., S. Huang, L. Szekely, K. G. Wiman and J. Samarut (1994). "Contrasting patterns of retinoblastoma protein expression in mouse embryonic stem cells and embryonic fibroblasts." Oncogene9(3): 809-18.

Sekiya, I., J. T. Vuoristo, B. L. Larson and D. J. Prockop (2002). "In vitro cartilage formation by human adult stem cells from bone marrow stroma defines the sequence of cellular and molecular events during chondrogenesis." Proc Natl Acad Sci U S A99(7): 4397-402.

Shakibaei, M., C. Csaki, M. Rahmanzadeh and R. Putz (2008). "Interaction between human chondrocytes and extracellular matrix in vitro. A contribution to autologous chondrocyte transplantation." Orthopade37(5): 440-+.

Shao Qiong, L., T. Quan, W. Lei, L. H. James, H. James Hoi Po, Y. Yi Yan and E. Pui Lai Rachel (2009). "Injectable Biodegradable Poly(ethylene glycol)/RGD Peptide Hybrid Hydrogels for in vitro Chondrogenesis of Human Mesenchymal Stem Cells." Macromolecular Rapid Communications31(13): 1148-1154.

Shimizu, H., S. Yokoyama and H. Asahara (2007). "Growth and differentiation of the developing limb bud from the perspective of chondrogenesis." Dev Growth Differ49(6): 449-54.

Shum, L. and G. Nuckolls (2002). "The life cycle of chondrocytes in the developing skeleton." Arthritis Res4(2): 94-106.

Silva, T. S. N., D. C. Machado, C. Viezzer, A. N. Silva and M. G. de Oliveira (2009). "Effect of titanium surface roughness on human bone marrow cell proliferation and differentiation. An experimental study." Acta Cirurgica Brasileira24(3): 200-205.

Smith, A. G., J. K. Heath, D. D. Donaldson, G. G. Wong, J. Moreau, M. Stahl and D. Rogers (1988). "Inhibition of pluripotential embryonic stem cell differentiation by purified polypeptides." Nature336(6200): 688-690.

Smits, P., P. Li, J. Mandel, Z. Zhang, J. M. Deng, R. R. Behringer, B. de Crombrugghe and V. Lefebvre (2001). "The transcription factors L-Sox5 and Sox6 are essential for cartilage formation." Dev Cell1: 277-90.

Son, B. R., L. A. Marquez-Curtis, M. Kucia, M. Wysoczynski, A. R. Turner, J. Ratajczak, M. Z. Ratajczak and A. Janowska-Wieczorek (2006). "Migration of bone marrow and cord blood mesenchymal stem cells in vitro is regulated by stromal-derived factor-1-CXCR4 and hepatocyte growth factor-c-met axes and involves matrix metalloproteinases." Stem Cells24(5): 1254-64.

Soncin, F., L. Mohamet, D. Eckardt, S. Ritson, A. M. Eastham, N. Bobola, A. Russell, S. Davies, R. Kemler, C. L. R. Merry and C. M. Ward (2009). "Abrogation of E-Cadherin-Mediated Cell-Cell Contact in Mouse Embryonic Stem Cells Results in Reversible LIF-Independent Self-Renewal." Stem Cells27(9): 2069-2080.

Steele, J. G., B. A. Dalton, G. Johnson and P. A. Underwood (1995). "Adsorption of fibronectin and vitronectin onto Primaria and tissue culture polystyrene and relationship to the mechanism of initial attachment of human vein endothelial cells and BHK-21 fibroblasts." Biomaterials16(14): 1057-67.

Steele, J. G., G. Johnson and P. A. Underwood (1992). "Role of serum vitronectin and fibronectin in adhesion of fibroblasts following seeding onto tissue culture polystyrene." J Biomed Mater Res26(7): 861-84.

Szabo, E., T. S. Feng, E. Dziak and M. Opas (2009). "Cell Adhesion and Spreading Affect Adipogenesis from Embryonic Stem Cells: The Role of Calreticulin." Stem Cells27(9): 2092-2102.

Tavella, S., G. Bellese, P. Castagnola, I. Martin, D. Piccini, R. Doliana, A. Colombatti, R. Cancedda and C. Tacchetti (1997). "Regulated expression of fibronectin, laminin and related integrin receptors during the early chondrocyte differentiation." J Cell Sci110 (Pt 18): 2261-70.

Tavella, S., P. Raffo, C. Tacchetti, R. Cancedda and P. Castagnola (1994). "N-CAM and N-cadherin expression during in vitro chondrogenesis." Exp Cell Res215(2): 354-62.

Tigli, R. S. and M. Gumusderelioglu (2008). "Evaluation of RGD- or EGF-immobilized chitosan scaffolds for chondrogenic activity." International Journal of Biological Macromolecules43(2): 121-128.

Tsuji, Y., N. Yoshimura, H. Aoki, A. A. Sharov, M. S. Ko, T. Motohashi and T. Kunisada (2008). "Maintenance of undifferentiated mouse embryonic stem cells in suspension by the serum- and feeder-free defined culture condition." Developmental dynamics : an official publication of the American Association of Anatomists237(8): 2129-38.

Underwood, P. A., J. G. Steele and B. A. Dalton (1993). "Effects of polystyrene surface chemistry on the biological activity of solid phase fibronectin and vitronectin, analysed with monoclonal antibodies." J Cell Sci104 (Pt 3): 793-803.

van der Linden, P. J. (1996). "Cell adhesion, cell adhesion molecules and their functional role in the human endometrium." Early Pregnancy2(1): 5-14.

Vanwachem, P. B., A. H. Hogt, T. Beugeling, J. Feijen, A. Bantjes, J. P. Detmers and W. G. Vanaken (1987). "Adhesion of cultured human-endothelial cells onto metharylate polymers with varying surface wettability and charge." Biomaterials8(5): 323-328.

Villa-Diaz, L. G., H. Nandivada, J. Ding, N. C. Nogueira-De-Souza, P. H. Krebsbach, K. S. O'Shea, J. Lahann and G. D. Smith (2010). "Synthetic polymer coatings for

long-term growth of human embryonic stem cells." Nature Biotechnology28(6): 581-583.

Vlodavsky, I., H. Q. Miao, B. Medalion, P. Danagher and D. Ron (1996). "Involvement of heparan sulfate and related molecules in sequestration and growth promoting activity of fibroblast growth factor." Cancer and Metastasis Reviews15(2): 177-186.

Wang, J. H., P. M. Claesson, J. L. Parker and H. Yasuda (1994). "Dynamic contact angles and contact-angle hystersis of plasma polymers." Langmuir10(10): 3887-3897.

Wang, Y. L., K. J. Addess, J. Chen, L. Y. Geer, J. He, S. Q. He, S. N. Lu, T. Madej, A. Marchler-Bauer, P. A. Thiessen, N. G. Zhang and S. H. Bryant (2007). "MMDB: annotating protein sequences with Entrez's 3D-structure database." Nucleic Acids Research35: D298-D300.

Webb, K., V. Hlady and P. A. Tresco (2000). "Relationships among cell attachment, spreading, cytoskeletal organization, and migration rate for anchorage-dependent cells on model surfaces." J Biomed Mater Res49(3): 362-8.

Wei, J. H., T. Igarashi, N. Okumori, T. Igarashi, T. Maetani, B. L. Liu and M. Yoshinari (2009). "Influence of surface wettability on competitive protein adsorption and initial attachment of osteoblasts." Biomedical Materials4(4): 7.

Wells, N. (2009). The role of synthetic substrates and separen sulphate in regulating embryonic stem cell fate. School of Biological Sciences. University of Liverpool. **PhD**.

Wells, N., M. A. Baxter, J. E. Turnbull, P. Murray, D. Edgar, K. L. Parry, D. A. Steele and R. D. Short (2009). "The geometric control of E14 and R1 mouse embryonic stem cell pluripotency by plasma polymer surface chemical gradients." Biomaterials30(6): 1066-70.

White, D. G., H. P. Hershey, J. J. Moss, H. Daniels, R. S. Tuan and V. D. Bennett (2003). "Functional analysis of fibronectin isoforms in chondrogenesis: Full-length recombinant mesenchymal fibronectin reduces spreading and promotes condensation and chondrogenesis of limb mesenchymal cells." Differentiation71(4-5): 251-61.

Widelitz, R. B., T. X. Jiang, B. A. Murray and C. M. Chuong (1993). "Adhesion molecules in skeletogenesis: II. Neural cell adhesion molecules mediate precartilaginous mesenchymal condensations and enhance chondrogenesis." J Cell Physiol156(2): 399-411.

Willenberg, B. J., T. Hamazaki, F. W. Meng, N. Terada and C. Batich (2006). "Self-assembled copper-capillary alginate gel scaffolds with oligochitosan support embryonic stem cell growth." Journal of Biomedical Materials Research Part A79A(2): 440-450.

Williams, C. G., T. K. Kim, A. Taboas, A. Malik, P. Manson and J. Elisseeff (2003). "In vitro chondrogenesis of bone marrow-derived mesenchymal stem cells in a photopolymerizing hydrogel." Tissue Engineering9(4): 679-688.

Williams, R. L., D. J. Hilton, S. Pease, T. A. Willson, C. L. Stewart, D. P. Gearing, E. F. Wagner, D. Metcalf, N. A. Nicola and N. M. Gough (1988). "Myeloid leukaemia inhibitory factor maintains the developmental potential of embryonic stem cells." Nature336(6200): 684-687.

Woods, A., G. Wang and F. Beier (2005). "RhoA/ROCK signaling regulates Sox9 expression and actin organization during chondrogenesis." J Biol Chem280(12): 11626-34.

Woods, A., G. Wang and F. Beier (2007). "Regulation of chondrocyte differentiation by the actin cytoskeleton and adhesive interactions." J Cell Physiol213(1): 1-8.

Woods, A., G. Wang, H. Dupuis, Z. Shao and F. Beier (2007). "Rac1 signaling stimulates N-cadherin expression, mesenchymal condensation, and chondrogenesis." J Biol Chem282(32): 23500-8.

Xu, H. W., X. T. Fan, X. Wu, J. Tang and H. Yang (2005). "Neural precursor cells differentiated from mouse embryonic stem cells relieve symptomatic motor behavior in a rat model of Parkinson's disease." Biochemical and Biophysical Research Communications326(1): 115-122.

Yim, E. K. F., J. Wen and K. W. Leong (2006). "Enhanced extracellular matrix production and differentiation of human embryonic germ cell derivatives in

biodegradable poly(epsilon-caprolactone-co-ethyl ethylene phosphate) scaffold." Acta Biomaterialia2(4): 365-376.

Ying, G., H. Giao, B. Huimin, M. P. Louis and E. B. Hal (2005). "SDF-1/CXCL12 Enhances Survival and Chemotaxis of Murine Embryonic Stem Cells and Production of Primitive and Definitive Hematopoietic Progenitor Cells." Stem Cells23(9): 1324-1332.

Ying, Q.-L., J. Wray, J. Nichols, L. Batlle-Morera, B. Doble, J. Woodgett, P. Cohen and A. Smith (2008). "The ground state of embryonic stem cell self-renewal." Nature453(7194): 519-523.

Yoo, J. U., T. S. Barthel, K. Nishimura, L. Solchaga, A. I. Caplan, V. M. Goldberg and B. Johnstone (1998). "The chondrogenic potential of human bone-marrow-derived mesenchymal progenitor cells." J Bone Joint Surg Am80(12): 1745-57.

Yoon, B. S. and K. M. Lyons (2004). "Multiple functions of BMPs in chondrogenesis." J Cell Biochem93(1): 93-103.

Yoon, B. S., D. A. Ovchinnikov, I. Yoshii, Y. Mishina, R. R. Behringer and K. M. Lyons (2005). "Bmpr1a and Bmpr1b have overlapping functions and are essential for chondrogenesis in vivo." Proc Natl Acad Sci U S A102(14): 5062-7.

Young, T. (1805). "An Essay on the Cohesion of Fluids." Philosophical Transactions of the Royal Society of London95: 65-87.

Zaidel-Bar, R., S. Itzkovitz, A. Ma'ayan, R. Iyengar and B. Geiger (2007). "Functional atlas of the integrin adhesome." Nat Cell Biol9: 858-67.

Zanetti, N. C. and M. Solursh (1984). "Induction of chondrogenesis in limb mesenchymal cultures by disruption of the actin cytoskeleton." J Cell Biol99(1 Pt 1): 115-23.

Zhu, Y., A. Oganesian, D. R. Keene and L. J. Sandell (1999). "Type IIA procollagen containing the cysteine-rich amino propeptide is deposited in the extracellular matrix of prechondrogenic tissue and binds to TGF-beta 1 and BMP-2." Journal of Cell Biology144(5): 1069-1080.

Zhu, Y. B., C. Y. Gao, Y. X. Liu and J. C. Shen (2004). "Endothelial cell functions in vitro cultured on poly(L-lactic acid) membranes modified with different methods." Journal of Biomedical Materials Research Part A69A(3): 436-443.

Zuzarte-Luis, V., J. A. Montero, J. Rodriguez-Leon, R. Merino, J. C. Rodriguez-Rey and J. M. Hurle (2004). "A new role for BMP5 during limb development acting through the synergic activation of Smad and MAPK pathways." Dev Biol272(1): 39-52.